

Dissertation zur Erlangung des Doktorgrades
der Fakultät für Chemie und Pharmazie
der Ludwig-Maximilians-Universität München



Reactivity Parameters
for
Enamine Activated Reactions

Tanja Kanzian

aus

Füssen

2010

Erklärung

Diese Dissertation wurde im Sinne von §13 Abs. 3 bzw. 4 der Promotionsordnung vom 29. Januar 1998 von Herrn Prof. Dr. Herbert Mayr betreut.

Ehrenwörtliche Versicherung

Diese Dissertation wurde selbständig und ohne unerlaubte Hilfe erarbeitet.

München, 02.08.2010

.....
Tanja Kanzian

Dissertation eingereicht am	06.08.2010
1.Gutachter	Prof. Dr. Herbert Mayr
2.Gutachter	Prof. Dr. Hendrik Zipse
Mündliche Prüfung am	01.10.2010

FÜR MEINE ELTERN

Danksagung

Besonders möchte ich Herrn Prof. Dr. Herbert Mayr für seine herausragende und beispielhafte Betreuung während der Durchführung meiner Arbeit, die interessante Themenstellung und seine stete Hilfs- und Diskussionsbereitschaft danken.

Weiterhin gilt mein Dank Herrn Prof. Dr. Orazio Attanasí für die Möglichkeit sechs Wochen in seinem Labor in Urbino arbeiten zu dürfen. Seinen Mitarbeitern, insbesondere Simona Nicolini danke ich für die freundliche Aufnahme in ihre Arbeitsgruppe und ihre Hilfsbereitschaft, die meinen Forschungsaufenthalt in wissenschaftlicher sowie privater Natur zu einem Erfolg gemacht haben.

Ich danke allen Mitgliedern des Prüfungsausschusses für ihre Teilnahmebereitschaft.

Dr. Armin Ofial sei ganz herzlich gedankt für die zügige und kritische Durchsicht meiner Publikationen.

Den Mitgliedern des Arbeitskreises möchte ich für das freundliche und kollegiale Arbeitsklima, ihre Diskussionsbereitschaft und die stets lustigen Feiern danken. Ich hoffe die entstandenen Freundschaften werden auch über diese Arbeit hinaus bestehen.

Besonderer Dank gilt auch meinen Kollegen des „Olah“-Labors, insbesondere Roland Appel, Martin Breugst, Sami Lakhdar, Christoph Nolte und Dr. André Streiter, und meinem Bürokollegen Nicolas Streidl, die mich durch Höhen und Tiefen des Laboralltags begleitet haben, und durch ihre anregenden fachlichen und privaten Gespräche und ihre nette Art wesentlich dazu beigetragen haben diese Zeit in guter Erinnerung zu behalten.

Bedanken möchte ich mich auch bei Nathalie Hampel, Brigitte Janker und Hildegard Lípfer, die mir durch die Bereitstellung von Chemikalien und ihrer Hilfe bei organisatorischen Fragen den Arbeitsalltag sehr erleichtert haben.

Ich danke meinem Forschungspraktikanten Stefan Píchl für seine erfolgreiche Mitarbeit.

Für die kritische und zügige Durchsicht dieser Arbeit danke ich Roland Appel, Martin Breugst, Hans Laub, Christoph Nolte und Tobias Nígst.

Auch möchte ich mich bei meinen Freunden und meiner Schwester bedanken, die immer an mich geglaubt und mich unterstützt haben und für die erforderliche Abwechslung sorgten.

Der größte Dank gebührt meinen Eltern ohne die mein Studium und die Promotion nicht möglich gewesen wären und denen deshalb diese Arbeit gewidmet ist.

Publikationen

- (1) T. Kanzian, T. A. Nigst, A. Maier, S. Pichl, H. Mayr in *Eur. J. Org. Chem.* **2009**, 6379–6385: “NUCLEOPHILIC REACTIVITIES OF PRIMARY AND SECONDARY AMINES IN ACETONITRILE”
- (2) T. Kanzian, S. Nicolini, L. De Crescentini, O. A. Attanasi, A. R. Ofial, H. Mayr, *Chem. Eur. J.* **2010**, *16*, 12008–12016: “ELECTROPHILIC REACTIVITIES OF 1,2-DIAZA-1,3-DIENES”
- (3) T. Kanzian, H. Mayr, *Chem. Eur. J.* **2010**, *16*, 11670–11677: “ELECTROPHILIC REACTIVITIES OF AZODICARBOXYLATES”
- (4) T. Kanzian, S. Lakhdar, H. Mayr, *Angew. Chem.* **2010**, accepted: “KINETIC EVIDENCE FOR OXAZOLIDINONE FORMATION IN THE STEREOGENIC STEP OF PROLINE-CATALYZED REACTIONS”

Konferenzbeiträge

- (1) 12/2007 Berichtskolloquium Organokatalyse (DFG-Schwerpunktprogramm SPP 1179), Posterpräsentation: “ELECTROPHILIC REACTIVITIES OF AZODICARBOXYLATES”
- (2) 09/2008 2nd EuCheMS Chemistry Congress, Posterpräsentation: “ELECTROPHILIC REACTIVITIES OF AZODICARBOXYLATES”

Table of Contents

0	SUMMARY	1
1	INTRODUCTION AND OBJECTIVES	12
2	NUCLEOPHILIC REACTIVITIES OF PRIMARY AND SECONDARY AMINES IN ACETONITRILE	16
	2.1 INTRODUCTION	16
	2.2 RESULTS AND DISCUSSION	17
	2.2.1 Product Characterization	17
	2.2.2 Kinetics of the Reactions of the Amines 2-15 with the Reference Electrophiles 1	19
	2.3 CONCLUSION	29
	2.4 EXPERIMENTAL SECTION	29
	2.4.1 General comment	29
	2.4.2 Kinetic Experiments	30
	2.4.3 Synthetic Experiments	64
	2.5 REFERENCES	66
3	ELECTROPHILIC REACTIVITIES OF 1,2-DIAZA-1,3-DIENES	69
	3.1 INTRODUCTION	69
	3.2 RESULTS AND DISCUSSION	71
	3.2.1 Reactions of 1,2-Diaza-1,3-dienes 1 with Carbanions 2	71
	3.2.2 Reactions of the 1,2-Diaza-1,3-dienes 1 with Other Nucleophiles	77
	3.3 CONCLUSION	87
	3.4 EXPERIMENTAL SECTION	89
	3.4.1 General comment	89
	3.4.2 Kinetic Experiments	90
	3.4.3 Synthetic Experiments	134
	3.5 REFERENCES	146

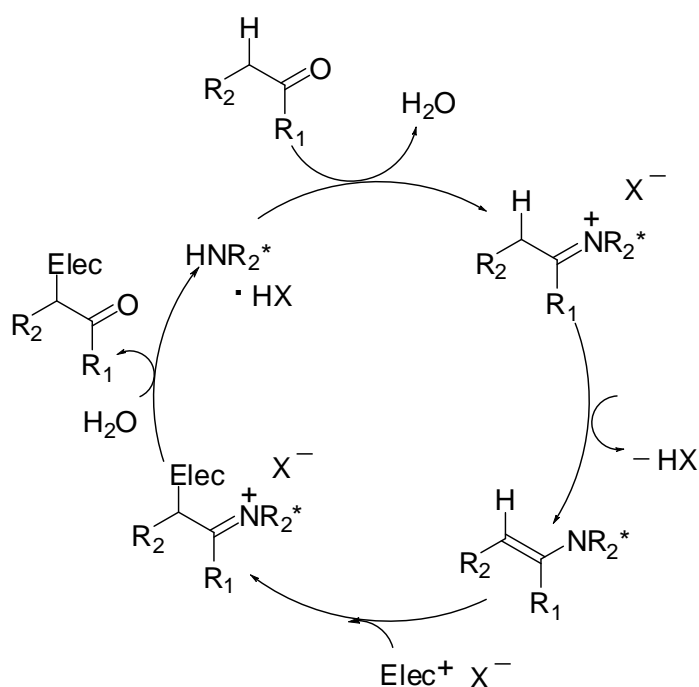
4	ELECTROPHILIC REACTIVITIES OF AZODICARBOXYLATES	148
4.1	INTRODUCTION	148
4.2	RESULTS AND DISCUSSION	150
4.2.1	Reactions of Azodicarboxylates 1 with Enamines 2	150
4.2.2	Reactions with Triarylphosphines 4	155
4.2.3	Reactions with Amines 5	158
4.2.4	Pericyclic Reactions	165
4.3	CONCLUSION	167
4.4	EXPERIMENTAL SECTION	167
4.4.1	General comment	167
4.4.2	Kinetic Experiments	168
4.4.3	Synthetic Experiments	212
4.5	REFERENCES	217
5	KINETIC EVIDENCE FOR OXAZOLIDINONE FORMATION IN THE STEREOREGENIC STEP IN PROLINE CATALYZED REACTIONS	220
5.1	INTRODUCTION	220
5.2	RESULTS AND DISCUSSION	223
5.3	CONCLUSION	228
5.4	EXPERIMENTAL SECTION	229
5.4.1	General comment	229
5.4.2	Kinetic Experiments	230
5.4.3	Synthetic Experiments	239
5.5	REFERENCES	240

Chapter 0

SUMMARY

0.1 General

Enamine activated reactions have become an important method for enantioselective α -functionalizations of carbonyl compounds (Scheme 0.1).



Scheme 0.1. Catalytic cycle of secondary amine catalyzed reactions of aldehydes and ketones with electrophiles.

Key-steps of the reaction cascade shown in Scheme 0.1 are combinations of electrophiles with nucleophiles, the rates of which should be accessible by Equation (0.1), where nucleophiles are described by a nucleophilicity parameter N and a nucleophile-specific sensitivity parameter s , and electrophiles are characterized by an electrophilicity parameter E .

$$\log k_2(20\text{ }^\circ\text{C}) = s(N+E) \quad (0.1)$$

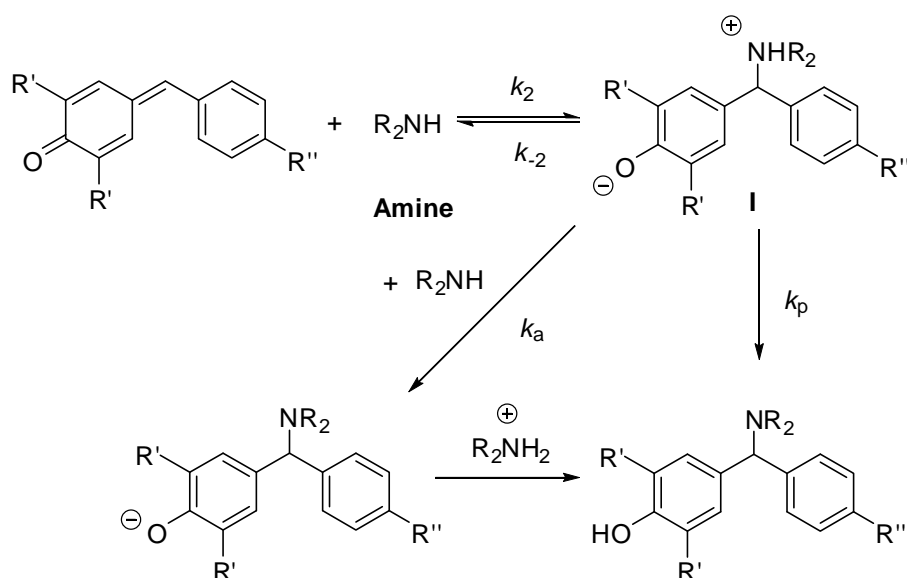
In this work, we have used Equation (0.1) to derive electrophilicity parameters E and nucleophile-specific parameters N and s for substrates and intermediates of enamine activated reactions in order to get insight in the mechanism and scope of some enamine activated reactions.

0.2 Nucleophilic Reactivities of Primary and Secondary Amines in Acetonitrile

The kinetics of the reactions of primary and secondary amines (for structures see Figure 0.2) with benzhydrylium ions and quinone methides in acetonitrile were studied under pseudo-first-order conditions (high excess of amines) by UV/Vis spectroscopy. Generally, the plots of k_{obs} versus the amine concentrations were linear, in line with a second-order rate law (0.2).

$$k_{\text{obs}} = k_2 [\text{Amine}] \quad (0.2)$$

However, for some reactions of secondary amines with quinone methides, an upward curvature was observed in plots of k_{obs} vs. the amine concentration, indicating rate limiting deprotonation of the initially formed adduct **I** by a second molecule of amine (Scheme 0.2).



Scheme 0.2. Reactions of secondary amines with quinone methides in acetonitrile.

For these reactions the initial electrophile-nucleophile combination step is reversible, and the more complicated rate law (0.3) has to be employed for deriving the rate constant k_2 for the attack of the amines on the electrophiles.

$$k_{\text{obs}} = k_2 [\text{Amine}]^2 k_a / (k_{-2} + k_a [\text{Amine}]) \quad (0.3)$$

From the second-order rate constants k_2 , the nucleophilicity parameters N and s for the amines according to Equation (0.1) were determined (as exemplified for selected examples in Figure 0.1) and cover a reactivity range of $10 < N < 19$. The less reactive amines react with similar rates as silyl ketene acetals, trialkyl-substituted pyrroles and pyridines, whereas the more reactive amines show a similar nucleophilicity as stabilized carbanions (Figure 0.2).

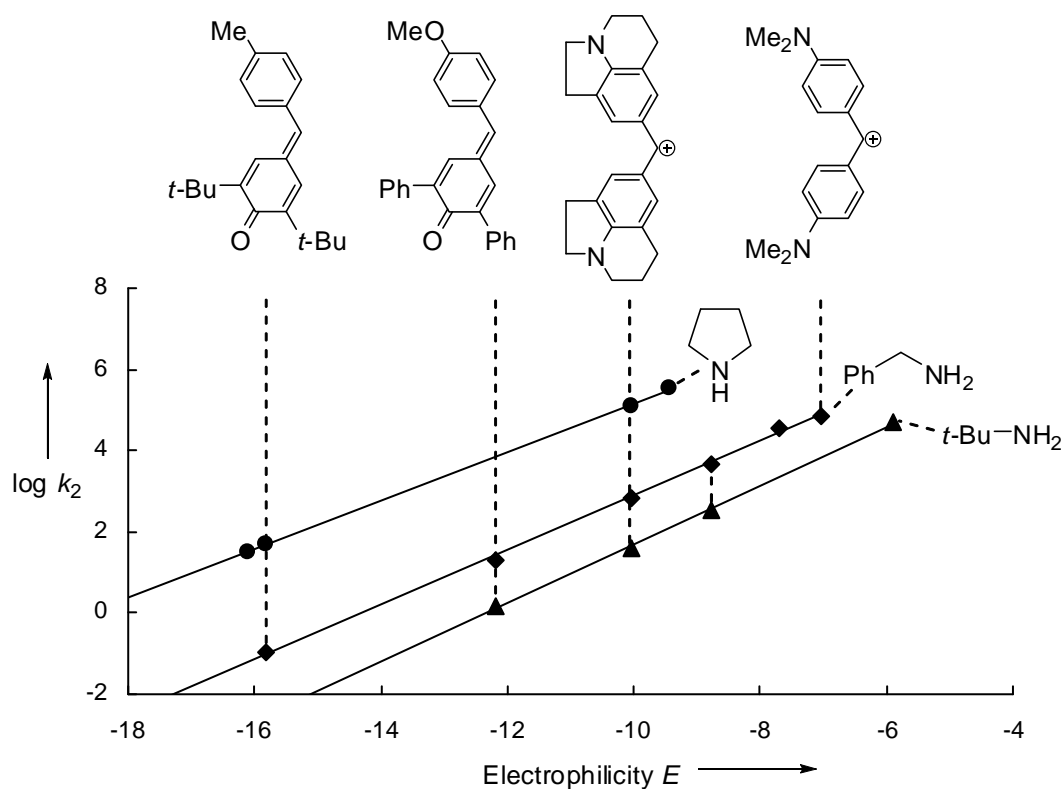


Figure 0.1. Plots of the second-order rate constants $\log k_2$ (20 °C) for the reactions of pyrrolidine, benzylamine, and *tert*-butylamine with benzhydrylium ions and quinone methides in CH_3CN against the E -parameters of the reference electrophiles.

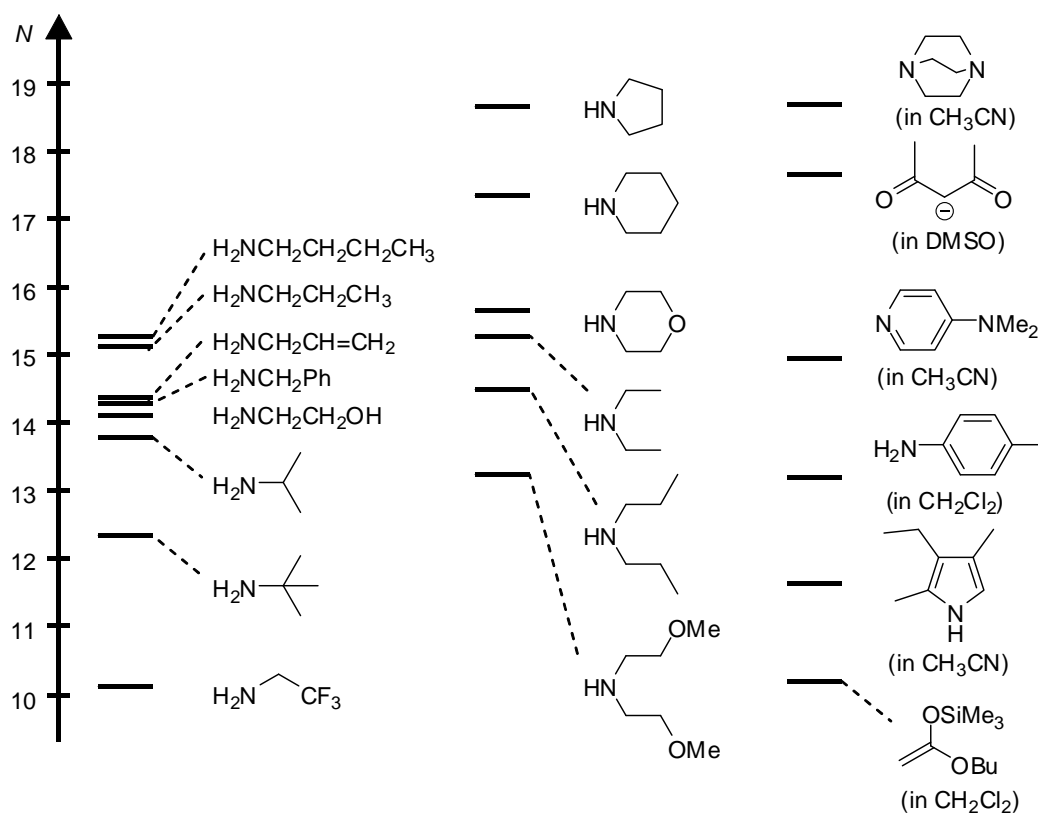
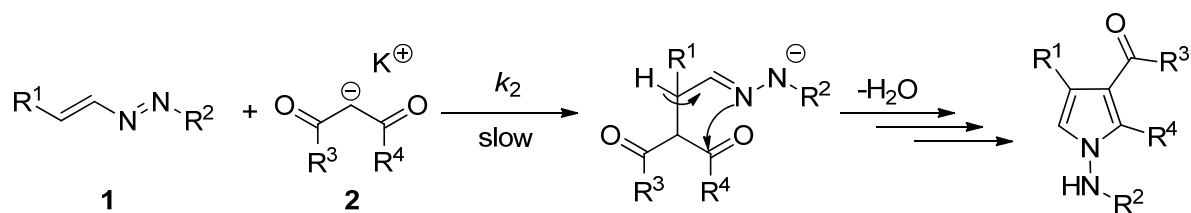


Figure 0.2. Comparison of the nucleophilic reactivities of amines in acetonitrile with other nucleophiles.

A poor correlation between N and pK_{aH} has been found and shows that also in acetonitrile, relative basicities cannot be used for predicting relative nucleophilicities. Solvent polarity affects the reactivities of alkylamines and anilines quite differently: Whereas anilines react approximately two times faster with benzhydrylium ions in water than in acetonitrile, primary alkylamines react at least 10 times faster in acetonitrile than in water. The opposite solvent effect on these closely related reactions demonstrates the limitation of Hughes-Ingold rules to predict solvent effects on polar organic reactions on the basis of the relative charge dispersal in the ground and transition states.

0.3 Electrophilic Reactivities of 1,2-Diaza-1,3-dienes

The kinetics of the reactions of 1,2-diaza-1,3-dienes **1** (for structures see Figure 0.4) with acceptor substituted carbanions **2** (for structures see Figure 0.3) have been studied at 20 °C. ^1H - and ^{13}C -NMR analysis of the addition products confirmed the formation of 1,4-adducts or of pyrroles after subsequent cyclization (Scheme 0.3).



Scheme 0.3. Michael-addition of β -dicarbonyl compounds to 1,2-diaza-1,3-dienes **1** and subsequent cyclization.

In these reactions the attack of the carbanions **2** at the electrophiles **1** is rate limiting; the reactions follow a second-order rate law and can be described by the linear free-energy relationship (0.1). With Equation (0.1) and the known nucleophile-specific parameters N and s for the carbanions **2**, the electrophilicity parameters E of the 1,2-diaza-1,3-dienes **1** were determined as exemplified for **1b** and **1d** in Figure 0.3.

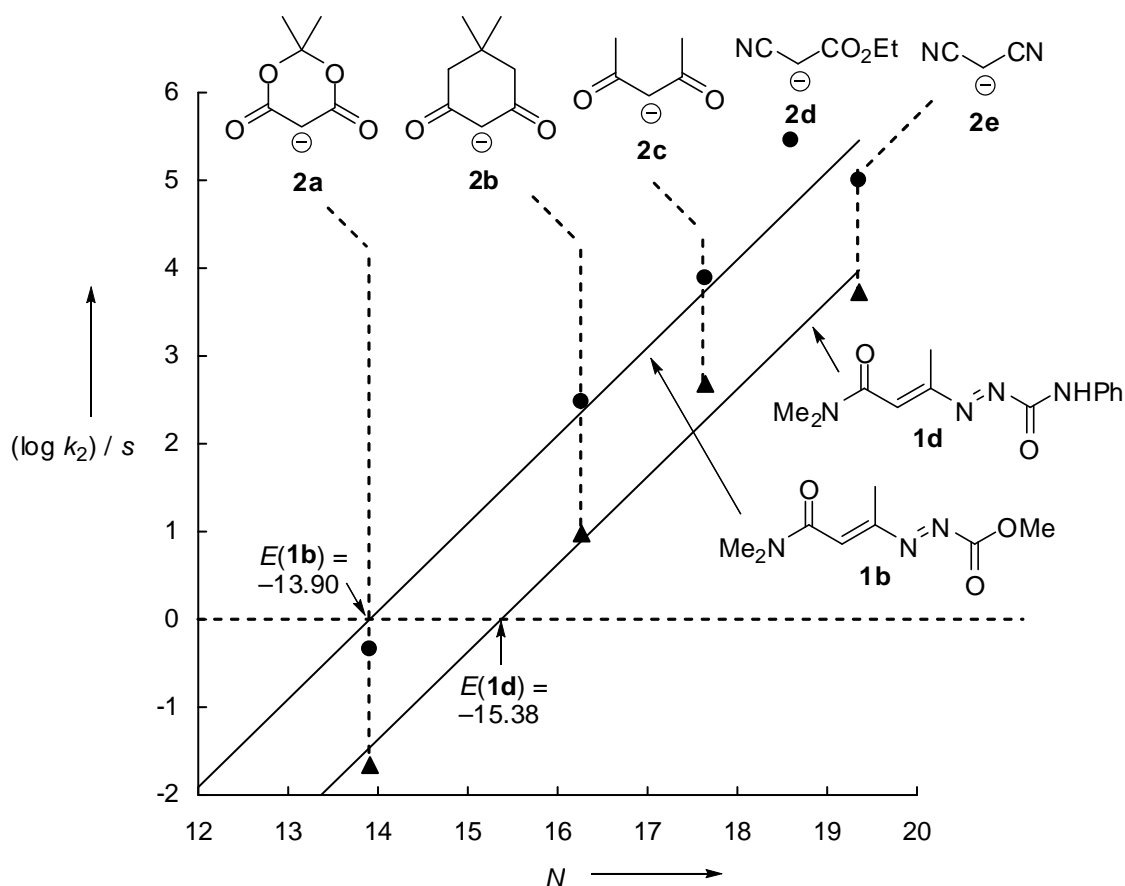


Figure 0.3. Plots of $(\log k_2)/s$ versus the N -parameters of the carbanions **2a–e** for the reactions of the 1,2-diaza-1,3-dienes **1b** and **1d** with **2a–e** in DMSO at 20 °C (the slopes are fixed to 1.0 as required by Equation (0.1); reaction of **2d** in methanol).

With E -parameters in the range of -15.4 to -13.3 , the electrophilic reactivities of **1a–d** are comparable to those of benzylidenemalononitriles, 2-benzylideneindan-1,3-diones, and benzylidenebarbituric acids (Figure 0.4).

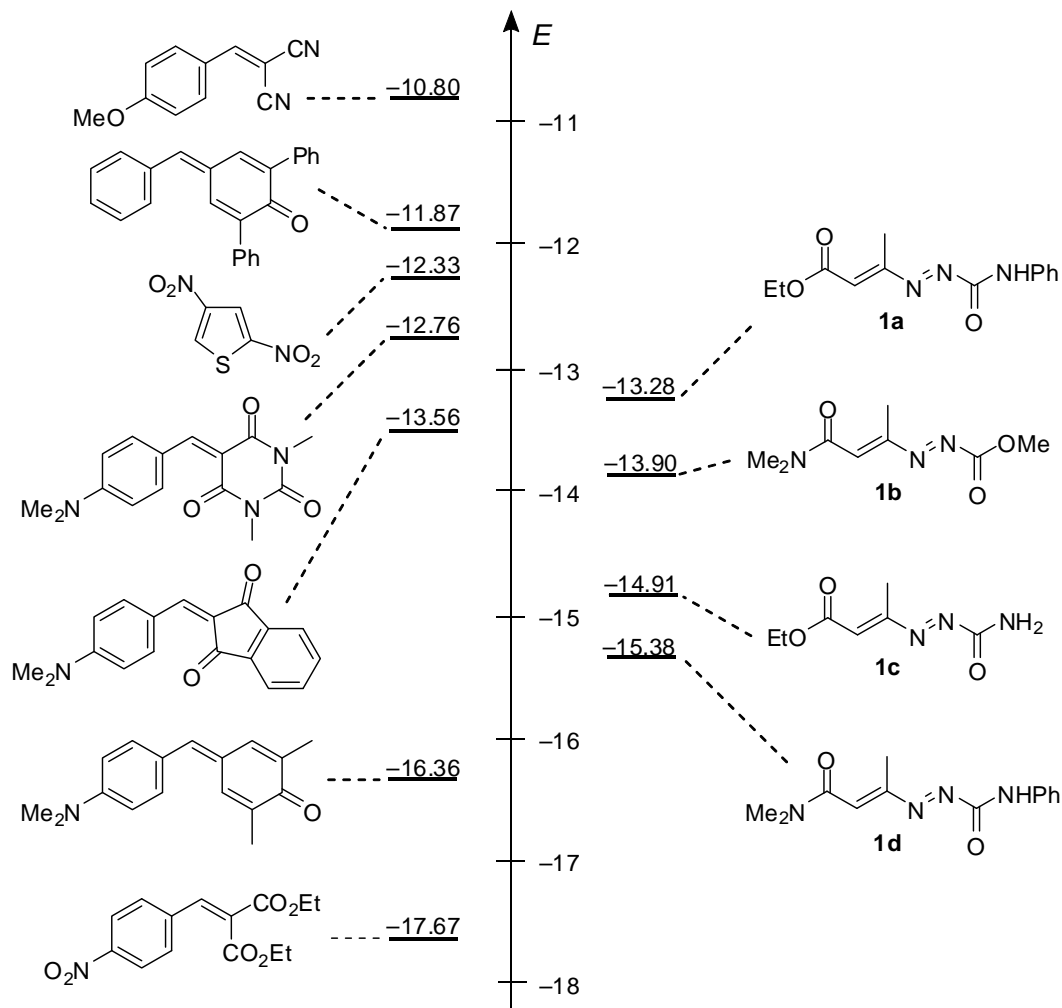


Figure 0.4. Comparison of the electrophilic reactivities of 1,2-diaza-1,3-dienes **1** with those of other classes of electrophiles.

The experimental second-order rate constants for the reactions of **1a–d** with amines and triarylphosphines agreed with those calculated from E , N , and s (Figure 0.5), indicating the applicability of the linear free-energy relationship (0.1) for predicting potential nucleophilic reaction partners of 1,2-diaza-1,3-dienes **1**. The positive deviations of the enamines from the correlation line in Figure 0.5 show that enamines react up to 10^2 – 10^3 times faster with compounds **1** than predicted by Equation (0.1). This deviation is indicative for a mechanistic change; possibly an initial concerted [4+2]-cycloaddition is operating where the transition

state profits from the simultaneous formation of two new bonds. The isolated pyrroles may be formed via rearrangement of the initial Diels-Alder adducts.

The Diels-Alder adducts obtained in the reactions of enol ethers with the diene **1c** must be generated by concerted mechanisms, because the stepwise processes can be estimated by Equation (0.1) to require more than 10^2 years.

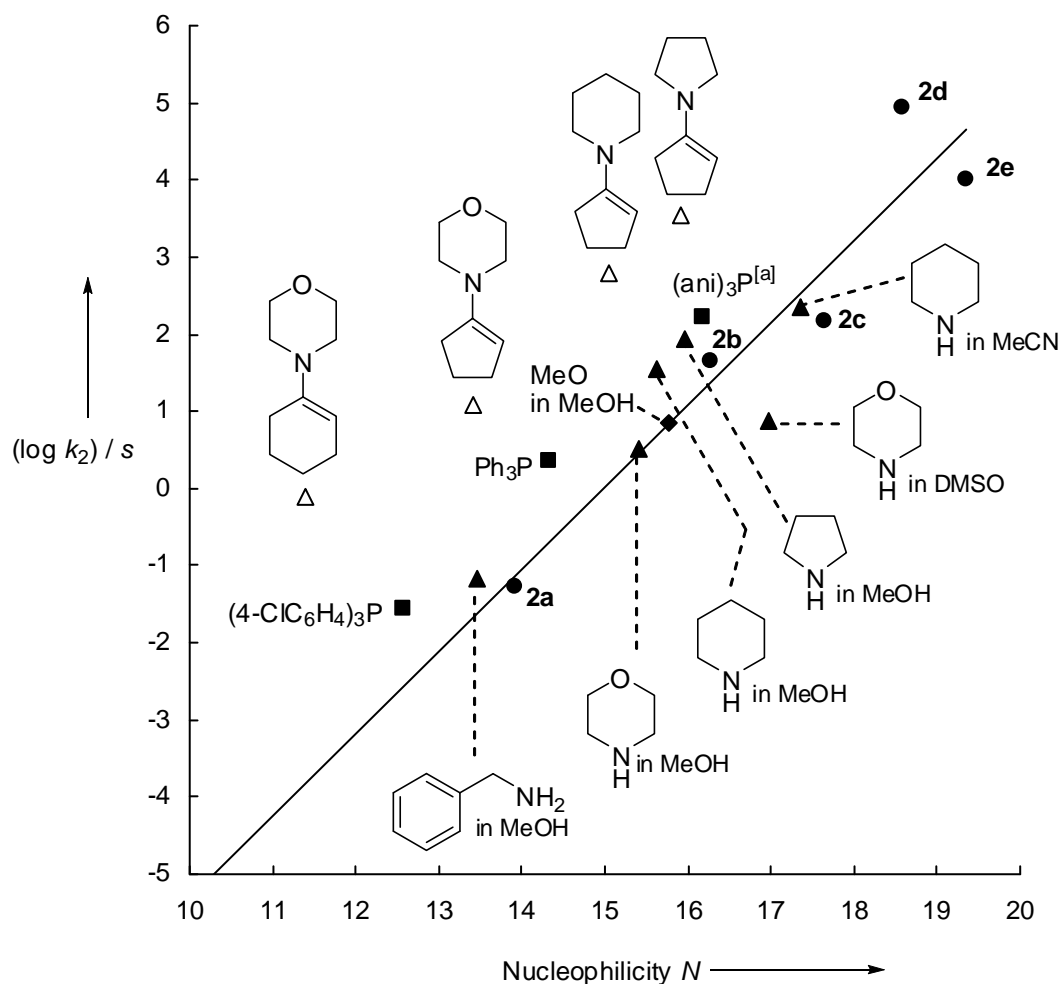


Figure 0.5. Plot of $(\log k_2)/s$ for the reactions of the 1,2-diaza-1,3-diene **1c** with carbanions **2**, amines, phosphines, and enamines at 20 °C against the N parameters of the carbanions **2a–e** (filled circles), amines (filled triangles), phosphines (filled squares, in CH_2Cl_2), enamines (open triangles, in MeCN) and methanolate (filled rhomb). - The linear curve refers to the plot of $(\log k_2)/s$ against the N parameters of the carbanions **2a–e**, and the slope is fixed to unity as required by Equation (0.1). ^[a] $\text{P}(\text{ani})_3$ = tris(*p*-anisyl)phosphine.

0.4 Electrophilic Reactivities of Azodicarboxylates

The kinetics of the reactions of the azodicarboxylates **3** (for structures see Figure 0.7) with enamines (for structures see Figure 0.6) have been studied in CH₃CN at 20 °C. The reactions follow a second-order rate law and can be described by the linear free-energy relationship (0.1) (Figure 0.6).

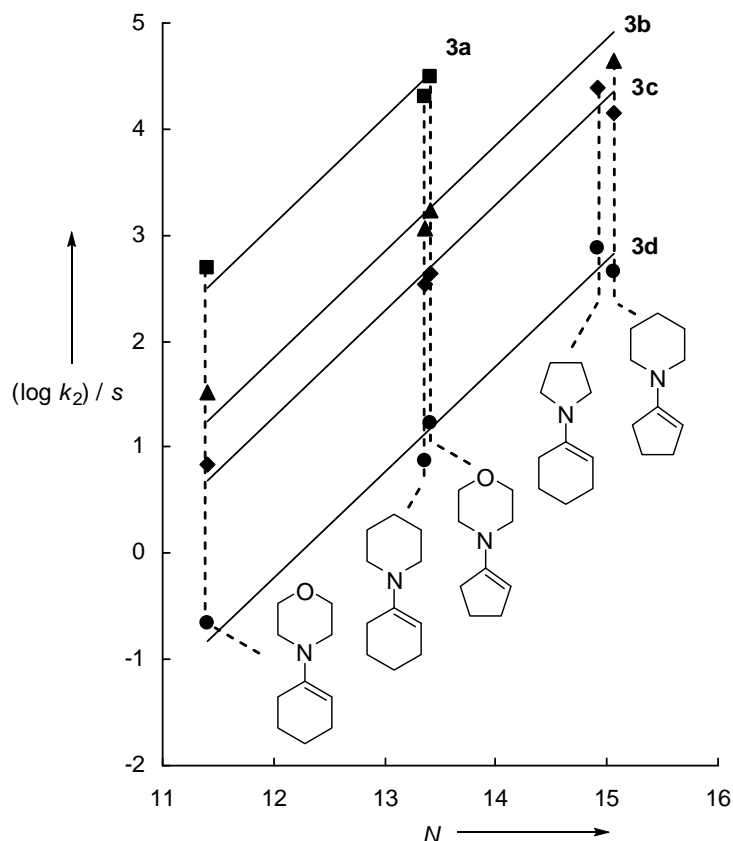


Figure 0.6. Correlation of $(\log k_2)/s$ against the corresponding nucleophile parameters N of the enamines for the reactions of azodicarboxylates **3a-d** (for structures see Figure 0.7) with enamines [the slopes are fixed to 1.0 as required by Equation (0.1)].

With E parameters from -12.2 to -8.9, the electrophilicities of **3** cover a surprisingly wide range of reactivity, and turned out to be comparable to those of α,β -unsaturated iminium ions, amino-substituted benzhydrylium ions, and ordinary Michael acceptors (Figure 0.7).

Unexpectedly, the E parameters of the azodicarboxylates **3** also hold for their reactions with triarylphosphines, though none of the reaction centers is carbon, a prerequisite for the applicability of Equation (0.1). The potential of Equation (0.1) to predict rates of P-N bond formations may be due to comparable bond energies of the P-N and the C-N bond. In contrast,

Equation (0.1) cannot be applied to N-N bond forming reactions, as the reactions of the azodicarboxylates with secondary amines are 10^3 - 10^6 times slower than predicted by Equation (0.1).

Concerted cycloadditions with the azodicarboxylate **3b** proceed 10^5 to 10^8 times faster than calculated by Equation (0.1). In these reactions the concerted formation of two new σ -bonds stabilizes the transition state and gives rise to a higher reaction rate. The difference between experimental and calculated rate constants for concerted cycloadditions and ene reactions of azodicarboxylates provides a measure for the energy of concert of these reactions.

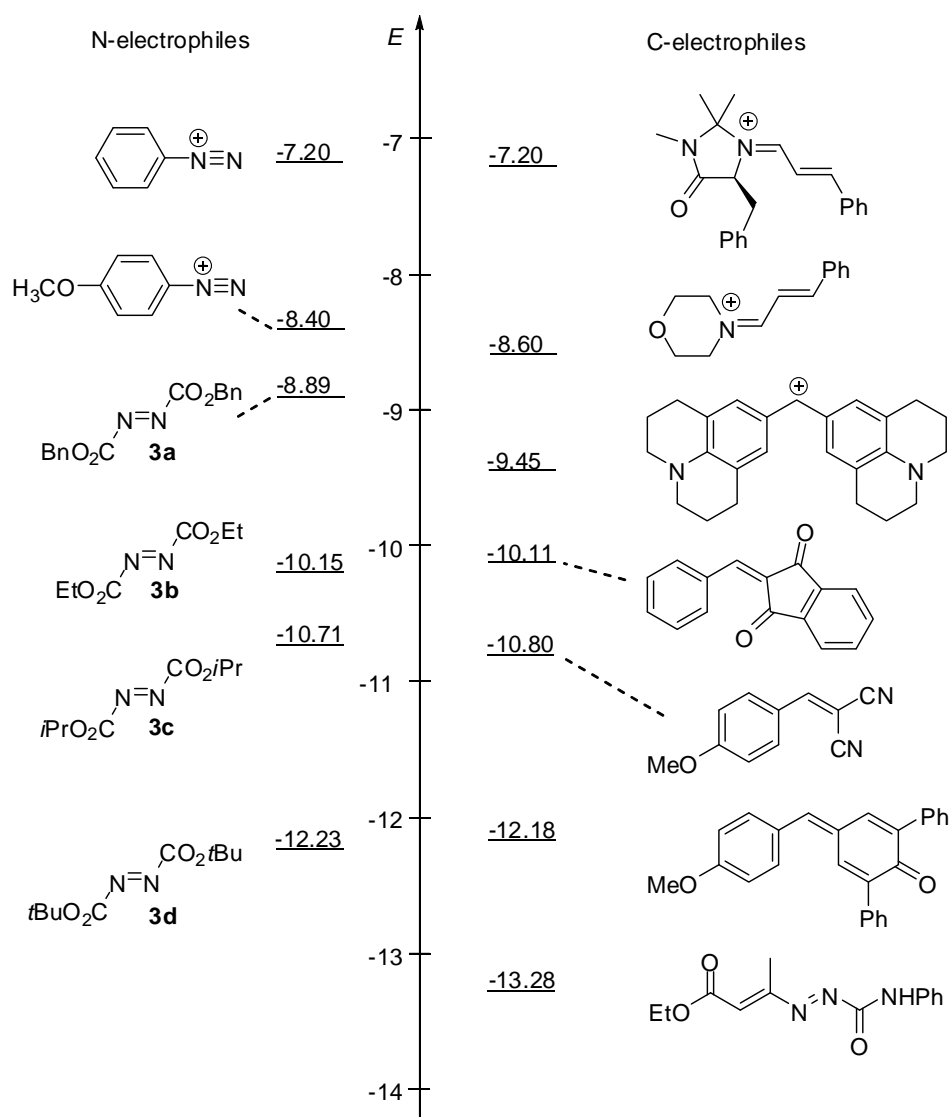


Figure 0.7. Comparison of the electrophilicity parameters of azodicarboxylates **3** with other electrophiles.

0.5 Kinetic Evidence for Oxazolidinone Formation in the Stereogenic Step of Proline-Catalyzed Reactions

The kinetics of the reactions of the proline-, pyrrolidine-, and proline methyl ester derived enamines **4** (for structures see Figure 0.8) with benzhydrylium ions and quinone methides in acetonitrile were studied under pseudo-first-order conditions (high excess of enamines) by UV/Vis spectroscopy. The reactions follow a second-order rate law, and the N and s parameters of **4a⁻**, **4b**, and **4c** were determined by plotting the logarithms of the second order rate constants against the E parameters of the electrophiles according to Equation (0.1) (Figure 0.8).

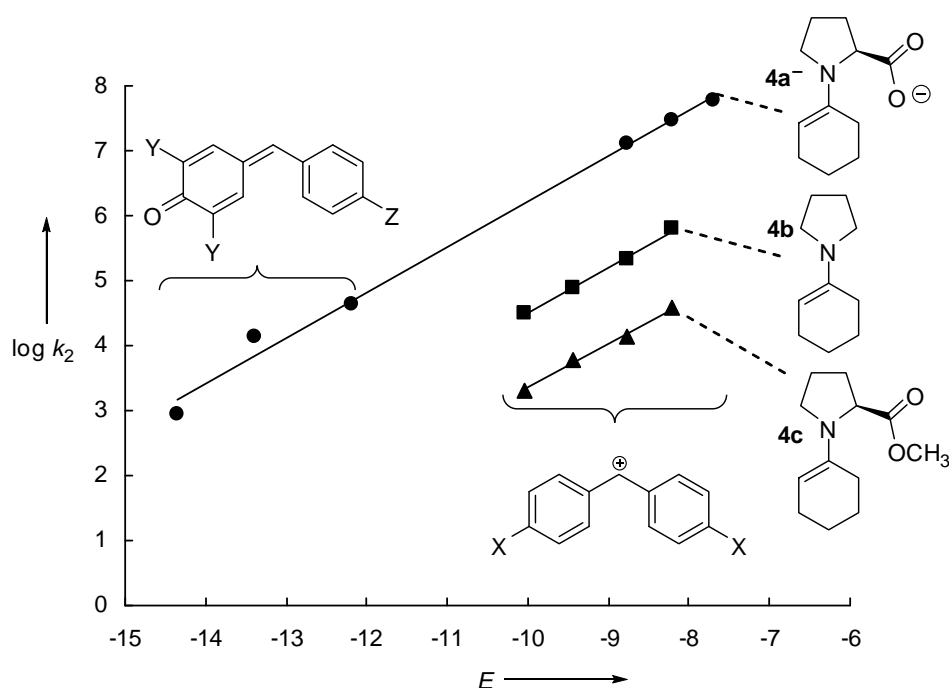
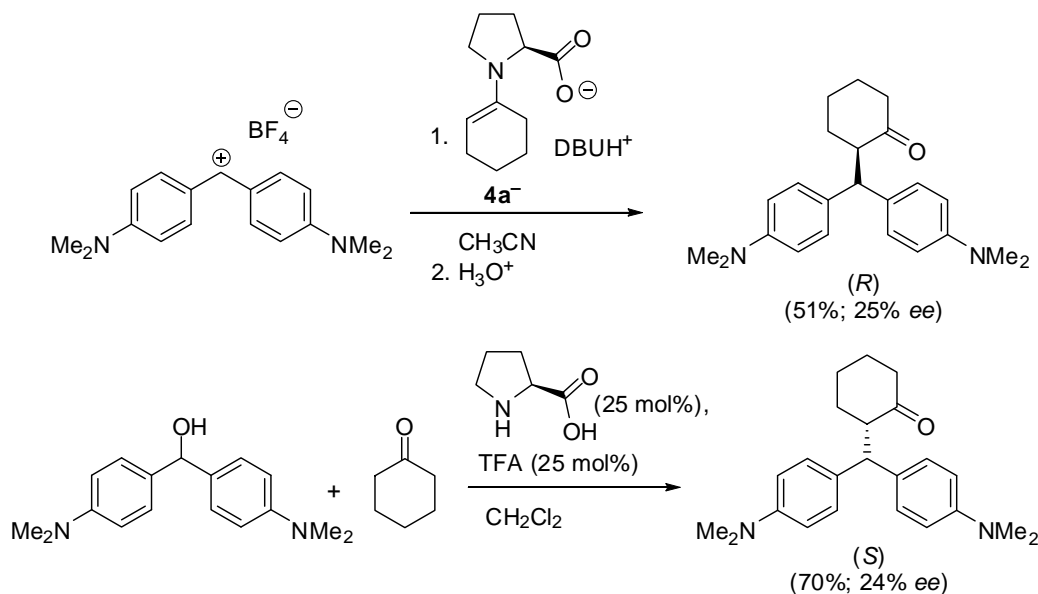


Figure 0.8. Plots of $\log k_2$ for the reactions of the enamines **4** with reference electrophiles (for detailed structures see Table 5.1 in Chapter 5) at 20 °C in acetonitrile versus their electrophilicity parameters E .

The considerably higher reactivity of the enamine carboxylate **4a⁻** reflects anchimeric assistance of the electrophilic attack by the carboxylate group. The high reactivity of the enamino carboxylate **4a⁻** and the reversed stereochemistry of the product of the reaction of 4,4'-bis(dimethylamino)benzhydrylium tetrafluoroborate with the enamino carboxylate **4a⁻**, in comparison to the proline catalyzed reaction of cyclohexanone with 4,4'-bis(dimethylamino)-benzhydrol (Scheme 0.4) supports Blackmond's and Armstrong's suggestion of an attack of

the electrophiles on the *s-trans* isomer of the enamine carboxylate **4a⁻** in proline catalyzed reactions in the presence of base (Figure 0.9).



Scheme 0.4. Stereoselectivities of the reactions of 4,4'-bis(dimethylamino)benzhydrylium tetrafluoroborate with the enamino carboxylate **4a⁻** and the proline catalyzed reaction of cyclohexanone with 4,4'-bis(dimethylamino)benzhydrol.

Nevertheless, the low stereoselectivities of these reactions indicate that there is no clear preference for the *s-cis* or the *s-trans* conformation of the enamine (Figure 0.9).

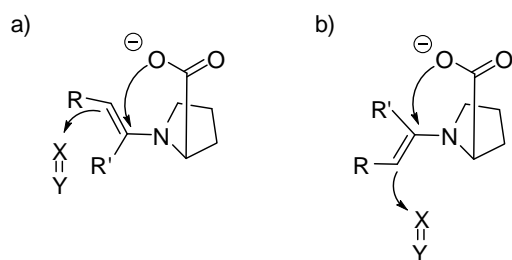


Figure 0.9. Transition state models of the proline-catalyzed reactions of carbonyl compounds with electrophiles: a) anti addition of the electrophiles to the *s-trans* isomer of the enamine; b) anti addition of the electrophiles to the *s-cis* isomer of the enamine.

While the increased reactivity of **4a⁻** (compared with **4b**) toward benzhydrylium ions can partially be due to Coulombic attraction, the 100 times faster reaction of β -nitrostyrene with **4a⁻** than with **4b** can fully be assigned to anchimeric assistance of the carboxylate group. The observation that di-*t*-butyl azodicarboxylate reacts only six times faster with the enamine carboxylate **4a⁻** than with the unsubstituted pyrrolidinocyclohexene **4b** indicates that the magnitude of anchimeric assistance is strongly dependent on the nature of the electrophiles.

Chapter 1

INTRODUCTION AND OBJECTIVES

In the 1930s, electron-deficient and electron-rich species were defined as ‘electrophiles’ and ‘nucleophiles’, respectively, by Ingold.^[1] Since then it has been a goal for organic chemists to quantify electrophilicity and nucleophilicity as general concepts. Swain and Scott were the first to find a constant order of reactivity for different nucleophilic reagents toward different substrates in S_N2 reactions.^[2] Later, Ritchie discovered that the rates of the reactions of diazonium ions and stabilized carbocations with various *n*-nucleophiles can be described by a constant selectivity relationship (1.1).^[3] The relative reactivities of nucleophiles do not depend on the absolute reactivities of the electrophiles. Ritchie constructed a nucleophilicity scale, covering a range of about 13 orders of magnitude, which allowed to calculate reaction rates from only one parameter for electrophiles (log *k*₀) and one for nucleophiles (*N*₊).

$$\log (k/k_0) = N_+ \quad (1.1)$$

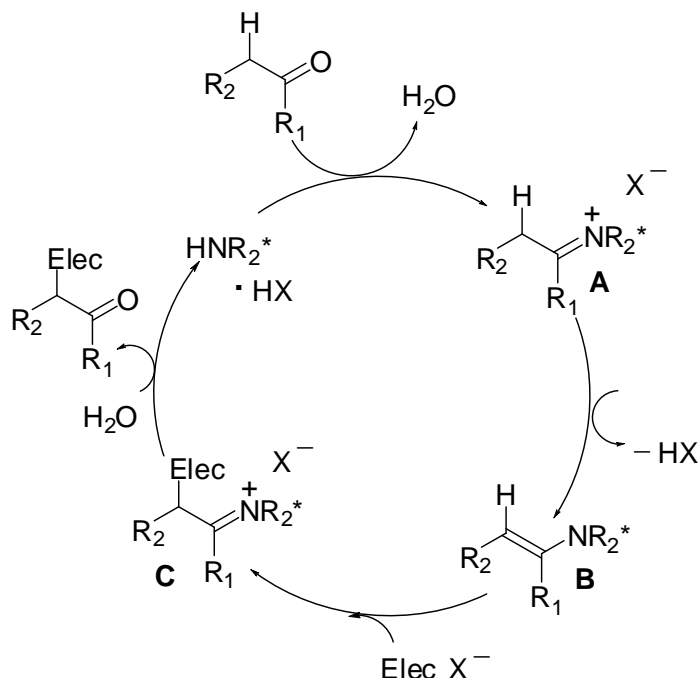
Later it turned out, that Equation (1.1) is not strictly valid and that better correlations are obtained when different classes of electrophiles are treated separately.^[4]

In 1994, Mayr and Patz introduced the three parameter linear free-energy relationship (1.2), where nucleophiles are described by a nucleophilicity parameter *N* and a nucleophile-specific sensitivity parameter *s*, and electrophiles are described by an electrophilicity parameter *E*.^[5]

$$\log k(20\text{ }^\circ\text{C}) = s(N+E) \quad (1.2)$$

Benzhydrylium ions and structurally related quinone methides were chosen as reference electrophiles, as the steric surroundings at the reaction centers can be kept constant while the reactivity can widely be varied by introducing different substituents in meta and para position of the aromatic rings.^[6] With Equation (1.2) reactivity scales, presently including 569 nucleophiles and 145 electrophiles, have been constructed.

After realizing the potential of the first proline-catalyzed enantioselective intramolecular aldol reaction, known as the Hajos-Parrish-Eder-Sauer-Wiechert reaction,^[7] enamine activated reactions have become an important method for enantioselective α -functionalizations of carbonyl compounds (Scheme 1.1).^[7,8]



Scheme 1.1. Catalytic cycle of secondary amine catalyzed reactions of aldehydes and ketones with electrophiles.

In enamine catalysis, an iminium ion **A** is formed by the reversible reaction of the catalyst, a secondary amine with a carbonyl compound, which is transformed into the enamine **B** by removing the α -proton. Subsequent addition of the electrophile leads to a second iminium ion **C**, which regenerates the amine catalyst and liberates the α -functionalized carbonyl compound by hydrolysis (Scheme 1.1).

In order to get insight in the mechanism and the scope of enamine activated reactions, we were interested in the rates of the key-steps of the reaction cascade of Scheme 1.1 by quantifying the reactivity of substrates and intermediates of such reactions. Equation (1.2) should provide access to these data as it was shown to be applicable for many nucleophile-electrophile combination reactions.^[6,9]

Proline-catalyzed α -functionalizations of carbonyl compounds are considered to proceed either via the neutral^[10] or anionic^[11] enamine intermediates derived from proline and a carbonyl compound. Studying the kinetics of the reactions of enamines derived from

prolinate-, pyrrolidine-, and proline methyl ester and cyclohexanone with electrophiles seemed to be appropriate to elucidate the mechanism of proline-catalyzed reactions.

Azodicarboxylates are commonly used as electrophiles in organocatalytic α -aminations of carbonyl compounds.^[8,12] The knowledge of their electrophilic reactivities seemed to be of importance to locate the reactivity range of appropriate electrophiles in enamine activated reactions, as they should react fast with the enamine intermediates but not with the enols, which are formed from carbonyl compounds as tautomers.

In view of the great synthetic potential of 1,2-diaza-1,3-butadienes which has been demonstrated by Attanasi^[13] these compounds were considered as possible substrates in enamine activated reactions. Reactivity parameters for these electrophiles should provide a quantitative basis for the rational planning of (enantioselective) synthetic strategies.

Nucleophilic reactivities of secondary amines, catalysts in enamine activated reactions, in acetonitrile are of great importance in order to study and evaluate the reactions of azodicarboxylates and 1,2-diaza-1,3-butadienes with secondary amines in this solvent as acetonitrile is a commonly used solvent in organocatalytic reactions.

As all of the parts of this thesis have already been published, accepted or submitted for publication, individual introductions will be given at the beginning of each chapter.

References

- [1] a) C. K. Ingold, *Recl. Trav. Chim. Pays-Bas* **1929**, *42*, 797–812. b) C. K. Ingold, *J. Am. Chem. Soc.* **1933**, 1120–1127. c) C. K. Ingold, *Chem. Rev.* **1934**, *15*, 225–274.
- [2] C. G. Swain, C. B. Scott, *J. Am. Chem. Soc.* **1953**, *75*, 141–147.
- [3] a) C. D. Ritchie, *Acc. Chem. Res.* **1972**, *5*, 348–354. b) C. D. Ritchie, J. E. van Verth, P. O. I. Virtanen, *J. Am. Chem. Soc.* **1982**, *104*, 3491–3497. c) C. D. Ritchie, *J. Am. Chem. Soc.* **1984**, *106*, 7187–7194.
- [4] C. D. Ritchie, *Can. J. Chem.* **1986**, *64*, 2239–2250.
- [5] H. Mayr, M. Patz, *Angew. Chem.* **1994**, *106*, 990-1010; *Angew. Chem. Int. Ed.* **1994**, *33*, 938–955.
- [6] H. Mayr, T. Bug, M. F. Gotta, N. Hering, B. Irrgang, B. Janker, B. Kempf, R. Loos, A. R. Ofial, G. Remennikov, H. Schimmel, *J. Am. Chem. Soc.* **2001**, *123*, 9500–9512.

- [7] a) U. Eder, G. Sauer, R. Wiechert, *Angew. Chem.* **1971**, 83, 492–493; *Angew. Chem. Int. Ed. Engl.* **1971**, 10, 496–497. b) Z. G. Hajos, D. R. Parrish, *J. Org. Chem.* **1974**, 39, 1615–1621.
- [8] a) B. List, *Acc. Chem. Res.* **2004**, 37, 548–557. b) A. Berkessel, H. Gröger, *Asymmetric Organocatalysis*, Wiley-VCH, Weinheim, **2005**. c) *Enantioselective Organocatalysis* (Ed.: P. I. Dalko), Wiley-VCH, Weinheim, **2007**. d) S. Mukherjee, J. W. Yang, S. Hoffman, B. List, *Chem. Rev.* **2007**, 107, 5471–5569. e) D. W. C. McMillan, *Nature* **2008**, 455, 304–308.
- [9] a) H. Mayr, B. Kempf, A. R. Ofial, *Acc. Chem. Res.* **2003**, 36, 66–77. b) H. Mayr, A. R. Ofial, *Pure Appl. Chem.* **2005**, 77, 1807–1821.
- [10] a) B. List, R. A. Lerner, C. F. Barbas III, *J. Am. Chem. Soc.* **2000**, 122, 2395–2396. b) S. Bahmanyar, K. N. Houk, *J. Am. Chem. Soc.* **2001**, 123, 12911–12912. c) L. Hoang, S. Bahmanyar, K. N. Houk, B. List, *J. Am. Chem. Soc.* **2003**, 125, 16–17. d) S. Bahmanyar, K. N. Houk, H. J. Martin, B. List, *J. Am. Chem. Soc.* **2003**, 125, 2475–2479. e) F. R. Clemente, K. N. Houk, *Angew. Chem.* **2004**, 116, 5890–5892; *Angew. Chem. Int. Ed.* **2004**, 43, 5766–5768. f) P. H.-Y. Cheong, K. N. Houk, *J. Am. Chem. Soc.* **2004**, 126, 13912–13913. g) B. List, L. Hoang, H. J. Martin, *Proc. Nat. Acad. Sci. U.S.A.* **2004**, 101, 5839–5842. h) C. Allemann, R. Gordillo, F. R. Clemente, P. H.-Y. Cheong, K. N. Houk, *Acc. Chem. Res.* **2004**, 37, 558–569. i) P. H.-Y. Cheong, K. N. Houk, *Synthesis* **2005**, 9, 1533–1537. j) F. R. Clemente, K. N. Houk, *J. Am. Chem. Soc.* **2005**, 127, 11294–11302. k) B. List, *Chem. Commun.* **2006**, 819–824. l) S. Mukherjee, J. W. Yang, S. Hoffmann, B. List, *Chem. Rev.* **2007**, 107, 5471–5569.
- [11] a) D. Seebach, A. K. Beck, D. M. Badine, M. Limbach, A. Eschenmoser, A. M. Treasurywala, R. Hobi, W. Prikoszovich, B. Lindner, *Helv. Chim. Acta* **2007**, 90, 425–471. b) D. G. Blackmond, A. Moran, M. Hughes, A. Armstrong, *J. Am. Chem. Soc.* **2010**, 132, 7598–7599.
- [12] a) B. List, *J. Am. Chem. Soc.* **2002**, 124, 5656–5657; b) A. Bøgevig, K. Juhl, N. Kumaragurubaran, W. Zhuang, K. A. Jørgensen, *Angew. Chem.* **2002**, 114, 1868–1871, *Angew. Chem. Int. Ed.* **2002**, 41, 1790–1793.
- [13] Reviews: a) O. A. Attanasi, *Org. Prep. Proced. Int.* **1986**, 299–327; b) O. A. Attanasi, P. Filippone, *Synlett* **1997**, 1128–1140; c) O. A. Attanasi, L. De Crescentini, P. Filippone, F. Mantellini, S. Santeusanio, *Arkivoc* **2002**, xi, 274–292; d) O. A. Attanasi, L. De Crescentini, G. Favi, P. Filippone, F. Mantellini, F. R. Perrulli, S. Santeusanio, *Eur. J. Org. Chem.* **2009**, 3109–3127.

Chapter 2

NUCLEOPHILIC REACTIVITIES OF PRIMARY AND SECONDARY AMINES IN ACETONITRILE

Tanja Kanzian, Tobias A. Nigst, Andreas Maier, Stefan Pichl, and Herbert Mayr in *Eur. J. Org. Chem.* **2009**, 6379–6385.

The results obtained by T. A. Nigst are not listed in the Experimental Section.

2.1 Introduction

Amines belong to the most important reagents in organic synthesis, and numerous kinetic investigations have been performed to determine their nucleophilic reactivities in various types of reactions.^[1] They have been characterized on the Swain-Scott n scale as well as on the Ritchie N_+ scale.^[1d,2]

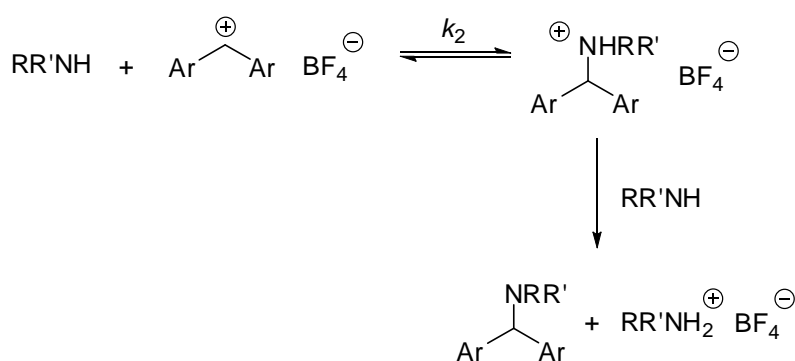
Recently, we have employed Equation (2.1), which characterizes nucleophiles a by the parameters N and s , and electrophiles are characterized by the parameter E ,^[3] for determining N and s of a variety of amines in aqueous solution.^[4] In this way it became possible to add amines to our comprehensive nucleophilicity scale, which includes n -, π -, and σ -nucleophiles.^[5] Comparison with the few available data in DMSO^[4a,6] and methanol^[7] showed that amine nucleophilicities are strongly dependent on the solvent, in contrast to the behavior of most neutral π - and σ -nucleophiles.

$$\log k_2(20\text{ }^\circ\text{C}) = s(N + E) \quad (2.1)$$

Systematic investigations of the nucleophilic reactivities of amines in acetonitrile have so far not been reported. Such data are of eminent importance for two reasons. (1) Acetonitrile is an ideal solvent for exploring the combat zone of nucleophilic aliphatic substitutions, i.e. the zone where the change from S_N1 to S_N2 mechanisms occurs.^[6,8] (2) Acetonitrile is the solvent of choice for the photoheterolytic cleavage of carbocation precursors.^[9] By using nanosecond-laser pulses, it is possible to generate carbocations in acetonitrile in the presence of various

nucleophiles and to determine rates of reactions along the borderline between activation and diffusion control, typically second-order rate constants from 10^8 to $10^{10} \text{ M}^{-1}\text{s}^{-1}$.^[10]

Knowledge of rate constants along this borderline is crucial for the understanding of structure-reactivity relationships, e.g., correlations between reactivity and selectivity as well as the breakdown of linear free energy relationships.^[11] Because many of these investigations involve reactions with amines in acetonitrile,^[9a,b] we have now determined the *N* and *s* parameters of primary and secondary amines using benzhydryl cations (Table 2.1) as reference electrophiles as described previously (Scheme 2.1).^[5a]



Scheme 2.1. Reactions of amines with benzhydrylium ions.

2.2 Results and Discussion

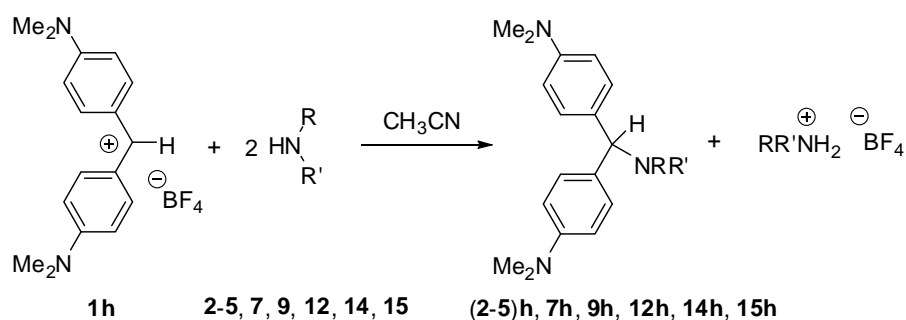
2.2.1 Product Characterization

A combination of the benzhydrylium salt **1h**-BF₄ with 2–3 equivalents of the amines **2**, **3**, **4**, **5**, **7**, **9**, **12**, **14**, and **15** in acetonitrile gave the corresponding benzhydrylamines **2h**, **3h**, **4h**, **5h**, **7h**, **9h**, **12h**, **14h**, and **15h** respectively (Scheme 2.2). The chemical shifts of the Ar₂CH-protons and the isolated yields are listed in Table 2.2.

Table 2.1. List of reference electrophiles used in this study.

reference electrophile ^[a]	$E^{\dagger[b]}$
	ani(<i>t</i> -Bu) ₂ QM (1a) -16.11
	tol(<i>t</i> -Bu) ₂ QM (1b) -15.83
	ani(Ph) ₂ QM (1c) -12.18
	(lil) ₂ CH ⁺ (1d) -10.04
	(jul) ₂ CH ⁺ (1e) -9.45
	(ind) ₂ CH ⁺ (1f) -8.76
	(pyr) ₂ CH ⁺ (1g) -7.69
	(dma) ₂ CH ⁺ (1h) -7.02
	(mpa) ₂ CH ⁺ (1i) -5.89
	(mfa) ₂ CH ⁺ (1j) -3.85
	(ani) ₂ CH ⁺ (1k) 0.00
	(ani)(tol)CH ⁺ (1l) 1.48
	(tol) ₂ CH ⁺ (1m) 3.63
	Ph(tol)CH ⁺ (1n) 4.59
	Ph ₂ CH ⁺ (1o) 5.90

[a] Counterion of the benzhydryl cations: BF₄⁻. [b] Electrophilicity parameters E were taken from refs. [5a,b].



Scheme 2.2. Reactions of amines with 4,4'-bis(dimethylamino)-benzhydrylium tetrafluoroborate **1h**-BF₄.

Table 2.2. ¹H-NMR chemical shifts of the Ar₂CH group of the products of the reactions of **1h** with **2-5, 7, 9, 12, 14**, and **15** and yields of the isolated products.

amine	product	δ_{H} / ppm	yield / %
2,2,2-trifluoroethylamine (2)	2h	4.80	85
<i>tert</i> -butylamine (3)	3h	4.88	98
isopropylamine (4)	4h	4.81	90
ethanolamine (5)	5h	4.69	98
allylamine (7)	7h	4.70	97
<i>n</i> -butylamine (9)	9h	4.65	95
diethylamine (12)	12h	4.50	45
piperidine (14)	14h	3.99	71
pyrrolidine (15)	15h	3.97	67

2.2.2 Kinetics of the Reactions of the Amines 2-15 with the Reference Electrophiles 1

The rates of the reactions of amines with the reference electrophiles **1a-j** were determined photometrically in CH₃CN at 20 °C. For the kinetic studies, the amines **2-15** were used in large excess (> 10 equiv.) over the electrophiles **1** to ensure first-order conditions. Details are given in the Experimental Section (Chapter 2.4). The first-order rate constants k_{obs} were obtained from the exponential decays of the absorbances of the electrophiles (Figure 2.1).

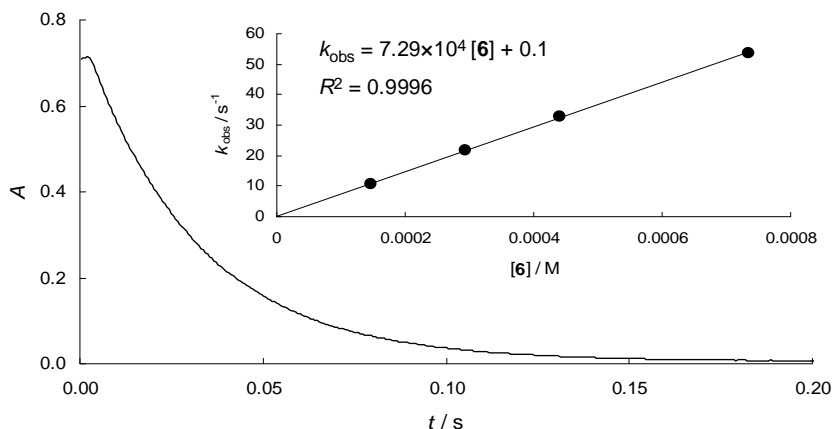


Figure 2.1. Exponential decay of the absorbance at 613 nm during the reaction of **1h** with benzylamine ($[\mathbf{6}] = 4.42 \times 10^{-4} \text{ M}$; $k_{\text{obs}} = 32.7 \text{ s}^{-1}$). Insert: Determination of the second-order rate constant k_2 ($7.29 \times 10^4 \text{ M}^{-1} \text{ s}^{-1}$) as the slope of the correlation of the first-order rate constants k_{obs} with the concentration of the amine **6**.

Plots of k_{obs} versus the amine concentrations were linear for the reactions of the primary and secondary amines **2–15** with all benzhydrylium ions **1d–o** (insert of Figure 2.1) and for the reactions of the primary amines **2–9** with the quinone methides **1a–c**. In these reactions the attack of the amines at the electrophiles is rate limiting, and the slopes of these plots gave the second-order rate constants k_2 [Equation (2.2)], which are listed in Table 2.3.

$$k_{\text{obs}} = k_2 [\text{amine}] \quad (2.2)$$

In the case of trifluoroethylamine (**2**) and *N,N*-bis(2-methoxyethyl)amine (**10**) the reactions with benzhydrylium ions of low reactivity become reversible, which is reflected by the positive intercepts in the plots of k_{obs} versus the amine concentrations.

Table 2.3. Second-order rate constants for the reactions of the reference electrophiles **1** with the amines **2-15** in acetonitrile at 20 °C.


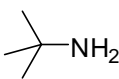
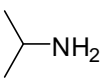
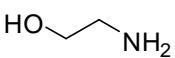
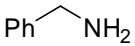
Amine	<i>N</i>	<i>s</i>	Electrophile	$k_2 / \text{M}^{-1}\text{s}^{-1}$	
	2	10.13	0.75	1h	1.43×10^2
				1i	2.53×10^3
				1j	4.03×10^4
				1k	3.50×10^7 [a]
				1l	1.50×10^8 [a,b]
				1m	8.50×10^8 [a,b]
				1n	1.70×10^9 [a,b]
				1o	2.00×10^9 [a,b]
	3	12.35	0.72	1c	1.52
				1d	4.15×10^1
				1f	3.34×10^2
				1i	5.13×10^4
	4	13.77	0.70	1c	1.56×10^1
				1d	2.97×10^2
				1f	2.43×10^3
				1g	2.13×10^4
				1h	5.24×10^4
	5	14.11	0.71	1c	2.71×10^1
				1d	5.85×10^2
				1f	4.94×10^3
				1g	4.24×10^4
				1h	1.02×10^5
	6	14.29	0.67	1b	1.10×10^{-1}
				1c	2.06×10^1
				1d	6.53×10^2
				1f	4.61×10^3
				1g	3.48×10^4
				1h	7.29×10^4

Table 2.3 continued.

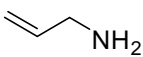
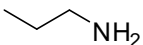
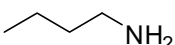
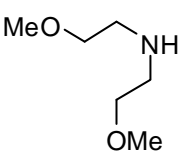
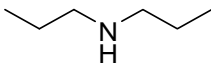
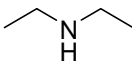
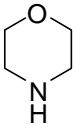
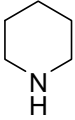
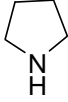
Amine	<i>N</i>	<i>s</i>	Electrophile	$k_2 / \text{M}^{-1}\text{s}^{-1}$	
	7	14.37	0.66	1b	1.25×10^{-1}
				1d	5.09×10^2
				1f	4.32×10^3
				1g	3.64×10^4
				1h	8.61×10^4
	8	15.11	0.63	1a	2.64×10^{-1}
				1b	3.82×10^{-1}
				1c	5.46×10^1
				1d	1.38×10^3
				1e	3.87×10^3
				1f	7.54×10^3
				1g	6.77×10^4
				1h	1.43×10^5
				1k	1.00×10^9 [a,b]
				1l	2.30×10^9 [a,b]
				1m	4.10×10^9 [a,b]
1n	4.40×10^9 [a,b]				
1o	4.50×10^9 [a,b]				
	9	15.27	0.63	1a	3.41×10^{-1}
				1c	7.49×10^1
				1f	1.03×10^4
				1h	2.12×10^5
	10	13.24	0.93	1c	7.89 [b,c]
				1d	1.12×10^3
				1e	4.47×10^3
				1f	1.25×10^4
				1g	1.17×10^5

Table 2.3 continued.

Amine	<i>N</i>	<i>s</i>	Electrophile	$k_2 / \text{M}^{-1}\text{s}^{-1}$	
	11	14.51	0.80	1c	$6.74 \times 10^{1[\text{c}]}$
				1d	3.95×10^3
				1e	1.38×10^4
				1f	3.17×10^4
				1g	2.77×10^5
	12	15.10	0.73	1c	$1.51 \times 10^{2[\text{c}]}$
				1d	4.62×10^3
				1e	1.29×10^4
				1f	3.49×10^4
				1g	3.24×10^5
	13	15.65	0.74	1b	$2.03 \times 10^{-1[\text{b,c}]}$
				1c	$3.85 \times 10^{2[\text{c}]}$
				1d	1.15×10^4
				1e	4.11×10^4
				1f	1.04×10^5
				1g	8.03×10^5
	14	17.35	0.68	1a	$6.04^{[\text{c}]}$
				1b	$1.23 \times 10^{1[\text{c}]}$
				1c	3.52×10^3
				1d	7.85×10^4
				1e	2.69×10^5
	15	18.64	0.60	1a	3.25×10^1
				1b	4.82×10^1
				1d	1.18×10^5
				1e	3.50×10^5

[a] Second-order rate constants k_2 from ref. [9b]. [b] Not included for the determination of the *N* and *s* parameters. [c] k_2 was derived from Equation (2.7) and is less precise.

For the reactions of the secondary amines **10-12** with the quinone methide **1c** (**1a** and **1b** were not studied), of morpholine (**13**) with the quinone methides **1b** and **1c**, and of piperidine (**14**)

with the quinone methides **1a** and **1b**, the plots of k_{obs} versus amine concentrations are not linear (Figure 2.2).

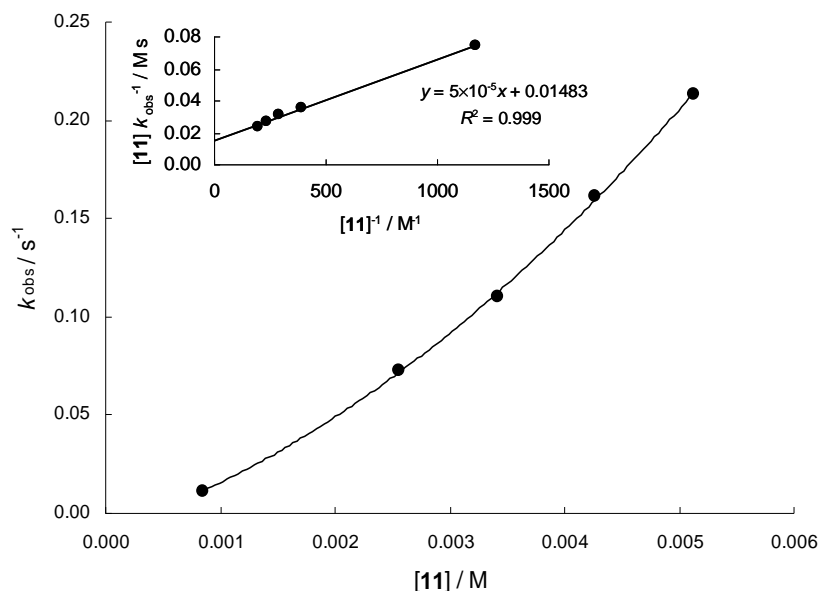
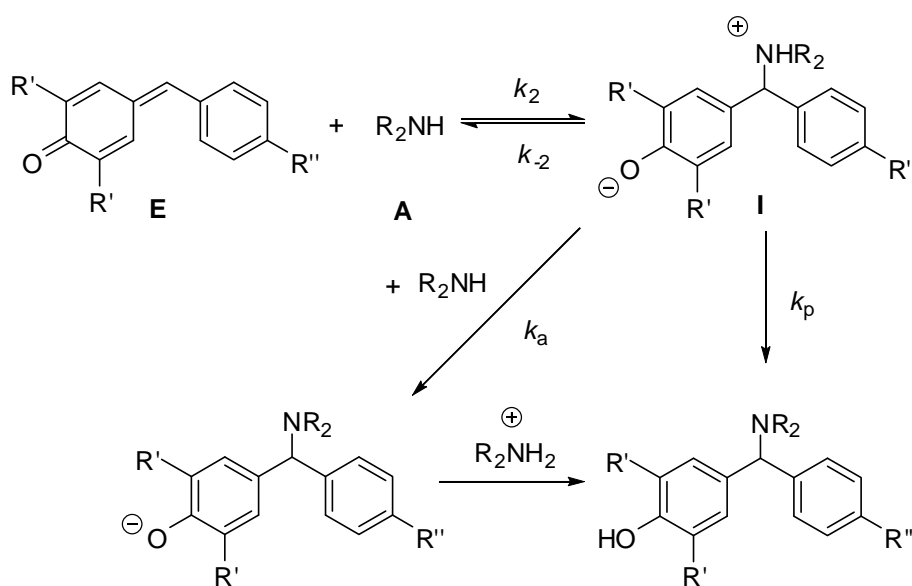


Figure 2.2. Plots of k_{obs} vs. **[11]** and $[11]/k_{\text{obs}}$ vs. $1/[\mathbf{11}]$ (insert) for the reaction of **11** with the quinone methide **1c**. The k_2 value for that reaction is $1/(0.0148 \text{ M s}) = 67.4 \text{ M}^{-1}\text{s}^{-1}$.

The upward curvature in the plots of k_{obs} versus amine concentration indicate that a second molecule of the amine is involved in the reaction as a base catalyst (Scheme 2.3).



Scheme 2.3. Reactions of secondary amines with quinone methides.

Analogous behavior has been reported for the reactions of secondary amines with thiocarbonates,^[12] thionobenzoates,^[13] and activated esters of indole-3-acetic acid.^[14] The change of the concentration of the zwitterionic intermediate **I** can be expressed by Equation (2.3).

$$d[\mathbf{I}]/dt = k_2[\mathbf{E}][\mathbf{A}] - k_{-2}[\mathbf{I}] - k_a[\mathbf{I}][\mathbf{A}] - k_p[\mathbf{I}] \quad (2.3)$$

With the assumption of a steady state concentration for the intermediate **I**, the rate law can be expressed by Equations (2.4) and (2.5).

$$-d[\mathbf{E}]/dt = k_2[\mathbf{E}][\mathbf{A}] (k_a[\mathbf{A}] + k_p)/(k_{-2} + k_a[\mathbf{A}] + k_p) \quad (2.4)$$

$$k_{\text{obs}} = k_2[\mathbf{A}] (k_a[\mathbf{A}] + k_p)/(k_{-2} + k_a[\mathbf{A}] + k_p) \quad (2.5)$$

Let us first neglect the direct proton-transfer from NH^+ to O^- in the zwitterionic intermediate **I**. Equation (2.5) is then reduced to Equation (2.6) which can be transformed into Equation (2.7).

$$k_{\text{obs}} = k_2[\mathbf{A}]^2 k_a/(k_{-2} + k_a[\mathbf{A}]) \quad (2.6)$$

$$[\mathbf{A}]/k_{\text{obs}} = 1/k_2 + k_{-2}/k_2[\mathbf{A}] k_a \quad (2.7)$$

The linear plot of $[\mathbf{A}]/k_{\text{obs}}$ against $1/[\mathbf{A}]$, as depicted in the insert of Figure 2.2, shows that this formalism holds for a wide range of concentrations. As shown in the Experimental Section (Chapter 2.4), deviations from these linear plots occur only at very low amine concentrations and are explained by the operation of k_p . If the k_{obs} values at very low amine concentrations are neglected, the k_2 values can be obtained from the intercepts ($1/k_2$) of the linear correlations [see insert of Figure 2.2 and Equation (2.7)]. If $k_{-2} \ll k_a[\mathbf{A}]$, Equation (2.6) is transformed to Equation (2.2), that is, a second-order reaction with rate-determining formation of the CN bond. Although this situation holds for all reactions with benzhydrylium ions, linearity between k_{obs} and [amine] was never reached, for reactions of the quinone methide **1a** with **14**, **1b** with **13** and **1c** with **10-14**, even when very high amine concentrations were used. The second-order rate constants k_2 are listed in Table 2.3.

When the logarithms of the second-order rate constants are plotted against the previously reported electrophilicity parameters E of the reference systems, linear correlations are obtained (Figure 2.3) which yield the nucleophile-specific parameters N and s that are listed

in Table 2.3. The rate constants for the reactions of trifluoroethylamine (**2**) with **1l–o** and for the reactions of *n*-propylamine (**8**) with **1k–o**^[9b] were not included for the determination of the nucleophilicity parameters, because these reactions are close to diffusion control. As the *s*-parameters of the amines differ only slightly, their relative nucleophilicities are almost independent of the nature of the electrophiles, and the reactivities of the amines can be compared by only regarding their *N*-parameters, which cover the reactivity range of $10 < N < 19$. The less reactive amines react with similar rates as silyl ketene acetals, trialkyl-substituted pyrroles and pyridines, whereas the more reactive amines show a similar nucleophilicity as stabilized carbanions (Figure 2.4).

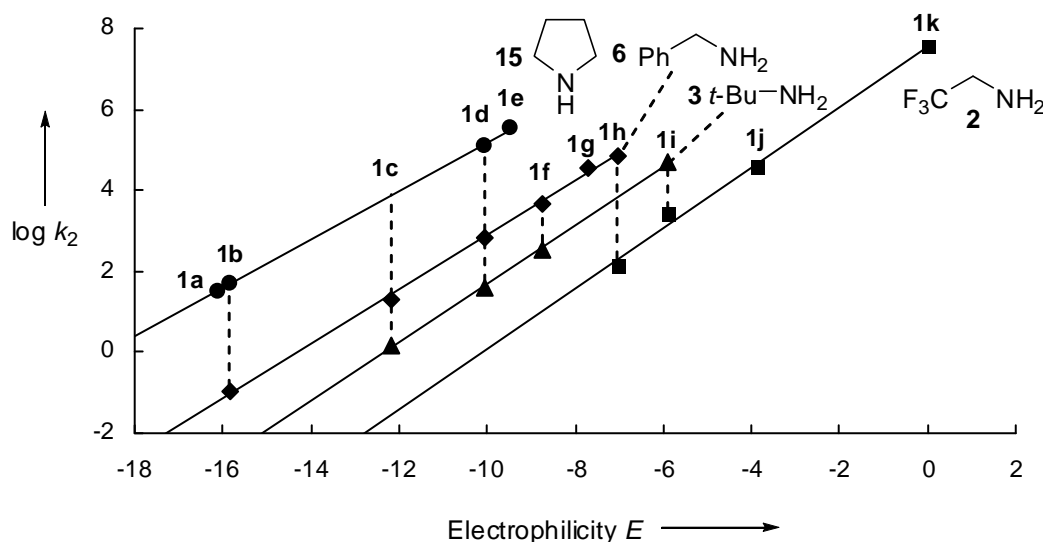


Figure 2.3. Plots of the second-order rate constants $\log k_2$ (20 °C) in CH_3CN against the *E*-parameters of the reference electrophiles for the reactions of **2**, **3**, **6**, and **15** with benzhydrylium ions and quinone methides.

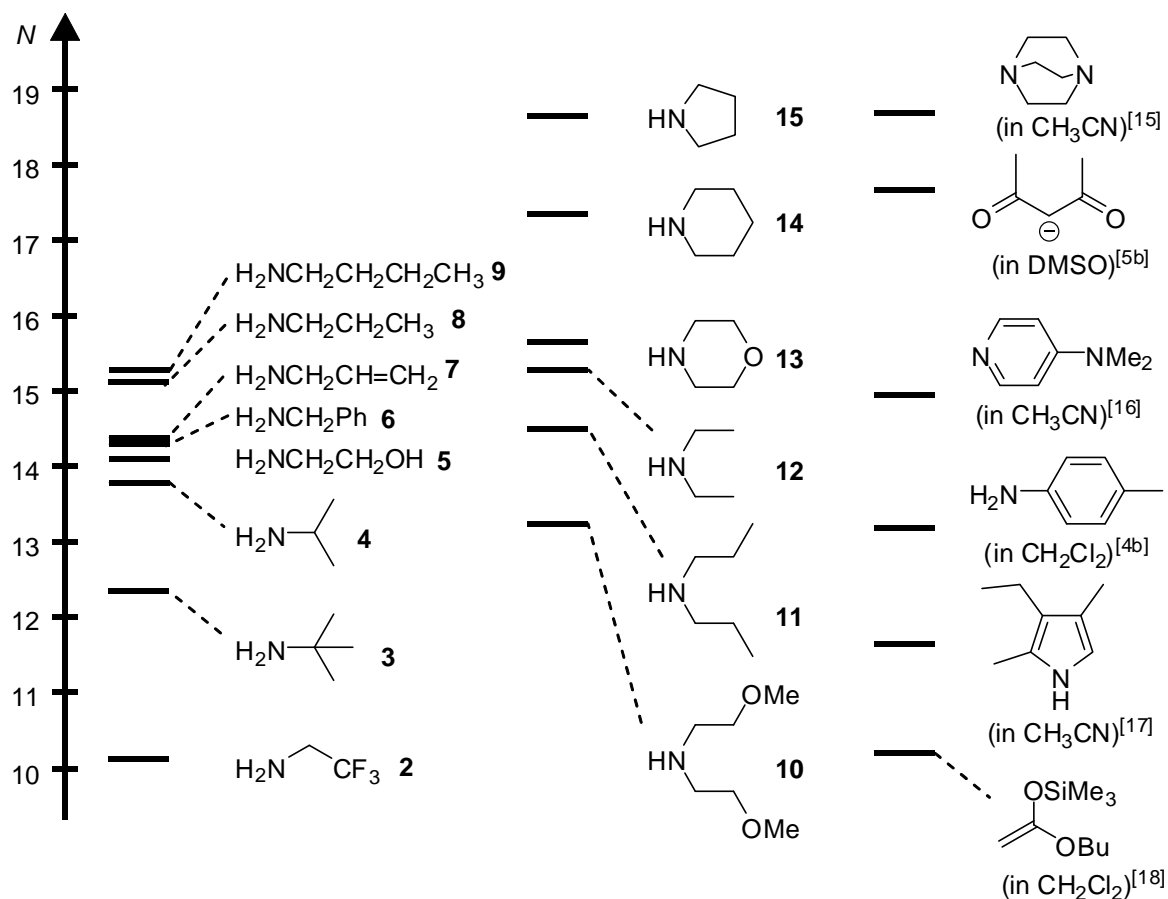


Figure 2.4. Comparison of the nucleophilic reactivities of amines in acetonitrile with other nucleophiles.

Figure 2.5 shows that the nucleophilic reactivities of the amines correlate only poorly with the corresponding $\text{p}K_{\text{aH}}$ values in acetonitrile.^[19] As previously reported for the reactions of amines in water^[4b], it is thus not possible to predict the nucleophilic reactivities of amines in CH_3CN on the basis of their $\text{p}K_{\text{aH}}$ values.

In previous work we reported that aniline is approximately 5 times more nucleophilic in water than propylamine^[4b] despite the considerably higher basicity ($\text{p}K_{\text{aH}}$) of the aliphatic amine. We now find that in CH_3CN the reactivity order is reversed and primary and secondary alkylamines are more nucleophilic than aniline ($N = 12.64$, $s = 0.68$)^[4b].

This reversal of the relative reactivities is due to the different solvent effects on the reactivities of aromatic and aliphatic amines. Whereas aniline and *p*-toluidine have similar nucleophilicities in water and acetonitrile (for aniline + **1h**: $k_{\text{CH}_3\text{CN}}/k_{\text{H}_2\text{O}} = 0.42$), alkylamines are typically one to two orders of magnitude more reactive in acetonitrile than in water (for propylamine + **1h**: $k_{\text{CH}_3\text{CN}}/k_{\text{H}_2\text{O}} = 46$).

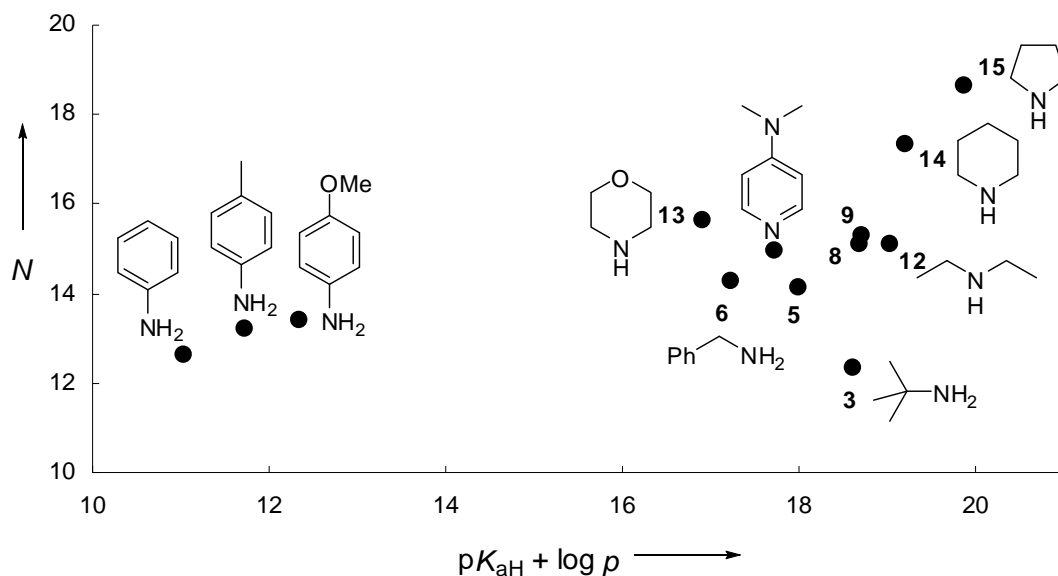


Figure 2.5. Plot of the N parameters of amines in acetonitrile versus the statistically corrected basicities in acetonitrile ($p =$ numbers of protons of the conjugated acid).^[4b,19]

Thus, although the nucleophilicity order alkylamines $>$ aniline in acetonitrile is the same as that of the relative basicities (pK_{aH}), the correlation in Figure 2.5 shows that also in acetonitrile anilines are considerably more reactive than expected on the basis of their basicities. In other words, the previously reported surprisingly high nucleophilicities of anilines are not a water-specific phenomenon.

In previous work, we have already mentioned that the reliability of Equation (2.1) to predict rate constants for the additions of amines to various Michael acceptors is limited because of variable stabilizing interactions between the NH protons and the different basic sites in the Michael acceptors.^[20] Although Figure 2.3 demonstrates^[20] that the reactivities of amines towards benzhydrylium ions and quinone methides correlate excellently with their electrophilicity parameters E , which have been derived from their reactivities towards C-nucleophiles, significant deviations are found by applying Equation (2.1) to additions of amines to other types of Michael acceptors in CH_3CN . In Chapter 2.4.2 (page 63) in the Experimental Section it is shown that in several cases the calculated rate constants deviate by more than a factor of 10^2 (the common confidence limit of Equation (2.1) from the experimental values). It is presently not clear whether these unusually high deviations are due to variable interactions of the NH protons with the basic sites of the Michael acceptors or whether the reactions under concern require a specific treatment of solvent effects.

2.3 Conclusion

The reactions of primary and secondary amines with benzhydrylium ions **1d–o** and of primary amines with quinone methides **1a–c** in acetonitrile follow a second-order rate law, which indicates rate-determining attack of the amines on the electrophiles. In contrast, for most of the reactions of the secondary amines **10–15** with the quinone methides **1a–c** the initial electrophile-nucleophile combination step is reversible and the more complicated rate law (2.6) has to be employed to derive the rate constants k_2 for the attack of the amines at the electrophiles. From the linear correlations of $\log k_2$ with the electrophilicity parameters E of the benzhydrylium ions, the nucleophile-specific parameters N and s for amines in CH_3CN have been derived. The poor correlation between N and $\text{p}K_{\text{aH}}$ shows that also in acetonitrile, relative basicities cannot be used for predicting relative nucleophilicities. Solvent polarity affects the reactivities of alkylamines and anilines quite differently: Whereas anilines react approximately two times faster with benzhydrylium ions in water than in acetonitrile, primary alkylamines react at least 10 times faster in acetonitrile than in water. The opposite solvent effect on these closely related reactions demonstrates the limitation of Hughes-Ingold rules^[21] to predict solvent effects on polar organic reactions on the basis of the relative charge dispersal in the ground and transition states.

2.4 Experimental Section

2.4.1 General comment

The benzhydrylium tetrafluoroborates **1**- BF_4 ^[5a] and quinone methides^[22] (see Table 2.1) were synthesized by literature procedures. *n*-propylamine (**8**), bis(2-methoxyethyl)amine (**10**), di-*n*-propylamine (**11**), diethylamine (**12**), morpholine (**13**), piperidine (**14**) and pyrrolidine (**15**) have been purchased and purified by distillation prior to use. ^1H - (400 MHz) and ^{13}C - (100 MHz) spectra were measured on a Varian Inova 400 instrument.

The kinetics of the reactions of the benzhydrylium ions and quinone methides with the amines were followed by UV-Vis spectroscopy in acetonitrile at 20 °C.

For slow reactions ($\tau_{1/2} > 10$ s) the UV-Vis spectra were collected at different times by a J&M TIDAS diode array spectrophotometer connected to a Hellma 661.502-QX quartz Suprasil immersion probe (5 mm light path) by fiber optic cables with standard SMA connectors. All the kinetic measurements were carried out in Schlenk glassware with the exclusion of

moisture. The temperature of the solutions during the kinetic studies was maintained to within ± 0.1 °C by using circulating bath cryostats and monitored with thermocouple probes that were inserted into the reaction mixture.

Stopped-flow spectrophotometer systems (Applied Photophysics SX.18MV-R or Hi-Tech SF-61DX2) were used for the investigation of fast reactions of benzhydrylium ions with nucleophiles ($10 \text{ ms} < \tau_{1/2} < 10 \text{ s}$). The kinetic runs were initiated by mixing equal volumes of acetonitrile solutions of the amines and the benzhydrylium salts.

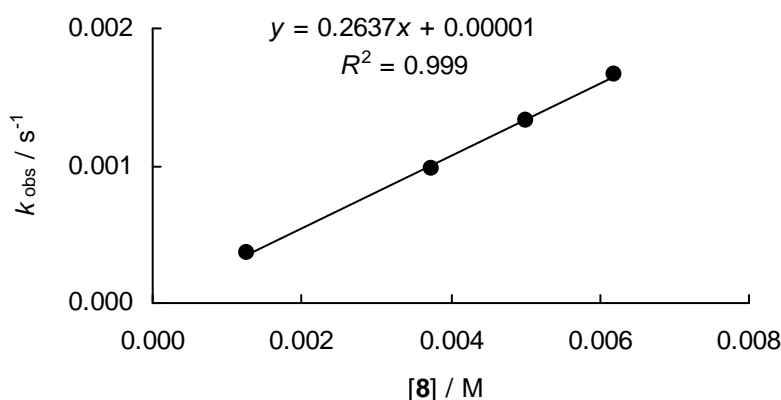
From the exponential decays of the absorbances at λ_{max} of the electrophiles **1**, the first-order rate constants k_{obs} (s^{-1}) were obtained.

2.4.2 Kinetic Experiments

Kinetics of the reactions of benzhydrylium ions and quinone methides (**1**) with *n*-propylamine (**8**)

Rate constants for the reactions of *n*-propylamine (**8**) with ani(*t*-Bu)₂QM (**1a**) in CH₃CN (diode array spectrophotometer, 20 °C, $\lambda = 393 \text{ nm}$).

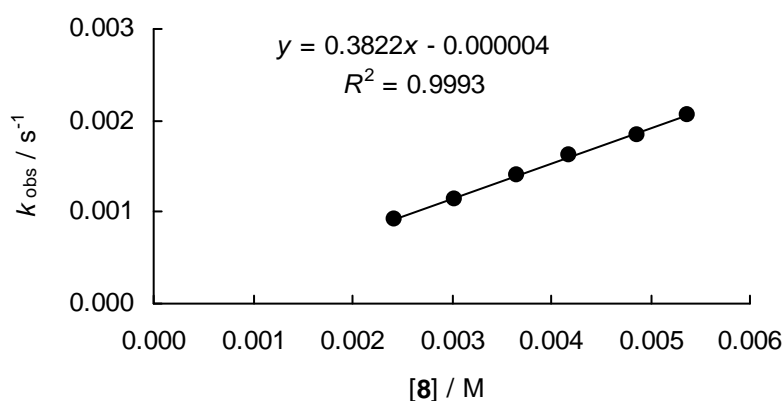
$[\mathbf{1a}]_0 / \text{M}$	$[\mathbf{8}]_0 / \text{M}$	$[\mathbf{8}]_0 / [\mathbf{1a}]_0$	$k_{\text{obs}} / \text{s}^{-1}$
4.92×10^{-5}	1.26×10^{-3}	26	3.59×10^{-4}
4.86×10^{-5}	3.74×10^{-3}	77	9.76×10^{-4}
4.89×10^{-5}	5.02×10^{-3}	103	1.33×10^{-3}
4.82×10^{-5}	6.18×10^{-3}	128	1.66×10^{-3}



$$k_2 = 2.64 \times 10^{-1} \text{ M}^{-1} \text{ s}^{-1}$$

Rate constants for the reactions of *n*-propylamine (**8**) with tol(*t*-Bu)₂QM (**1b**) in CH₃CN (diode array spectrophotometer, 20 °C, λ = 371 nm).

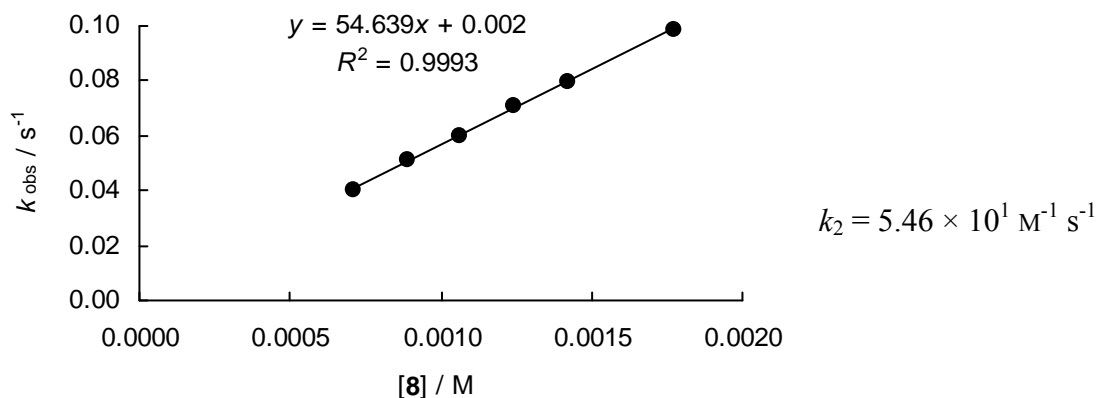
[1b] ₀ / M	[8] ₀ / M	[8] ₀ / [1b] ₀	<i>k</i> _{obs} / s ⁻¹
5.42 × 10 ⁻⁵	2.43 × 10 ⁻³	45	9.22 × 10 ⁻⁴
5.42 × 10 ⁻⁵	3.03 × 10 ⁻³	56	1.15 × 10 ⁻³
5.44 × 10 ⁻⁵	3.66 × 10 ⁻³	67	1.40 × 10 ⁻³
5.32 × 10 ⁻⁵	4.17 × 10 ⁻³	78	1.61 × 10 ⁻³
5.42 × 10 ⁻⁵	4.86 × 10 ⁻³	90	1.84 × 10 ⁻³
5.33 × 10 ⁻⁵	5.38 × 10 ⁻³	101	2.05 × 10 ⁻³



$$k_2 = 3.82 \times 10^{-1} \text{ M}^{-1} \text{ s}^{-1}$$

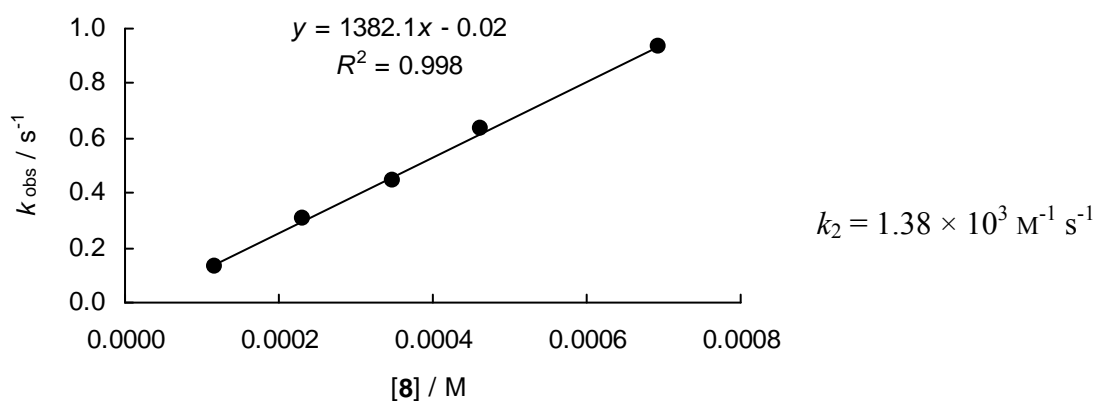
Rate constants for the reactions of *n*-propylamine (**8**) with ani(Ph)₂QM (**1c**) in CH₃CN (Stopped-flow, 20 °C, λ = 422 nm).

[1c] ₀ / M	[8] ₀ / M	[8] ₀ / [1c] ₀	<i>k</i> _{obs} / s ⁻¹
2.06 × 10 ⁻⁵	7.11 × 10 ⁻⁴	35	4.03 × 10 ⁻²
2.06 × 10 ⁻⁵	8.88 × 10 ⁻⁴	43	5.08 × 10 ⁻²
2.06 × 10 ⁻⁵	1.07 × 10 ⁻³	52	5.98 × 10 ⁻²
2.06 × 10 ⁻⁵	1.24 × 10 ⁻³	60	7.08 × 10 ⁻²
2.06 × 10 ⁻⁵	1.42 × 10 ⁻³	69	7.99 × 10 ⁻²
2.06 × 10 ⁻⁵	1.78 × 10 ⁻³	86	9.85 × 10 ⁻²



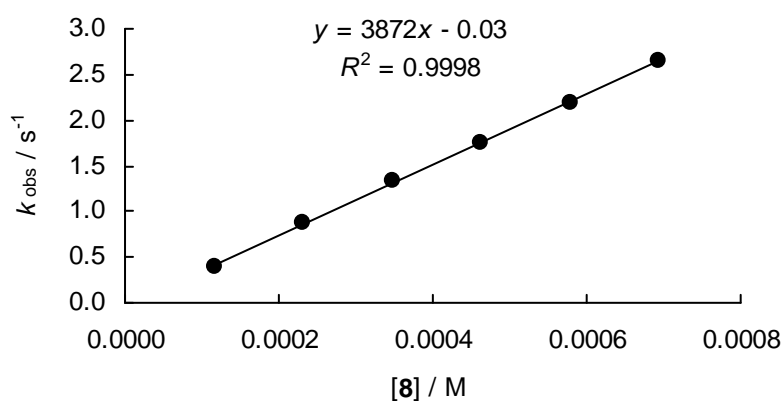
Rate constants for the reactions of n -propylamine ($\mathbf{8}$) with $(\text{liI})_2\text{CH}^+\text{BF}_4^-$ ($\mathbf{1d}$) in CH_3CN (Stopped-flow, 20°C , $\lambda = 639 \text{ nm}$).

$[\mathbf{1d}]_0 / \text{M}$	$[\mathbf{8}]_0 / \text{M}$	$[\mathbf{8}]_0 / [\mathbf{1d}]_0$	$k_{\text{obs}} / \text{s}^{-1}$
6.82×10^{-6}	1.16×10^{-4}	17	1.32×10^{-1}
6.82×10^{-6}	2.31×10^{-4}	34	3.09×10^{-1}
6.82×10^{-6}	3.47×10^{-4}	51	4.43×10^{-1}
6.82×10^{-6}	4.63×10^{-4}	68	6.34×10^{-1}
6.82×10^{-6}	6.94×10^{-4}	102	9.32×10^{-1}



Rate constants for the reactions of *n*-propylamine (**8**) with (jul)₂CH⁺BF₄⁻ (**1e**) in CH₃CN (Stopped-flow, 20 °C, λ = 642 nm).

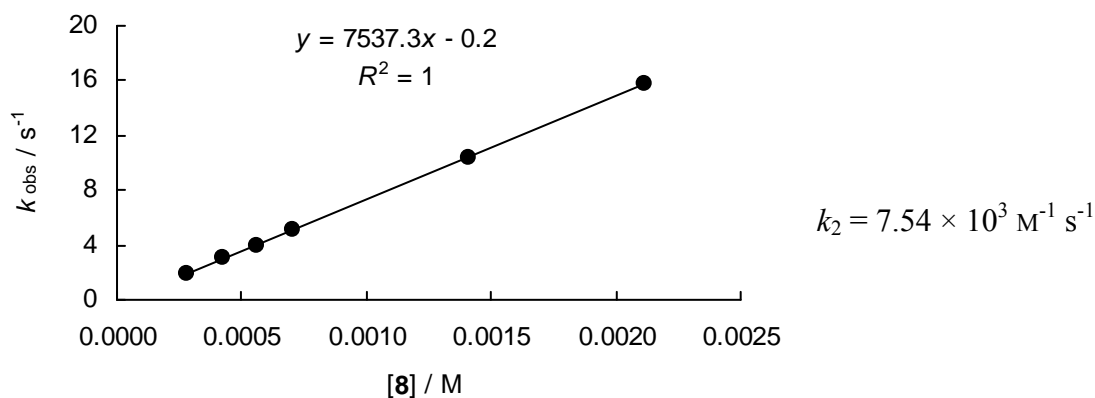
[1e] ₀ / M	[8] ₀ / M	[8] ₀ / [1e] ₀	<i>k</i> _{obs} / s ⁻¹
6.39 × 10 ⁻⁶	1.16 × 10 ⁻⁴	18	3.99 × 10 ⁻¹
6.39 × 10 ⁻⁶	2.31 × 10 ⁻⁴	36	8.71 × 10 ⁻¹
6.39 × 10 ⁻⁶	3.47 × 10 ⁻⁴	54	1.33
6.39 × 10 ⁻⁶	4.63 × 10 ⁻⁴	72	1.77
6.39 × 10 ⁻⁶	5.79 × 10 ⁻⁴	91	2.20
6.39 × 10 ⁻⁶	6.94 × 10 ⁻⁴	109	2.65



$$k_2 = 3.87 \times 10^3 \text{ M}^{-1} \text{ s}^{-1}$$

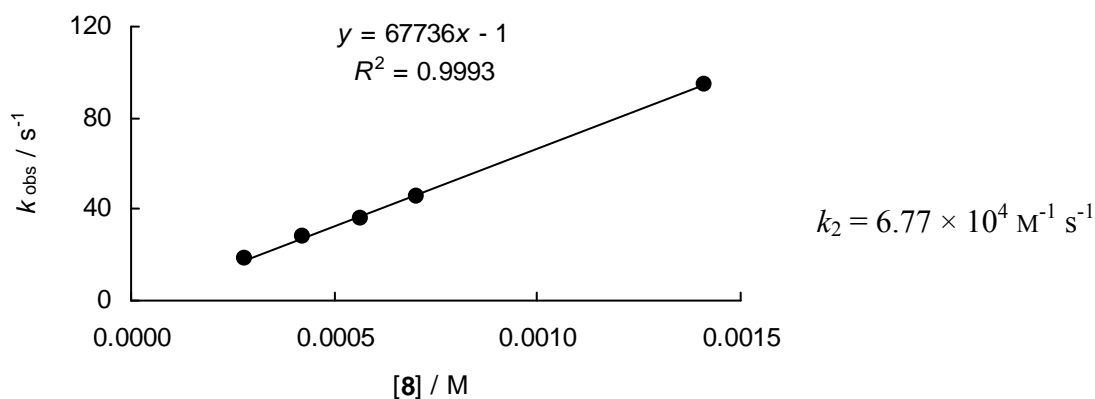
Rate constants for the reactions of *n*-propylamine (**8**) with (ind)₂CH⁺BF₄⁻ (**1f**) in CH₃CN (Stopped-flow, 20 °C, λ = 625 nm).

[1f] ₀ / M	[8] ₀ / M	[8] ₀ / [1f] ₀	<i>k</i> _{obs} / s ⁻¹
2.21 × 10 ⁻⁵	2.82 × 10 ⁻⁴	13	1.96
2.21 × 10 ⁻⁵	4.23 × 10 ⁻⁴	19	3.01
2.21 × 10 ⁻⁵	5.64 × 10 ⁻⁴	26	4.00
2.21 × 10 ⁻⁵	7.05 × 10 ⁻⁴	32	5.13
2.21 × 10 ⁻⁵	1.41 × 10 ⁻³	64	1.04 × 10 ¹
2.21 × 10 ⁻⁵	2.12 × 10 ⁻³	96	1.58 × 10 ¹



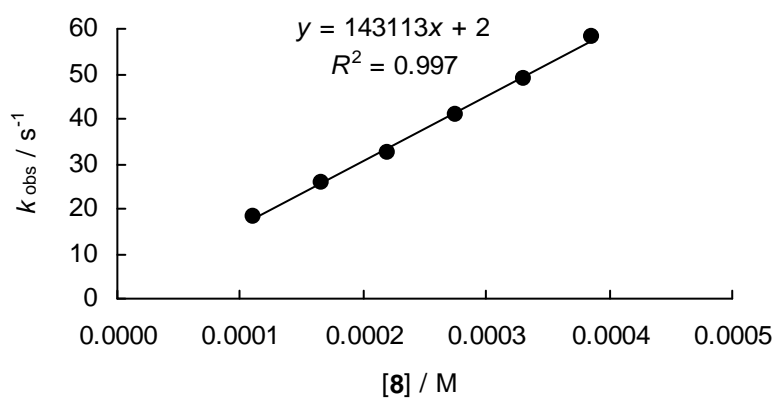
Rate constants for the reactions of n -propylamine ($\mathbf{8}$) with $(\text{pyr})_2\text{CH}^+\text{BF}_4^-$ ($\mathbf{1g}$) in CH_3CN (Stopped-flow, 20°C , $\lambda = 620 \text{ nm}$).

$[\mathbf{1g}]_0 / \text{M}$	$[\mathbf{8}]_0 / \text{M}$	$[\mathbf{8}]_0 / [\mathbf{1g}]_0$	$k_{\text{obs}} / \text{s}^{-1}$
1.71×10^{-5}	2.82×10^{-4}	16	1.81×10^1
1.71×10^{-5}	4.23×10^{-4}	25	2.82×10^1
1.71×10^{-5}	5.64×10^{-4}	33	3.60×10^1
1.71×10^{-5}	7.05×10^{-4}	41	4.57×10^1
1.71×10^{-5}	1.41×10^{-3}	82	9.46×10^1



Rate constants for the reactions of *n*-propylamine (**8**) with $(\text{dma})_2\text{CH}^+\text{BF}_4^-$ (**1h**) in CH_3CN (Stopped-flow, 20 °C, $\lambda = 613 \text{ nm}$).

$[\mathbf{1h}]_0 / \text{M}$	$[\mathbf{8}]_0 / \text{M}$	$[\mathbf{8}]_0 / [\mathbf{1h}]_0$	$k_{\text{obs}} / \text{s}^{-1}$
9.35×10^{-6}	1.10×10^{-4}	12	1.84×10^1
9.35×10^{-6}	1.65×10^{-4}	18	2.58×10^1
9.35×10^{-6}	2.21×10^{-4}	24	3.24×10^1
9.35×10^{-6}	2.76×10^{-4}	30	4.07×10^1
9.35×10^{-6}	3.31×10^{-4}	35	4.88×10^1
9.35×10^{-6}	3.86×10^{-4}	41	5.82×10^1



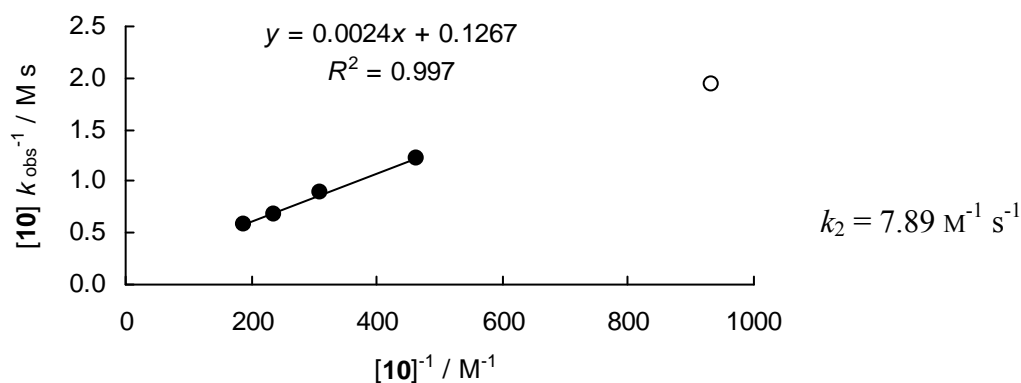
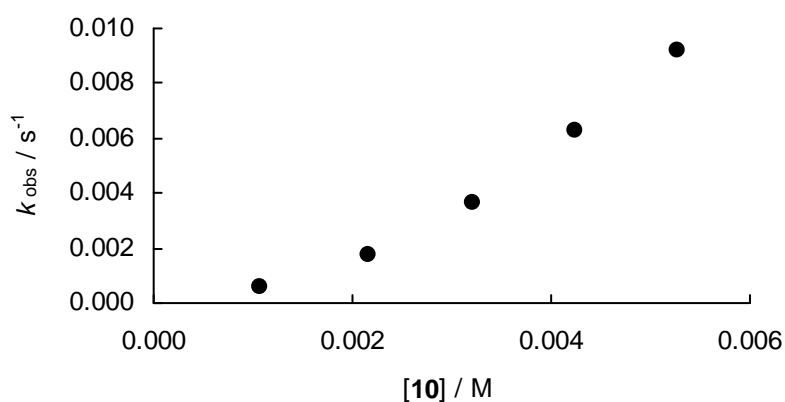
$$k_2 = 1.43 \times 10^5 \text{ M}^{-1} \text{ s}^{-1}$$

Kinetics of the reactions of benzhydrylium ions and quinone methides (1) with *N,N*-bis(2-methoxyethyl)amine (10)

Rate constants for the reactions of *N,N*-bis(2-methoxyethyl)amine (10) with ani(Ph)₂QM (1c) in CH₃CN (diode array spectrophotometer, 20 °C, λ = 422 nm).

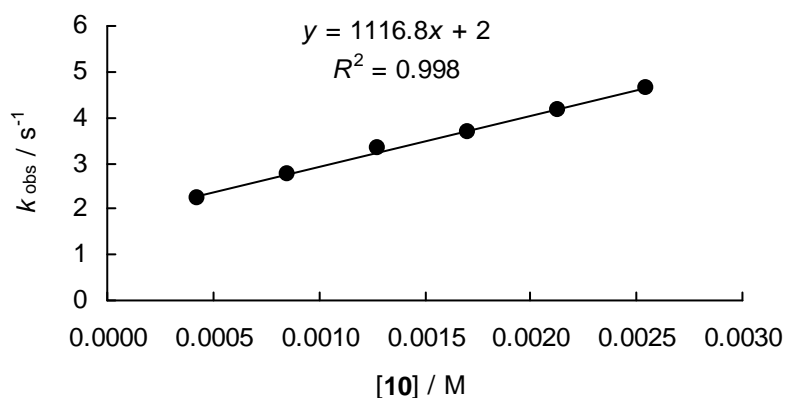
[1c] ₀ / M	[10] ₀ / M	[10] ₀ ⁻¹ / M ⁻¹	[10] ₀ / [1c] ₀	k _{obs} / s ⁻¹	[10] ₀ × k _{obs} ⁻¹ / Ms
5.16 × 10 ⁻⁵	1.07 × 10 ⁻³	9.33 × 10 ²	21	5.52 × 10 ⁻⁴	1.94 ^[a]
5.21 × 10 ⁻⁵	2.16 × 10 ⁻³	4.63 × 10 ²	42	1.78 × 10 ⁻³	1.21
5.16 × 10 ⁻⁵	3.21 × 10 ⁻³	3.11 × 10 ²	62	3.62 × 10 ⁻³	8.88 × 10 ⁻¹
5.11 × 10 ⁻⁵	4.24 × 10 ⁻³	2.36 × 10 ²	83	6.29 × 10 ⁻³	6.75 × 10 ⁻¹
5.07 × 10 ⁻⁵	5.27 × 10 ⁻³	1.90 × 10 ²	104	9.20 × 10 ⁻³	5.72 × 10 ⁻¹

^[a] not included for the evaluation of k₂, because at the low concentration of 10 the assumption that k_p << k_a × [10] seems to be invalid.



Rate constants for the reactions of *N,N*-bis(2-methoxyethyl)amine (**10**) with $(\text{tli})_2\text{CH}^+\text{BF}_4^-$ (**1d**) in CH_3CN (Stopped-flow, 20 °C, $\lambda = 639 \text{ nm}$).

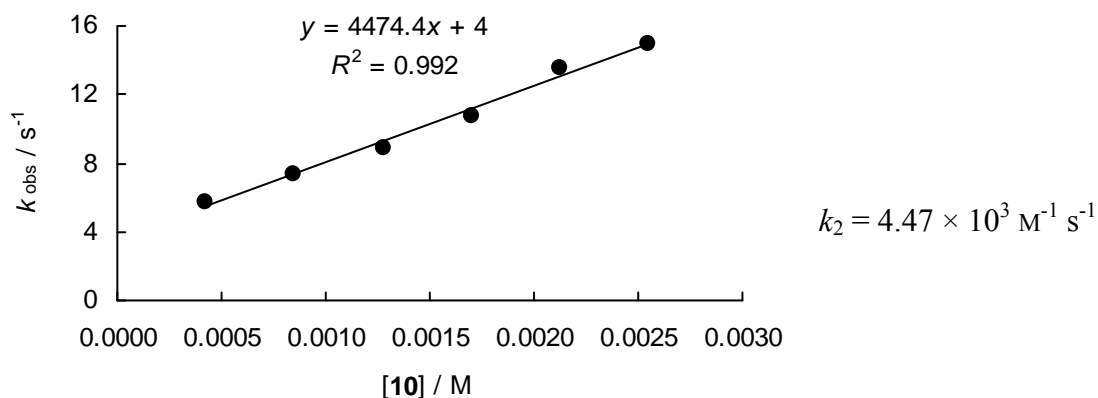
$[\mathbf{1d}]_0 / \text{M}$	$[\mathbf{10}]_0 / \text{M}$	$[\mathbf{10}]_0 / [\mathbf{1d}]_0$	$k_{\text{obs}} / \text{s}^{-1}$
1.83×10^{-5}	4.25×10^{-4}	23	2.24
1.83×10^{-5}	8.50×10^{-4}	47	2.75
1.83×10^{-5}	1.27×10^{-3}	70	3.31
1.83×10^{-5}	1.70×10^{-3}	93	3.69
1.83×10^{-5}	2.12×10^{-3}	116	4.16
1.83×10^{-5}	2.55×10^{-3}	140	4.64



$$k_2 = 1.12 \times 10^3 \text{ M}^{-1} \text{ s}^{-1}$$

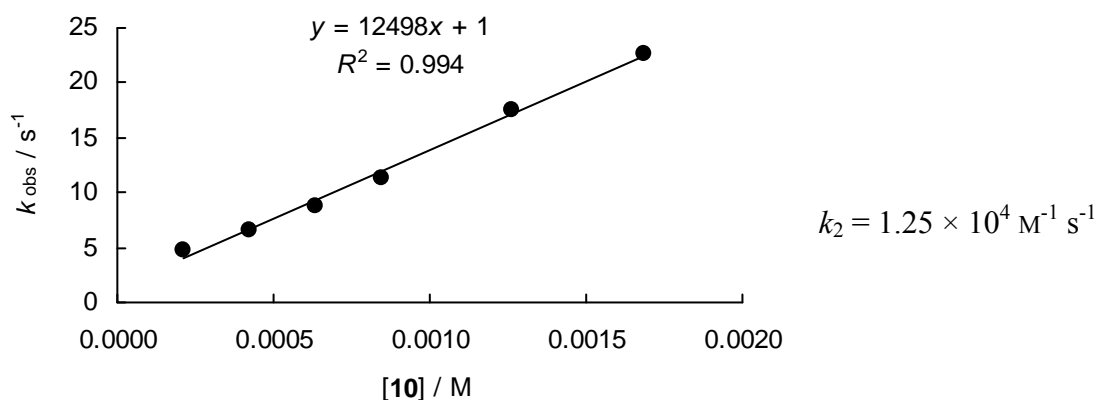
Rate constants for the reactions of *N,N*-bis(2-methoxyethyl)amine (**10**) with $(\text{jul})_2\text{CH}^+\text{BF}_4^-$ (**1e**) in CH_3CN (Stopped-flow, 20 °C, $\lambda = 642 \text{ nm}$).

$[\mathbf{1e}]_0 / \text{M}$	$[\mathbf{10}]_0 / \text{M}$	$[\mathbf{10}]_0 / [\mathbf{1e}]_0$	$k_{\text{obs}} / \text{s}^{-1}$
1.76×10^{-5}	4.25×10^{-4}	24	5.74
1.76×10^{-5}	8.50×10^{-4}	48	7.40
1.76×10^{-5}	1.27×10^{-3}	72	8.91
1.76×10^{-5}	1.70×10^{-3}	96	1.08×10^1
1.76×10^{-5}	2.12×10^{-3}	120	1.35×10^1
1.76×10^{-5}	2.55×10^{-3}	145	1.50×10^1



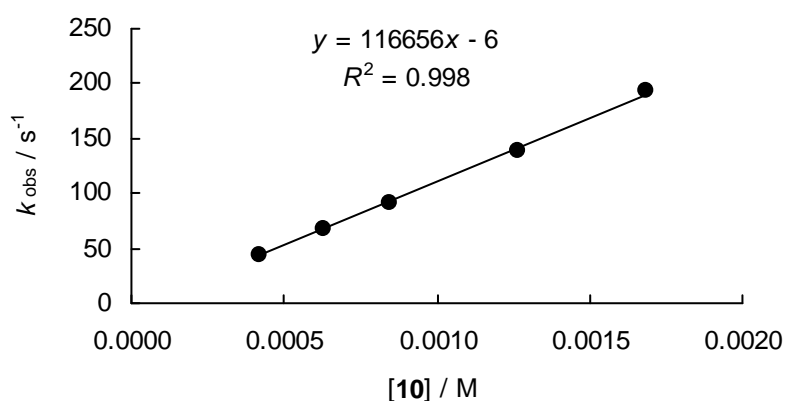
Rate constants for the reactions of *N,N*-bis(2-methoxyethyl)amine (**10**) with $(\text{ind})_2\text{CH}^+\text{BF}_4^-$ (**1f**) in CH_3CN (Stopped-flow, 20 °C, $\lambda = 625 \text{ nm}$).

$[\mathbf{1f}]_0 / \text{M}$	$[\mathbf{10}]_0 / \text{M}$	$[\mathbf{10}]_0 / [\mathbf{1f}]_0$	$k_{\text{obs}} / \text{s}^{-1}$
2.15×10^{-5}	2.11×10^{-4}	10	4.74
2.15×10^{-5}	4.22×10^{-4}	20	6.63
2.15×10^{-5}	6.32×10^{-4}	29	8.79
2.15×10^{-5}	8.43×10^{-4}	39	1.13×10^1
2.15×10^{-5}	1.26×10^{-3}	59	1.75×10^1
2.15×10^{-5}	1.69×10^{-3}	78	2.27×10^1



Rate constants for the reactions of *N,N*-bis(2-methoxyethyl)amine (**10**) with $(\text{pyr})_2\text{CH}^+\text{BF}_4^-$ (**1g**) in CH_3CN (Stopped-flow, 20 °C, $\lambda = 620$ nm).

$[\mathbf{1g}]_0 / \text{M}$	$[\mathbf{10}]_0 / \text{M}$	$[\mathbf{10}]_0 / [\mathbf{1g}]_0$	$k_{\text{obs}} / \text{s}^{-1}$
2.09×10^{-5}	4.22×10^{-4}	20	4.45×10^1
2.09×10^{-5}	6.32×10^{-4}	30	6.84×10^1
2.09×10^{-5}	8.43×10^{-4}	40	9.07×10^1
2.09×10^{-5}	1.26×10^{-3}	61	1.38×10^2
2.09×10^{-5}	1.69×10^{-3}	81	1.93×10^2

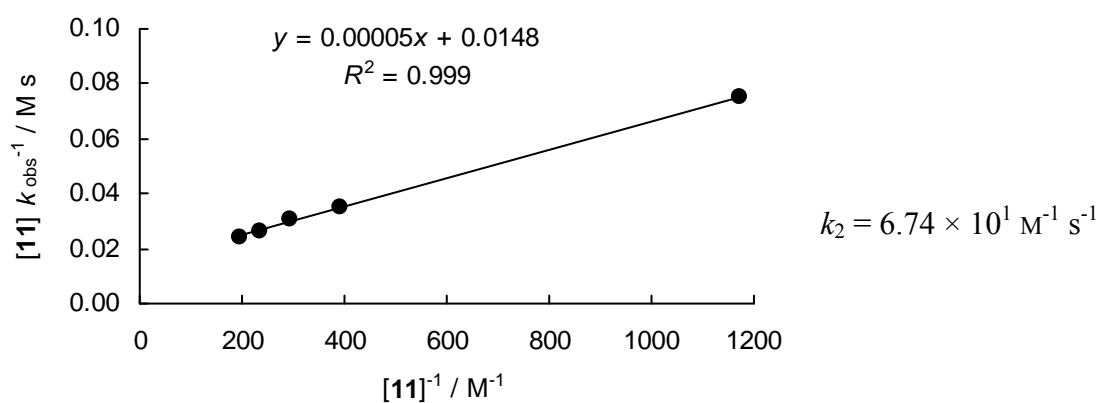
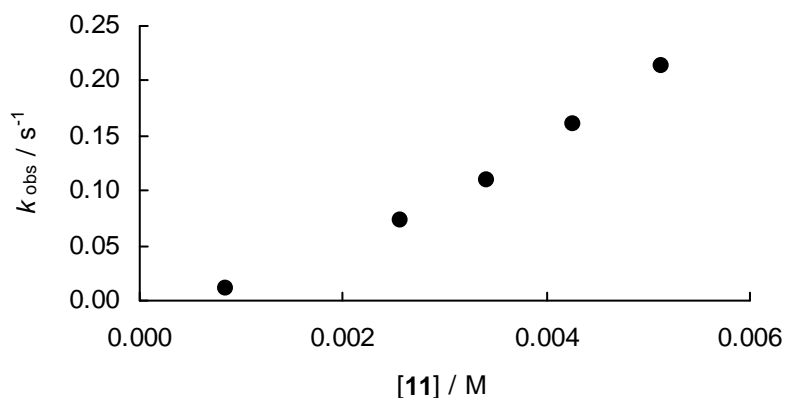


$$k_2 = 1.17 \times 10^5 \text{ M}^{-1} \text{ s}^{-1}$$

Kinetics of the reactions of benzhydrylium ions and quinone methides (**1**) with di-*n*-propylamine (**11**)

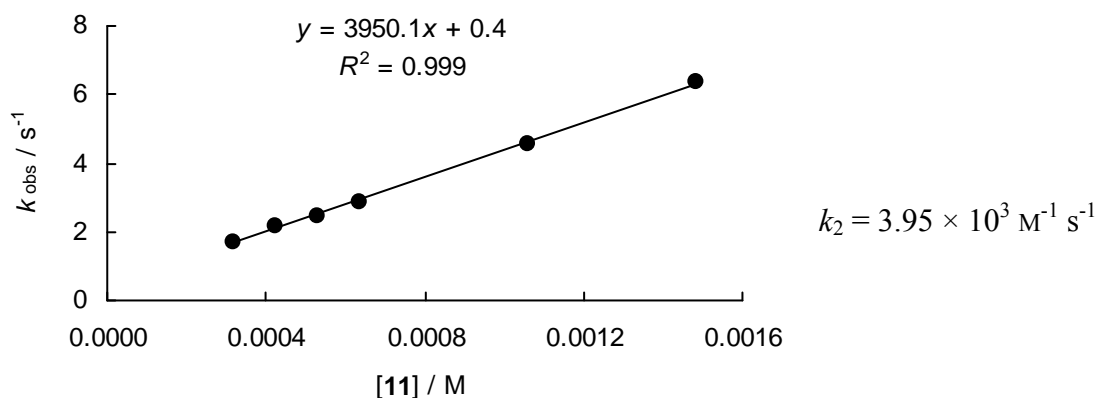
Rate constants for the reactions of di-*n*-propylamine (**11**) with ani(Ph)₂QM (**1c**) in CH_3CN (Stopped-flow, 20 °C, $\lambda = 422$ nm).

$[\mathbf{1c}]_0 / \text{M}$	$[\mathbf{11}]_0 / \text{M}$	$[\mathbf{11}]_0^{-1} / \text{M}^{-1}$	$[\mathbf{11}]_0 / [\mathbf{1c}]_0$	$k_{\text{obs}} / \text{s}^{-1}$	$[\mathbf{11}]_0 \times k_{\text{obs}}^{-1} / \text{Ms}$
5.14×10^{-5}	8.54×10^{-4}	1.17×10^3	17	1.14×10^{-2}	7.49×10^{-2}
5.14×10^{-5}	2.56×10^{-3}	3.90×10^2	50	7.28×10^{-2}	3.52×10^{-2}
5.14×10^{-5}	3.42×10^{-3}	2.93×10^2	66	1.10×10^{-1}	3.10×10^{-2}
5.14×10^{-5}	4.27×10^{-3}	2.34×10^2	83	1.61×10^{-1}	2.65×10^{-2}
5.14×10^{-5}	5.12×10^{-3}	1.95×10^2	100	2.13×10^{-1}	2.40×10^{-2}



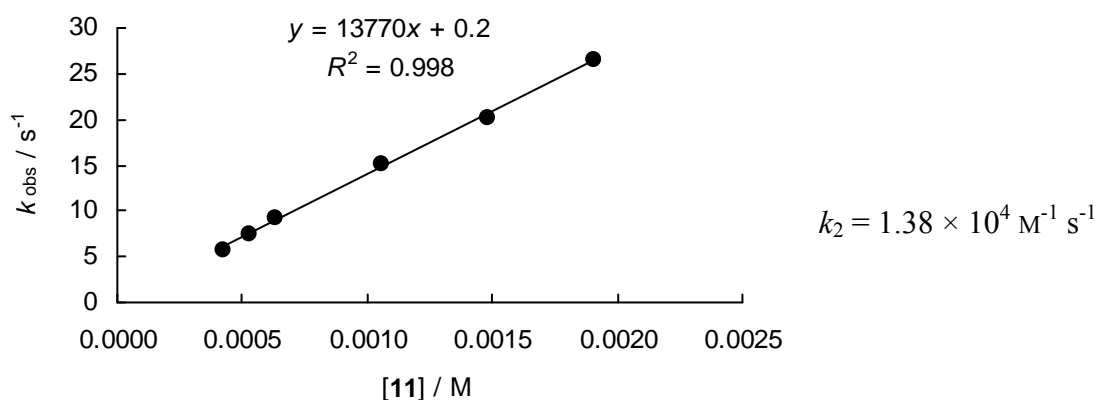
Rate constants for the reactions of di-*n*-propylamine (**11**) with $(\text{il})_2\text{CH}^+\text{BF}_4^-$ (**1d**) in CH_3CN (Stopped-flow, 20 °C, $\lambda = 639 \text{ nm}$).

$[\mathbf{1d}]_0 / \text{M}$	$[\mathbf{11}]_0 / \text{M}$	$[\mathbf{11}]_0 / [\mathbf{1d}]_0$	$k_{\text{obs}} / \text{s}^{-1}$
2.02×10^{-5}	3.18×10^{-4}	16	1.72
2.02×10^{-5}	4.24×10^{-4}	21	2.18
2.02×10^{-5}	5.30×10^{-4}	26	2.48
2.02×10^{-5}	6.36×10^{-4}	32	2.85
2.02×10^{-5}	1.06×10^{-3}	53	4.57
2.02×10^{-5}	1.48×10^{-3}	74	6.34



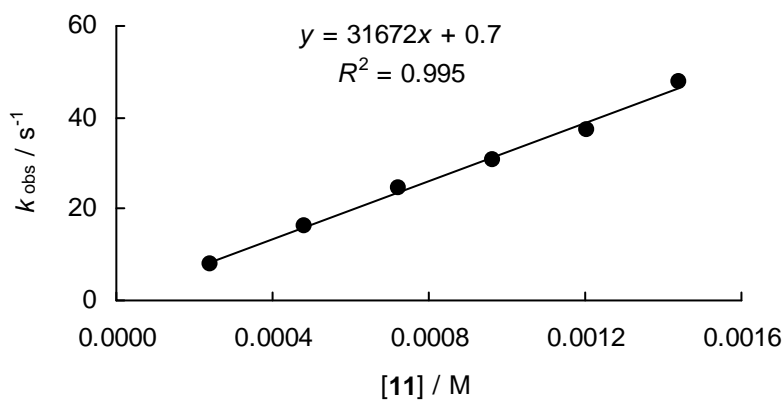
Rate constants for the reactions of di-*n*-propylamine (**11**) with $(\text{jul})_2\text{CH}^+\text{BF}_4^-$ (**1e**) in CH_3CN (Stopped-flow, 20 °C, $\lambda = 642 \text{ nm}$).

$[\mathbf{1e}]_0 / \text{M}$	$[\mathbf{11}]_0 / \text{M}$	$[\mathbf{11}]_0 / [\mathbf{1e}]_0$	$k_{\text{obs}} / \text{s}^{-1}$
1.94×10^{-5}	4.24×10^{-4}	22	5.60
1.94×10^{-5}	5.30×10^{-4}	27	7.52
1.94×10^{-5}	6.36×10^{-4}	33	9.29
1.94×10^{-5}	1.06×10^{-3}	55	1.52×10^1
1.94×10^{-5}	1.48×10^{-3}	76	2.02×10^1
1.94×10^{-5}	1.91×10^{-3}	98	2.66×10^1



Rate constants for the reactions of di-*n*-propylamine (**11**) with (ind)₂CH⁺BF₄⁻ (**1f**) in CH₃CN (Stopped-flow, 20 °C, λ = 625 nm).

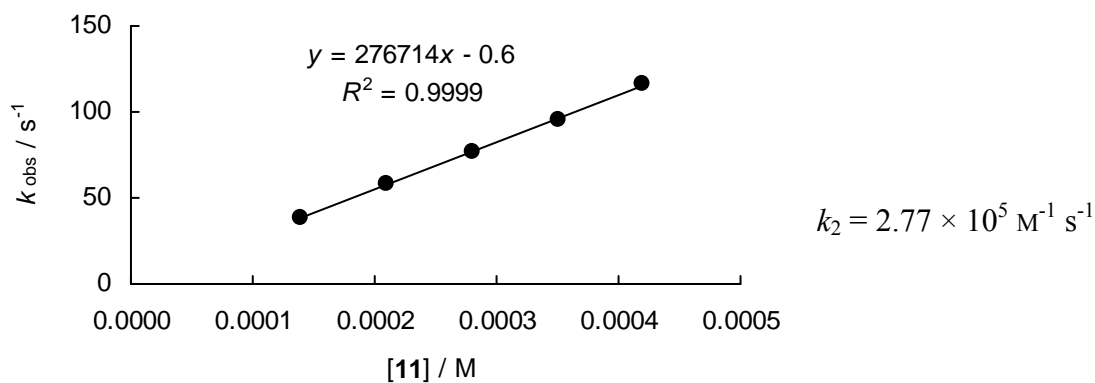
[1f] ₀ / M	[11] ₀ / M	[11] ₀ / [1f] ₀	<i>k</i> _{obs} / s ⁻¹
2.17 × 10 ⁻⁵	2.41 × 10 ⁻⁴	11	8.07
2.17 × 10 ⁻⁵	4.81 × 10 ⁻⁴	22	1.63 × 10 ¹
2.17 × 10 ⁻⁵	7.22 × 10 ⁻⁴	33	2.44 × 10 ¹
2.17 × 10 ⁻⁵	9.62 × 10 ⁻⁴	44	3.05 × 10 ¹
2.17 × 10 ⁻⁵	1.20 × 10 ⁻³	55	3.73 × 10 ¹
2.17 × 10 ⁻⁵	1.44 × 10 ⁻³	66	4.76 × 10 ¹



$$k_2 = 3.17 \times 10^4 \text{ M}^{-1} \text{ s}^{-1}$$

Rate constants for the reactions of di-*n*-propylamine (**11**) with (pyr)₂CH⁺BF₄⁻ (**1g**) in CH₃CN (Stopped-flow, 20 °C, λ = 611 nm).

[1g] ₀ / M	[11] ₀ / M	[11] ₀ / [1g] ₀	<i>k</i> _{obs} / s ⁻¹
1.06 × 10 ⁻⁵	1.40 × 10 ⁻⁴	13	3.82 × 10 ¹
1.06 × 10 ⁻⁵	2.10 × 10 ⁻⁴	20	5.78 × 10 ¹
1.06 × 10 ⁻⁵	2.80 × 10 ⁻⁴	26	7.67 × 10 ¹
1.06 × 10 ⁻⁵	3.50 × 10 ⁻⁴	33	9.59 × 10 ¹
1.06 × 10 ⁻⁵	4.20 × 10 ⁻⁴	40	1.16 × 10 ²

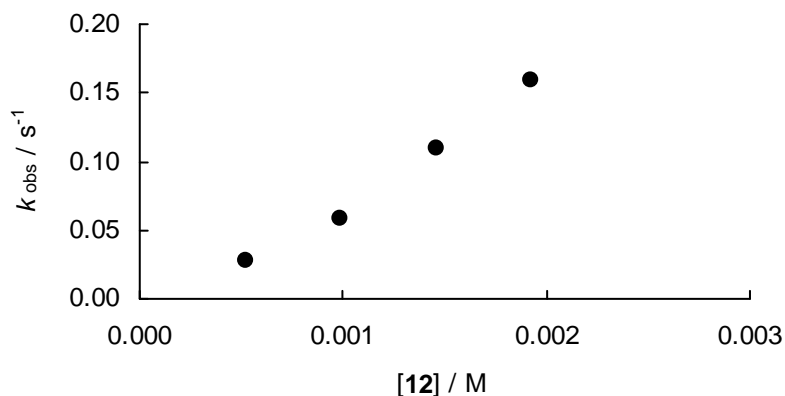


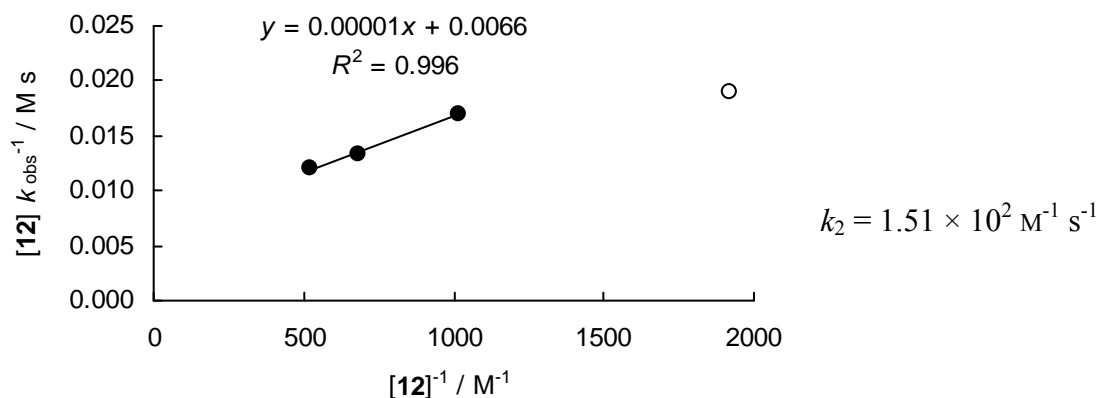
Kinetics of the reactions of benzhydrylium ions and quinone methides (**1**) with diethylamine (**12**)

Rate constants for the reactions of diethylamine (**12**) with ani(Ph)₂QM (**1c**) in CH₃CN (diode array spectrophotometer, 20 °C, $\lambda = 422 \text{ nm}$).

$[\mathbf{1c}]_0 / \text{M}$	$[\mathbf{12}]_0 / \text{M}$	$[\mathbf{12}]_0^{-1} / \text{M}^{-1}$	$[\mathbf{12}]_0 / [\mathbf{1c}]_0$	$k_{\text{obs}} / \text{s}^{-1}$	$[\mathbf{12}]_0 \times k_{\text{obs}}^{-1} / \text{Ms}$
4.54×10^{-5}	5.21×10^{-4}	1.92×10^3	11	2.75×10^{-2}	1.89×10^{-2} [a]
4.28×10^{-5}	9.82×10^{-4}	1.02×10^3	23	5.77×10^{-2}	1.70×10^{-2}
4.25×10^{-5}	1.46×10^{-3}	6.85×10^2	34	1.09×10^{-1}	1.34×10^{-2}
4.19×10^{-5}	1.92×10^{-3}	5.21×10^2	46	1.60×10^{-1}	1.20×10^{-2}

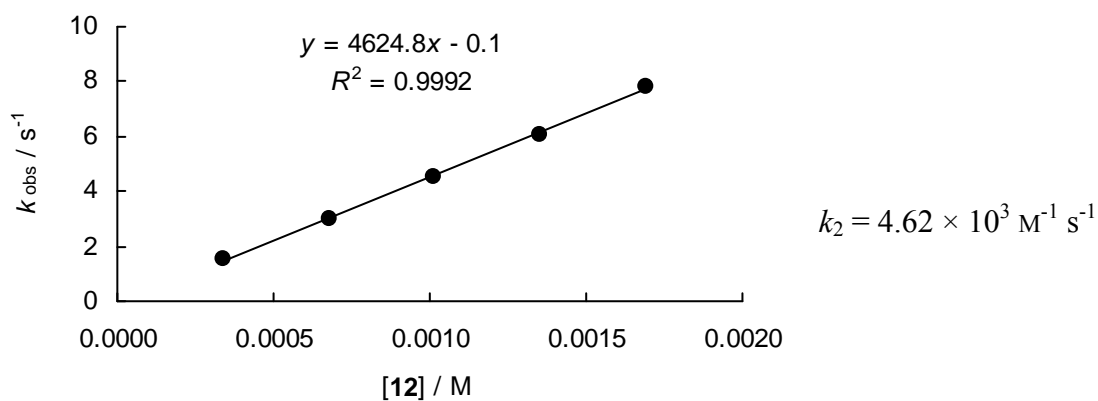
[a] not included for the evaluation of k_2 , because at the low concentration of **12** the assumption that $k_p \ll k_a \times [\mathbf{12}]$ seems to be invalid.





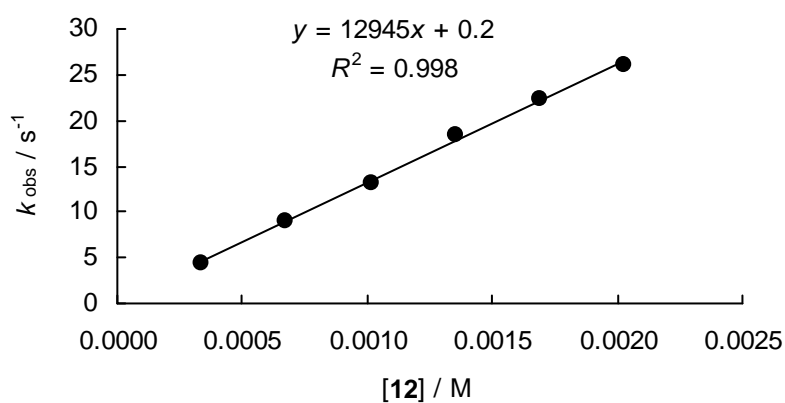
Rate constants for the reactions of diethylamine (**12**) with $(\text{il})_2\text{CH}^+\text{BF}_4^-$ (**1d**) in CH_3CN (Stopped-flow, 20 °C, $\lambda = 639 \text{ nm}$).

$[\mathbf{1d}]_0 / \text{M}$	$[\mathbf{12}]_0 / \text{M}$	$[\mathbf{12}]_0 / [\mathbf{1d}]_0$	$k_{\text{obs}} / \text{s}^{-1}$
2.00×10^{-5}	3.38×10^{-4}	17	1.52
2.00×10^{-5}	6.77×10^{-4}	34	2.98
2.00×10^{-5}	1.02×10^{-3}	51	4.56
2.00×10^{-5}	1.35×10^{-3}	68	6.07
2.00×10^{-5}	1.69×10^{-3}	85	7.80



Rate constants for the reactions of diethylamine (**12**) with (jul)₂CH⁺BF₄⁻ (**1e**) in CH₃CN (Stopped-flow, 20 °C, λ = 642 nm).

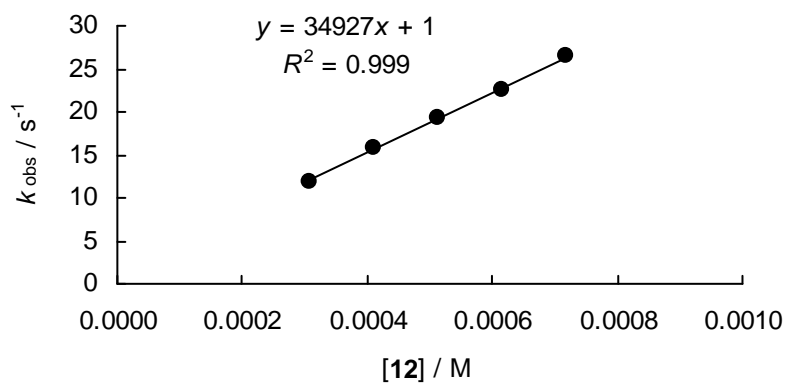
[1e] ₀ / M	[12] ₀ / M	[12] ₀ / [1e] ₀	k _{obs} / s ⁻¹
2.07 × 10 ⁻⁵	3.38 × 10 ⁻⁴	16	4.47
2.07 × 10 ⁻⁵	6.77 × 10 ⁻⁴	33	8.91 ⁰
2.07 × 10 ⁻⁵	1.02 × 10 ⁻³	49	1.31 × 10 ¹
2.07 × 10 ⁻⁵	1.35 × 10 ⁻³	65	1.83 × 10 ¹
2.07 × 10 ⁻⁵	1.69 × 10 ⁻³	82	2.24 × 10 ¹
2.07 × 10 ⁻⁵	2.03 × 10 ⁻³	98	2.60 × 10 ¹



$$k_2 = 1.29 \times 10^4 \text{ M}^{-1} \text{ s}^{-1}$$

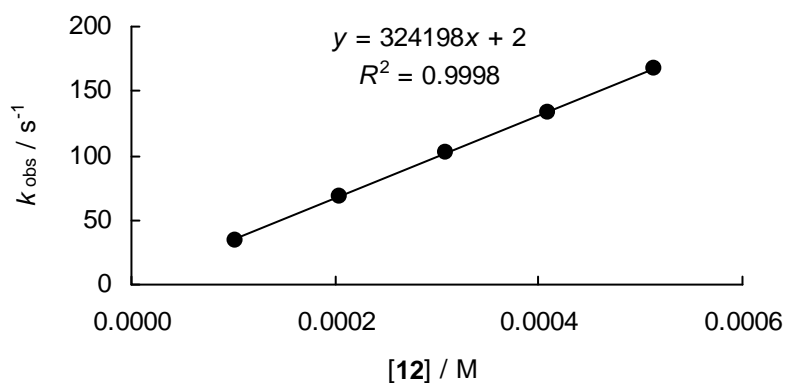
Rate constants for the reactions of diethylamine (**12**) with (ind)₂CH⁺BF₄⁻ (**1f**) in CH₃CN (Stopped-flow, 20 °C, λ = 616 nm).

[1f] ₀ / M	[12] ₀ / M	[12] ₀ / [1f] ₀	k _{obs} / s ⁻¹
2.04 × 10 ⁻⁵	3.08 × 10 ⁻⁴	15	1.19 × 10 ¹
2.04 × 10 ⁻⁵	4.10 × 10 ⁻⁴	20	1.58 × 10 ¹
2.04 × 10 ⁻⁵	5.13 × 10 ⁻⁴	25	1.94 × 10 ¹
2.04 × 10 ⁻⁵	6.15 × 10 ⁻⁴	30	2.26 × 10 ¹
2.04 × 10 ⁻⁵	7.18 × 10 ⁻⁴	35	2.64 × 10 ¹



Rate constants for the reactions of diethylamine (**12**) with $(\text{pyr})_2\text{CH}^+\text{BF}_4^-$ (**1g**) in CH_3CN (Stopped-flow, 20 °C, $\lambda = 611 \text{ nm}$).

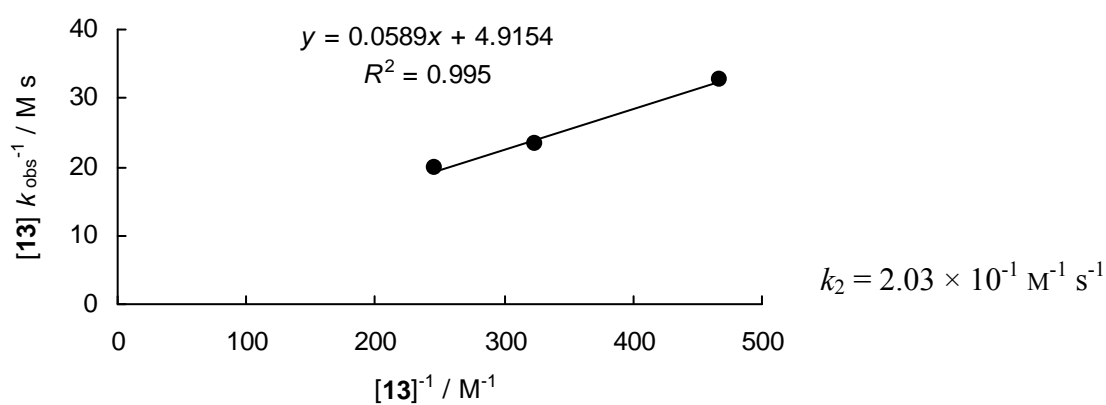
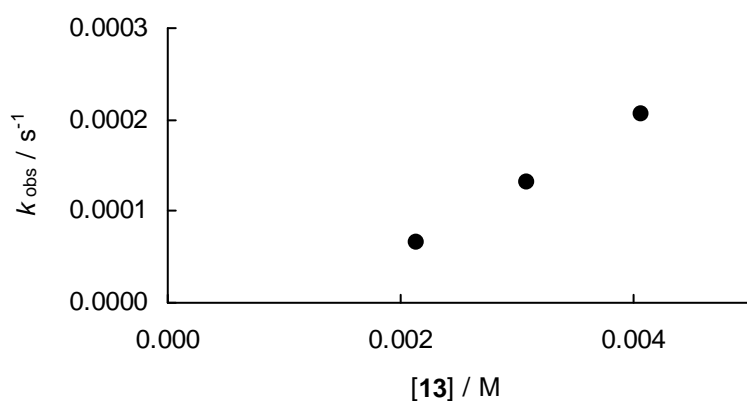
$[\mathbf{1g}]_0 / \text{M}$	$[\mathbf{12}]_0 / \text{M}$	$[\mathbf{12}]_0 / [\mathbf{1g}]_0$	$k_{\text{obs}} / \text{s}^{-1}$
1.02×10^{-5}	1.03×10^{-4}	10	3.47×10^1
1.02×10^{-5}	2.05×10^{-4}	20	6.83×10^1
1.02×10^{-5}	3.08×10^{-4}	30	1.03×10^2
1.02×10^{-5}	4.10×10^{-4}	40	1.34×10^2
1.02×10^{-5}	5.13×10^{-4}	50	1.68×10^2



Kinetics of the reactions of benzhydrylium ions and quinone methides (1) with morpholine (13)

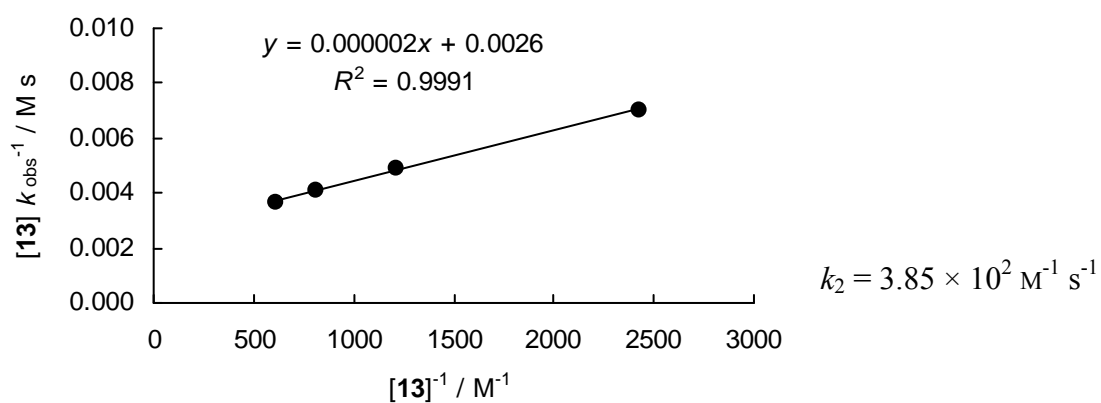
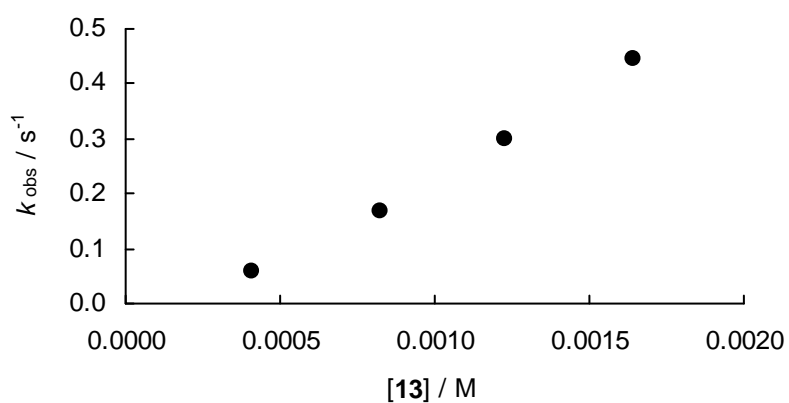
Rate constants for the reactions of morpholine (**13**) with $\text{tol}(t\text{-Bu})_2\text{QM}$ (**1b**) in CH_3CN (diode array spectrophotometer, $20\text{ }^\circ\text{C}$, $\lambda = 371\text{ nm}$).

$[\mathbf{1b}]_0 / \text{M}$	$[\mathbf{13}]_0 / \text{M}$	$[\mathbf{13}]_0^{-1} / \text{M}^{-1}$	$[\mathbf{13}]_0 / [\mathbf{1b}]_0$	$k_{\text{obs}} / \text{s}^{-1}$	$[\mathbf{13}]_0 \times k_{\text{obs}}^{-1} / \text{Ms}$
6.16×10^{-5}	2.14×10^{-3}	4.68×10^2	35	6.55×10^{-5}	3.26×10^1
6.84×10^{-5}	3.09×10^{-3}	3.23×10^2	45	1.32×10^{-4}	2.34×10^1
6.75×10^{-5}	4.07×10^{-3}	2.46×10^2	60	2.06×10^{-4}	1.97×10^1



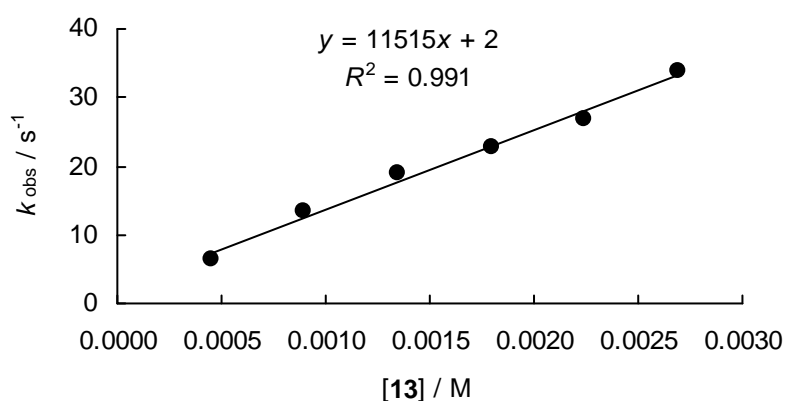
Rate constants for the reactions of morpholine (**13**) with ani(Ph)₂QM (**1c**) in CH₃CN (diode array spectrophotometer, 20 °C, $\lambda = 422$ nm).

$[\mathbf{1c}]_0 / \text{M}$	$[\mathbf{13}]_0 / \text{M}$	$[\mathbf{13}]_0^{-1} / \text{M}^{-1}$	$[\mathbf{13}]_0 / [\mathbf{1c}]_0$	$k_{\text{obs}} / \text{s}^{-1}$	$[\mathbf{13}]_0 \times k_{\text{obs}}^{-1} / \text{Ms}$
4.85×10^{-5}	4.11×10^{-4}	2.43×10^3	8	5.84×10^{-2}	7.04×10^{-3}
4.87×10^{-5}	8.25×10^{-4}	1.21×10^3	17	1.69×10^{-1}	4.88×10^{-3}
4.83×10^{-5}	1.23×10^{-3}	8.13×10^2	25	3.01×10^{-1}	4.09×10^{-3}
4.85×10^{-5}	1.64×10^{-3}	6.10×10^2	34	4.46×10^{-1}	3.68×10^{-3}



Rate constants for the reactions of morpholine (**13**) with $(\text{il})_2\text{CH}^+\text{BF}_4^-$ (**1d**) in CH_3CN (Stopped-flow, 20 °C, $\lambda = 639$ nm).

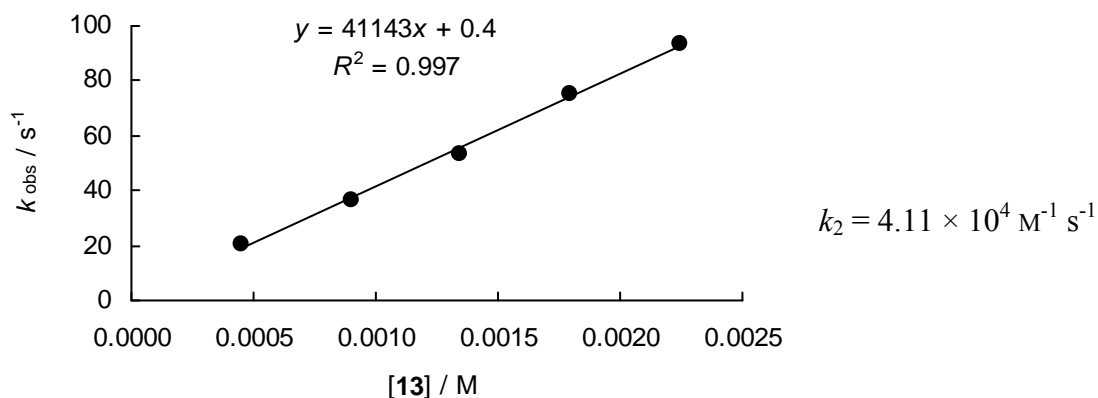
$[\mathbf{1d}]_0 / \text{M}$	$[\mathbf{13}]_0 / \text{M}$	$[\mathbf{13}]_0 / [\mathbf{1d}]_0$	$k_{\text{obs}} / \text{s}^{-1}$
2.33×10^{-5}	4.49×10^{-4}	19	6.50
2.33×10^{-5}	8.98×10^{-4}	39	1.34×10^1
2.33×10^{-5}	1.35×10^{-3}	58	1.89×10^1
2.33×10^{-5}	1.80×10^{-3}	77	2.28×10^1
2.33×10^{-5}	2.24×10^{-3}	96	2.69×10^1
2.33×10^{-5}	2.69×10^{-3}	116	3.38×10^1



$$k_2 = 1.15 \times 10^4 \text{ M}^{-1} \text{ s}^{-1}$$

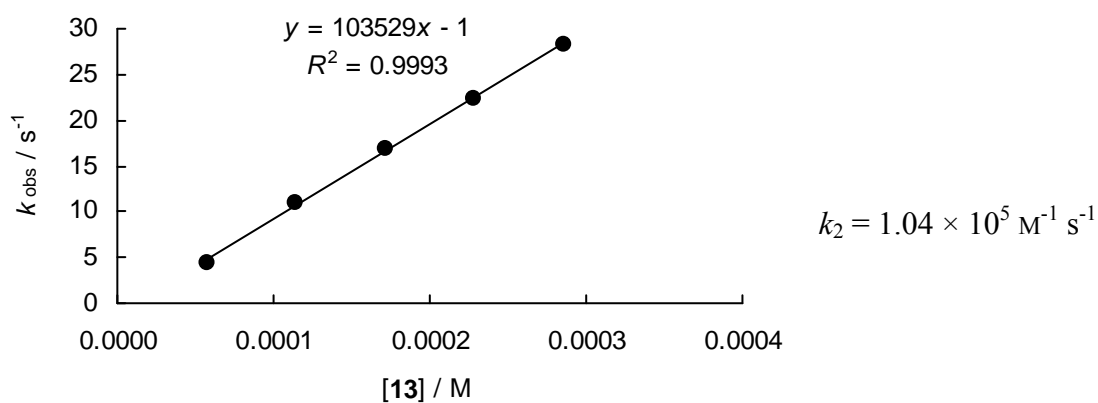
Rate constants for the reactions of morpholine (**13**) with $(\text{jul})_2\text{CH}^+\text{BF}_4^-$ (**1e**) in CH_3CN (Stopped-flow, 20 °C, $\lambda = 642$ nm).

$[\mathbf{1e}]_0 / \text{M}$	$[\mathbf{13}]_0 / \text{M}$	$[\mathbf{13}]_0 / [\mathbf{1e}]_0$	$k_{\text{obs}} / \text{s}^{-1}$
2.18×10^{-5}	4.49×10^{-4}	21	2.05×10^1
2.18×10^{-5}	8.98×10^{-4}	41	3.65×10^1
2.18×10^{-5}	1.35×10^{-3}	62	5.34×10^1
2.18×10^{-5}	1.80×10^{-3}	82	7.51×10^1
2.18×10^{-5}	2.24×10^{-3}	103	9.35×10^1



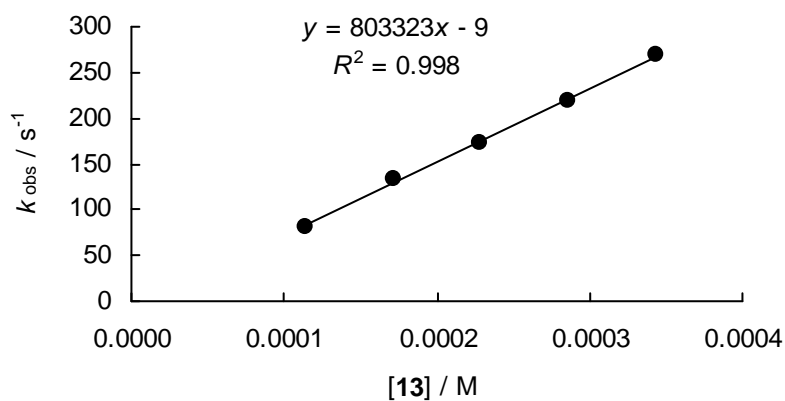
Rate constants for the reactions of morpholine (**13**) with $(\text{ind})_2\text{CH}^+\text{BF}_4^-$ (**1f**) in CH_3CN (Stopped-flow, 20 °C, $\lambda = 625 \text{ nm}$).

$[\mathbf{1f}]_0 / \text{M}$	$[\mathbf{13}]_0 / \text{M}$	$[\mathbf{13}]_0 / [\mathbf{1f}]_0$	$k_{\text{obs}} / \text{s}^{-1}$
1.54×10^{-5}	5.72×10^{-5}	4	4.48
1.54×10^{-5}	1.14×10^{-4}	7	1.09×10^1
1.54×10^{-5}	1.71×10^{-4}	11	1.69×10^1
1.54×10^{-5}	2.29×10^{-4}	15	2.24×10^1
1.54×10^{-5}	2.86×10^{-4}	19	2.83×10^1



Rate constants for the reactions of morpholine (**13**) with $(\text{pyr})_2\text{CH}^+\text{BF}_4^-$ (**1g**) in CH_3CN (Stopped-flow, 20 °C, $\lambda = 620 \text{ nm}$).

$[\mathbf{1g}]_0 / \text{M}$	$[\mathbf{13}]_0 / \text{M}$	$[\mathbf{13}]_0 / [\mathbf{1g}]_0$	$k_{\text{obs}} / \text{s}^{-1}$
1.33×10^{-5}	1.14×10^{-4}	9	8.19×10^1
1.33×10^{-5}	1.71×10^{-4}	13	1.33×10^2
1.33×10^{-5}	2.29×10^{-4}	17	1.73×10^2
1.33×10^{-5}	2.86×10^{-4}	22	2.18×10^2
1.33×10^{-5}	3.43×10^{-4}	26	2.69×10^2

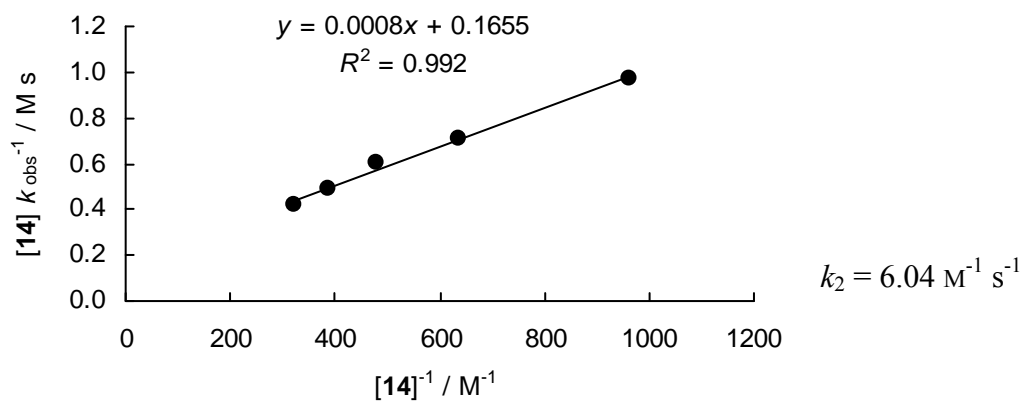
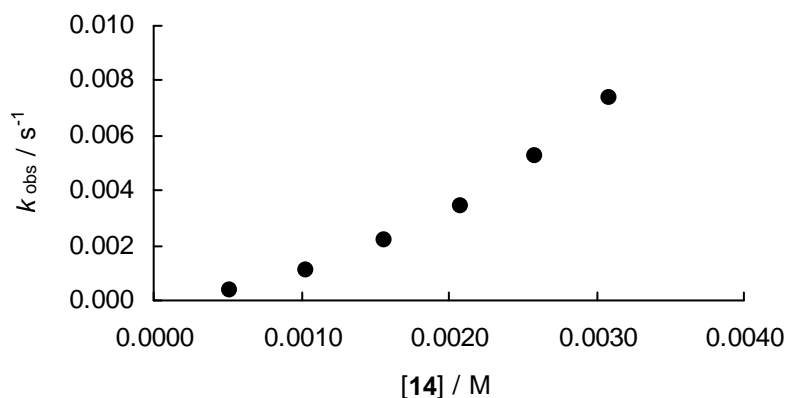


$$k_2 = 8.03 \times 10^5 \text{ M}^{-1} \text{ s}^{-1}$$

Kinetics of the reactions of benzhydrylium ions and quinone methides (1) with piperidine (14)

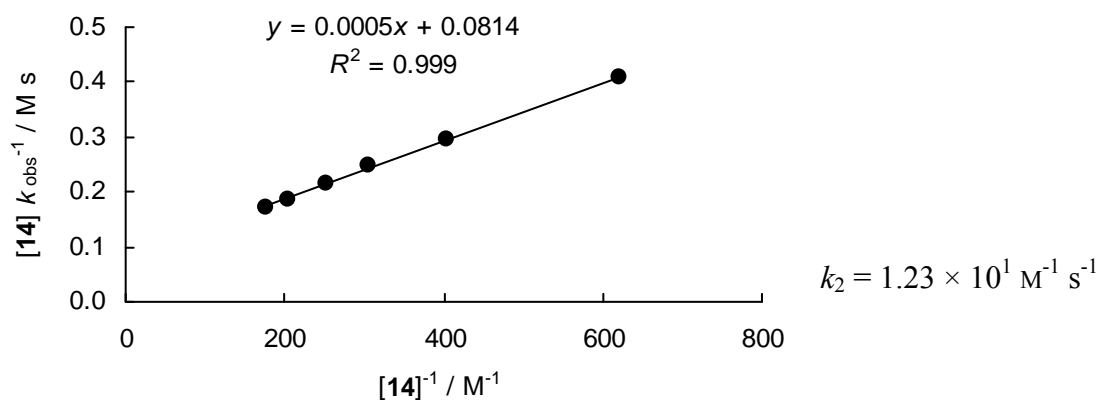
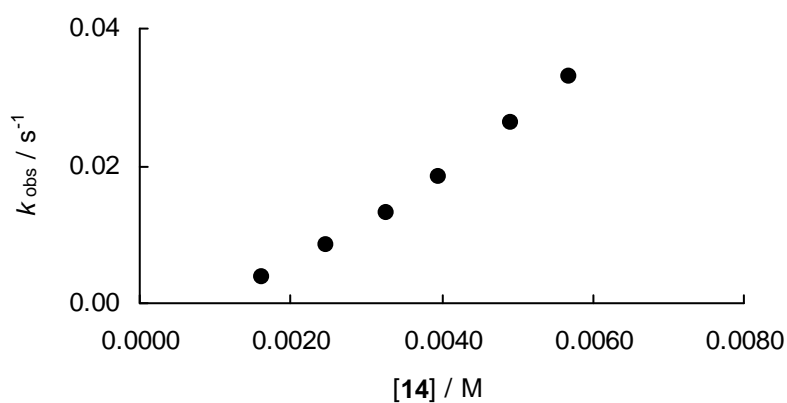
Rate constants for the reactions of piperidine (**14**) with ani(*t*-Bu)₂QM (**1a**) in CH₃CN (diode array spectrophotometer, 20 °C, $\lambda = 393$ nm).

$[\mathbf{1a}]_0 / \text{M}$	$[\mathbf{14}]_0 / \text{M}$	$[\mathbf{14}]_0^{-1} / \text{M}^{-1}$	$[\mathbf{14}]_0 / [\mathbf{1a}]_0$	$k_{\text{obs}} / \text{s}^{-1}$	$[\mathbf{14}]_0 \times k_{\text{obs}}^{-1} / \text{Ms}$
5.33×10^{-5}	1.04×10^{-3}	9.62×10^2	20	1.07×10^{-3}	9.72×10^{-1}
5.32×10^{-5}	1.57×10^{-3}	6.37×10^2	30	2.22×10^{-3}	7.07×10^{-1}
5.29×10^{-5}	2.08×10^{-3}	4.81×10^2	39	3.44×10^{-3}	6.05×10^{-1}
5.27×10^{-5}	2.58×10^{-3}	3.88×10^2	49	5.27×10^{-3}	4.90×10^{-1}
5.26×10^{-5}	3.09×10^{-3}	3.24×10^2	59	7.38×10^{-3}	4.19×10^{-1}



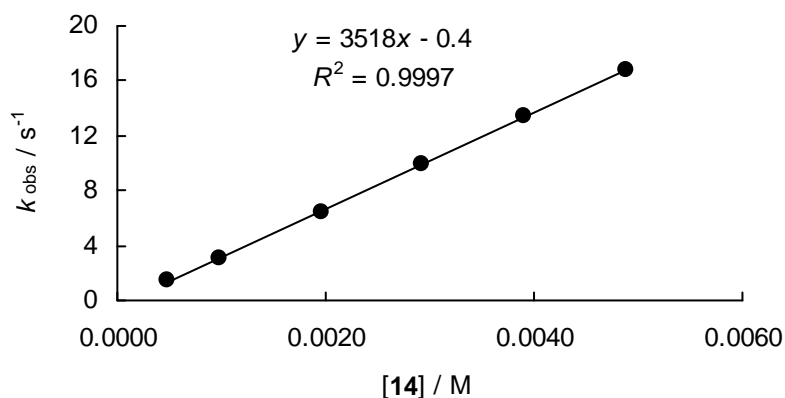
Rate constants for the reactions of piperidine (**14**) with $\text{tol}(t\text{-Bu})_2\text{QM}$ (**1b**) in CH_3CN (diode array spectrophotometer, 20 °C, $\lambda = 371 \text{ nm}$).

$[\mathbf{1b}]_0 / \text{M}$	$[\mathbf{14}]_0 / \text{M}$	$[\mathbf{14}]_0^{-1} / \text{M}^{-1}$	$[\mathbf{14}]_0 / [\mathbf{1b}]_0$	$k_{\text{obs}} / \text{s}^{-1}$	$[\mathbf{14}]_0 \times k_{\text{obs}}^{-1} / \text{Ms}$
6.10×10^{-5}	1.61×10^{-3}	6.21×10^2	26	3.94×10^{-3}	4.09×10^{-1}
6.25×10^{-5}	2.47×10^{-3}	4.05×10^2	40	8.34×10^{-3}	2.96×10^{-1}
6.23×10^{-5}	3.28×10^{-3}	3.05×10^2	53	1.32×10^{-2}	2.48×10^{-1}
6.00×10^{-5}	3.96×10^{-3}	2.53×10^2	66	1.83×10^{-2}	2.16×10^{-1}
6.20×10^{-5}	4.91×10^{-3}	2.04×10^2	79	2.64×10^{-2}	1.86×10^{-1}
6.18×10^{-5}	5.70×10^{-3}	1.75×10^2	92	3.31×10^{-2}	1.72×10^{-1}



Rate constants for the reactions of piperidine (**14**) with ani(Ph)₂QM (**1c**) in CH₃CN (Stopped-flow, 20 °C, $\lambda = 422$ nm).

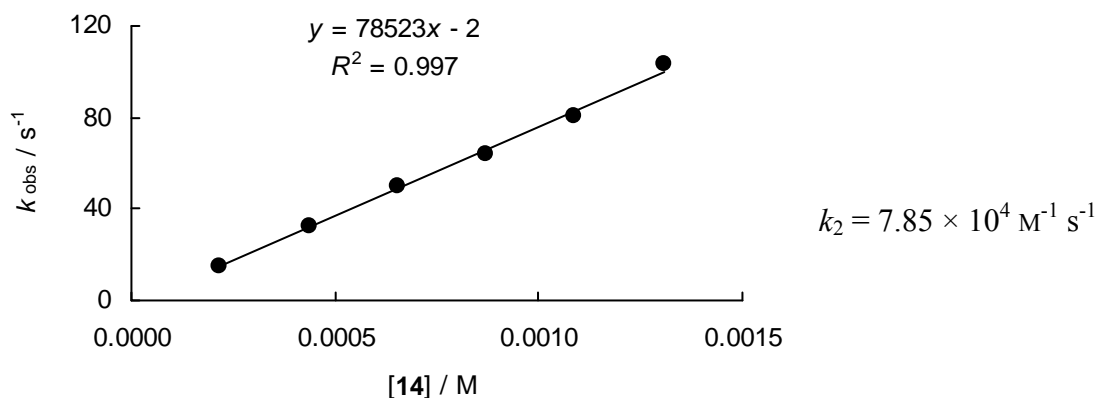
[1c] ₀ / M	[14] ₀ / M	[14] ₀ / [1c] ₀	k_{obs} / s ⁻¹
4.80×10^{-5}	4.89×10^{-4}	10	1.47
4.80×10^{-5}	9.77×10^{-4}	20	3.02
4.80×10^{-5}	1.95×10^{-3}	41	6.37
4.80×10^{-5}	2.93×10^{-3}	61	9.87
4.80×10^{-5}	3.91×10^{-3}	81	1.35×10^1
4.80×10^{-5}	4.89×10^{-3}	102	1.68×10^1



$$k_2 = 3.52 \times 10^3 \text{ M}^{-1} \text{ s}^{-1}$$

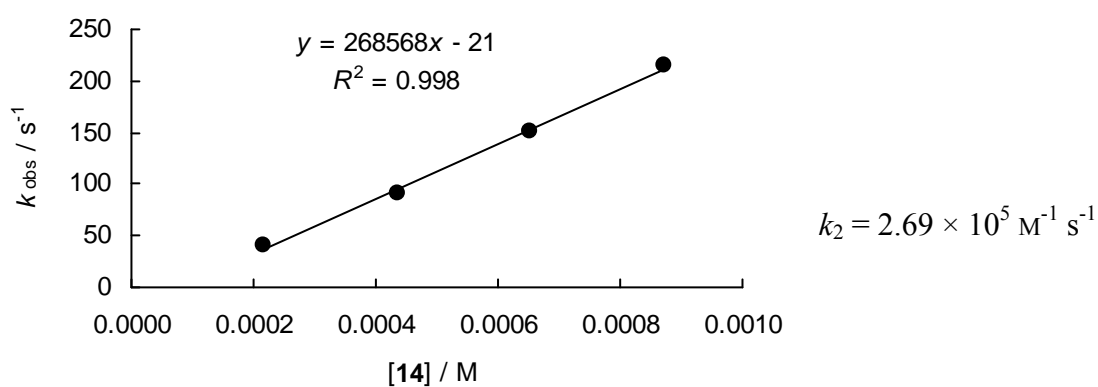
Rate constants for the reactions of piperidine (**14**) with (lil)₂CH⁺BF₄⁻ (**1d**) in CH₃CN (Stopped-flow, 20 °C, $\lambda = 639$ nm).

[1d] ₀ / M	[14] ₀ / M	[14] ₀ / [1d] ₀	k_{obs} / s ⁻¹
1.91×10^{-5}	2.18×10^{-4}	11	1.53×10^1
1.91×10^{-5}	4.36×10^{-4}	23	3.23×10^1
1.91×10^{-5}	6.54×10^{-4}	34	4.97×10^1
1.91×10^{-5}	8.71×10^{-4}	46	6.38×10^1
1.91×10^{-5}	1.09×10^{-3}	57	8.10×10^1
1.91×10^{-5}	1.31×10^{-3}	68	1.03×10^2



Rate constants for the reactions of piperidine (**14**) with $(\text{jul})_2\text{CH}^+\text{BF}_4^-$ (**1e**) in CH_3CN (Stopped-flow, 20 °C, $\lambda = 642 \text{ nm}$).

$[\mathbf{1e}]_0 / \text{M}$	$[\mathbf{14}]_0 / \text{M}$	$[\mathbf{14}]_0 / [\mathbf{1e}]_0$	$k_{\text{obs}} / \text{s}^{-1}$
2.16×10^{-5}	2.18×10^{-4}	10	3.98×10^1
2.16×10^{-5}	4.36×10^{-4}	20	9.19×10^1
2.16×10^{-5}	6.54×10^{-4}	30	1.51×10^2
2.16×10^{-5}	8.71×10^{-4}	40	2.15×10^2

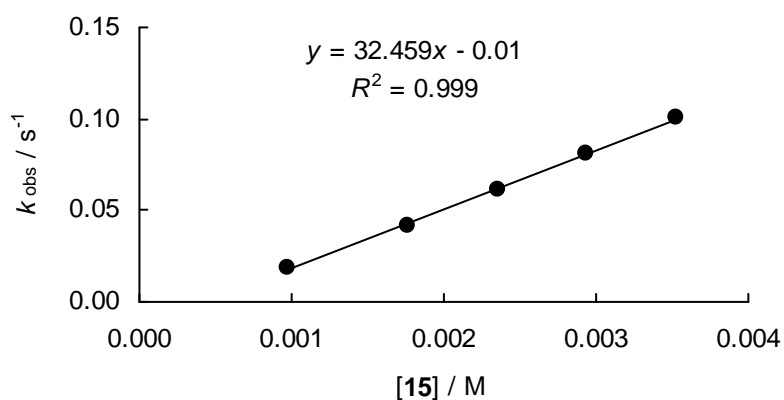


Kinetics of the reactions of benzhydrylium ions and quinone methides (1) with pyrrolidine (15)

Rate constants for the reactions of pyrrolidine (**15**) with ani(^t-Bu)₂QM (**1a**) in CH₃CN (diode array spectrophotometer or Stopped-flow, 20 °C, λ = 393 nm).

[1a] ₀ / M	[15] ₀ / M	[15] ₀ / [1a] ₀	k _{obs} / s ⁻¹
5.90 × 10 ⁻⁵	9.79 × 10 ⁻⁴	17	1.85 × 10 ⁻² [a]
4.25 × 10 ⁻⁵	1.76 × 10 ⁻³	41	4.14 × 10 ⁻² [b]
4.25 × 10 ⁻⁵	2.35 × 10 ⁻³	55	6.16 × 10 ⁻² [b]
4.25 × 10 ⁻⁵	2.94 × 10 ⁻³	69	8.05 × 10 ⁻² [b]
4.25 × 10 ⁻⁵	3.53 × 10 ⁻³	83	1.01 × 10 ⁻¹ [b]

[a] diode array spectrometer; [b] Stopped-flow.

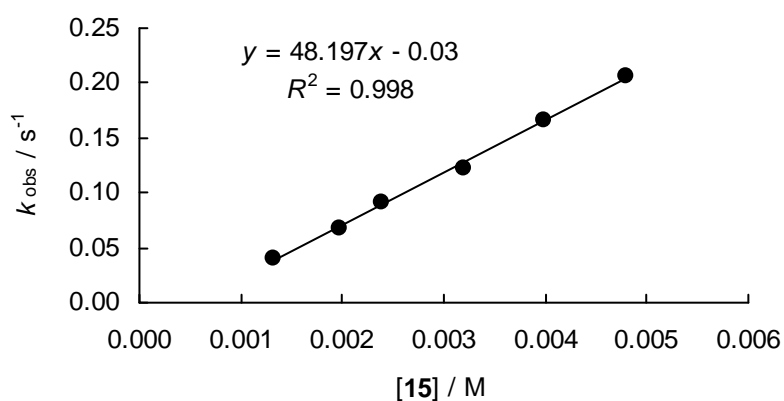


$$k_2 = 3.25 \times 10^1 \text{ M}^{-1} \text{ s}^{-1}$$

Rate constants for the reactions of pyrrolidine (**15**) with tol(*t*-Bu)₂QM (**1b**) in CH₃CN (diode array spectrophotometer or Stopped-flow, 20 °C, λ = 371 nm).

[1b] ₀ / M	[15] ₀ / M	[15] ₀ / [1b] ₀	<i>k</i> _{obs} / s ⁻¹
7.21 × 10 ⁻⁵	1.33 × 10 ⁻³	18	3.96 × 10 ⁻² [a]
7.13 × 10 ⁻⁵	1.97 × 10 ⁻³	28	6.77 × 10 ⁻² [a]
5.20 × 10 ⁻⁵	2.39 × 10 ⁻³	46	9.10 × 10 ⁻² [b]
5.20 × 10 ⁻⁵	3.19 × 10 ⁻³	61	1.22 × 10 ⁻¹ [b]
5.20 × 10 ⁻⁵	3.99 × 10 ⁻³	77	1.66 × 10 ⁻¹ [b]
5.20 × 10 ⁻⁵	4.79 × 10 ⁻³	92	2.07 × 10 ⁻¹ [b]

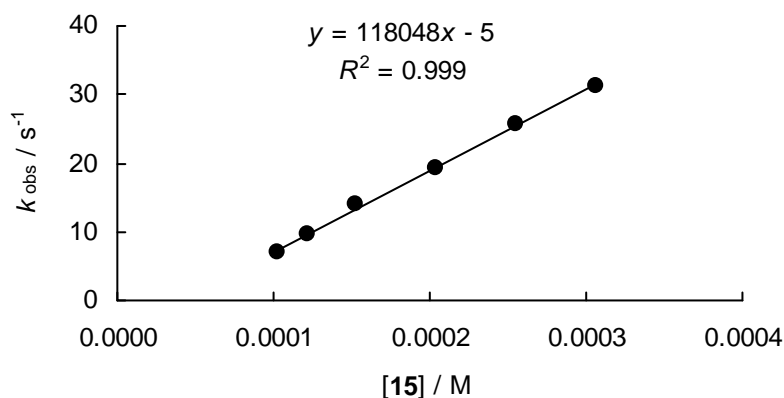
[a] diode array spectrometer; [b] Stopped-flow.



$$k_2 = 4.82 \times 10^1 \text{ M}^{-1} \text{ s}^{-1}$$

Rate constants for the reactions of pyrrolidine (**15**) with $(\text{lil})_2\text{CH}^+\text{BF}_4^-$ (**1d**) in CH_3CN (Stopped-flow, 20 °C, $\lambda = 639$ nm).

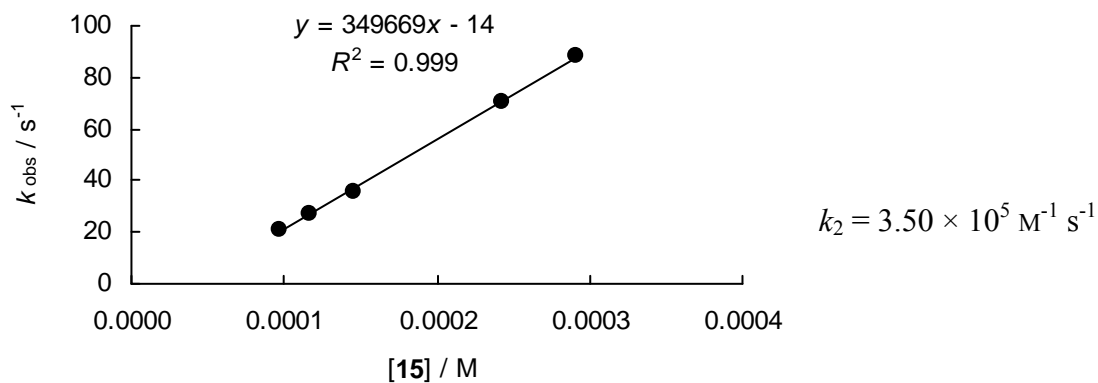
$[\mathbf{1d}]_0 / \text{M}$	$[\mathbf{15}]_0 / \text{M}$	$[\mathbf{15}]_0 / [\mathbf{1d}]_0$	$k_{\text{obs}} / \text{s}^{-1}$
6.73×10^{-6}	1.02×10^{-4}	15	7.07
6.73×10^{-6}	1.22×10^{-4}	18	9.72
6.73×10^{-6}	1.53×10^{-4}	23	1.40×10^1
6.73×10^{-6}	2.04×10^{-4}	30	1.93×10^1
6.73×10^{-6}	2.55×10^{-4}	38	2.56×10^1
6.73×10^{-6}	3.06×10^{-4}	45	3.13×10^1



$$k_2 = 1.18 \times 10^5 \text{ M}^{-1} \text{ s}^{-1}$$

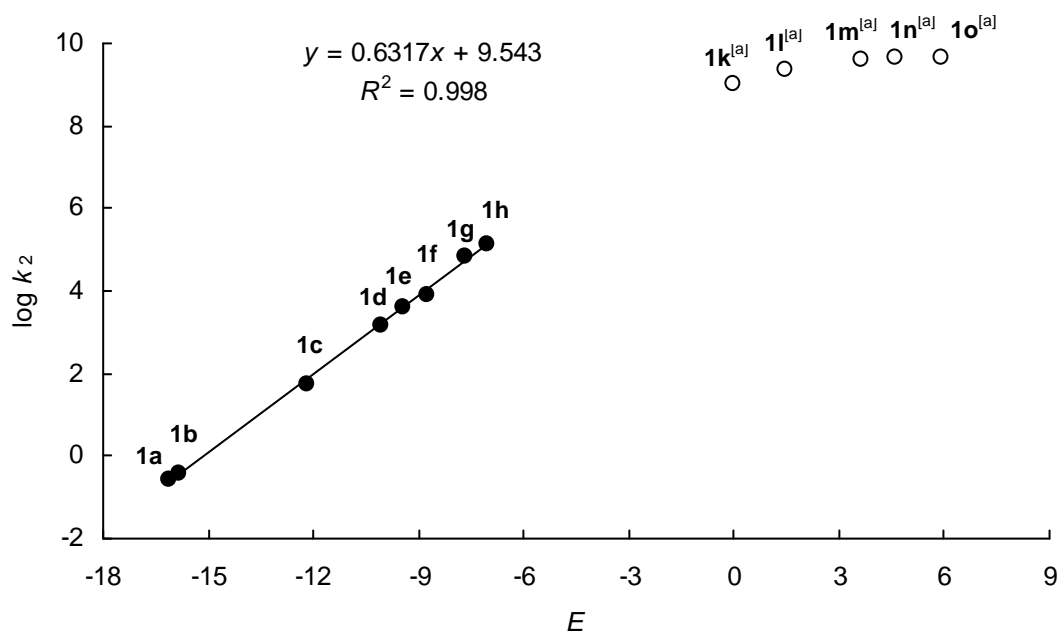
Rate constants for the reactions of pyrrolidine (**15**) with $(\text{jul})_2\text{CH}^+\text{BF}_4^-$ (**1e**) in CH_3CN (Stopped-flow, 20 °C, $\lambda = 642$ nm).

$[\mathbf{1e}]_0 / \text{M}$	$[\mathbf{15}]_0 / \text{M}$	$[\mathbf{15}]_0 / [\mathbf{1e}]_0$	$k_{\text{obs}} / \text{s}^{-1}$
6.39×10^{-6}	9.70×10^{-5}	15	2.08×10^1
6.39×10^{-6}	1.16×10^{-4}	18	2.71×10^1
6.39×10^{-6}	1.46×10^{-4}	23	3.58×10^1
6.39×10^{-6}	2.43×10^{-4}	38	7.05×10^1
6.39×10^{-6}	2.91×10^{-4}	45	8.86×10^1



Correlations analysis

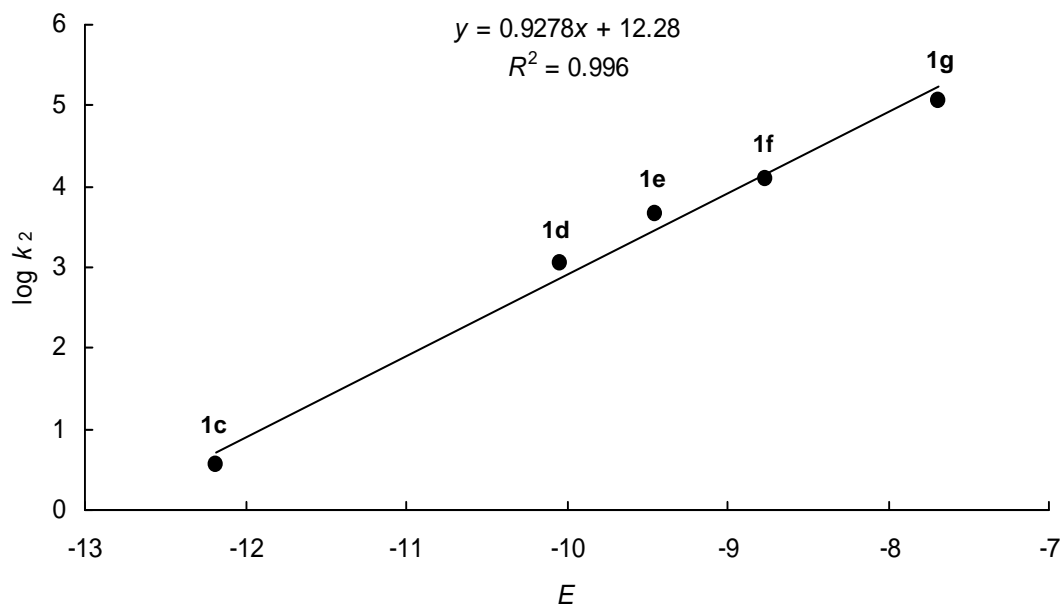
Plot of $\log k_2$ versus E for the reactions of *n*-propylamine (8).



^[a] rate constants taken from rate constants taken from ref [9b]; not included for the determination of N and s parameter due to diffusion control

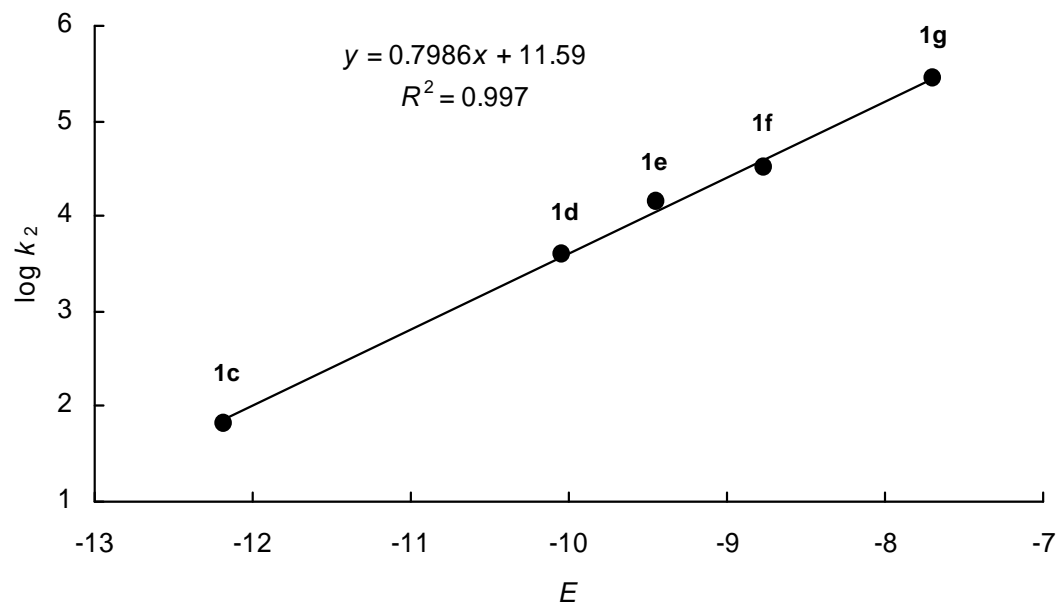
$$N = 15.11, s = 0.63$$

Plot of $\log k_2$ versus E for the reactions of *N,N*-bis(2-methoxyethyl)amine (**10**).



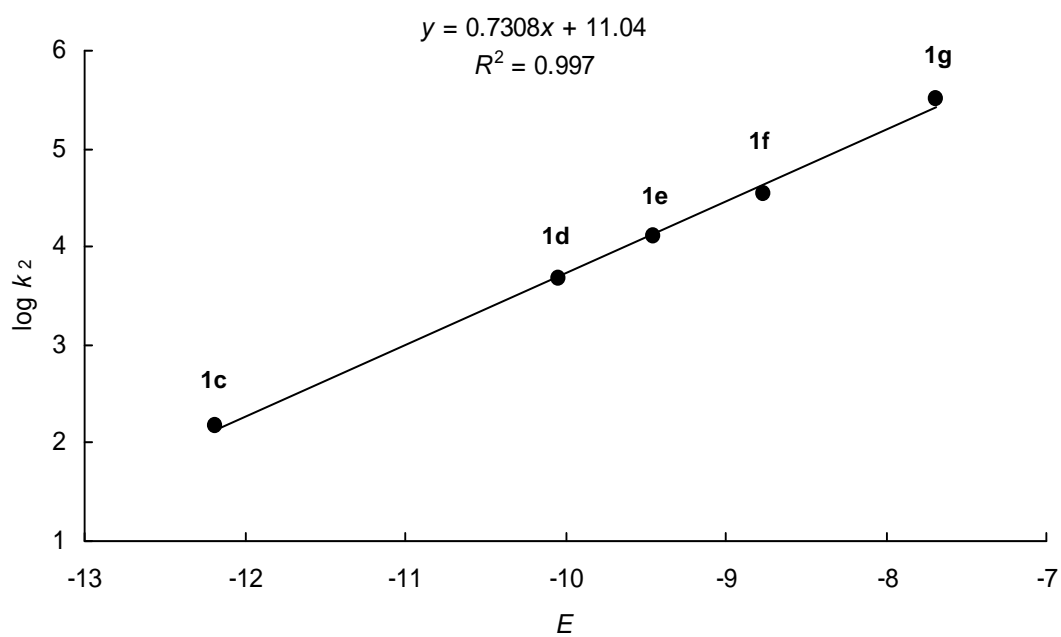
$$N = 13.24, s = 0.93$$

Plot of $\log k_2$ versus E for the reactions of di-*n*-propylamine (**11**).



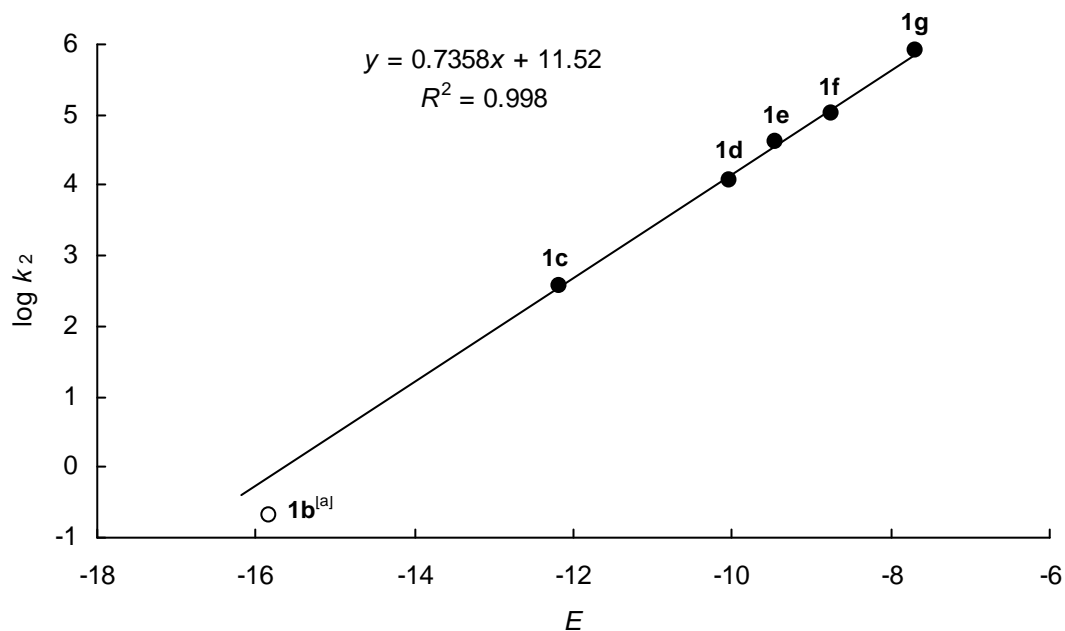
$$N = 14.51, s = 0.80$$

Plot of $\log k_2$ versus E for the reactions of diethylamine (**12**).



$$N = 15.10, s = 0.73$$

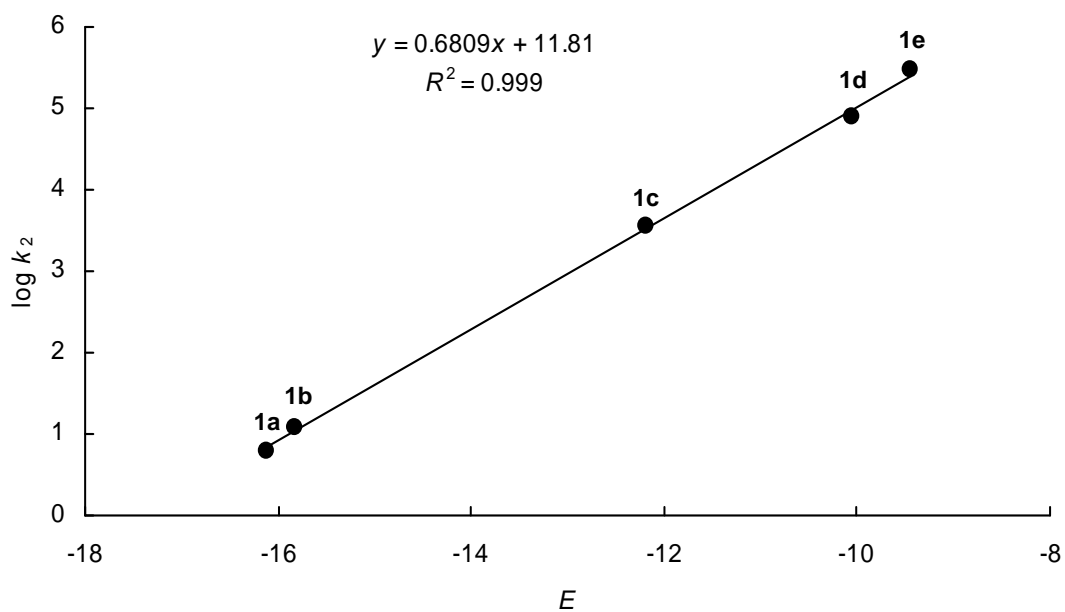
Plot of $\log k_2$ versus E for the reactions of morpholine (**13**).



^[a] not included for the determination of the N - and s -parameters due to the low accuracy of the determination of k_2 (only 3 k_{obs} values measured which correlate moderately)

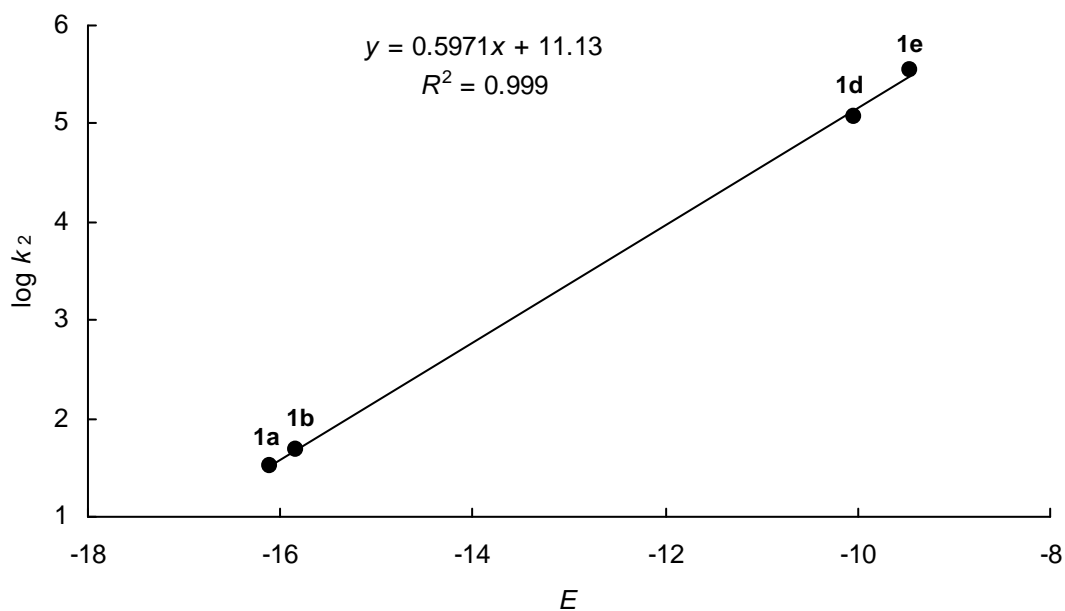
$$N = 15.65, s = 0.74$$

Plot of $\log k_2$ versus E for the reactions of piperidine (**14**).



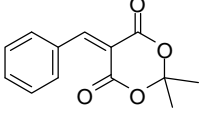
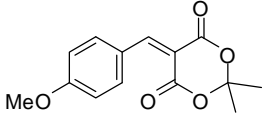
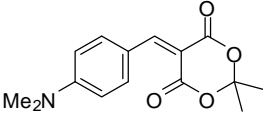
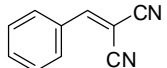
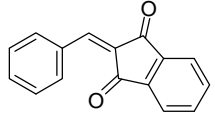
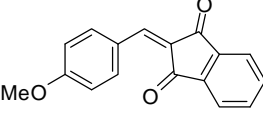
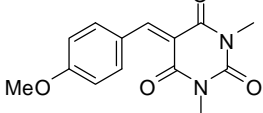
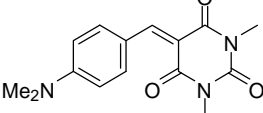
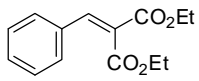
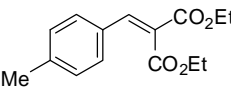
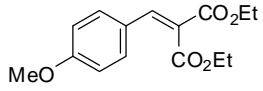
$$N = 17.35, s = 0.68$$

Plot of $\log k_2$ versus E for the reactions of pyrrolidine (**15**).



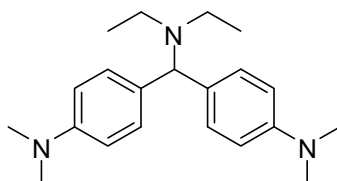
$$N = 18.64, s = 0.60$$

Comparison of calculated and experimental rate constants ($M^{-1}s^{-1}$) for the additions of amines to Michael acceptors in acetonitrile

Electrophile	E	Amine	N / s	k_{calc} (20 °C) ^[f]	k_{exp}
	-9.15 ^[a]	14	17.35 / 0.68	3.8×10^5	2.3×10^6 (25 °C) ^[g]
		13	15.65 / 0.74	6.5×10^4	4.0×10^5 (25 °C) ^[g]
		6	14.29 / 0.67	2.8×10^3	8.7×10^1 (20 °C) ^[h]
	-10.28 ^[a]	14	17.35 / 0.68	6.4×10^4	9.5×10^5 (25 °C) ^[g]
		6	14.29 / 0.67	4.9×10^2	6.7×10^1 (20 °C) ^[h]
	-12.76 ^[a]	14	17.35 / 0.68	1.3×10^3	1.1×10^5 (25 °C) ^[g]
	-9.42 ^[b]	6	14.29 / 0.67	1.8×10^3	1.5×10^0 (20 °C) ^[i]
	-10.11 ^[c]	6	14.29 / 0.67	6.3×10^2	1.5×10^0 (25 °C) ^[j]
		6	14.29 / 0.67	9.8×10^1	1.1×10^0 (25 °C) ^[j]
	-11.32 ^[c]	6	14.29 / 0.67	9.8×10^1	1.1×10^0 (25 °C) ^[j]
		6	14.29 / 0.67	9.8×10^1	1.1×10^0 (25 °C) ^[j]
	-10.37 ^[d]	14	17.35 / 0.68	5.6×10^4	3.2×10^5 (25 °C) ^[g]
		14	17.35 / 0.68	5.6×10^4	3.2×10^5 (25 °C) ^[g]
	-12.76 ^[d]	14	17.35 / 0.68	1.3×10^3	2.9×10^4 (25 °C) ^[g]
		14	17.35 / 0.68	1.3×10^3	2.9×10^4 (25 °C) ^[g]
	-20.55 ^[e]	6	14.29 / 0.67	6.4×10^{-5}	2.5×10^{-2} (20 °C) ^[k]
		6	14.29 / 0.67	6.4×10^{-5}	2.5×10^{-2} (20 °C) ^[k]
	-21.11 ^[e]	6	14.29 / 0.67	2.7×10^{-5}	1.8×10^{-2} (20 °C) ^[k]
		6	14.29 / 0.67	2.7×10^{-5}	1.8×10^{-2} (20 °C) ^[k]
	-21.47 ^[e]	6	14.29 / 0.67	1.5×10^{-5}	1.3×10^{-2} (20 °C) ^[k]

[a] Ref. [20c]; [b] ref. [23]; [c] ref. [20a]; [d] ref. [20b]; [e] ref. [24]; [f] calculated on the basis of $\log k_2$ (20 °C) = $s(N + E)$; [g] ref. [1b]; [h] ref. [1w]; [i] ref. [1m]; [j] ref. [1q]; [k] ref. [1y].

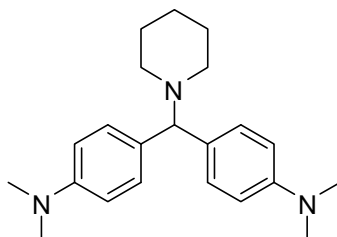
2.4.3 Synthetic Experiments

[Bis-(4-dimethylaminophenyl)methyl]-diethylamine (**12h**)**12h**

A solution of diethylamine (**12**, 77 μ L, 0.74 mmol) in 3 mL acetonitrile was added to a solution of $(\text{dma})_2\text{CH}^+\text{BF}_4^-$ (**1h**, 69 mg, 0.20 mmol) in acetonitrile (10 mL) over 5 min. at 20 °C. The solvent was removed under reduced pressure, the remaining solid was extracted with diethyl ether after which the ether was evaporated: **12h** (29 mg, 0.089 mmol, 45%) colorless crystals.

$^1\text{H-NMR}$ (400 MHz, CD_3CN) δ = 0.93 (t, J = 7.1 Hz, 6 H, $2 \times \text{CH}_2\text{CH}_3$), 2.55 (q, J = 7.1 Hz, 4 H, $2 \times \text{CH}_2\text{CH}_3$), 2.85 (s, 12 H, $2 \times \text{NMe}_2$), 4.50 (s, 1 H, Ar_2CH), 6.66 (d, J = 8.9 Hz, 4 H, H_{ar}), 7.22 (d, J = 8.8 Hz, 4 H, H_{ar}).

$^{13}\text{C-NMR}$ (100 MHz, CD_3CN) δ = 11.3 (q), 41.0 (q), 43.5 (t), 70.9 (d, Ar_2CH), 113.5 (d), 129.3 (d), 133.6 (s), 150.7 (s).

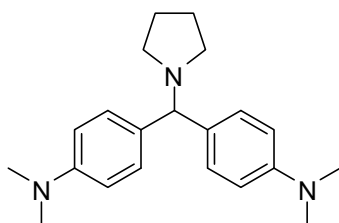
N-[Bis-(4-dimethylaminophenyl)methyl]-piperidine (**14h**)**14h**

A solution of piperidine (**14**, 77 μ L, 0.78 mmol) in 3 mL acetonitrile was added to a solution of $(\text{dma})_2\text{CH}^+\text{BF}_4^-$ (**1h**, 86 mg, 0.25 mmol) in acetonitrile (10 mL) over 5 min. at 20 °C. The solvent was removed under reduced pressure, the remaining solid was extracted with diethyl ether after which the ether was evaporated: **14h** (60 mg, 0.18 mmol, 71%) colorless crystals.

$^1\text{H-NMR}$ (400 MHz, CD_3CN) $\delta = 1.38\text{--}1.45$ (m, 2 H, CH_2), 1.49–1.55 (m, 4 H, 2 \times CH_2), 2.23–2.30 (m, 4 H, 2 \times NCH_2) 2.84 (s, 12 H, 2 \times NMe_2), 3.99 (s, 1 H, Ar_2CH), 6.66 (d, $J = 8.9$ Hz, 4 H, H_{ar}), 7.18 (d, $J = 8.9$ Hz, 4 H, H_{ar}).

$^{13}\text{C-NMR}$ (100 MHz, CD_3CN) $\delta = 25.6$ (t), 27.1 (t), 41.0 (q), 53.9 (t), 76.2 (d, Ar_2CH), 113.6 (d), 129.2 (d), 134.3 (s), 150.8 (s).

N-[Bis-(4-dimethylaminophenyl)methyl]-pyrrolidine (**15h**)



15h

A solution of pyrrolidine (**15**, 48 μL , 0.58 mmol) in 3 mL acetonitrile was added to a solution of $(\text{dma})_2\text{CH}^+\text{BF}_4^-$ (**1h**, 57 mg, 0.17 mmol) in acetonitrile (10 mL) over 5 min. at 20 $^\circ\text{C}$. The solvent was removed under reduced pressure, the remaining solid was extracted with diethyl ether after which the ether was evaporated: **15h** (37 mg, 0.11 mmol, 67%) colorless crystals.

$^1\text{H-NMR}$ (400 MHz, CD_3CN) $\delta = 1.70\text{--}1.75$ (m, 4 H, 2 \times NCH_2CH_2), 2.34–2.38 (m, 4 H, 2 \times NCH_2) 2.84 (s, 12 H, 2 \times NMe_2), 3.97 (s, 1 H, Ar_2CH), 6.65 (d, $J = 8.9$ Hz, 4 H, H_{ar}), 7.23 (d, $J = 8.8$ Hz, 4 H, H_{ar}).

$^{13}\text{C-NMR}$ (100 MHz, CD_3CN) $\delta = 24.4$ (t), 41.0 (q), 54.3 (t), 75.8 (d, Ar_2CH), 113.6 (d), 128.7 (d), 134.6 (s), 150.8 (s).

2.5 References

- [1] a) W. P. Jencks, M. Gilchrist, *J. Am. Chem. Soc.* **1968**, *90*, 2622–2637. b) B. Schreiber, H. Martinek, P. Wolschann, P. Schuster, *J. Am. Chem. Soc.* **1979**, *101*, 4708–4713. c) L. A. P. Kane-Maguire, E. D. Honig, D. A. Sweigart, *Chem. Rev.* **1984**, *84*, 525–543. d) C. D. Ritchie, *Can. J. Chem.* **1986**, *64*, 2239–2250. e) C. F. Bernasconi, M. Panda, *J. Org. Chem.* **1987**, *52*, 3042–3050. f) Z. Rappoport, A. Topol, *J. Org. Chem.* **1989**, *54*, 5967–5977. g) N. S. Nudelman, *J. Phys. Org. Chem.* **1989**, *2*, 1–14. h) C. F. Bernasconi, M. W. Stronach, *J. Am. Chem. Soc.* **1991**, *113*, 2222–2227. i) J. P. Richard, T. L. Amyes, T. Vontor, *J. Am. Chem. Soc.* **1992**, *114*, 5626–5634. j) C. F. Bernasconi, A. E. Leyes, *J. Am. Chem. Soc.* **1993**, *115*, 7513–7514. k) L. García-Río, E. Iglesias, J. R. Leis, M. E. Peña, A. Ríos, *J. Chem. Soc. Perkin Trans. 2* **1993**, 29–37. l) C. K. M. Heo, J. W. Bunting, *J. Chem. Soc. Perkin Trans. 2* **1994**, 2279–2290. m) B. Varghese, S. Kothari, K. K. Banerji, *Int. J. Chem. Kinet.* **1999**, *31*, 245–252. n) A. D. Allen, T. T. Tidwell, *J. Org. Chem.* **1999**, *64*, 266–271. o) M. R. Crampton, J. Delaney, L. C. Rabbitt, *J. Chem. Soc. Perkin Trans. 2* **1999**, 2473–2480. p) J. P. Richard, M. M. Toteva, J. Crueiras, *J. Am. Chem. Soc.* **2000**, *122*, 1664–1674. q) H. K. Oh, J. H. Yang, H. W. Lee, *J. Org. Chem.* **2000**, *65*, 5391–5395. r) I.-H. Um, J.-S. Min, J.-A. Ahn, H.-J. Hahn, *J. Org. Chem.* **2000**, *65*, 5659–5663. s) C. F. Bernasconi, C. Whitesell, R. A. Johnson, *Tetrahedron* **2000**, *56*, 4917–4924. t) E. A. Castro, M. G. Ruiz, J. G. Santos, *Int. J. Chem. Kinet.* **2001**, *33*, 281–287. u) N. C. de Lucas, J. C. Netto-Ferreira, J. Andraos, J. C. Scaiano, *J. Org. Chem.* **2001**, *66*, 5016–5021. v) D. Rajarathnam, T. Jeyakumar, P. A. Nadar, *Int. J. Chem. Kinet.* **2002**, *34*, 366–373. w) H. K. Oh, T. S. Kim, H. W. Lee, I. Lee, *Bull. Korean Chem. Soc.* **2003**, *24*, 193–196. x) P. M. Mancini, G. G. Fortunato, L. R. Vottero, *J. Phys. Org. Chem.* **2004**, *17*, 138–147. y) H. K. Oh, I. K. Kim, H. W. Lee, I. Lee, *J. Org. Chem.* **2004**, *69*, 3806–3810. z) M. R. Crampton, T. A. Emokpae, C. Isanbor, *J. Phys. Org. Chem.* **2006**, *19*, 75–80.
- [2] a) C. G. Swain, C. B. Scott, *J. Am. Chem. Soc.* **1953**, *75*, 141–147. b) C. D. Ritchie, *Acc. Chem. Res.* **1972**, *5*, 348–354. (c) C. D. Ritchie, R. J. Minasz, A. A. Kamego, M. Sawada, *J. Am. Chem. Soc.* **1977**, *99*, 3747–3753. d) C. D. Ritchie, C. Kubisty, G. Y. Ting, *J. Am. Chem. Soc.* **1983**, *105*, 279–284.
- [3] H. Mayr, M. Patz, *Angew. Chem.* **1994**, *106*, 990–1010; *Angew. Chem. Int. Ed. Engl.* **1994**, *33*, 938–957.

- [4] a) S. Minegishi, H. Mayr, *J. Am. Chem. Soc.* **2003**, *125*, 286–295. b) F. Brotzel, Y. C. Chu, H. Mayr, *J. Org. Chem.* **2007**, *72*, 3679–3688.
- [5] a) H. Mayr, T. Bug, M. F. Gotta, N. Hering, B. Irrgang, B. Janker, B. Kempf, R. Loos, A. R. Ofial, G. Remennikov, H. Schimmel, *J. Am. Chem. Soc.* **2001**, *123*, 9500–9512. b) R. Lucius, R. Loos, H. Mayr, *Angew. Chem.* **2002**, *114*, 97–102; *Angew. Chem. Int. Ed.* **2002**, *41*, 91–95. c) H. Mayr, B. Kempf, A. R. Ofial, *Acc. Chem. Res.* **2003**, *36*, 66–77. d) H. Mayr, A. R. Ofial, *Pure Appl. Chem.* **2005**, *77*, 1807–1821. e) H. Mayr, A. R. Ofial, *J. Phys. Org. Chem.* **2008**, *21*, 584–595.
- [6] T. B. Phan, C. Nolte, S. Kobayashi, A. R. Ofial, H. Mayr, *J. Am. Chem. Soc.* **2009**, *131*, 11392–11401.
- [7] T. B. Phan, M. Breugst, H. Mayr, *Angew. Chem.* **2006**, *118*, 3954–3959; *Angew. Chem. Int. Ed.* **2006**, *45*, 3869–3874.
- [8] a) W. P. Jencks, *Chem. Soc. Rev.* **1981**, *10*, 345–375. b) J. P. Richards in *Advances in Carbocation Chemistry* (Ed.: X. Creary), JAI Press, Greenwich, London, **1989**; vol. 1, pp 121–169. c) T. L. Amyes, M. M. Toteva, J. P. Richard in *Reactive Intermediate Chemistry* (Eds.: R. A. Moss, M. S. Platz, M. Jones Jr.), Wiley-Interscience, Hoboken, NJ, **2004**, pp. 41–68. d) J. P. Richard, T. L. Amyes, M. M. Toteva, Y. Tsuji, *Adv. Phys. Org. Chem.* **2004**, *39*, 1–26.
- [9] a) R. A. McClelland, N. Banait, S. Steenken, *J. Am. Chem. Soc.* **1989**, *111*, 2929–2935. b) R. A. McClelland, V. M. Kanagasabapathy, N. S. Banait, S. Steenken, *J. Am. Chem. Soc.* **1992**, *114*, 1816–1823. c) R. A. McClelland in *Reactive Intermediate Chemistry* (Eds.: R. A. Moss, M. S. Platz, M. Jones Jr.), Wiley-Interscience, Hoboken, NJ, **2004**, pp. 3–40.
- [10] a) J. Bartl, S. Steenken, H. Mayr, R. A. McClelland, *J. Am. Chem. Soc.* **1990**, *112*, 6918–6928. b) J. Bartl, S. Steenken, H. Mayr, *J. Am. Chem. Soc.* **1991**, *113*, 7710–7716. c) S. Minegishi, R. Loos, S. Kobayashi, H. Mayr, *J. Am. Chem. Soc.* **2005**, *127*, 2641–2649.
- [11] H. Mayr, A. R. Ofial, *Angew. Chem.* **2006**, *118*, 1876–1886; *Angew. Chem. Int. Ed.* **2006**, *45*, 1844–1854.
- [12] a) I.-H. Um, S. Yoon, H.-R. Park, H.-J. Han, *Org. Biomol. Chem.* **2008**, *6*, 1618–1624. b) E. A. Castro, *Pure Appl. Chem.* **2009**, *81*, 685–696.
- [13] I.-H. Um, J.-A. Seok, H.-T. Kim, S.-K. Bae, *J. Org. Chem.* **2003**, *68*, 7742–7746.
- [14] M. J. Pfeiffer, S. B. Hanna, *J. Org. Chem.* **1993**, *58*, 735–740.

- [15] M. Baidya, S. Kobayashi, F. Brotzel, U. Schmidhammer, E. Riedle, H. Mayr, *Angew. Chem.* **2007**, *119*, 6288–6292; *Angew. Chem. Int. Ed.* **2007**, *46*, 6176–6179.
- [16] F. Brotzel, B. Kempf, T. Singer, H. Zipse, H. Mayr, *Chem. Eur. J.* **2007**, *13*, 336–345.
- [17] T. A. Nigst, M. Westermaier, A. R. Ofial, H. Mayr, *Eur. J. Org. Chem.* **2008**, 2369–2374.
- [18] T. Tokuyasu, H. Mayr, *Eur. J. Org. Chem.* **2004**, 2791–2796.
- [19] a) R. P. Bell, *The Proton in Chemistry*, Methuen, London, **1959**, 159.
b) J. F. Coetzee, G. R. Padmanabhan, *J. Am. Chem. Soc.* **1965**, *87*, 5005–5010. c) I. Kaljurand, T. Rodima, I. Leito, I. A. Koppel, R. Schwesinger, *J. Org. Chem.* **2000**, *65*, 6202–6208. d) I. Kaljurand, A. Kütt, L. Sooväli, T. Rodima, V. Mäemets, I. Leito, I. A. Koppel, *J. Org. Chem.* **2005**, *70*, 1019–1028.
- [20] a) S. T. A. Berger, F. H. Seeliger, F. Hofbauer, H. Mayr, *Org. Biomol. Chem.* **2007**, *5*, 3020–3026. b) F. Seeliger, S. T. A. Berger, G. Y. Remennikov, K. Polborn, H. Mayr, *J. Org. Chem.* **2007**, *72*, 9170–9180. c) O. Kaumanns, H. Mayr, *J. Org. Chem.* **2008**, *73*, 2738–2745. See also: d) C. F. Bernasconi, *Tetrahedron* **1989**, *45*, 4017–4090.
- [21] For a discussion of the Hughes-Ingold rules and their limitation see C. Reichardt in *Solvents and Solvent Effects in Organic Chemistry* 3rd, (Ed.: H. F. Ebel), Wiley-VCH, Weinheim, **2003**, pp. 163, 215.
- [22] a) S. Evans, P. Nesvadba, S. Allenbach, Ciba-Geigy AG, EP-B744392, 1996; *Chem. Abstr.* **1997**, *126*, 46968v. b) R. Lucius; H. Mayr, *Angew. Chem.* **2000**, *112*, 2086–2089; *Angew. Chem. Int. Ed.* **2000**, *39*, 1995–1997. c) D. Richter, N. Hampel, T. Singer, A. R. Ofial, H. Mayr, *Eur. J. Org. Chem.* **2009**, 3203–3211.
- [23] T. Lemek, H. Mayr, *J. Org. Chem.* **2003**, *68*, 6880–6886.
- [24] O. Kaumanns, R. Lucius, H. Mayr, *Chem. Eur. J.* **2008**, *14*, 9675–9682.

Chapter 3

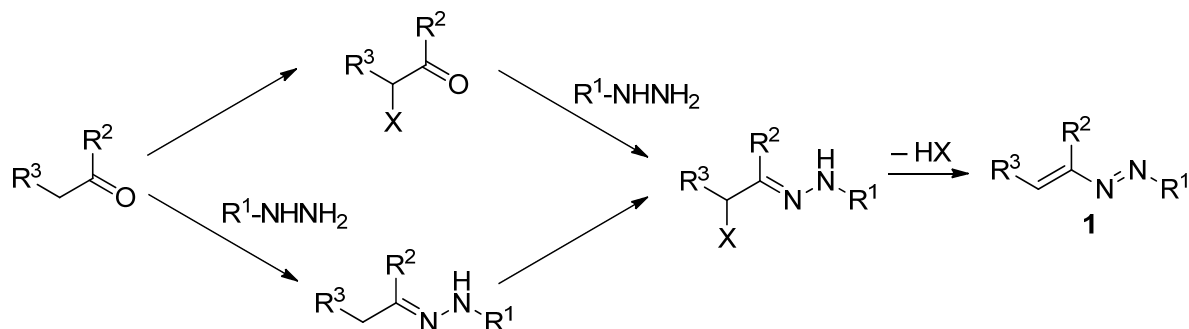
ELECTROPHILIC REACTIVITIES OF 1,2-DIAZA-1,3-DIENES

Tanja Kanzian, Simona Nicolini, Lucia De Crescentini, Orazio A. Attanasi, Armin R. Ofial and Herbert Mayr, *Chem. Eur. J.* **2010**, *16*, 12008-12016.

Results obtained by S. Nicolini are not listed in the Experimental Section.

3.1 Introduction

In recent years 1,2-diaza-1,3-dienes **1** have become increasingly important as tools for the construction of a variety of heterocycles.^[1] The electron withdrawing effect of the azo group in the heterodiene system controls the regioselectivity of the nucleophilic attack at the terminal carbon. This regioselectivity is further enhanced by appropriate electron withdrawing groups at the terminal carbon and/or nitrogen atom of the conjugated azo-ene system. As a consequence, typical reactions of conjugated azoalkenes with a variety of carbon, nitrogen, oxygen, phosphorus, sulfur, and selenium nucleophiles result in the formation of 1,4-hydrazone adducts by Michael-type addition. From these intermediates, different intramolecular cyclizations lead to a variety of five- and six-membered heterocycles, e.g. pyrroles, pyrazoles, imidazoles, thiazoles, selenazoles, 1,2,3-thiadiazoles, 1,2,3-selenadiazoles, 1,2,3-diazaphospholes, pyridazines, pyrazines, 1,4-thiazines, 1,2,4-triazines, and 1,2,4-oxadiazines. In many cases, the 1,4-additions of nucleophiles at 1,2-diaza-1,3-dienes are accompanied by spontaneous subsequent formations of heterocycles. Accordingly heterocycles are frequently accessible by one-pot syntheses that do not require the use of anhydrous solvents or work under an inert atmosphere. Another advantage which makes **1** attractive intermediates in organic chemistry is their good accessibility. Usually they are synthesized by elimination of a leaving group X in the α -position of a hydrazone. The leaving group X can either be present in the starting material, that is a cyclic or acyclic carbonyl compound, or it can be introduced in the hydrazone derivative (Scheme 3.1).

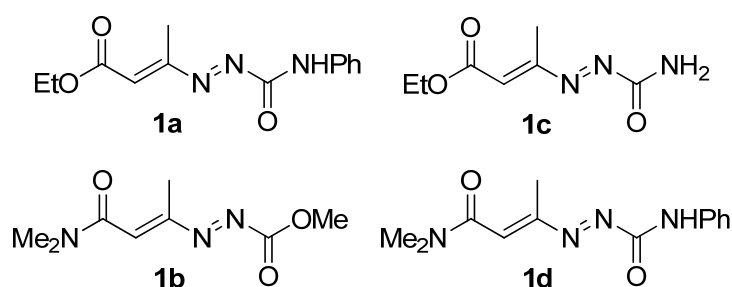
Scheme 3.1. Synthetic pathways to 1,2-diaza-1,3-dienes **1**.

In order to make synthetic strategies which include the use of **1** more predictable and efficient, it was our goal to quantify the electrophilicity of different substituted 1,2-diaza-1,3-dienes **1**. We have, therefore, determined the reactivities of **1** towards nucleophiles in the first step of the complex, sequential transformations that lead to different products.

Recently, the München group has shown that the reactions of carbocations and various electron-deficient alkenes with n -, π -, and σ -nucleophiles can be described by Equation (3.1), where nucleophiles are characterized by the parameters N and s , and electrophiles are characterized by the parameter E .^[2] In this way, it was possible to construct comprehensive nucleophilicity and electrophilicity scales.^[3] Reactions of carbanions with typical Michael acceptors, such as benzylidenemalononitriles, benzylideneindandiones, benzylidene Meldrum's acids, benzylidenemalonates have been shown to follow Equation (3.1).^[4]

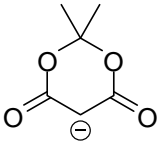
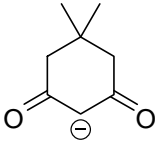
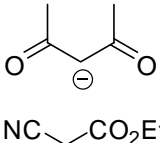
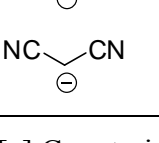
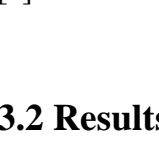
$$\log k_2(20\text{ }^\circ\text{C}) = s(N + E) \quad (3.1)$$

Assuming that the reactions of **1** with carbanions can also be described by Equation (3.1) we have determined the electrophilicities of four conjugated azoalkenes (1,2-diaza-1,3-dienes **1a-d**) with ester or amido substituents at the positions 1 and 4 (Scheme 3.2).

Scheme 3.2. 1,2-Diaza-1,3-dienes **1a-d** used in this study.

For that purpose, we have investigated the rates of the reactions of **1a-d** with the carbanions **2a-e**, for which *N* and *s* parameters are known (Table 3.1).^[3b,5]

Table 3.1. Reference carbanions **2** used in this study and their nucleophilicity parameters *N* and *s*.

carbanion ^[a]		<i>N</i> (<i>s</i>) ^[b]
	2a	13.91 (0.86) in DMSO
	2b	16.27 (0.77) in DMSO
	2c	17.64 (0.73) in DMSO
	2d	18.59 (0.65) in MeOH
	2e	19.36 (0.67) in DMSO

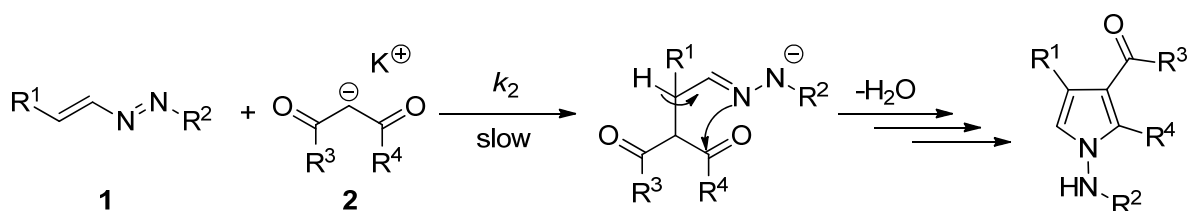
[a] Counterion for **2a**, **2b**, **2c**, and **2e**: K^+ ; counterion for **2d**: Na^+ . [b] Refs. [3b,5].

3.2 Results and Discussion

3.2.1 Reactions of 1,2-Diaza-1,3-dienes **1** with Carbanions **2**

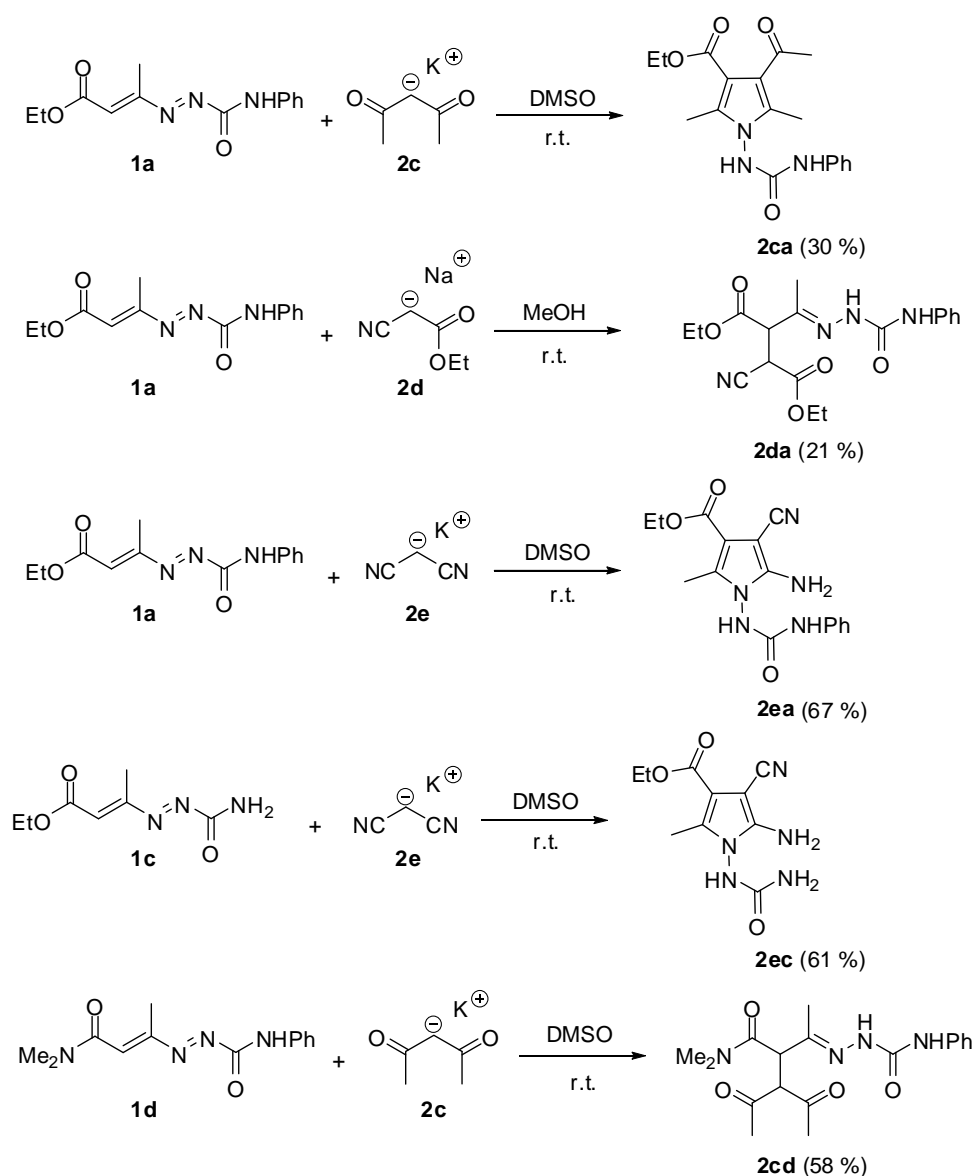
Product Characterization

Many base-activated reactions of 1,2-diaza-1,3-dienes **1** with CH-acidic compounds, such as β -dicarbonyl compounds have been reported to result in the formation of pyrroles (Scheme 3.3).^[6]



Scheme 3.3. Michael-addition of β -dicarbonyl compounds to 1,2-diaza-1,3-dienes **1** and subsequent cyclization.

In previous investigations,^[1,6] the majority of the reactions between carbanions **2** and **1** were carried out in THF. As the structure of the resulting products was reported to depend on the solvent, we repeated some of the relevant reactions in those solvents used for the kinetic studies in this work, i.e., DMSO or MeOH (Table 3.1, Scheme 3.4). The reactions of **1a** with the carbanions **2c,e** and of **1c** with carbanion **2e** gave the expected pyrroles **2ca**, **2ea**, and **2ec**, while the reactions of **1a** with **2d** and of **1d** with carbanion **2c** yielded the acyclic 1,4-adducts **2da** and **2cd**, respectively. Because the products shown in Scheme 3.4 accordingly indicate initial attack of the carbanions at C-4 of the diazadiene system, we have assumed that all other combinations of **1a-d** with **2** which were kinetically studied in this work proceed in an analogous manner.



Scheme 3.4. Products of the reactions of **1a**, **c** and **d** with carbanions **2** (isolated yields after column chromatography).

Kinetic Investigations

The rates of the reactions of **1** with the carbanions **2** were determined photometrically at 20 °C by using conventional or stopped-flow UV-Vis spectrometers. The carbanions **2** were used as preformed potassium salts or were prepared in solution by deprotonation of the CH acids with 1.05 equiv. of KO^tBu (or NaOMe in the case of **2d**). The reaction progress was monitored by the decrease of the absorbances of the electrophiles. By using the nucleophiles **2** in excess over the electrophiles **1**, first-order conditions were achieved. From the mono-exponential decays of the absorbances the first-order rate constants k_{obs} were obtained by a least squares fit to $A = A_0 e^{-k_{\text{obs}}t} + C$. Details are given in the Experimental Section (Chapter 3.4).

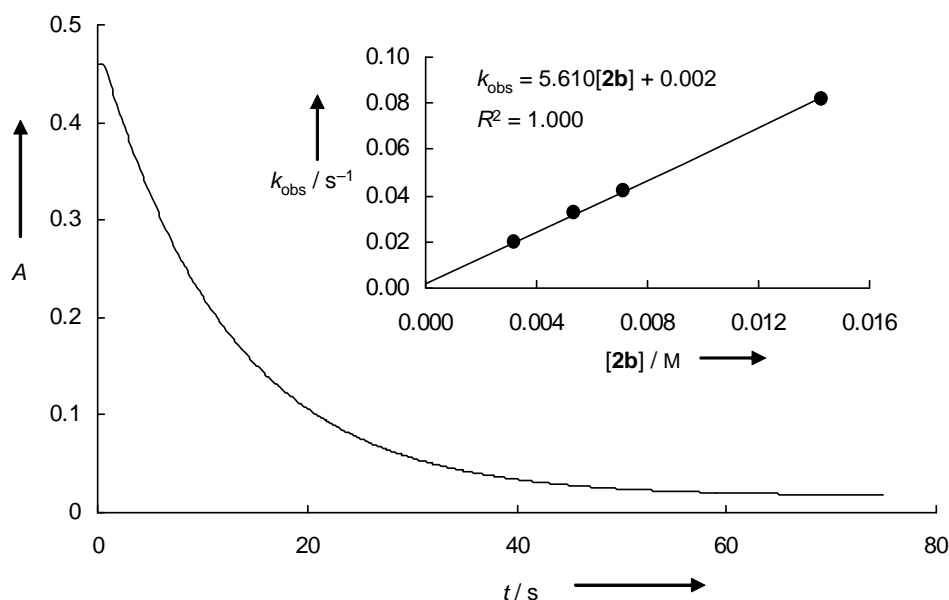


Figure 3.1. Exponential decay of the absorbance at 350 nm during the reaction of **1d** with the anion of dimedone in DMSO at 20 °C ($[2b] = 1.43 \times 10^{-2} \text{ M}$; $k_{\text{obs}} = 8.21 \times 10^{-2} \text{ s}^{-1}$, counter-ion: K^+). Inset: Determination of the second-order rate constant $k_2 = 5.61 \text{ M}^{-1} \text{ s}^{-1}$ from the slope of the correlation of the first-order rate constants k_{obs} with the concentration of **2b**.

The reactions of **1** with the carbanion **2d** have been performed in methanol where **2d** was generated by treatment of **2d-H** with sodium methanolate. Because ethyl cyanoacetate (**2d-H**) is only partially deprotonated by methoxide in methanol, the evaluation of the kinetics of the reaction of **1** with **2d** has to consider the acid-base equilibrium ($\text{2d-Na} + \text{MeOH} \rightleftharpoons \text{2d-H} + \text{MeO}^- \text{Na}^+$) as well as the parallel reaction of **1** with MeO^- . The actual concentrations of **2d**

and MeO^- can be calculated by using the known equilibrium constant $K_{2\mathbf{d}}$.^[7] The independently determined second-order rate constants $k_{2,\text{MeO}}$ for the reactions of MeO^- with the electrophiles **1** have then been employed to subtract $k_{2,\text{MeO}}[\text{MeO}^-]$ from k_{obs} to get to the pseudo first-order rate constants for the reaction of **2d** with the 1,2-diaza-1,3-dienes **1** (for details see the Experimental Section (Chapter 3.4) and ref. [5]).

As exemplified in Figure 3.1 for the reaction of **1d** with **2b**, plots of k_{obs} (or $k_{\text{obs}} - k_{2,\text{OMe}}[\text{MeO}^-]$ in the case of the reactions with **2d**) versus the carbanion concentrations were linear for all reactions of **1** with **2**. In these reactions, the attack of the carbanions at the electrophiles is rate limiting, and the slopes of the plots of k_{obs} versus $[\mathbf{2}]$ gave the second-order rate constants k_2 [Equation (3.2)], which are listed in Table 3.2.

$$k_{\text{obs}} = k_2[\mathbf{2}] \quad (3.2)$$

Figure 3.2 shows linear correlations of $(\log k_2)/s$ versus N with slopes of unity, as required by Equation (3.1). Consequently, the electrophilicity parameters E of **1a–d** could be derived from a least-squares fit of experimental and calculated rate constants by minimization of $\Delta^2 = \sum(\log k_2 - s(N + E))^2$. As discussed in previous reviews,^[3] the special type of linear free energy relationship (3.1) avoids long-ranging extrapolations, because $E = -N$ for $(\log k_2)/s = 0$ as shown graphically in Figure 3.2. While in most cases calculated (from E , N , s) and experimental rate constants agree within a factor of 3 (Table 3.2), **1c** reacts 7-times faster with **2d** than calculated. Because this deviation is within the confidence limit of Equation (3.1), we abstain from an interpretation of this deviation.

Table 3.2. Experimental and calculated second-order rate constants for the reactions of **1a–d** with carbanions **2a–e** at 20 °C in DMSO.

Electrophile (<i>E</i>)	Nucleophile	k_2^{exp} [$\text{M}^{-1} \text{s}^{-1}$]	k_2^{calcd} [$\text{M}^{-1} \text{s}^{-1}$] ^[a]	$k_2^{\text{exp}}/k_2^{\text{calcd}}$
1a (−13.28)	2a	1.52	3.48	0.44
	2b	4.39×10^2	2.01×10^2	2.2
	2c	4.02×10^3	1.52×10^3	2.6
	2d	2.96×10^3 ^[b]	2.83×10^3	1.0
	2e	4.44×10^3	1.18×10^4	0.37
1b (−13.90)	2a	5.15×10^{-1}	1.02	0.51
	2b	8.11×10^1	6.68×10^1	1.2
	2c	6.93×10^2	5.37×10^2	1.3
	2d	3.50×10^3 ^[b]	1.12×10^3	3.1
	2e	2.21×10^3	4.55×10^3	0.49
1c (−14.91)	2a	7.98×10^{-2}	1.38×10^{-1}	0.58
	2b	1.88×10^1	1.11×10^1	1.7
	2c	3.86×10^1	9.84×10^1	0.39
	2d	1.64×10^3 ^[b]	2.47×10^2	6.7
	2e	4.82×10^2	9.58×10^2	0.50
1d (−15.38)	2a	3.69×10^{-2}	5.41×10^{-2}	0.67
	2b	5.61	4.82	1.2
	2c	8.98×10^1	4.44×10^1	2.0
	2e	3.13×10^2	4.68×10^2	0.67

[a] Calculated by using Equation (3.1), *N* and *s* parameters from Table 3.1 and *E* from this Table. [b] Solvent: MeOH.

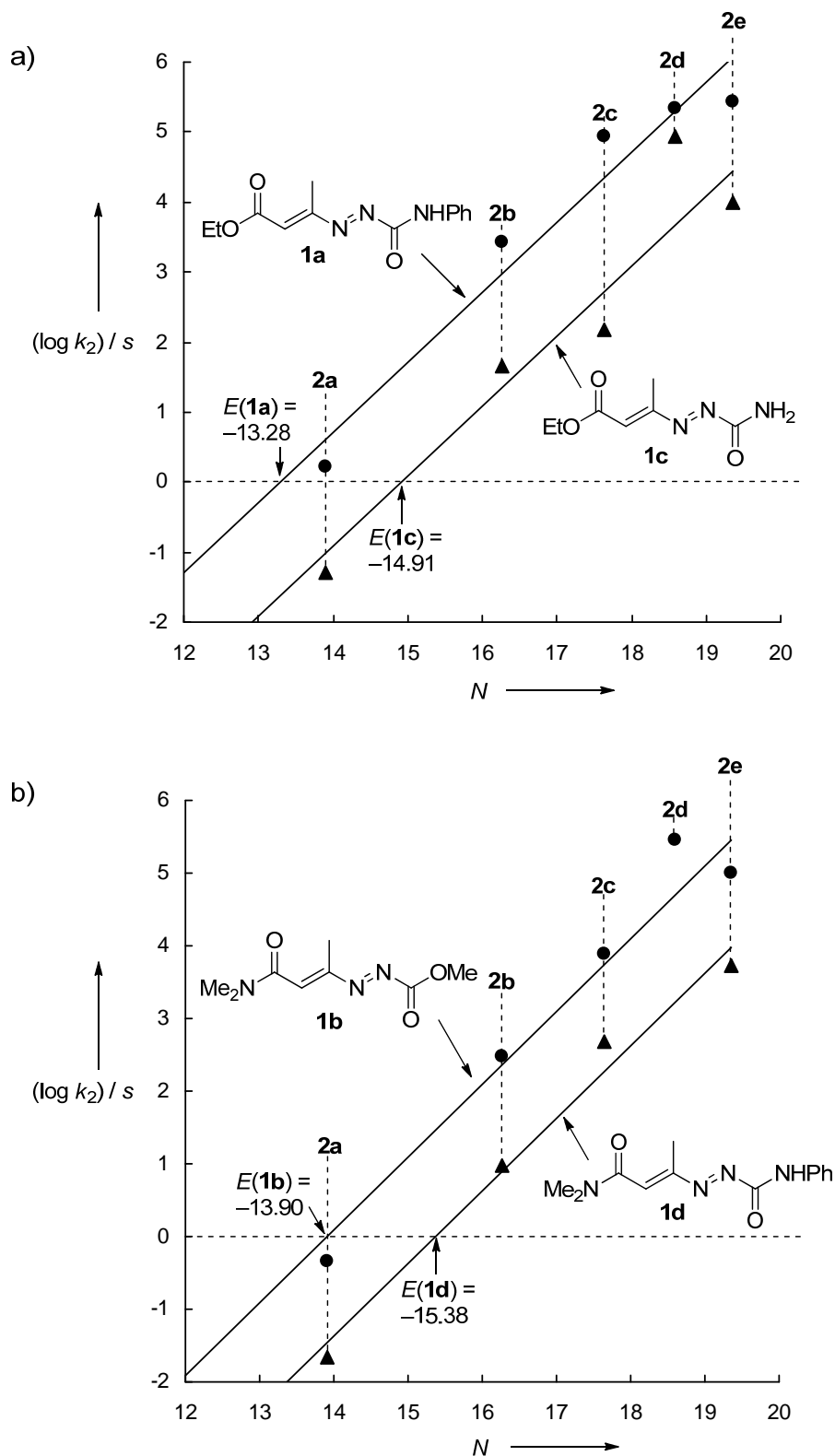


Figure 3.2. Plots of $(\log k_2)/s$ against the N -parameters of the carbanions **2a–e** for the reactions of the 1,2-diaza-1,3-dienes **1a**, **1c** (Figure 3.2a), **1b** and **1d** (Figure 3.2b) with **2a–e** in DMSO at 20 °C (the slopes are fixed to one as required by Equation (3.1); reactions of **2d** in methanol).

The electrophiles **1a–d** cover a reactivity range of two orders of magnitude and can be compared to benzylidenemalononitriles,^[4a] benzylideneindandiones,^[4b] benzylidenebarbituric acids,^[4c] benzylidene Meldrum's acids,^[4d] electron deficient arenes^[8] and quinone methides^[3g] (Figure 3.3). 1,2-Diaza-1,3-dienes (**1**) are considerably more reactive than benzylidenemalonates ($E < -17.5$).^[4e]

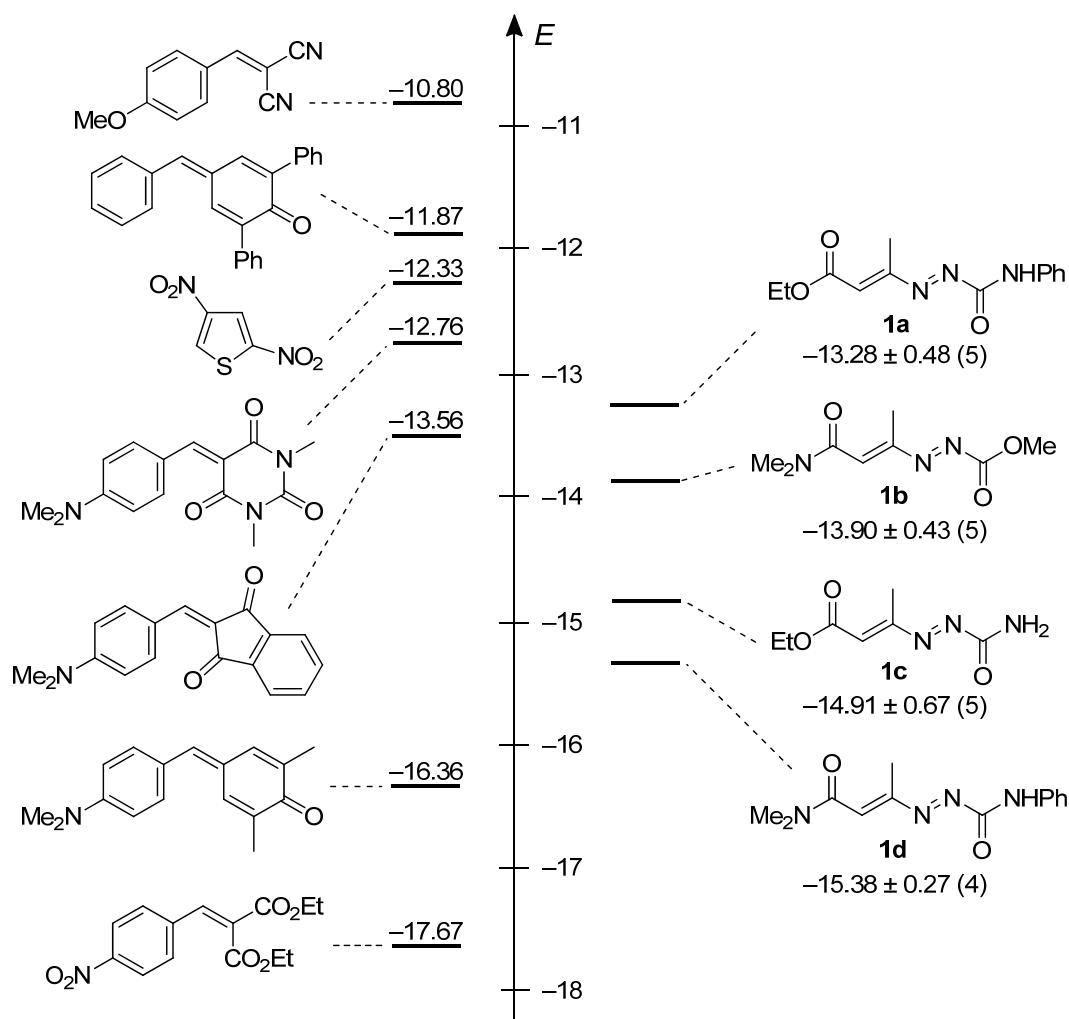


Figure 3.3. Comparison of the electrophilic reactivities of 1,2-diaza-1,3-dienes **1** with those of other classes of electrophiles (standard deviations are given for $E(1)$ with the number of experiments in parentheses).

3.2.2 Reactions of the 1,2-Diaza-1,3-dienes **1** with Other Nucleophiles

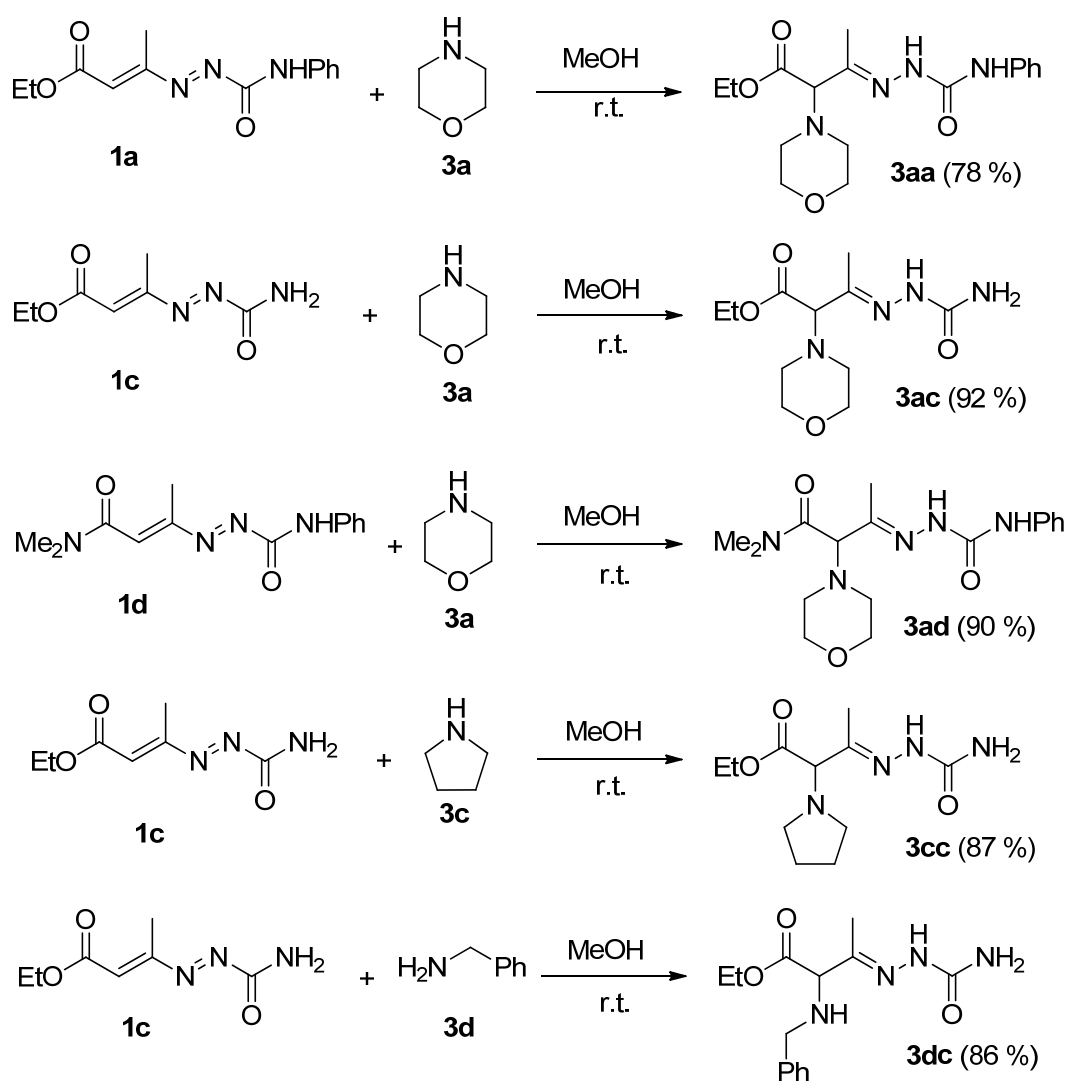
In order to examine whether the electrophilicity parameters of 1,2-diaza-1,3-dienes **1a–d** derived from the rates of their reactions with carbanions, which are listed in Figure 3.3, are suitable for the prediction of their reaction rates with other types of nucleophiles, we studied

the kinetics of the reactions of **1a-d** with amines **3**, triarylphosphines **4**, and enamines **5** of known nucleophilicities.^[3a, 9]

Product Characterization

Products of the reactions of **1** with amines **3**.

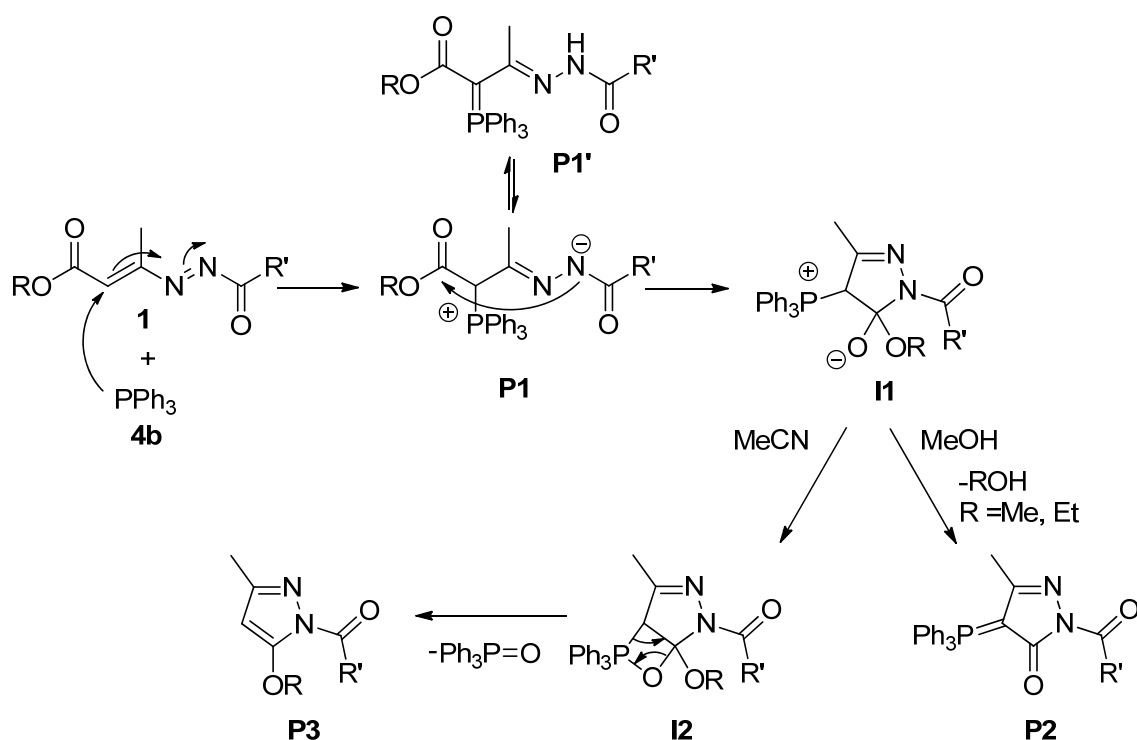
The reactions of **1a,c,d** with the amines **3a,c,d** in MeOH furnished the expected^[10] α -aminohydrazones **3aa,ac,ad,cc,dc** in high yield (Scheme 3.5).



Scheme 3.5. Product studies of the reactions of **1** with amines **3** (isolated yields).

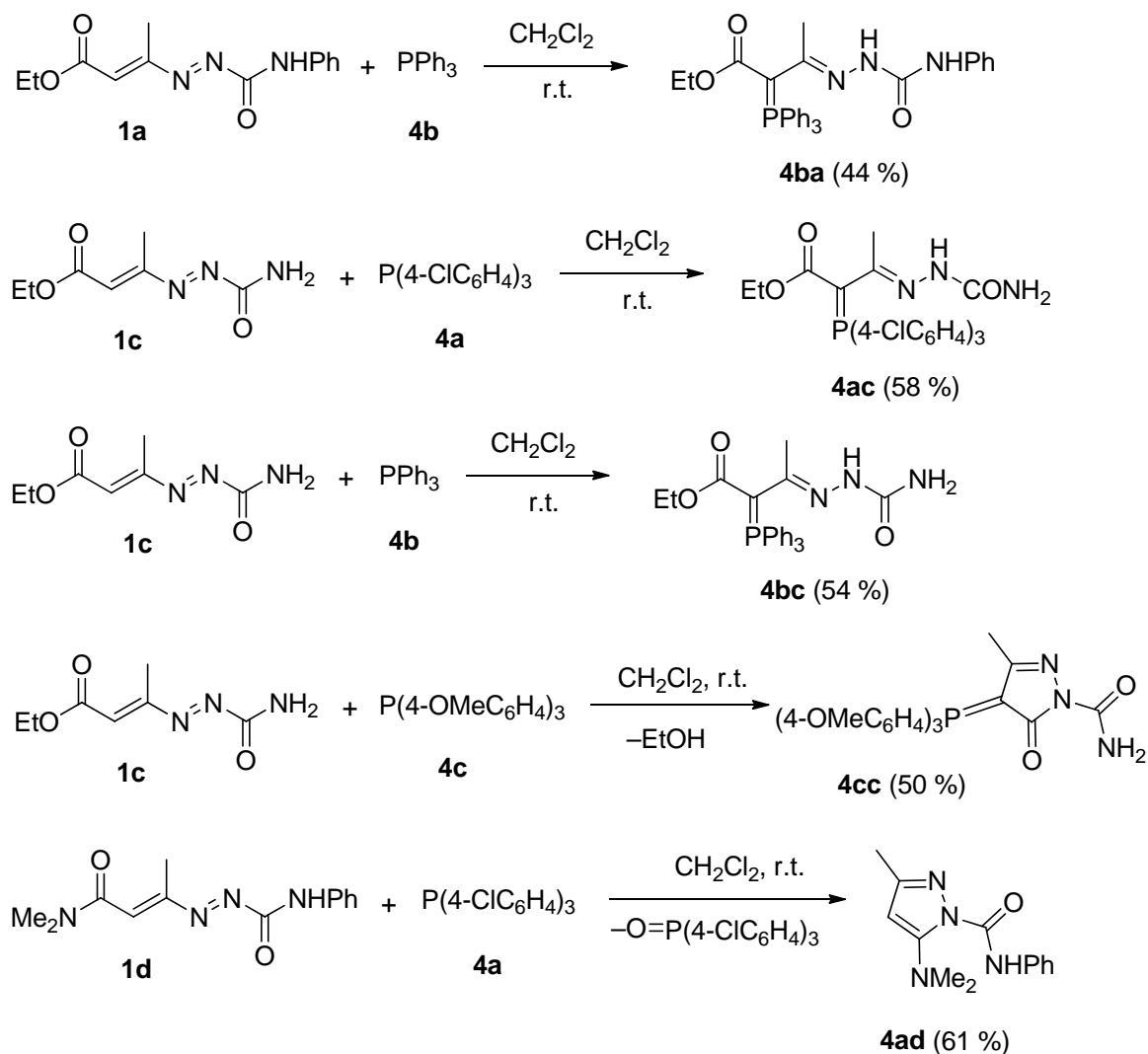
Products of the reactions of **1** with triarylphosphines **4**.

Some of us^[11] reported previously that the reactions of **1** with triphenylphosphine (**4b**) in ethyl acetate produced the 1,5-zwitterions **P1** which precipitated from the solvent (Scheme 3.6). These intermediates undergo different heterocyclizations, depending on the nature of the solvent used: in methanol the 1,4-adduct **P1** is transformed into a betaine intermediate **I1** by intramolecular attack of the nitrogen at the ester group. Subsequent loss of MeOH or EtOH yields 4-triphenylphosphoranilidene-4,5-dihydropyrazol-5-ones **P2**. Also in acetonitrile, the cyclic betaine intermediates **I1** are formed, which then cyclize to the oxaphosphetane intermediates **I2**. Finally, loss of triphenylphosphine oxide transforms **I2** into the corresponding pyrazoles **P3**.



Scheme 3.6. Mechanism of the reactions of **1** with triphenylphosphine (**4b**).

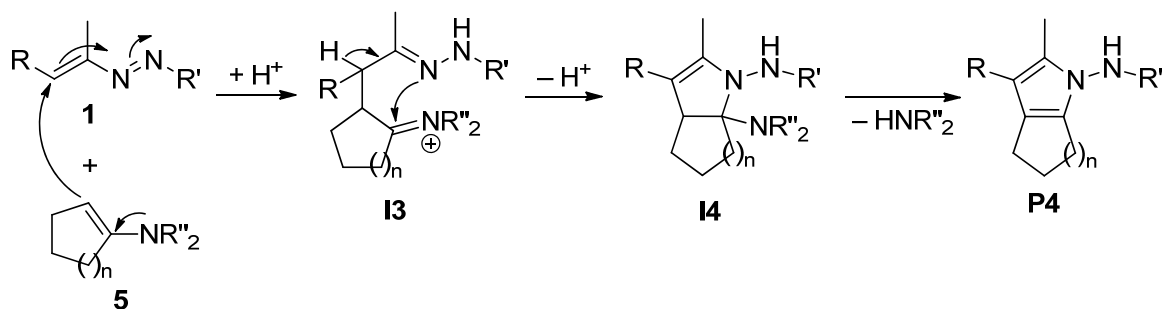
Because the kinetic experiments have been performed in CH_2Cl_2 , we have also studied products of the reactions between **1a,c** and **4a,b** in this solvent. Scheme 3.7 shows the formation of the expected phosphorus ylides **4ba**, **4ac**, and **4bc**.^[11a] In contrast, the reaction between **1c** and tris(4-methoxyphenyl)phosphine (**4c**) gave the 4-tris(4-methoxyphenyl)phosphoranilidene-4,5-dihydropyrazol-5-one (**4cc**),^[11] and the reaction between **1d** and 4-tris(4-chlorophenyl)phosphine (**4a**) afforded the pyrazole **4ad**^[11a] (Scheme 3.7).



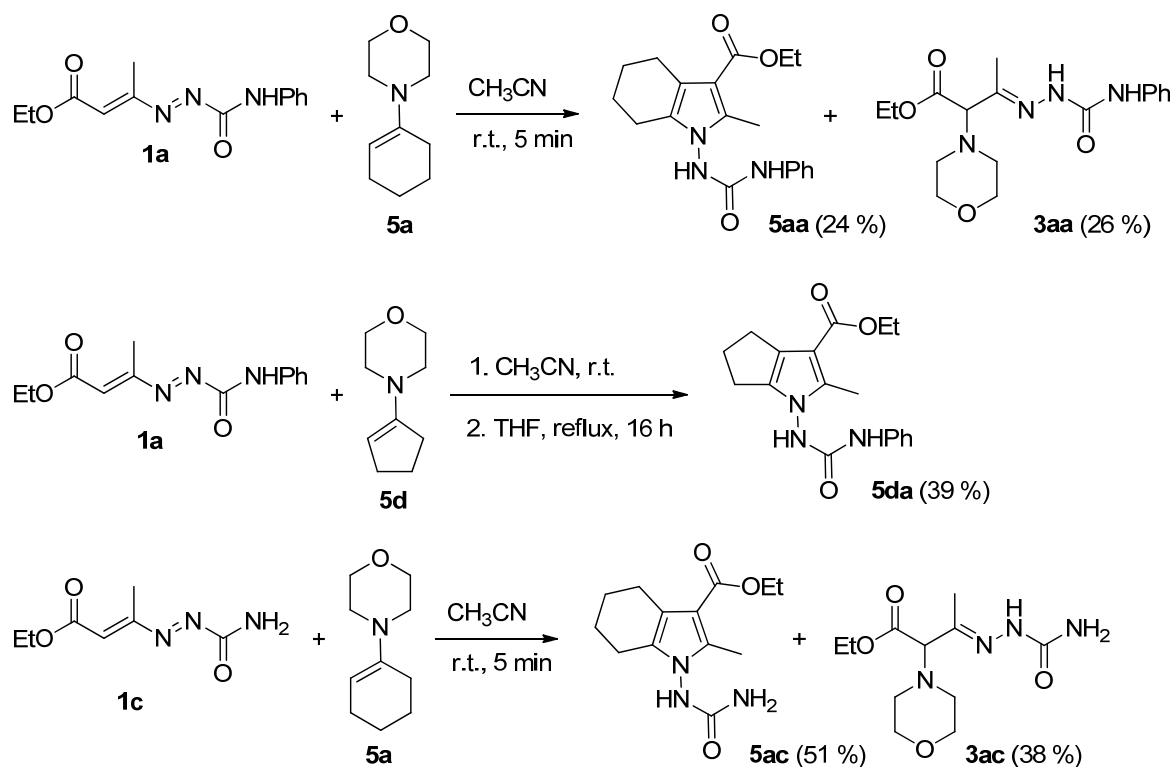
Scheme 3.7. Products of the reactions of **1a**, **c** and **d** with triarylphosphines (**4**) (isolated yields after column chromatography).

Products of the reactions of **1** with enamines **5**.

Reactions of the conjugated azoalkenes **1** with α,β -disubstituted enamines **5** have been reported to yield 1-aminopyrroles **P4** in polar and apolar solvents. The initial attack of the nucleophilic carbon atom of the enamine **5** at the terminal carbon atom of the azo-ene system **1** produces hydrazone intermediates **I3**, which undergo a [3+2]-cyclization to furnish the 2-amino substituted dihydropyrroles **I4**. The spontaneous subsequent loss of the secondary amine results in the formation of the 1-aminopyrrole derivatives **P4** (Scheme 3.8).^[12]

Scheme 3.8. Formation of 1-aminopyrroles **P4** from the reactions of **1** with enamines **5**.

For the product investigations, we have chosen the reactions between **1a,c** and the 1-morpholinocycloalkenes **5a,d** in acetonitrile. The reactions of **1a** and **1c** with morpholinocyclohexene (**5a**) delivered the 1-aminopyrroles **5aa** and **5ac**, respectively. The accompanying 1,4-adducts **3aa** and **3ac** are formed by addition of morpholine (a side product of the formation of the pyrroles, see Scheme 3.8) to the electrophiles **1a** and **1c**.^[12a] In the reaction of **1a** with **5d**, the loss of morpholine did not occur spontaneously; therefore, the reaction mixture in THF was refluxed until the complete conversion into pyrrole **5da** was observed by TLC (Scheme 3.9).

Scheme 3.9. Product studies of the reactions of **1a** and **1c** with enamines **5** (isolated yields after chromatographic workup).

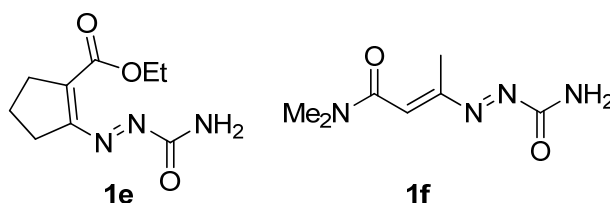
Kinetic Studies

The kinetics of the reactions of **1** with amines **3**, triarylphosphines **4**, and enamines **5** were determined photometrically as described above for the reactions of **1** with carbanions **2**.

Reactions of **1** with amines **3**.

The reactions of **1** with amines **3a-d** were studied in different solvents. Table 3.3 shows that the experimental rate constants for these reactions agree within a factor of 7 with those calculated by Equation (3.1) from the electrophilicity parameters E of **1** (Table 3.2) and the N and s parameters of the amines **3a-c** previously determined from the rates of their reactions with benzhydrylium ions.^[9b,d,e]

The rate constants for the reactions of morpholine (**3a**) and piperidine (**3b**) with two additional 1,2-diaza-1,3-dienes **1e** and **1f** were studied in methanol. Tentative E parameters for **1e** and **1f** can be calculated by Equation (3.1), from the known N and s parameters of **3a** and **3b** and the second-order rate constants listed in Table 3.3. The averaged values of the electrophilicity parameters E are -14.9 for **1e** and -15.3 for **1f**.



1,2-Diaza-1,3-dienes **1** with amido groups at the 1- and the 4-terminus are the least reactive ones (**1d/1f**). Their reactivity increases slightly when the amido substituents at the terminal carbon or the nitrogen atom are replaced by the stronger electron-withdrawing ester group (**1d** is less reactive than **1b** and **1a**). However, these substituent effects are small, and the electrophilicities of the 1,2-diaza-1,3-butadienes studied in this work cover a very narrow reactivity range of only 2 orders of magnitude.

Table 3.3. Experimental and calculated second-order rate constants for the reactions of 1,2-diaza-1,3-dienes **1** with amines **3** at 20 °C.

1	Amine 3	<i>N/s</i> ^[a]	k_2^{exp} [M ⁻¹ s ⁻¹]	k_2^{calcd} [M ⁻¹ s ⁻¹] ^[b]	$k_2^{\text{exp}}/k_2^{\text{calcd}}$
1a	morpholine (3a) in MeOH	15.40/0.64	4.72	2.27×10^1	0.21
1a	morpholine (3a) in DMSO	16.96/0.67	4.12×10^1	2.92×10^2	0.14
1a	piperidine (3b) in MeOH	15.63/0.64	1.92×10^1	3.19×10^1	0.60
1a	piperidine (3b) in MeCN	17.35/0.68	2.22×10^2	5.86×10^2	0.38
1a	pyrrolidine (3c) in MeOH	15.97/0.63	3.18×10^1	4.95×10^1	0.64
1b	morpholine (3a) in MeOH	15.40/0.64	1.15×10^1	9.12	1.3
1b	morpholine (3a) in DMSO	16.96/0.67	1.45×10^2	1.12×10^2	1.3
1b	piperidine (3b) in MeOH	15.63/0.64	2.63×10^1	1.28×10^1	2.1
1c	morpholine (3a) in MeOH	15.40/0.64	2.17	2.06	1.1
1c	morpholine (3a) in DMSO	16.96/0.67	3.83	2.36×10^1	0.16
1c	piperidine (3b) in MeOH	15.63/0.64	9.81	3.11	3.2
1c	piperidine (3b) in MeCN	17.35/0.68	4.00×10^1	2.89×10^1	0.88
1c	pyrrolidine (3c) in MeOH	15.97/0.63	1.68×10^1	4.65	3.6
1c	benzylamine (3d) in MeOH	13.46/0.62	1.91×10^{-1}	1.26×10^{-1}	1.5
1d	morpholine (3a) in MeOH	15.40/0.64	1.69	1.03	1.6
1d	piperidine (3b) in MeOH	15.63/0.64	4.95	1.45	3.4
1e	morpholine (3a) in MeOH	15.40/0.64	1.19		
1e	piperidine (3b) in MeOH	15.63/0.64	4.94		
1f	morpholine (3a) in MeOH	15.40/0.64	8.04×10^{-1}		
1f	piperidine (3b) in MeOH	15.63/0.64	2.35		

[a] *N* and *s* parameters of amines from refs. [9b, 9d, 9e]. [b] Calculated by using Equation (3.1).

Reactions of **1** with triarylphosphines **4**.

The rates of the reactions of **1** with triarylphosphines **4a-c** were studied in CH₂Cl₂ by following the decay of the electrophiles' absorbance. In analogy to the reactions of **1** with amines, the linearity of the k_{obs} vs [PR₃] plots proved that second-order rate laws were obeyed for all studied reactions. This fact allowed us to determine the second-order rate constants for the attack of PR₃ at the CC double bond of **1**. Comparison of the experimentally obtained rate

constants with those predicted by Equation (3.1) shows an excellent agreement of these values within a factor of 5 (Table 3.4).

Table 3.4. Experimental and calculated second-order rate constants for the reactions of 1,2-diaza-1,3-dienes **1** with phosphines **4** in CH₂Cl₂ at 20 °C.

1	Phosphine (4)	$N/s^{[a]}$	$k_2^{\text{exp}} [\text{M}^{-1} \text{s}^{-1}]$	$k_2^{\text{calcd}} [\text{M}^{-1} \text{s}^{-1}]^{[b]}$	$k_2^{\text{exp}}/k_2^{\text{calcd}}$
1a	(4-ClC ₆ H ₄) ₃ P (4a)	12.58/0.65	3.12×10^{-1}	3.51×10^{-1}	0.89
1a	Ph ₃ P (4b)	14.33/0.65	6.59	4.74	1.4
1a	(4-OMeC ₆ H ₄) ₃ P (4c)	16.17/0.62	1.02×10^2	6.19×10^1	1.6
1b	Ph ₃ P (4b)	14.33/0.65	9.63×10^{-1}	1.90	0.5
1c	(4-ClC ₆ H ₄) ₃ P (4a)	12.58/0.65	1.05×10^{-1}	3.06×10^{-2}	3.4
1c	Ph ₃ P (4b)	14.33/0.65	1.73	4.14×10^{-1}	4.2
1c	(4-OMeC ₆ H ₄) ₃ P (4c)	16.17/0.62	2.41×10^1	6.04	4.0

[a] N and s parameters of triarylphosphines **4a–c** from ref. [9c]. [b] Calculated by using Equation (3.1), N and s parameters from ref. [9c], and the E parameters from Table 3.2.

Reactions of **1** with enamines **5**.

The reactions of **1** with the α,β -disubstituted enamines **5a–c** were studied in acetonitrile by following the decay of the electrophiles' absorbance. The progress of the reaction of **1c** with morpholinocyclopentene (**5d**) can be monitored by the decrease of the absorbance of the electrophile and, additionally, by the increase of the absorbance of the reaction product. From the mono-exponential increases (as from the mono-exponential decays) the k_{obs} values were obtained by a least squares fit to the function $A = (1 - A_0 e^{-k_{\text{obs}}t}) + C$. The slope of the linear plot of k_{obs} versus [**5d**] yielded the second-order rate constants k_2 . Figure 3.4 shows the reaction progress by the mono-exponential increase of the product and the mono-exponential decay of **1c** for the same reaction ($[\mathbf{1c}]_0 = 2.19 \times 10^{-4} \text{ M}$; $[\mathbf{5d}]_0 = 9.40 \times 10^{-4} \text{ M}$). The first-order rate constants for the reactions of **1c** with **5d** obtained by the two different methods are in fair agreement; however, because of the high molar absorption coefficient of the product, the concentration of **1c** had to be kept small, which resulted in a very low absorption for **1c** and a less precise k_{obs} value determined from the decay of [**1c**].

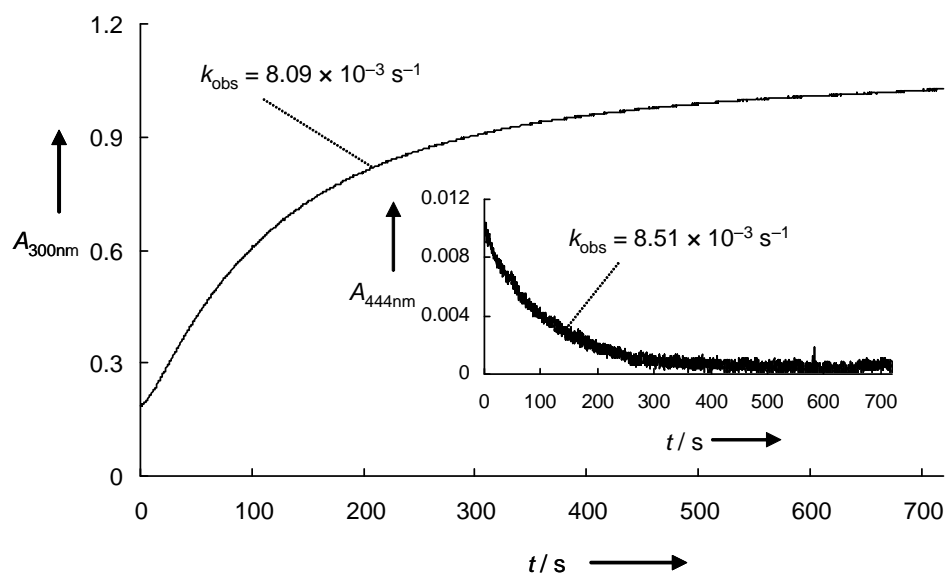


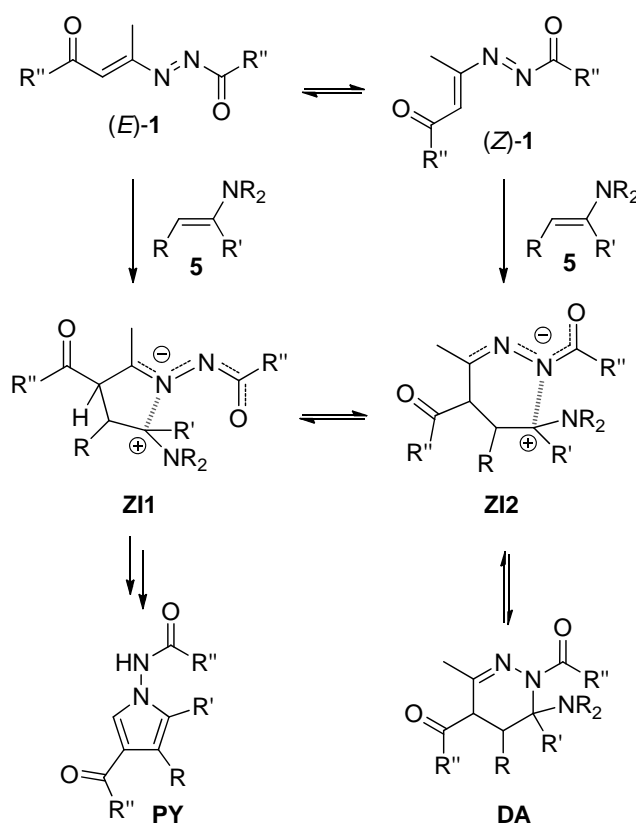
Figure 3.4. Exponential increase of the absorbance at 300 nm during the reaction of **1c** with morpholinocyclopentene (**5d**) ($[\mathbf{5d}]_0 = 9.40 \times 10^{-4}$ M). Insert: Exponential decay of the absorbance of **1c** at 444 nm during the reaction of **1c** with **5d**.

Table 3.5. Experimental and calculated second-order rate constants for the reactions of 1,2-diaza-1,3-dienes **1** with enamines **5** in acetonitrile at 20 °C.

1	Enamine 5	N/s ^[a]	k_2^{exp} [$\text{M}^{-1} \text{s}^{-1}$]	k_2^{calcd} [$\text{M}^{-1} \text{s}^{-1}$] ^[b]	$k_2^{\text{exp}}/k_2^{\text{calcd}}$
1a	morpholinocyclohexene (5a)	11.40/0.83	4.73	2.75×10^{-2}	172
1a	piperidinocyclopentene (5b)	15.06/0.82	1.23×10^3	2.88×10^1	43
1a	pyrrolidinocyclopentene (5c)	15.91/0.86	6.44×10^3	1.83×10^2	35
1b	morpholinocyclohexene (5a)	11.40/0.83	8.88×10^{-1}	8.41×10^{-3}	106
1b	piperidinocyclopentene (5b)	15.06/0.82	1.40×10^2	8.94	16
1b	pyrrolidinocyclopentene (5c)	15.91/0.86	1.07×10^3	5.35×10^1	20
1c	morpholinocyclohexene (5a)	11.40/0.83	8.05×10^{-1}	1.22×10^{-3}	660
1c	morpholinocyclopentene (5d)	13.41/0.82	7.59 ^[c]	5.89×10^{-2}	128
1c	piperidinocyclopentene (5b)	15.06/0.82	1.96×10^2	1.33	148
1c	pyrrolidinocyclopentene (5c)	15.91/0.86	1.12×10^3	7.24	155
1d	morpholinocyclohexene (5a)	11.40/0.83	3.75×10^{-1}	4.97×10^{-4}	754
1d	morpholinocyclopentene (5d)	13.41/0.82	3.89	2.42×10^{-2}	160
1d	piperidinocyclopentene (5b)	15.06/0.82	6.47×10^1	5.47×10^{-1}	118

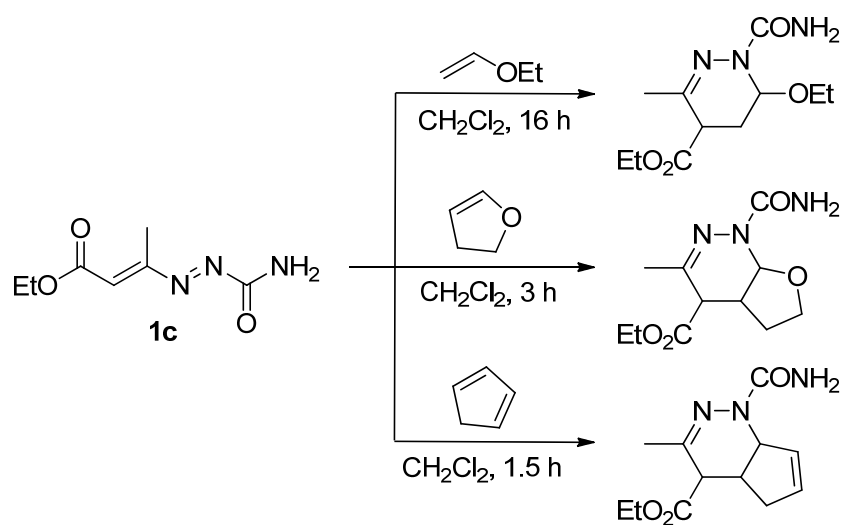
[a] N and s parameters from refs. [3a, 9a]. [b] Calculated by using Equation (3.1). [c] k_{obs} values were obtained from the mono-exponential increases of the product.

Though some of the rate constants listed in Table 3.5 agree with the calculated ones within a factor of 10^2 , all experimental rate constants are larger than calculated; most of the reactions are 10^2 - 10^3 times faster than derived from Equation (3.1), and the strongest deviation is found for the reactions of the least nucleophilic enamine **5a** with the least electrophilic azadienes **1c** and **1d**. One, therefore, can assume that these reactions experience a special acceleration. As shown in Scheme 3.10, **5** may react with the (*Z,E*)-conformational isomers of the diazadienes **1** to give the zwitterions **ZI1** or **ZI2**. Stabilization of these intermediates and the preceding transition states by Coulombic attraction of the oppositely charged fragments may explain the increased reactivity of the enamines. The observation that the acceleration is highest for the slowest reactions may indicate that the transition state is even stabilized by partial formation of the second bond (hatched lines in **ZI1** and **ZI2**) leading to the heterocycles **DA** and **PY**, respectively.^[13] In accord with this interpretation, aldehyde-derived enamines **5** ($R' = H$) have been reported to undergo [4+2]-cycloadditions with 1,2-diaza-1,3-dienes.^[12d] Possibly analogous [4+2]-cycloadditions also occur with the enamines **5a-d** studied in this work. However, when $R' = \text{alkyl}$, the zwitterion **ZI2** is sufficiently stabilized that it can be regenerated from the Diels-Alder adduct **DA** and finally gives the pyrrole **PY** as indicated in Scheme 3.10.



Scheme 3.10. Mechanism for the reactions of **1** with aldehyde and ketone derived enamines **5**.

From the nucleophilicity parameters N and s for ethyl vinyl ether ($N = 3.92$, $s = 0.90$), 2,3-dihydrofuran ($N = 4.37$, $s = 0.90$), and cyclopentadiene ($N = 2.30$, $s = 1.09$)^[3c] one can derive that nucleophilic attack of these π -systems at the 4-position of the 1,2-diaza-1,3-diene **1c** would occur with rate constants between 2×10^{-14} and $3 \times 10^{-10} \text{ M}^{-1} \text{ s}^{-1}$. From these calculated rate constants one can estimate that the Diels-Alder reactions with inverse electron demand depicted in Scheme 3.11 would require 10^2 to 10^6 years at 20 °C (half reaction times for 1 M solutions) if they proceeded stepwise through a zwitterionic intermediate. The reported reaction times of 1.5 to 16 h at 15 °C are, therefore, clear evidence for the occurrence of concerted Diels-Alder reactions.^[14]



Scheme 3.11. Diels-Alder reactions of **1c** with ethyl vinyl ether, 2,3-dihydrofuran, and cyclopentadiene (at 15 °C, from ref. [14]).

The considerably smaller deviations between calculated and experimental rate constants for the reactions of **1** with enamines **5** indicate that the potentially involved initial Diels-Alder reactions would profit much less from concertedness.

3.3 Conclusion

Figure 3.5 illustrates that the N and s parameters for carbanions **2**, amines **3**, and phosphines **4** derived from reactions with benzhydrylium ions also hold for their reactions with 1,2-diaza-1,3-dienes **1**. Though belonging to different classes of compounds, the deviations of these nucleophiles from the correlation line in Figure 3.5 are small. The positive deviations of

enamines from this correlation line are indicative for a mechanistic change toward concerted [4+2]-cycloadditions which must be operating in the reactions of enol ethers with the dienes **1**, because the stepwise mechanism can be estimated to require more than 10^2 years.

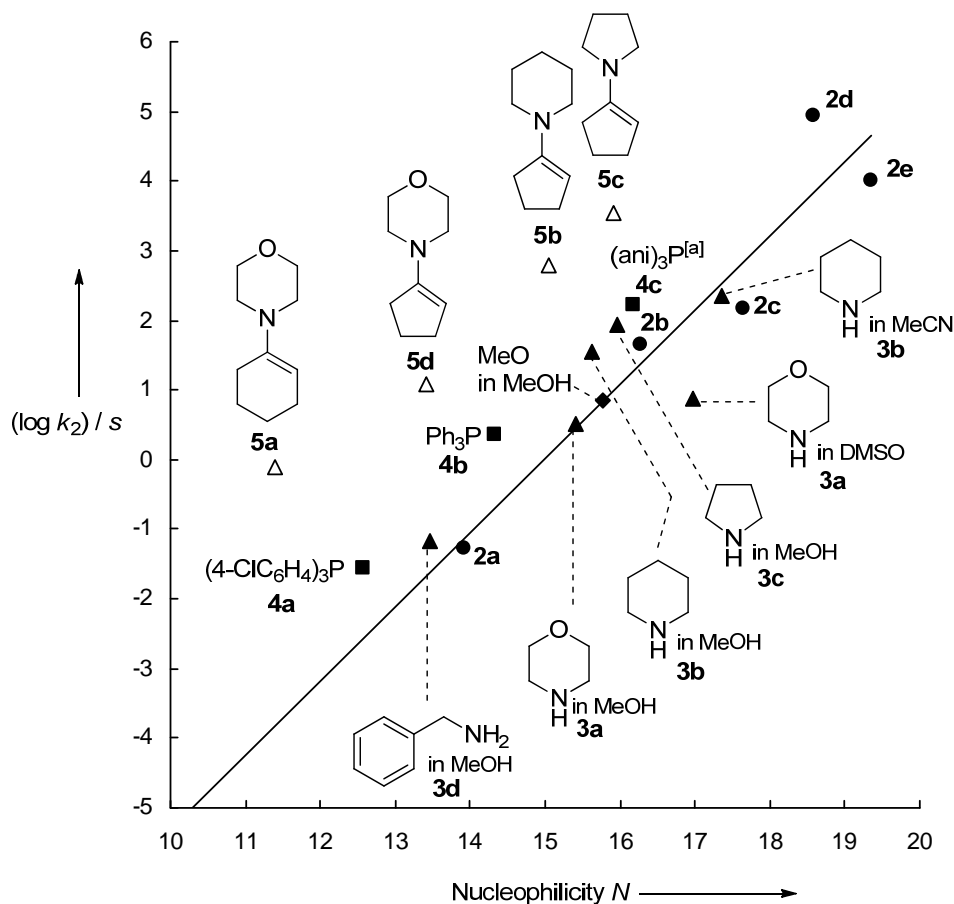


Figure 3.5. Plot of $(\log k_2)/s$ for the reactions of the 1,2-diaza-1,3-diene **1c** with **2–5** at 20 °C against the N parameters of the carbanions **2a–e** (filled circles), the amines **3a–c** (filled triangles), the phosphines **4a–c** (filled squares, in CH_2Cl_2), the enamines **5a–c** (open triangles, in MeCN) and methanolate (filled rhomb). The linear curve refers to the plot of $(\log k_2)/s$ against the N parameters of the carbanions **2a–e**, and the slope is fixed to unity as required by Equation (3.1). ^[a] $\text{P}(\text{ani})_3$ = tris(*p*-anisyl)phosphine **4c**.

3.4 Experimental Section

3.4.1 General comment

1,2-Diaza-1,3-dienes **1a-f**, the potassium salts of **2a-c** and **2e**, and the enamines **5a-d** were synthesized by following literature procedures.^[1c, 6b, 15, 16] Tris(4-chlorophenyl)phosphine (**4a**), triphenylphosphine (**4b**) and tris(4-chlorophenyl)phosphine (**4c**) were purchased. Morpholine (**3a**), piperidine (**3b**), pyrrolidine (**3c**) and benzylamine (**3d**) were purchased and purified by distillation prior to use. ¹H (400 MHz) and ¹³C (100 MHz) NMR spectra were measured on a Varian Inova 400 or Varian Mercury 400 NMR spectrometer.

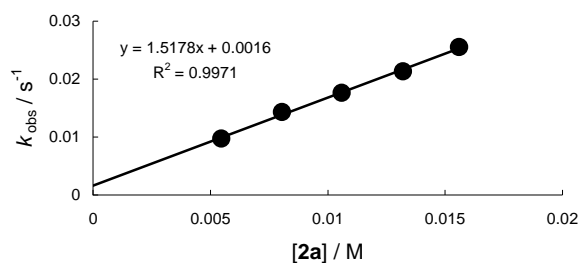
The kinetics of the reactions of the conjugated azoalkenes **1** with the nucleophiles **2-5** were followed by UV-Vis spectroscopy by using working stations similar to those described previously.^[3a, 3f, 17] For slow reactions ($\tau_{1/2} > 10$ s) the UV-visible spectra were collected at different times by a J&M TIDAS diode array spectrophotometer that was connected to a Hellma 661.502-QX quartz Suprasil immersion probe (5 mm light path) by fiber optic cables with standard SMA connectors. All kinetic measurements were carried out in Schlenk glassware under exclusion of moisture. The temperature of the solutions during the kinetic studies was maintained to 20 °C within ± 0.1 °C by using circulating bath cryostats and monitored with thermo-couple probes that were inserted into the reaction mixture. Stopped-flow spectrophotometer systems (Applied Photophysics SX.18MV-R or Hi-Tech SF-61DX2) were used for the investigation of fast reactions of 1,2-diaza-1,3-dienes with nucleophiles ($10 \text{ ms} < \tau_{1/2} < 10$ s). The kinetic runs were initiated by mixing equal volumes of solutions of the 1,2-diaza-1,3-dienes and the nucleophiles.

3.4.2 Kinetic Experiments

Kinetics of the reactions of 4-ethoxycarbonyl-3-methyl-1-phenylaminocarbonyl-1,2-diaza-1,3-butadiene (**1a**) with nucleophilesRate constants for the reactions of 4-ethoxycarbonyl-3-methyl-1-phenylaminocarbonyl-1,2-diaza-1,3-butadiene (**1a**) with carbanions **2**

Rate constants for the reactions of **1a** with the anion of Meldrum's acid (**2a-K**) in DMSO (conventional UV-Vis spectroscopy, 20 °C, $\lambda = 400$ nm).

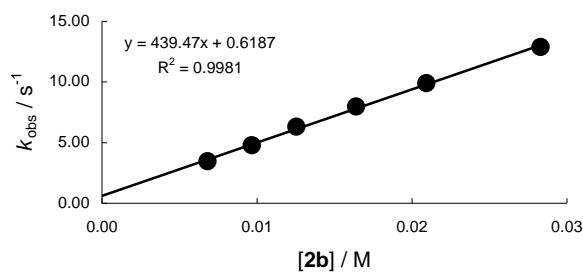
$[\mathbf{1a}]_0 / \text{M}$	$[\mathbf{2a}]_0 / \text{M}$	$[\mathbf{2a}]_0 / [\mathbf{1a}]_0$	$k_{\text{obs}} / \text{s}^{-1}$
5.30×10^{-4}	5.47×10^{-3}	10	9.71×10^{-3}
5.21×10^{-4}	8.05×10^{-3}	15	1.43×10^{-2}
5.12×10^{-4}	1.06×10^{-2}	21	1.76×10^{-2}
5.14×10^{-4}	1.32×10^{-2}	26	2.13×10^{-2}
5.05×10^{-4}	1.56×10^{-2}	31	2.55×10^{-2}



$$k_2 = 1.52 \text{ M}^{-1} \text{ s}^{-1}$$

Rate constants for the reactions of **1a** with the anion of dimedone (**2b-K**) in DMSO (stopped-flow method, 20 °C, $\lambda = 400$ nm).

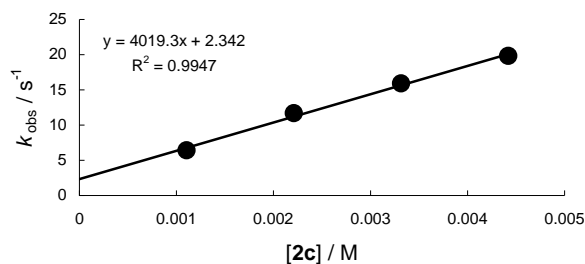
$[\mathbf{1a}]_0 / \text{M}$	$[\mathbf{2b}]_0 / \text{M}$	$[\mathbf{2b}]_0 / [\mathbf{1a}]_0$	$k_{\text{obs}} / \text{s}^{-1}$
5.45×10^{-4}	6.82×10^{-3}	13	3.45
5.45×10^{-4}	9.68×10^{-3}	18	4.79
5.45×10^{-4}	1.25×10^{-2}	23	6.30
5.45×10^{-4}	1.64×10^{-2}	30	7.97
5.45×10^{-4}	2.09×10^{-2}	38	9.90
5.45×10^{-4}	2.83×10^{-2}	52	1.29×10^1



$$k_2 = 4.39 \times 10^2 \text{ M}^{-1} \text{ s}^{-1}$$

Rate constants for the reactions of **1a** with the anion of acetylacetone (**2c-K**) in DMSO (stopped-flow method, 20 °C, $\lambda = 360$ nm).

$[\mathbf{1a}]_0 / \text{M}$	$[\mathbf{2c}]_0 / \text{M}$	$[\mathbf{2c}]_0 / [\mathbf{1a}]_0$	$k_{\text{obs}} / \text{s}^{-1}$
1.09×10^{-4}	1.11×10^{-3}	10	6.39
1.09×10^{-4}	2.21×10^{-3}	20	1.17×10^1
1.09×10^{-4}	3.32×10^{-3}	30	1.59×10^1
1.09×10^{-4}	4.42×10^{-3}	41	1.98×10^1



$$k_2 = 4.02 \times 10^3 \text{ M}^{-1} \text{ s}^{-1}$$

Rate constants for the reactions of **1a** with the anion of ethylcyanoacetate (**2d**-Na) in MeOH (deprotonation of **2d**-H with NaOMe, stopped-flow method, 20 °C, $\lambda = 400 \text{ nm}$).

$[\mathbf{1a}]_0 / \text{M}$	$[\mathbf{2d-H}]_0 / \text{M}$	$[\text{MeO}^-]_0 / \text{M}$	$[\mathbf{2d}]^a / \text{M}$	$[\text{MeO}^-]^a / \text{M}$	$[\mathbf{2d}] / [\mathbf{1a}]_0$	$k_{\text{obs}} / \text{s}^{-1}$	$k_{1\psi} / \text{s}^{-1b}$
3.49×10^{-4}	8.71×10^{-2}	8.33×10^{-3}	2.76×10^{-3}	1.41×10^{-3}	8	8.57	8.56
3.49×10^{-4}	8.71×10^{-2}	1.67×10^{-2}	5.39×10^{-3}	2.94×10^{-3}	15	1.69×10^1	1.69×10^1
3.49×10^{-4}	8.71×10^{-2}	2.50×10^{-2}	7.89×10^{-3}	4.61×10^{-3}	23	2.49×10^1	2.49×10^1
3.49×10^{-4}	8.71×10^{-2}	3.33×10^{-2}	1.02×10^{-2}	6.41×10^{-3}	29	3.10×10^1	3.10×10^1
3.49×10^{-4}	8.71×10^{-2}	4.17×10^{-2}	1.25×10^{-2}	8.36×10^{-3}	36	3.75×10^1	3.75×10^1

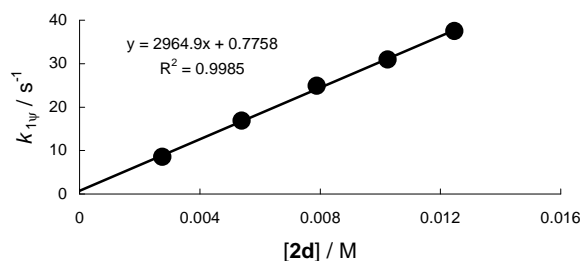
^a were calculated based on $K_{2dH} = 2.40 \times 10^1 \text{ M}^{-1}$ [7]

$$K_{2dH} = [\mathbf{2d}] / ([\mathbf{2dH}] [\text{MeO}^-])$$

$$[\mathbf{2d}] = [\mathbf{2dH}]_0 - [\mathbf{2dH}]$$

$$[\text{MeO}^-] = [\text{MeO}^-]_0 - [\mathbf{2d}]$$

$$k_{\text{obs}} = k_{1\psi} + [\text{MeO}^-] k_{2,\text{MeO}^-}; k_{2,\text{MeO}^-} = 4.25 \text{ M}^{-1} \text{ s}^{-1*}$$

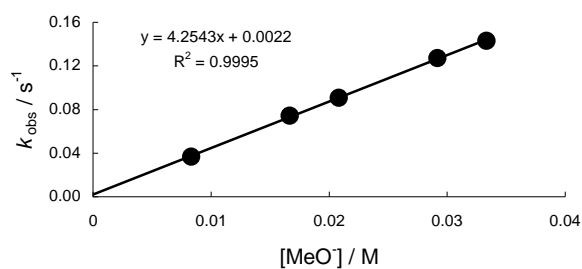


$$k_2 = 2.96 \times 10^3 \text{ M}^{-1} \text{ s}^{-1}$$

Chapter 3: Electrophilic Reactivities of 1,2-Diaza-1,3-dienes

* Rate constants for the reactions of **1a** with sodium methanolate in CH₃OH (stopped-flow method, 20 °C, $\lambda = 400$ nm).

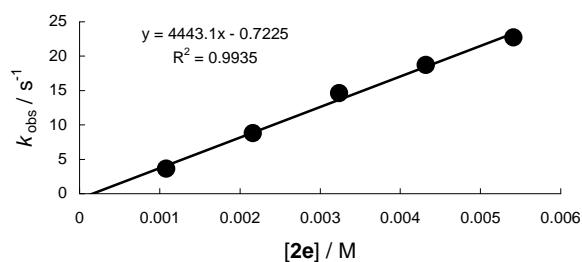
$[\mathbf{1a}]_0 / \text{M}$	$[\text{NaOMe}]_0 / \text{M}$	$[\text{NaOMe}]_0 / [\mathbf{1a}]_0$	$k_{\text{obs}} / \text{s}^{-1}$
3.49×10^{-4}	8.33×10^{-3}	24	3.67×10^{-2}
3.49×10^{-4}	1.67×10^{-2}	48	7.43×10^{-2}
3.49×10^{-4}	2.08×10^{-2}	60	9.08×10^{-2}
3.49×10^{-4}	2.92×10^{-2}	84	1.27×10^{-1}
3.49×10^{-4}	3.33×10^{-2}	96	1.43×10^{-1}



$$k_2 = 4.25 \text{ M}^{-1} \text{ s}^{-1}$$

Rate constants for the reactions of **1a** with the anion of malononitrile (**2e-K**) in DMSO (stopped-flow method, 20 °C, $\lambda = 350$ nm).

$[\mathbf{1a}]_0 / \text{M}$	$[\mathbf{2e}]_0 / \text{M}$	$[\mathbf{2e}]_0 / [\mathbf{1a}]_0$	$k_{\text{obs}} / \text{s}^{-1}$
1.09×10^{-4}	1.08×10^{-3}	10	3.61
1.09×10^{-4}	2.16×10^{-3}	20	8.80
1.09×10^{-4}	3.24×10^{-3}	30	1.46×10^1
1.09×10^{-4}	4.32×10^{-3}	40	1.87×10^1
1.09×10^{-4}	5.41×10^{-3}	50	2.27×10^1

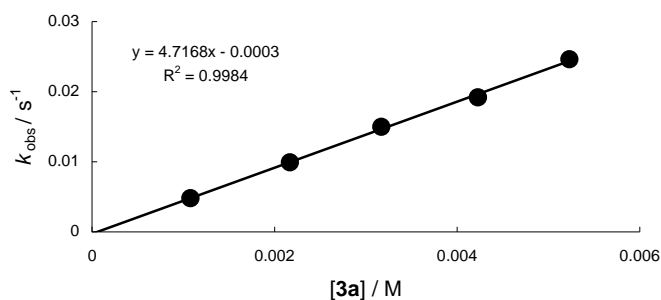


$$k_2 = 4.44 \times 10^3 \text{ M}^{-1} \text{ s}^{-1}$$

Rate constants for the reactions of 4-ethoxycarbonyl-3-methyl-1-phenylaminocarbonyl-1,2-diaza-1,3-butadiene (**1a**) with secondary amines **3**

Rate constants for the reactions of **1a** with morpholine (**3a**) in CH₃OH (conventional UV-Vis spectroscopy, 20 °C, $\lambda = 340$ nm).

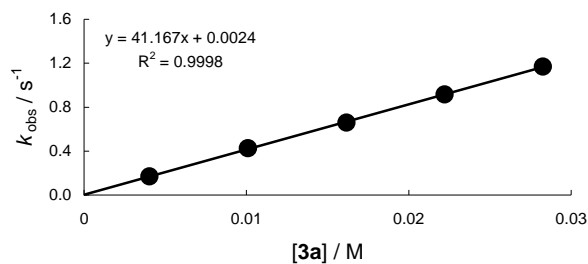
$[\mathbf{1a}]_0 / \text{M}$	$[\mathbf{3a}]_0 / \text{M}$	$[\mathbf{3a}]_0 / [\mathbf{1a}]_0$	$k_{\text{obs}} / \text{s}^{-1}$
3.09×10^{-4}	1.08×10^{-3}	4	4.80×10^{-3}
3.11×10^{-4}	2.17×10^{-3}	7	9.92×10^{-3}
3.02×10^{-4}	3.17×10^{-3}	11	1.50×10^{-2}
3.02×10^{-4}	4.23×10^{-3}	14	1.92×10^{-2}
2.99×10^{-4}	5.23×10^{-3}	17	2.46×10^{-2}



$$k_2 = 4.72 \text{ M}^{-1} \text{ s}^{-1}$$

Rate constants for the reactions of **1a** with morpholine (**3a**) in DMSO (stopped-flow method, 20 °C, $\lambda = 400$ nm).

$[\mathbf{1a}]_0 / \text{M}$	$[\mathbf{3a}]_0 / \text{M}$	$[\mathbf{3a}]_0 / [\mathbf{1a}]_0$	$k_{\text{obs}} / \text{s}^{-1}$
3.63×10^{-4}	4.04×10^{-3}	11	1.68×10^{-1}
3.63×10^{-4}	1.01×10^{-2}	28	4.25×10^{-1}
3.63×10^{-4}	1.62×10^{-2}	44	6.60×10^{-1}
3.63×10^{-4}	2.22×10^{-2}	61	9.15×10^{-1}
3.63×10^{-4}	2.83×10^{-2}	78	1.17×10^0

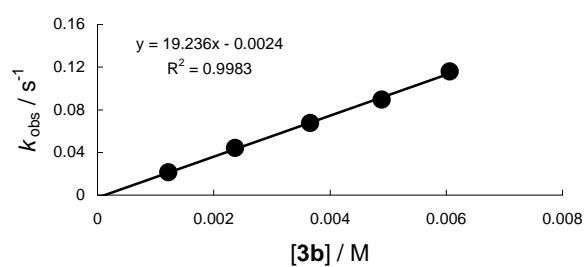


$$k_2 = 4.12 \times 10^1 \text{ M}^{-1} \text{ s}^{-1}$$

Rate constants for the reactions of **1a** with piperidine (**3b**) in CH₃OH (conventional UV-Vis spectroscopy, 20 °C).

$[\mathbf{1a}]_0 / \text{M}$	$[\mathbf{3b}]_0 / \text{M}$	$[\mathbf{3b}]_0 / [\mathbf{1a}]_0$	$k_{\text{obs}} / \text{s}^{-1}$	$\lambda / \text{nm}^{[a]}$
6.65×10^{-4}	2.37×10^{-3}	4	4.40×10^{-2}	425
3.06×10^{-4}	1.22×10^{-3}	4	2.13×10^{-2}	340
3.05×10^{-4}	3.66×10^{-3}	12	6.76×10^{-2}	340
3.06×10^{-4}	4.89×10^{-3}	16	8.94×10^{-2}	340
3.03×10^{-4}	6.06×10^{-3}	20	1.16×10^{-1}	340

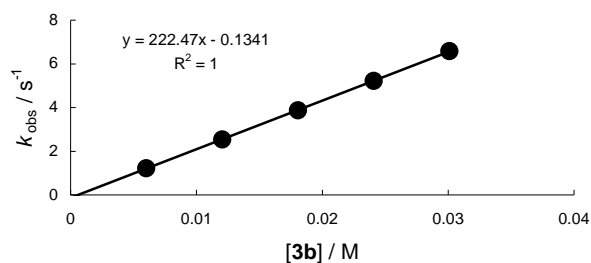
[a] evaluated at different wavelengths to show the consistency of all reactions, which were collected at different wavelengths



$$k_2 = 1.92 \times 10^1 \text{ M}^{-1} \text{ s}^{-1}$$

Rate constants for the reactions of **1a** with piperidine (**3b**) in CH₃CN (stopped-flow method, 20 °C, $\lambda = 400$ nm).

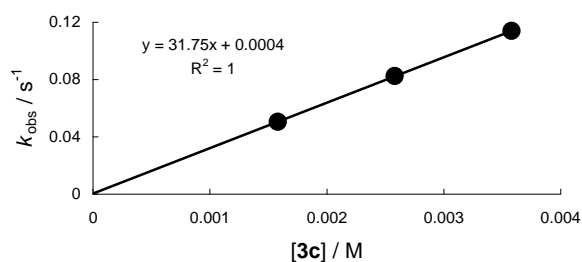
$[\mathbf{1a}]_0 / \text{M}$	$[\mathbf{3b}]_0 / \text{M}$	$[\mathbf{3b}]_0 / [\mathbf{1a}]_0$	$k_{\text{obs}} / \text{s}^{-1}$
6.18×10^{-4}	6.02×10^{-3}	10	1.22
6.18×10^{-4}	1.21×10^{-2}	20	2.54
6.18×10^{-4}	1.81×10^{-2}	30	3.87
6.18×10^{-4}	2.41×10^{-2}	39	5.22
6.18×10^{-4}	3.01×10^{-2}	49	6.58



$$k_2 = 2.22 \times 10^2 \text{ M}^{-1} \text{ s}^{-1}$$

Rate constants for the reactions of **1a** with pyrrolidine (**3c**) in CH₃CN (conventional UV-Vis spectroscopy, 20 °C, $\lambda = 340$ nm).

$[\mathbf{1a}]_0 / \text{M}$	$[\mathbf{3c}]_0 / \text{M}$	$[\mathbf{3c}]_0 / [\mathbf{1a}]_0$	$k_{\text{obs}} / \text{s}^{-1}$
3.04×10^{-4}	1.58×10^{-3}	5	5.05×10^{-2}
3.04×10^{-4}	2.58×10^{-3}	9	8.24×10^{-2}
3.01×10^{-4}	3.58×10^{-3}	12	1.14×10^{-1}

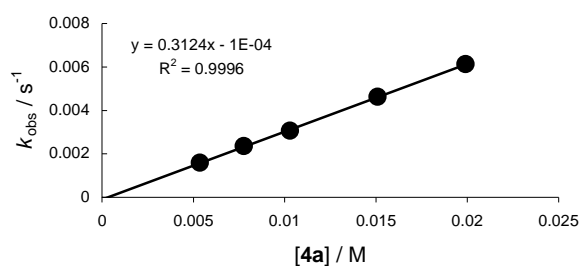


$$k_2 = 3.18 \times 10^1 \text{ M}^{-1} \text{ s}^{-1}$$

Rate constants for the reactions of 4-ethoxycarbonyl-3-methyl-1-phenylaminocarbonyl-1,2-diaza-1,3-butadiene (**1a**) with triarylphosphines **4**

Rate constants for the reactions of **1a** with tris(4-chlorophenyl)phosphine (**4a**) in CH₂Cl₂ (conventional UV-Vis spectroscopy, 20 °C, $\lambda = 400$ nm).

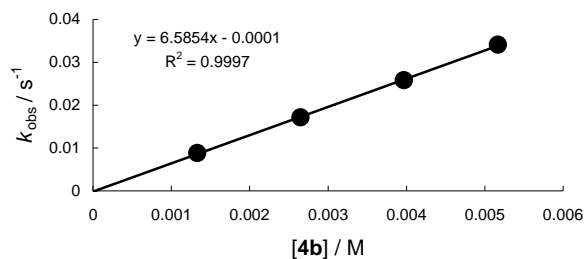
$[\mathbf{1a}]_0 / \text{M}$	$[\mathbf{4a}]_0 / \text{M}$	$[\mathbf{4a}]_0 / [\mathbf{1a}]_0$	$k_{\text{obs}} / \text{s}^{-1}$
5.34×10^{-4}	5.36×10^{-3}	10	1.59×10^{-3}
5.16×10^{-4}	7.77×10^{-3}	15	2.36×10^{-3}
5.13×10^{-4}	1.03×10^{-2}	20	3.06×10^{-3}
5.02×10^{-4}	1.51×10^{-2}	30	4.63×10^{-3}
5.03×10^{-4}	1.99×10^{-2}	40	6.13×10^{-3}



$$k_2 = 3.12 \times 10^{-1} \text{ M}^{-1} \text{ s}^{-1}$$

Rate constants for the reactions of **1a** with triphenylphosphine (**4b**) in CH₂Cl₂ (conventional UV-Vis spectroscopy, 20 °C, $\lambda = 400$ nm).

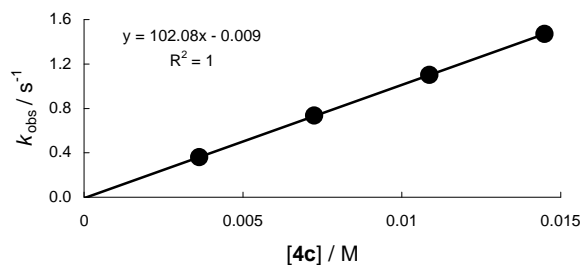
$[\mathbf{1a}]_0 / \text{M}$	$[\mathbf{4b}]_0 / \text{M}$	$[\mathbf{4b}]_0 / [\mathbf{1a}]_0$	$k_{\text{obs}} / \text{s}^{-1}$
2.79×10^{-4}	1.33×10^{-3}	5	8.77×10^{-3}
2.78×10^{-4}	2.65×10^{-3}	10	1.72×10^{-2}
2.78×10^{-4}	3.97×10^{-3}	14	2.58×10^{-2}
2.71×10^{-4}	5.17×10^{-3}	19	3.41×10^{-2}



$$k_2 = 6.59 \text{ M}^{-1} \text{ s}^{-1}$$

Rate constants for the reactions of **1a** with tris(4-methoxyphenyl)phosphine (**4c**) in CH_2Cl_2 (stopped-flow method, 20 °C, $\lambda = 400 \text{ nm}$).

$[\mathbf{1a}]_0 / \text{M}$	$[\mathbf{4c}]_0 / \text{M}$	$[\mathbf{4c}]_0 / [\mathbf{1a}]_0$	$k_{\text{obs}} / \text{s}^{-1}$
3.49×10^{-4}	3.62×10^{-3}	10	3.59×10^{-1}
3.49×10^{-4}	7.25×10^{-3}	21	7.34×10^{-1}
3.49×10^{-4}	1.09×10^{-2}	31	1.10
3.49×10^{-4}	1.45×10^{-2}	42	1.47

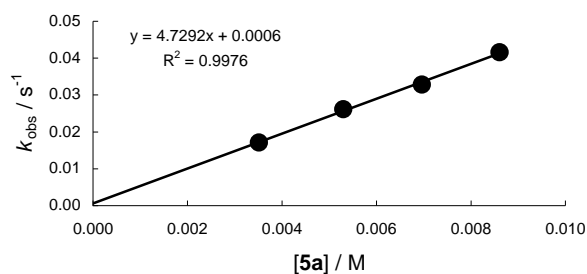


$$k_2 = 1.02 \times 10^2 \text{ M}^{-1} \text{ s}^{-1}$$

Rate constants for the reactions of 4-ethoxycarbonyl-3-methyl-1-phenylaminocarbonyl-1,2-diaza-1,3-butadiene (**1a**) with enamines **5**

Rate constants for the reactions of **1a** with morpholinocyclohexene (**5a**) in CH₃CN (conventional UV-Vis spectroscopy, 20 °C, $\lambda = 400$ nm).

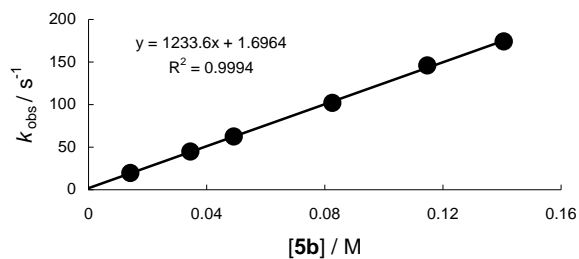
$[\mathbf{1a}]_0 / \text{M}$	$[\mathbf{5a}]_0 / \text{M}$	$[\mathbf{5a}]_0 / [\mathbf{1a}]_0$	$k_{\text{obs}} / \text{s}^{-1}$
7.50×10^{-4}	3.51×10^{-3}	5	1.71×10^{-2}
7.55×10^{-4}	5.30×10^{-3}	7	2.61×10^{-2}
7.45×10^{-4}	6.96×10^{-3}	9	3.28×10^{-2}
7.35×10^{-4}	8.61×10^{-3}	12	4.16×10^{-2}



$$k_2 = 4.73 \text{ M}^{-1} \text{ s}^{-1}$$

Rate constants for the reactions of **1a** with piperidinocyclopentene (**5b**) in CH₃CN (stopped-flow method, 20 °C, $\lambda = 444$ nm).

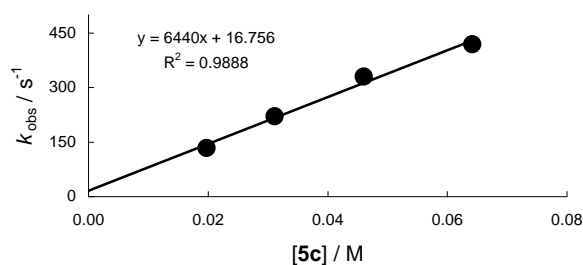
$[\mathbf{1a}]_0 / \text{M}$	$[\mathbf{5b}]_0 / \text{M}$	$[\mathbf{5b}]_0 / [\mathbf{1a}]_0$	$k_{\text{obs}} / \text{s}^{-1}$
1.07×10^{-3}	1.42×10^{-2}	13	1.94×10^1
1.07×10^{-3}	3.46×10^{-2}	32	4.46×10^1
1.07×10^{-3}	4.93×10^{-2}	46	6.23×10^1
1.07×10^{-3}	8.26×10^{-2}	77	1.02×10^2
1.07×10^{-3}	1.15×10^{-1}	108	1.46×10^2
1.07×10^{-3}	1.41×10^{-1}	132	1.74×10^2



$$k_2 = 1.23 \times 10^3 \text{ M}^{-1} \text{ s}^{-1}$$

Rate constants for the reactions of **1a** with pyrrolidinocyclopentene (**5c**) in CH₃CN (stopped-flow method, 20 °C, $\lambda = 444 \text{ nm}$).

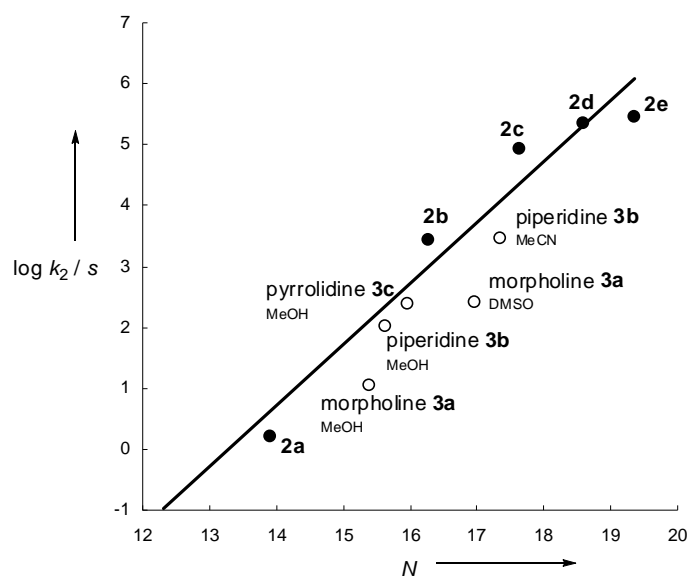
$[\mathbf{1a}]_0 / \text{M}$	$[\mathbf{5c}]_0 / \text{M}$	$[\mathbf{5c}]_0 / [\mathbf{1a}]_0$	$k_{\text{obs}} / \text{s}^{-1}$
1.04×10^{-3}	1.97×10^{-2}	19	1.34×10^2
1.04×10^{-3}	3.11×10^{-2}	30	2.21×10^2
1.04×10^{-3}	4.60×10^{-2}	44	3.30×10^2
1.04×10^{-3}	6.42×10^{-2}	62	4.19×10^2



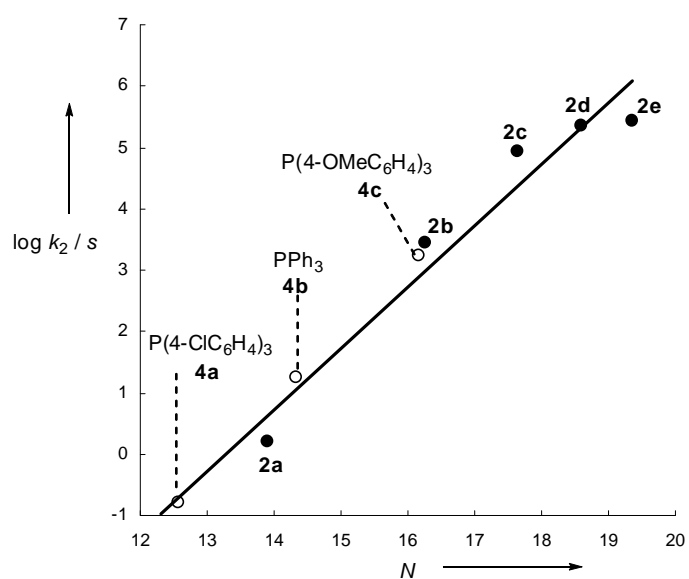
$$k_2 = 6.44 \times 10^3 \text{ M}^{-1} \text{ s}^{-1}$$

Correlations of the second-order rate constants ($\log k_2$ (20 °C)/s) of the reactions of **1a** with the nucleophiles **2-5** versus the corresponding N parameters of the nucleophiles

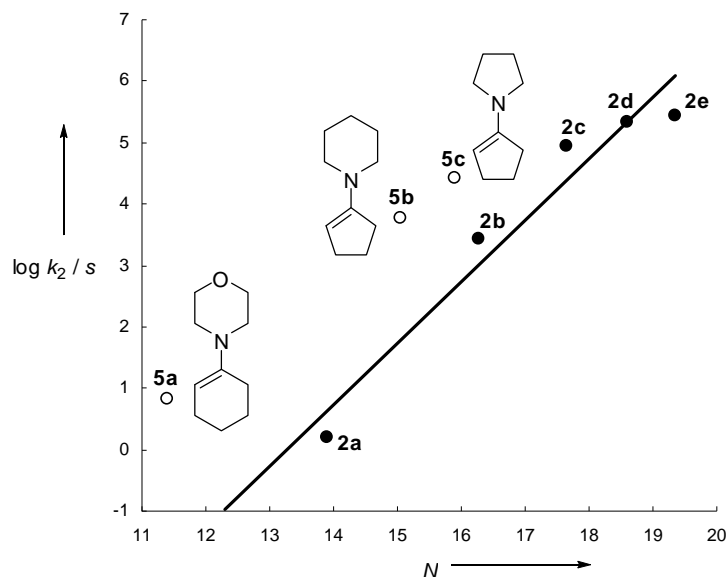
Plot of $\log k_2/s$ versus N for the reactions of **1a** with carbanions **2** (filled symbols) in DMSO and with amines **3** (open symbols) in different solvents.



Plot of $\log k_2/s$ versus N for the reactions of **1a** with carbanions **2** (filled symbols) in DMSO and with phosphines **4** (open symbols) in CH_2Cl_2 .



Plot of $\log k_2/s$ versus N for the reactions of **1a** with carbanions **2** (filled symbols) in DMSO and with enamines **5** (open symbols) in MeCN.

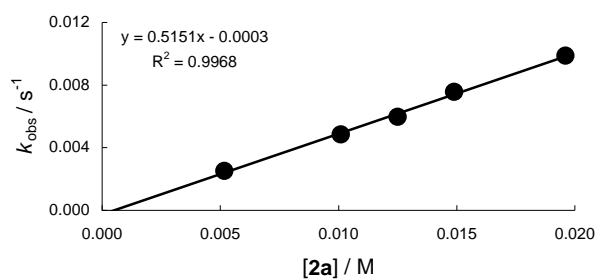


Kinetics of the reactions of 4-(dimethylaminocarbonyl)-3-methyl-1-methoxycarbonyl-aza-1,3-butadiene (**1b**) with nucleophiles

Rate constants for the reactions of 4-(dimethylaminocarbonyl)-3-methyl-1-methoxycarbonyl-1,2-diaza-1,3-butadiene (**1b**) with carbanions **2**

Rate constants for the reactions of **1b** with the anion of Meldrum's acid (**2a-K**) in DMSO (conventional UV-Vis spectroscopy, 20 °C, $\lambda = 340$ nm).

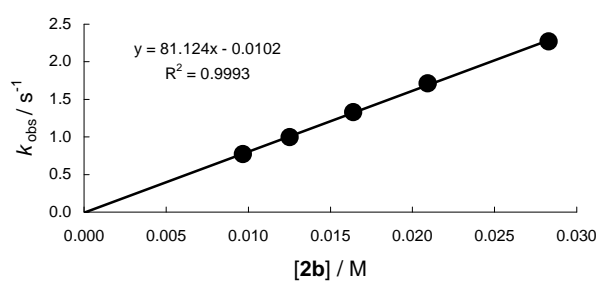
$[\mathbf{1b}]_0 / \text{M}$	$[\mathbf{2a}]_0 / \text{M}$	$[\mathbf{2a}]_0 / [\mathbf{1b}]_0$	$k_{\text{obs}} / \text{s}^{-1}$
6.01×10^{-4}	5.17×10^{-3}	9	2.52×10^{-3}
5.84×10^{-4}	1.01×10^{-2}	17	4.84×10^{-3}
5.81×10^{-4}	1.25×10^{-2}	22	5.96×10^{-3}
5.79×10^{-4}	1.49×10^{-2}	26	7.57×10^{-3}
5.70×10^{-4}	1.96×10^{-2}	34	9.87×10^{-3}



$$k_2 = 5.15 \times 10^{-1} \text{ M}^{-1} \text{ s}^{-1}$$

Rate constants for the reactions of **1b** with the anion of dimedone (**2b-K**) in DMSO (stopped-flow method, 20 °C, $\lambda = 350 \text{ nm}$).

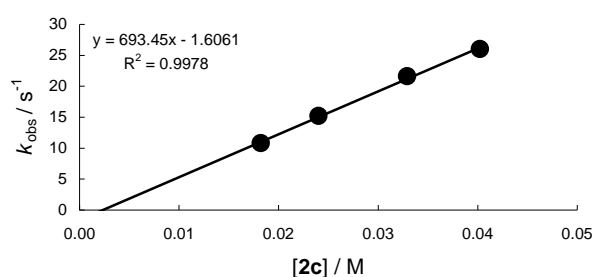
$[\mathbf{1b}]_0 / \text{M}$	$[\mathbf{2b}]_0 / \text{M}$	$[\mathbf{2b}]_0 / [\mathbf{1b}]_0$	$k_{\text{obs}} / \text{s}^{-1}$
1.50×10^{-3}	9.68×10^{-3}	6	7.69×10^{-1}
1.50×10^{-3}	1.25×10^{-2}	8	9.96×10^{-1}
1.50×10^{-3}	1.64×10^{-2}	11	1.33
1.50×10^{-3}	2.09×10^{-2}	14	1.71
1.50×10^{-3}	2.83×10^{-2}	19	2.27



$$k_2 = 8.11 \times 10^1 \text{ M}^{-1} \text{ s}^{-1}$$

Rate constants for the reactions of **1b** with the anion of acetylacetonate (**2c-K**) in DMSO (stopped-flow method, 20 °C, $\lambda = 350$ nm).

$[\mathbf{1b}]_0 / \text{M}$	$[\mathbf{2c}]_0 / \text{M}$	$[\mathbf{2c}]_0 / [\mathbf{1b}]_0$	$k_{\text{obs}} / \text{s}^{-1}$
1.66×10^{-3}	1.82×10^{-2}	11	1.08×10^1
1.66×10^{-3}	2.40×10^{-2}	15	1.52×10^1
1.66×10^{-3}	3.29×10^{-2}	20	2.16×10^1
1.66×10^{-3}	4.02×10^{-2}	24	2.60×10^1



$$k_2 = 6.93 \times 10^2 \text{ M}^{-1} \text{ s}^{-1}$$

Rate constants for the reactions of **1b** with the anion of ethylcyanoacetate (**2d-Na**) in CH_3OH (deprotonation of **2d-H** with NaOMe, stopped-flow method, 20 °C, $\lambda = 300$ nm).

$[\mathbf{1b}]_0 / \text{M}$	$[\mathbf{2d-H}]_0 / \text{M}$	$[\text{MeO}^-]_0 / \text{M}$	$[\mathbf{2d}]^a / \text{M}$	$[\text{MeO}^-]^a / \text{M}$	$[\mathbf{2d}] / [\mathbf{1b}]_0$	$k_{\text{obs}} / \text{s}^{-1}$	$k_{1\psi} / \text{s}^{-1}$
1.36×10^{-3}	9.60×10^{-2}	9.50×10^{-2}	2.49×10^{-2}	2.26×10^{-2}	18	4.14×10^1	4.14×10^1
1.36×10^{-3}	9.60×10^{-2}	1.43×10^{-1}	3.16×10^{-2}	4.00×10^{-2}	23	6.27×10^1	6.26×10^1
1.36×10^{-3}	1.40×10^{-1}	8.90×10^{-2}	2.94×10^{-2}	1.51×10^{-2}	22	5.49×10^1	5.49×10^1
1.36×10^{-3}	1.24×10^{-1}	1.78×10^{-1}	4.27×10^{-2}	4.63×10^{-2}	31	1.03×10^2	1.03×10^2

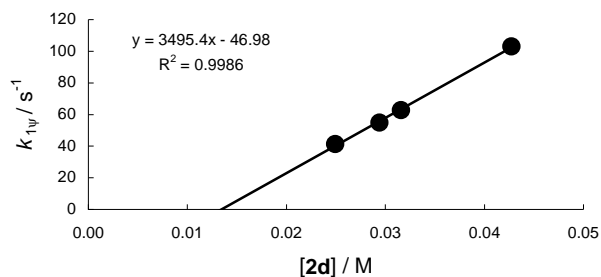
^a were calculated based on $K_{2\text{dH}} = 2.40 \times 10^1 \text{ M}^{-1}$ [7]

$$K_{2\text{dH}} = [\mathbf{2d}] / ([\mathbf{2dH}] [\text{MeO}^-])$$

$$[\mathbf{2d}] = [\mathbf{2dH}]_0 - [\mathbf{2dH}]$$

$$[\text{MeO}^-] = [\text{MeO}^-]_0 - [\mathbf{2d}]$$

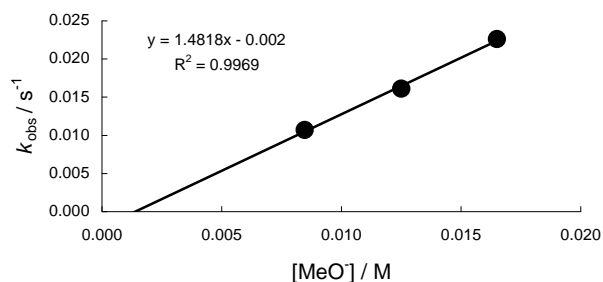
^b $k_{\text{obs}} = k_{1\psi} + [\text{MeO}^-] k_{2,\text{MeO}^-}$; $k_{2,\text{MeO}^-} = 1.48 \text{ M}^{-1} \text{ s}^{-1}$ *



$$k_2 = 3.50 \times 10^3 \text{ M}^{-1} \text{ s}^{-1}$$

*Rate constants for the reactions of **1b** with sodium methanolate in CH₃OH (conventional UV-Vis spectroscopy, 20 °C, $\lambda = 300 \text{ nm}$).

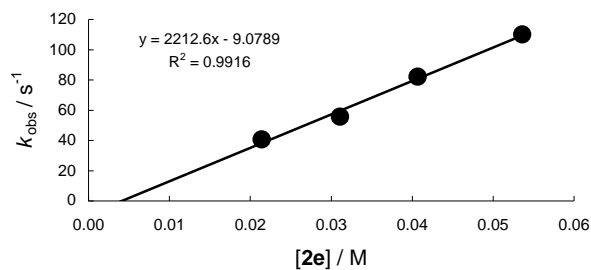
$[\mathbf{1b}]_0 / \text{M}$	$[\text{NaOMe}]_0 / \text{M}$	$[\text{NaOMe}]_0 / [\mathbf{1b}]_0$	$k_{\text{obs}} / \text{s}^{-1}$
2.30×10^{-3}	8.47×10^{-3}	4	1.07×10^{-2}
2.26×10^{-3}	1.25×10^{-2}	6	1.61×10^{-2}
2.24×10^{-3}	1.65×10^{-2}	7	2.26×10^{-2}



$$k_2 = 1.48 \text{ M}^{-1} \text{ s}^{-1}$$

Rate constants for the reactions of **1b** with the anion of malononitrile (**2e-K**) in DMSO (stopped-flow method, 20 °C, $\lambda = 350 \text{ nm}$).

$[\mathbf{1b}]_0 / \text{M}$	$[\mathbf{2e}]_0 / \text{M}$	$[\mathbf{2e}]_0 / [\mathbf{1b}]_0$	$k_{\text{obs}} / \text{s}^{-1}$
2.46×10^{-3}	2.14×10^{-2}	9	4.06×10^1
2.46×10^{-3}	3.11×10^{-2}	13	5.57×10^1
2.46×10^{-3}	4.07×10^{-2}	17	8.22×10^1
2.46×10^{-3}	5.36×10^{-2}	22	1.10×10^2

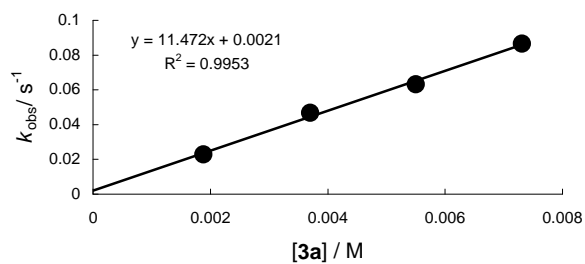


$$k_2 = 2.21 \times 10^3 \text{ M}^{-1} \text{ s}^{-1}$$

Rate constants for the reactions of 4-(dimethylaminocarbonyl)-3-methyl-1-methoxycarbonyl-1,2-diaza-1,3-butadiene (**1b**) with amines **3**

Rate constants for the reactions of **1b** with morpholine (**3a**) in CH₃OH (conventional UV-Vis spectroscopy, 20 °C, $\lambda = 300 \text{ nm}$).

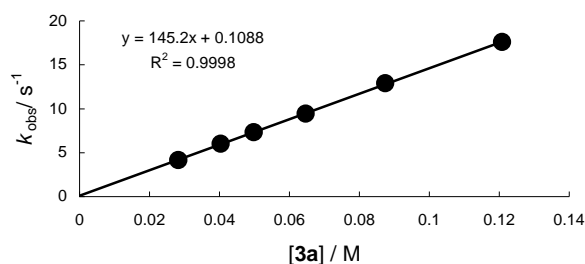
$[\mathbf{1b}]_0 / \text{M}$	$[\mathbf{3a}]_0 / \text{M}$	$[\mathbf{3a}]_0 / [\mathbf{1b}]_0$	$k_{\text{obs}} / \text{s}^{-1}$
2.64×10^{-4}	1.88×10^{-3}	7	2.28×10^{-2}
3.47×10^{-4}	3.70×10^{-3}	11	4.68×10^{-2}
3.44×10^{-4}	5.50×10^{-3}	16	6.32×10^{-2}
3.43×10^{-4}	7.31×10^{-3}	21	8.65×10^{-2}



$$k_2 = 1.15 \times 10^1 \text{ M}^{-1} \text{ s}^{-1}$$

Rate constants for the reactions of **1b** with morpholine (**3a**) in DMSO (stopped-flow method, 20 °C, $\lambda = 420$ nm).

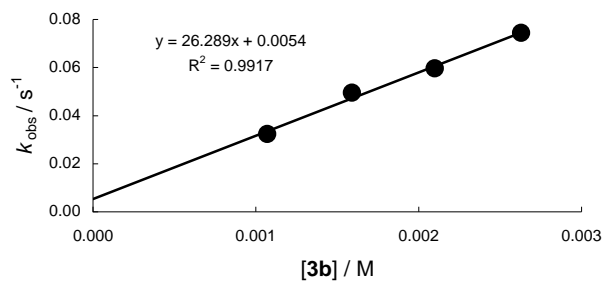
$[\mathbf{1b}]_0 / \text{M}$	$[\mathbf{3a}]_0 / \text{M}$	$[\mathbf{3a}]_0 / [\mathbf{1b}]_0$	$k_{\text{obs}} / \text{s}^{-1}$
3.42×10^{-3}	2.83×10^{-2}	8	4.17
3.42×10^{-3}	4.04×10^{-2}	12	6.02
3.42×10^{-3}	4.98×10^{-2}	15	7.34
3.42×10^{-3}	6.47×10^{-2}	19	9.45
3.42×10^{-3}	8.74×10^{-2}	26	1.29×10^1
3.42×10^{-3}	1.21×10^{-1}	35	1.76×10^1



$$k_2 = 1.45 \times 10^2 \text{ M}^{-1} \text{ s}^{-1}$$

Rate constants for the reactions of **1b** with piperidine (**3b**) in CH₃OH (conventional UV-Vis spectroscopy, 20 °C, $\lambda = 300$ nm).

$[\mathbf{1b}]_0 / \text{M}$	$[\mathbf{3b}]_0 / \text{M}$	$[\mathbf{3b}]_0 / [\mathbf{1b}]_0$	$k_{\text{obs}} / \text{s}^{-1}$
3.54×10^{-4}	1.07×10^{-3}	3	3.23×10^{-2}
3.51×10^{-4}	1.59×10^{-3}	5	4.95×10^{-2}
3.47×10^{-4}	2.10×10^{-3}	6	5.96×10^{-2}
3.47×10^{-4}	2.63×10^{-3}	8	7.44×10^{-2}

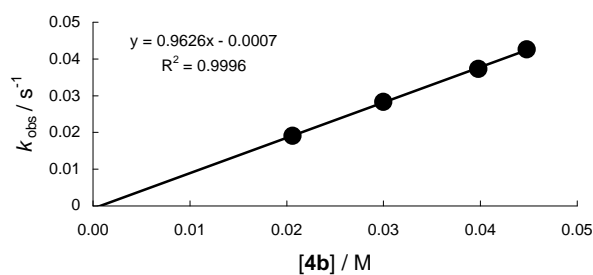


$$k_2 = 2.63 \times 10^1 \text{ M}^{-1} \text{ s}^{-1}$$

Rate constants for the reactions of 4-(dimethylaminocarbonyl)-3-methyl-1-methoxycarbonyl-1,2-diaza-1,3-butadiene (**1b**) with triarylphosphines **4** and enamines **5**

Rate constants for the reactions of **1b** with triphenylphosphine (**4b**) in CH₂Cl₂ (conventional UV-Vis spectroscopy, 20 °C, λ = 420 nm).

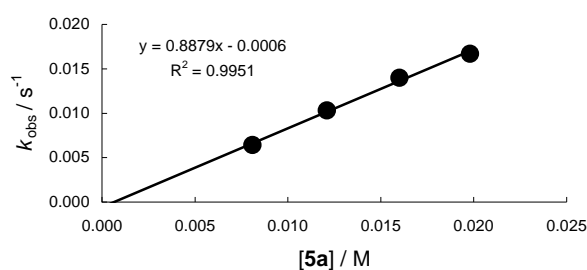
$[\mathbf{1b}]_0 / \text{M}$	$[\mathbf{4b}]_0 / \text{M}$	$[\mathbf{4b}]_0 / [\mathbf{1b}]_0$	$k_{\text{obs}} / \text{s}^{-1}$
4.29×10^{-3}	2.06×10^{-2}	5	1.91×10^{-2}
4.17×10^{-3}	3.00×10^{-2}	7	2.83×10^{-2}
4.14×10^{-3}	3.98×10^{-2}	10	3.73×10^{-2}
4.00×10^{-3}	4.48×10^{-2}	11	4.26×10^{-2}



$$k_2 = 9.63 \times 10^1 \text{ M}^{-1} \text{ s}^{-1}$$

Rate constants for the reactions of **1b** with morpholinocyclohexene (**5a**) in CH₃CN (conventional UV-Vis spectroscopy, 20 °C, $\lambda = 350$ nm).

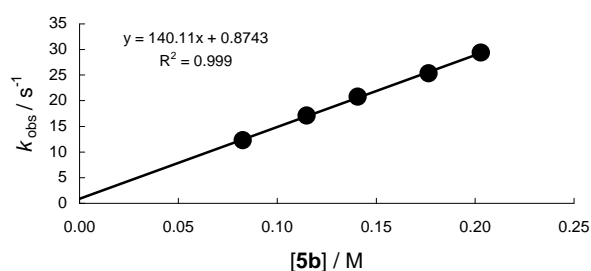
$[\mathbf{1b}]_0 / \text{M}$	$[\mathbf{5a}]_0 / \text{M}$	$[\mathbf{5a}]_0 / [\mathbf{1b}]_0$	$k_{\text{obs}} / \text{s}^{-1}$
2.20×10^{-3}	8.10×10^{-3}	4	6.40×10^{-3}
2.20×10^{-3}	1.21×10^{-2}	6	1.03×10^{-2}
2.18×10^{-3}	1.60×10^{-2}	7	1.40×10^{-2}
2.16×10^{-3}	1.98×10^{-2}	9	1.67×10^{-2}



$$k_2 = 8.88 \times 10^1 \text{ M}^{-1} \text{ s}^{-1}$$

Rate constants for the reactions of **1b** with piperidinocyclopentene (**5b**) in CH₃CN (stopped-flow method, 20 °C, $\lambda = 420$ nm).

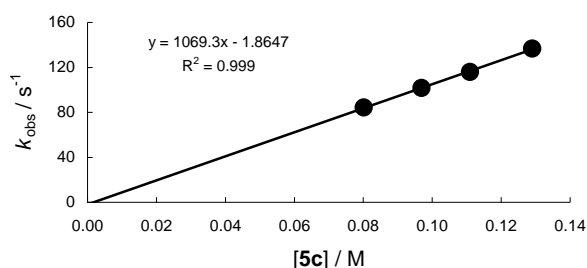
$[\mathbf{1b}]_0 / \text{M}$	$[\mathbf{5b}]_0 / \text{M}$	$[\mathbf{5b}]_0 / [\mathbf{1b}]_0$	$k_{\text{obs}} / \text{s}^{-1}$
8.24×10^{-3}	8.26×10^{-2}	10	1.23×10^1
8.24×10^{-3}	1.15×10^{-1}	14	1.71×10^1
8.24×10^{-3}	1.41×10^{-1}	17	2.08×10^1
8.24×10^{-3}	1.76×10^{-1}	21	2.53×10^1
8.24×10^{-3}	2.03×10^{-1}	25	2.94×10^1



$$k_2 = 1.40 \times 10^2 \text{ M}^{-1} \text{ s}^{-1}$$

Rate constants for the reactions of **1b** with pyrrolidinocyclopentene (**5c**) in CH₃CN (stopped-flow method, 20 °C, $\lambda = 420$ nm)

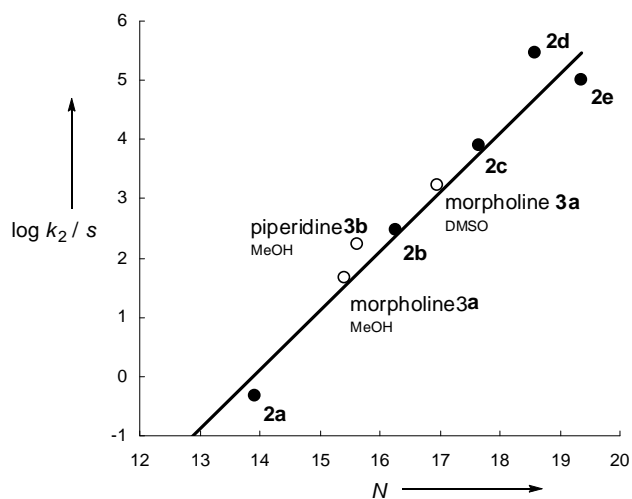
$[\mathbf{1b}]_0 / \text{M}$	$[\mathbf{5c}]_0 / \text{M}$	$[\mathbf{5c}]_0 / [\mathbf{1b}]_0$	$k_{\text{obs}} / \text{s}^{-1}$
8.24×10^{-3}	8.01×10^{-2}	10	8.42×10^1
8.24×10^{-3}	9.69×10^{-2}	12	1.02×10^2
8.24×10^{-3}	1.11×10^{-1}	13	1.16×10^2
8.24×10^{-3}	1.29×10^{-1}	16	1.37×10^2



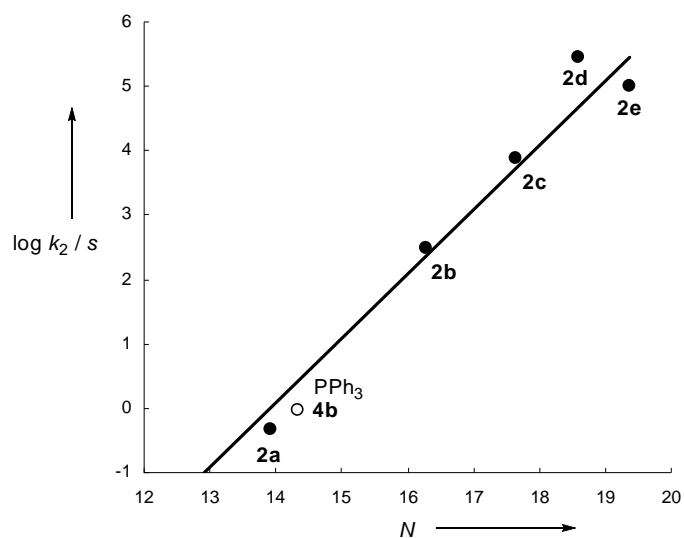
$$k_2 = 1.07 \times 10^3 \text{ M}^{-1} \text{ s}^{-1}$$

Correlations of the second-order rate constants ($\log k_2$ (20 °C)/s) of the reactions of **1b** with the nucleophiles **2-5** versus the corresponding N parameters of the nucleophiles

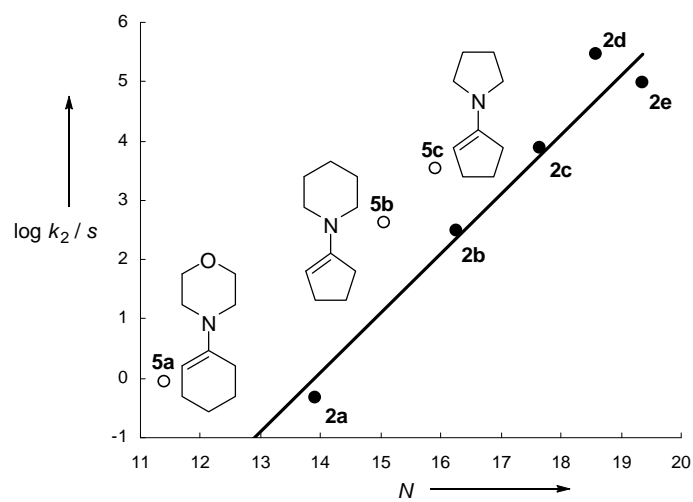
Plot of $\log k_2/s$ versus N for the reactions of **1b** with carbanions **2** (filled symbols) in DMSO and with amines **3** (open symbols) in different solvents.



Plot of $\log k_2/s$ versus N for the reactions of **1b** with carbanions **2** (filled symbols) in DMSO and with phosphines **4** (open symbols) in CH_2Cl_2 .



Plot of $\log k_2/s$ versus N for the reactions of **1b** with carbanions **2** (filled symbols) in DMSO and with enamines **5** (open symbols) in MeCN.

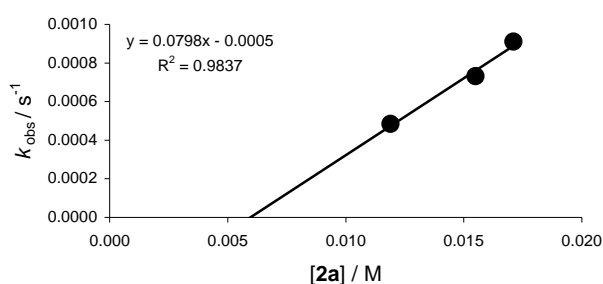


Kinetics of the reactions of 4-ethoxycarbonyl-3-methyl-1-aminocarbonyl-1,2-diaza-1,3-butadiene (**1c**) with nucleophiles

Rate constants for the reactions of 4-ethoxycarbonyl-3-methyl-1-aminocarbonyl-1,2-diaza-1,3-butadiene (**1c**) with carbanions **2**

Rate constants for the reactions of **1c** with the anion of Meldrum's acid (**2a-K**) in DMSO (conventional UV-Vis spectroscopy, 20 °C, $\lambda = 400$ nm).

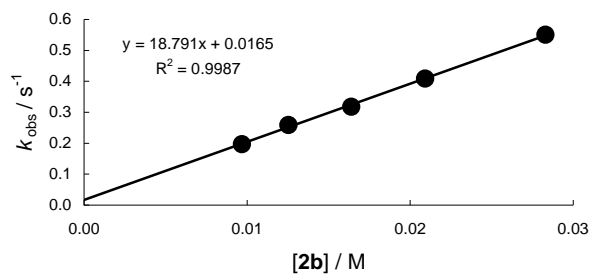
$[\mathbf{1c}]_0 / \text{M}$	$[\mathbf{2a}]_0 / \text{M}$	$[\mathbf{2a}]_0 / [\mathbf{1c}]_0$	$k_{\text{obs}} / \text{s}^{-1}$
1.65×10^{-3}	1.19×10^{-2}	7	4.84×10^{-4}
1.66×10^{-3}	1.55×10^{-2}	9	7.31×10^{-4}
1.66×10^{-3}	1.71×10^{-2}	10	4.84×10^{-2}



$$k_2 = 7.98 \times 10^{-2} \text{ M}^{-1} \text{ s}^{-1}$$

Rate constants for the reactions of **1c** with the anion of dimedone (**2b-K**) in DMSO (stopped-flow method, 20 °C, $\lambda = 444$ nm).

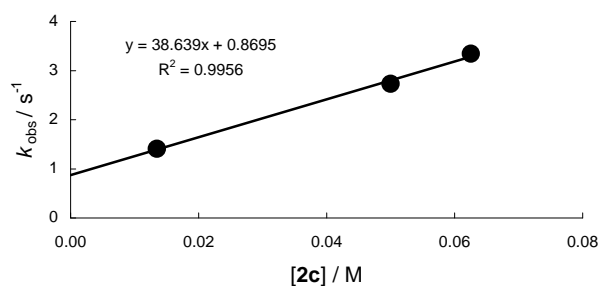
$[\mathbf{1c}]_0 / \text{M}$	$[\mathbf{2b}]_0 / \text{M}$	$[\mathbf{2b}]_0 / [\mathbf{1c}]_0$	$k_{\text{obs}} / \text{s}^{-1}$
1.49×10^{-3}	9.68×10^{-3}	6	1.97×10^{-1}
1.49×10^{-3}	1.25×10^{-2}	8	2.59×10^{-1}
1.49×10^{-3}	1.64×10^{-2}	11	3.18×10^{-1}
1.49×10^{-3}	2.09×10^{-2}	14	4.09×10^{-1}
1.49×10^{-3}	2.83×10^{-2}	19	5.50×10^{-1}



$$k_2 = 1.88 \times 10^1 \text{ M}^{-1} \text{ s}^{-1}$$

Rate constants for the reactions of **1c** with the anion of acetylacetone (**2c-K**) in DMSO (stopped-flow method, 20 °C, $\lambda = 360 \text{ nm}$).

$[\mathbf{1c}]_0 / \text{M}$	$[\mathbf{2c}]_0 / \text{M}$	$[\mathbf{2c}]_0 / [\mathbf{1c}]_0$	$k_{\text{obs}} / \text{s}^{-1}$
2.19×10^{-4}	1.35×10^{-2}	6	1.41
2.19×10^{-4}	5.00×10^{-2}	23	2.73
2.19×10^{-4}	6.25×10^{-2}	29	3.34



$$k_2 = 3.86 \times 10^1 \text{ M}^{-1} \text{ s}^{-1}$$

Rate constants for the reactions of **1c** with the anion of ethylcyanoacetate (**2d-Na**) in CH₃OH (deprotonation of **2d-H** with NaOMe, stopped-flow method, 20 °C, $\lambda = 444$ nm).

[1c] ₀ / M	[2d-H] ₀ / M	[MeO ⁻] ₀ / M	[2d] ^a / M	[MeO ⁻] ^a / M	[2d] / [1c] ₀	$k_{\text{obs}} / \text{s}^{-1}$	$k_{1\psi} / \text{s}^{-1}$
1.39×10^{-3}	9.60×10^{-2}	4.70×10^{-2}	1.45×10^{-2}	9.01×10^{-3}	10	1.84×10^1	1.84×10^1
1.39×10^{-3}	9.60×10^{-2}	9.50×10^{-2}	2.49×10^{-2}	2.26×10^{-2}	18	3.35×10^1	3.34×10^1
1.39×10^{-3}	1.40×10^{-1}	8.90×10^{-2}	2.94×10^{-2}	1.51×10^{-2}	21	4.03×10^1	4.04×10^1
1.39×10^{-3}	9.60×10^{-2}	1.43×10^{-1}	3.16×10^{-2}	4.00×10^{-2}	23	4.51×10^1	4.46×10^1
1.39×10^{-3}	1.24×10^{-1}	1.78×10^{-1}	4.27×10^{-2}	4.63×10^{-2}	31	6.48×10^1	6.47×10^1

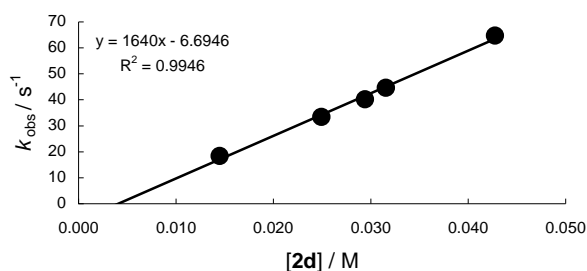
^a were calculated based on $K_{2\text{dH}} = 2.40 \times 10^1 \text{ M}^{-1}$ [7]

$$K_{2\text{dH}} = \frac{[\mathbf{2d}]}{([\mathbf{2dH}] [\text{MeO}^-])}$$

$$[\mathbf{2d}] = [\mathbf{2dH}]_0 - [\mathbf{2dH}]$$

$$[\text{MeO}^-] = [\text{MeO}^-]_0 - [\mathbf{2d}]$$

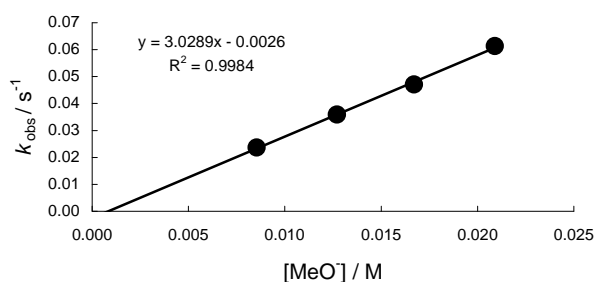
$$k_{\text{obs}} = k_{1\psi} + [\text{MeO}^-] k_{2,\text{MeO}^-}; k_{2,\text{MeO}^-} = 3.03 \text{ M}^{-1} \text{ s}^{-1*}$$



$$k_2 = 1.64 \times 10^3 \text{ M}^{-1} \text{ s}^{-1}$$

*Rate constants for the reactions of **1c** with sodium methanolate in CH₃OH (conventional UV-Vis spectroscopy, 20 °C, $\lambda = 444$ nm).

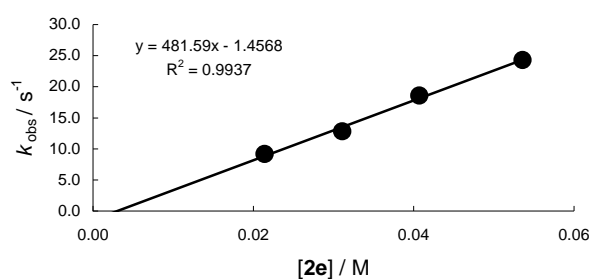
[1c] ₀ / M	[NaOMe] ₀ / M	[NaOMe] ₀ / [1c] ₀	$k_{\text{obs}} / \text{s}^{-1}$
2.25×10^{-3}	8.55×10^{-3}	3.80	2.36×10^{-2}
2.23×10^{-3}	1.27×10^{-2}	5.70	3.59×10^{-2}
2.20×10^{-3}	1.67×10^{-2}	7.61	4.71×10^{-2}
2.20×10^{-3}	2.09×10^{-2}	9.50	6.13×10^{-2}



$$k_2 = 3.03 \text{ M}^{-1} \text{ s}^{-1}$$

Rate constants for the reactions of **1c** with the anion of malononitrile (**2e-K**) in DMSO (stopped-flow method, 20 °C, $\lambda = 444$ nm).

$[\mathbf{1c}]_0 / \text{M}$	$[\mathbf{2e}]_0 / \text{M}$	$[\mathbf{2e}]_0 / [\mathbf{1c}]_0$	$k_{\text{obs}} / \text{s}^{-1}$
1.46×10^{-3}	2.14×10^{-2}	15	9.17
1.46×10^{-3}	3.11×10^{-2}	21	1.28×10^1
1.46×10^{-3}	4.07×10^{-2}	28	1.86×10^1
1.46×10^{-3}	5.36×10^{-2}	37	2.43×10^1

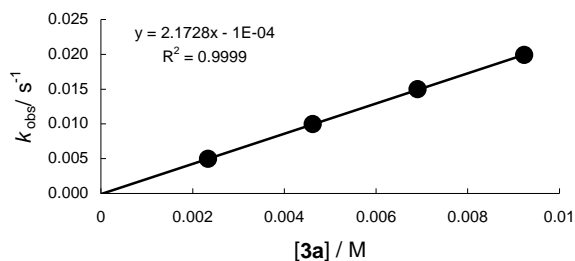


$$k_2 = 4.82 \times 10^2 \text{ M}^{-1} \text{ s}^{-1}$$

Rate constants for the reactions of 4-ethoxycarbonyl-3-methyl-1-aminocarbonyl-1,2-diaza-1,3-butadiene (**1c**) with amines **3**

Rate constants for the reactions of **1c** with morpholine (**3a**) in CH_3OH (conventional UV-Vis spectroscopy, 20 °C, $\lambda = 300$ nm).

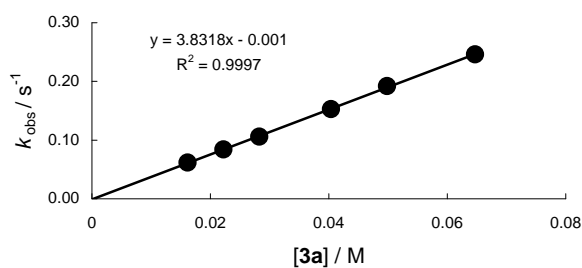
$[\mathbf{1c}]_0 / \text{M}$	$[\mathbf{3a}]_0 / \text{M}$	$[\mathbf{3a}]_0 / [\mathbf{1c}]_0$	$k_{\text{obs}} / \text{s}^{-1}$
7.65×10^{-4}	2.34×10^{-3}	3	4.95×10^{-3}
7.55×10^{-4}	4.62×10^{-3}	6	9.96×10^{-3}
7.55×10^{-4}	6.91×10^{-3}	9	1.50×10^{-2}
7.45×10^{-4}	9.23×10^{-3}	12	1.99×10^{-2}



$$k_2 = 2.17 \text{ M}^{-1} \text{ s}^{-1}$$

Rate constants for the reactions of **1c** with morpholine (**3a**) in DMSO (stopped-flow method, 20 °C, $\lambda = 444 \text{ nm}$).

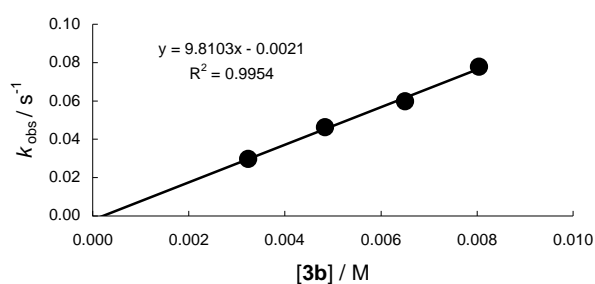
$[\mathbf{1c}]_0 / \text{M}$	$[\mathbf{3a}]_0 / \text{M}$	$[\mathbf{3a}]_0 / [\mathbf{1c}]_0$	$k_{\text{obs}} / \text{s}^{-1}$
1.54×10^{-3}	1.62×10^{-2}	10	6.17×10^{-2}
1.54×10^{-3}	2.22×10^{-2}	14	8.39×10^{-2}
1.54×10^{-3}	2.83×10^{-2}	18	1.06×10^{-1}
1.54×10^{-3}	4.04×10^{-2}	26	1.53×10^{-1}
1.54×10^{-3}	4.98×10^{-2}	32	1.92×10^{-1}
1.54×10^{-3}	6.47×10^{-2}	42	2.46×10^{-1}



$$k_2 = 3.83 \text{ M}^{-1} \text{ s}^{-1}$$

Rate constants for the reactions of **1c** with piperidine (**3b**) in CH₃OH (conventional UV-Vis spectroscopy, 20 °C, $\lambda = 300$ nm).

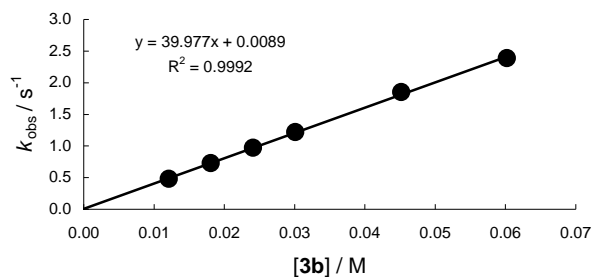
$[\mathbf{1c}]_0 / \text{M}$	$[\mathbf{3b}]_0 / \text{M}$	$[\mathbf{3b}]_0 / [\mathbf{1c}]_0$	$k_{\text{obs}} / \text{s}^{-1}$
6.65×10^{-4}	3.24×10^{-3}	5	2.97×10^{-2}
6.60×10^{-4}	4.84×10^{-3}	7	4.63×10^{-2}
6.65×10^{-4}	6.50×10^{-3}	10	5.97×10^{-2}
6.65×10^{-4}	8.04×10^{-3}	12	7.78×10^{-2}



$$k_2 = 9.81 \text{ M}^{-1} \text{ s}^{-1}$$

Rate constants for the reactions of **1c** with piperidine (**3b**) in CH₃CN (stopped-flow method, 20 °C, $\lambda = 300$ nm).

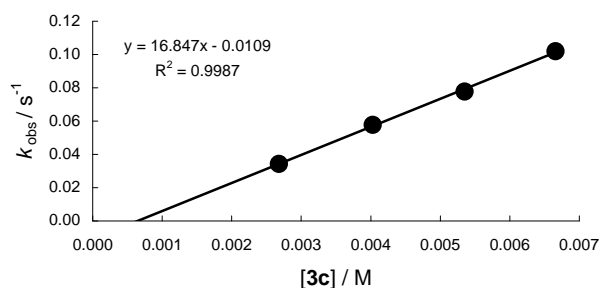
$[\mathbf{1c}]_0 / \text{M}$	$[\mathbf{3b}]_0 / \text{M}$	$[\mathbf{3b}]_0 / [\mathbf{1c}]_0$	$k_{\text{obs}} / \text{s}^{-1}$
1.65×10^{-3}	1.21×10^{-2}	7	4.82×10^{-1}
1.65×10^{-3}	1.81×10^{-2}	11	7.28×10^{-1}
1.65×10^{-3}	2.41×10^{-2}	15	9.71×10^{-1}
1.65×10^{-3}	3.01×10^{-2}	18	1.22
1.65×10^{-3}	4.52×10^{-2}	27	1.85
1.65×10^{-3}	6.02×10^{-2}	36	2.39



$$k_2 = 4.00 \times 10^1 \text{ M}^{-1} \text{ s}^{-1}$$

Rate constants for the reactions of **1c** with pyrrolidine (**3c**) in CH₃OH (conventional UV-Vis spectroscopy, 20 °C, $\lambda = 300$ nm).

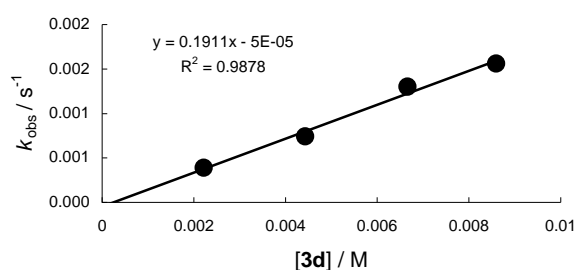
[1c] ₀ / M	[3c] ₀ / M	[3c] ₀ / [1c] ₀	$k_{\text{obs}} / \text{s}^{-1}$
7.90×10^{-4}	2.68×10^{-3}	3	3.42×10^{-2}
7.90×10^{-4}	4.03×10^{-3}	5	5.77×10^{-2}
7.85×10^{-4}	5.35×10^{-3}	7	7.77×10^{-2}
7.85×10^{-4}	6.66×10^{-3}	8	1.02×10^{-1}



$$k_2 = 1.68 \times 10^1 \text{ M}^{-1} \text{ s}^{-1}$$

Rate constants for the reactions of **1c** with benzylamine (**3d**) in CH₃OH (conventional UV-Vis spectroscopy, 20 °C, $\lambda = 300$ nm).

$[\mathbf{1c}]_0 / \text{M}$	$[\mathbf{3d}]_0 / \text{M}$	$[\mathbf{3d}]_0 / [\mathbf{1c}]_0$	$k_{\text{obs}} / \text{s}^{-1}$
7.00×10^{-4}	2.22×10^{-3}	3	3.90×10^{-4}
6.95×10^{-4}	4.43×10^{-3}	6	7.41×10^{-4}
6.70×10^{-4}	6.66×10^{-3}	10	1.30×10^{-3}
6.75×10^{-4}	8.59×10^{-3}	13	1.56×10^{-3}

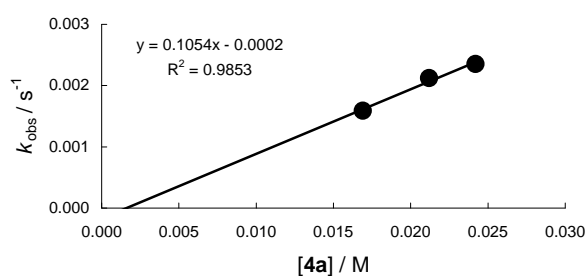


$$k_2 = 1.91 \times 10^{-1} \text{ M}^{-1} \text{ s}^{-1}$$

Rate constants for the reactions of 4-ethoxycarbonyl-3-methyl-1-aminocarbonyl-1,2-diaza-1,3-butadiene (**1c**) with triarylphosphines **4**

Rate constants for the reactions of **1c** with tris(4-chlorophenyl)phosphine (**4a**) in CH₂Cl₂ (conventional UV-Vis spectroscopy, 20 °C, $\lambda = 444$ nm).

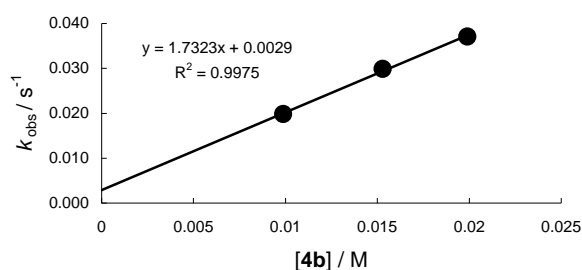
$[\mathbf{1c}]_0 / \text{M}$	$[\mathbf{4a}]_0 / \text{M}$	$[\mathbf{4a}]_0 / [\mathbf{1c}]_0$	$k_{\text{obs}} / \text{s}^{-1}$
2.65×10^{-3}	1.69×10^{-2}	6	1.59×10^{-3}
2.62×10^{-3}	2.12×10^{-2}	8	2.12×10^{-3}
2.61×10^{-3}	2.35×10^{-2}	9	2.35×10^{-3}



$$k_2 = 1.05 \times 10^{-1} \text{ M}^{-1} \text{ s}^{-1}$$

Rate constants for the reactions of **1c** with triphenylphosphine (**4b**) in CH₂Cl₂ (conventional UV-Vis spectroscopy, 20 °C, $\lambda = 444$ nm).

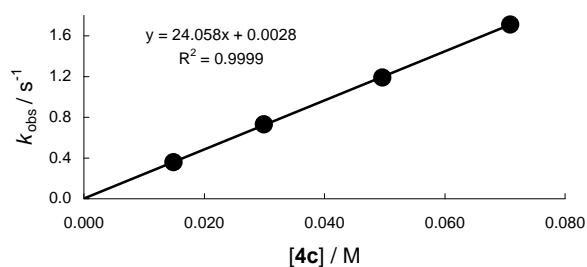
[1c] ₀ / M	[4b] ₀ / M	[4b] ₀ / [1c] ₀	$k_{\text{obs}} / \text{s}^{-1}$
2.40×10^{-3}	9.89×10^{-3}	4	1.98×10^{-2}
2.38×10^{-3}	1.53×10^{-2}	6	2.99×10^{-2}
2.32×10^{-3}	1.99×10^{-2}	9	3.71×10^{-2}



$$k_2 = 1.73 \text{ M}^{-1} \text{ s}^{-1}$$

Rate constants for the reactions of **1c** with tris(4-methoxyphenyl)phosphine (**4c**) in CH₂Cl₂ (stopped-flow method, 20 °C, $\lambda = 444$ nm).

[1c] ₀ / M	[4c] ₀ / M	[4c] ₀ / [1c] ₀	$k_{\text{obs}} / \text{s}^{-1}$
1.42×10^{-3}	1.49×10^{-2}	11	3.58×10^{-1}
1.42×10^{-3}	2.99×10^{-2}	21	7.30×10^{-1}
1.42×10^{-3}	4.96×10^{-2}	35	1.19×10^0
1.42×10^{-3}	7.09×10^{-2}	50	1.71×10^0

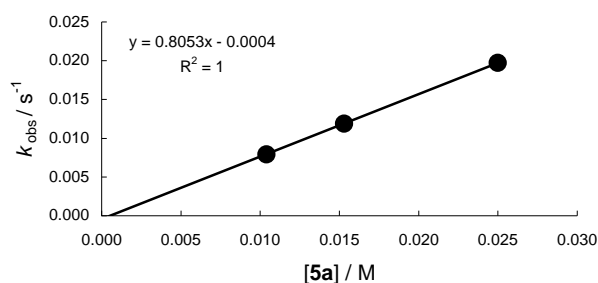


$$k_2 = 2.41 \times 10^1 \text{ M}^{-1} \text{ s}^{-1}$$

Rate constants for the reactions of 4-ethoxycarbonyl-3-methyl-1-aminocarbonyl-1,2-diaza-1,3-butadiene (**1c**) with enamines **5**

Rate constants for the reactions of **1c** with morpholinocyclohexene (**5a**) in CH₃CN (conventional UV-Vis spectroscopy, 20 °C, $\lambda = 444$ nm).

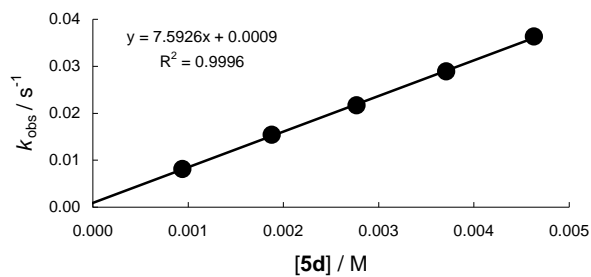
$[\mathbf{1c}]_0 / \text{M}$	$[\mathbf{5a}]_0 / \text{M}$	$[\mathbf{5a}]_0 / [\mathbf{1c}]_0$	$k_{\text{obs}} / \text{s}^{-1}$
2.30×10^{-3}	1.04×10^{-2}	5	7.94×10^{-3}
2.26×10^{-3}	1.53×10^{-2}	7	1.19×10^{-2}
2.21×10^{-3}	2.50×10^{-2}	11	1.97×10^{-2}



$$k_2 = 8.05 \times 10^{-1} \text{ M}^{-1} \text{ s}^{-1}$$

Rate constants for the reactions of **1c** with morpholinocyclopentene (**5d**) in CH₃CN (conventional UV-Vis spectroscopy, 20 °C, increase at $\lambda = 300$ nm).

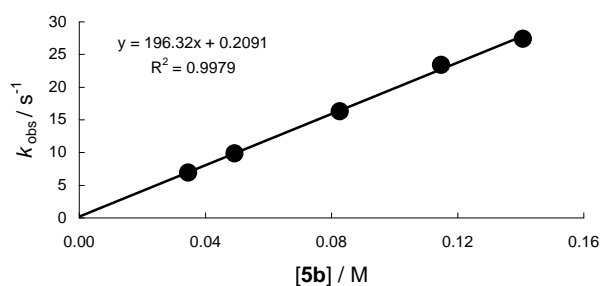
$[\mathbf{1c}]_0 / \text{M}$	$[\mathbf{5d}]_0 / \text{M}$	$[\mathbf{5d}]_0 / [\mathbf{1c}]_0$	$k_{\text{obs}} / \text{s}^{-1}$
2.19×10^{-4}	9.40×10^{-4}	4	8.09×10^{-3}
2.19×10^{-4}	1.88×10^{-3}	9	1.54×10^{-2}
2.16×10^{-4}	2.77×10^{-3}	13	2.17×10^{-2}
2.16×10^{-4}	3.71×10^{-3}	17	2.89×10^{-2}
2.16×10^{-4}	4.63×10^{-3}	21	3.63×10^{-2}



$$k_2 = 7.59 \text{ M}^{-1} \text{ s}^{-1}$$

Rate constants for the reactions of **1c** with piperidinocyclopentene (**5b**) in CH₃CN (stopped-flow method, 20 °C, $\lambda = 444 \text{ nm}$).

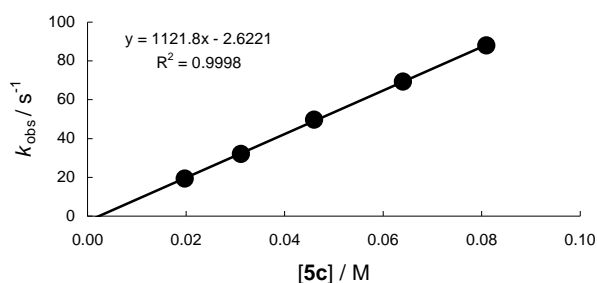
$[\mathbf{1c}]_0 / \text{M}$	$[\mathbf{5b}]_0 / \text{M}$	$[\mathbf{5b}]_0 / [\mathbf{1c}]_0$	$k_{\text{obs}} / \text{s}^{-1}$
1.49×10^{-3}	3.46×10^{-2}	23	6.94
1.49×10^{-3}	4.93×10^{-2}	33	9.85
1.49×10^{-3}	8.26×10^{-2}	55	1.63×10^1
1.49×10^{-3}	1.15×10^{-1}	77	2.34×10^1
1.49×10^{-3}	1.41×10^{-1}	94	2.74×10^1



$$k_2 = 1.96 \times 10^2 \text{ M}^{-1} \text{ s}^{-1}$$

Rate constants for the reactions of **1c** with pyrrolidinocyclopentene (**5c**) in CH₃CN (stopped-flow method, 20 °C, $\lambda = 444$ nm).

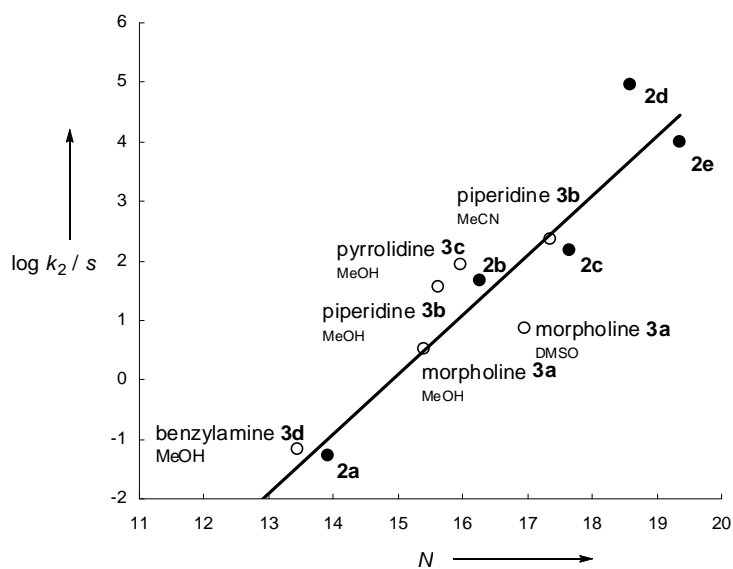
[1c] ₀ / M	[5c] ₀ / M	[5c] ₀ / [1c] ₀	k_{obs} / s ⁻¹
1.42×10^{-3}	1.97×10^{-2}	14	1.93×10^1
1.42×10^{-3}	3.11×10^{-2}	22	3.20×10^1
1.42×10^{-3}	4.60×10^{-2}	33	4.97×10^1
1.42×10^{-3}	6.40×10^{-2}	45	6.93×10^1
1.42×10^{-3}	8.10×10^{-2}	57	8.79×10^1



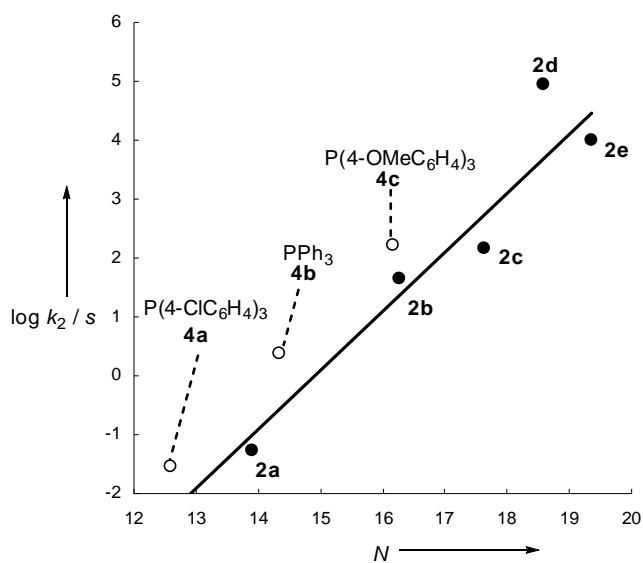
$$k_2 = 1.12 \times 10^3 \text{ M}^{-1} \text{ s}^{-1}$$

Correlations of the second-order rate constants ($\log k_2$ (20 °C)/s) of the reactions of **1c** with the nucleophiles **2-5** versus the corresponding N parameters of the nucleophiles

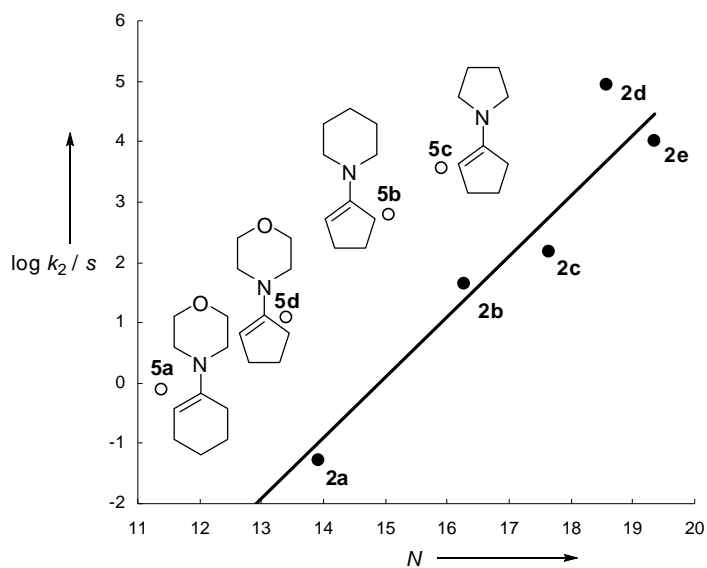
Plot of $\log k_2/s$ versus N for the reactions of **1c** with carbanions **2** (filled symbols) in DMSO and with amines **3** (open symbols) in different solvents.



Plot of $\log k_2/s$ versus N for the reactions of **1c** with carbanions **2** (filled symbols) in DMSO and with phosphines **4** (open symbols) in CH_2Cl_2 .



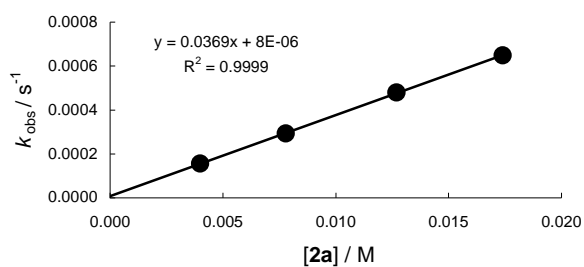
Plot of $\log k_2/s$ versus N for the reactions of **1c** with carbanions **2** (filled symbols) in DMSO and with enamines **5** (open symbols) in MeCN.



Kinetics of the reactions of 4-dimethylaminocarbonyl-3-methyl-1-phenylamino-carbonyl-1,2-diaza-1,3-butadiene (1d**) with nucleophiles**Reactions of 4-dimethylaminocarbonyl-3-methyl-1-phenylaminocarbonyl-1,2-diaza-1,3-butadiene (**1d**) with carbanions **2**

Rate constants for the reactions of **1d** with the anion of Meldrum's acid (**2a-K**) in DMSO (conventional UV-Vis spectroscopy, 20 °C, $\lambda = 350$ nm).

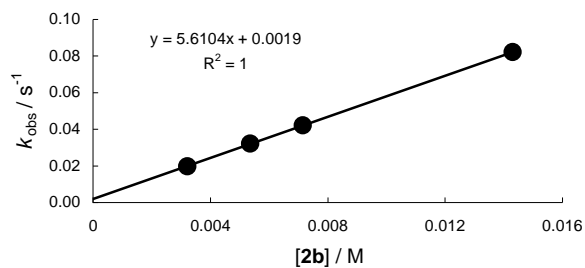
$[\mathbf{1d}]_0 / \text{M}$	$[\mathbf{2a}]_0 / \text{M}$	$[\mathbf{2a}]_0 / [\mathbf{1d}]_0$	$k_{\text{obs}} / \text{s}^{-1}$
2.84×10^{-4}	3.99×10^{-3}	14	1.56×10^{-4}
2.76×10^{-4}	7.79×10^{-3}	28	2.93×10^{-4}
2.71×10^{-4}	1.27×10^{-2}	47	4.80×10^{-4}
2.63×10^{-4}	1.74×10^{-2}	66	6.49×10^{-4}



$$k_2 = 3.69 \times 10^{-2} \text{ M}^{-1} \text{ s}^{-1}$$

Rate constants for the reactions of **1d** with the anion of dimedone (**2b-K**) in DMSO (stopped-flow method, 20 °C, $\lambda = 350$ nm).

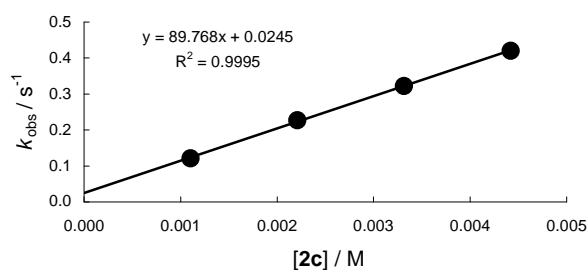
$[\mathbf{1d}]_0 / \text{M}$	$[\mathbf{2b}]_0 / \text{M}$	$[\mathbf{2b}]_0 / [\mathbf{1d}]_0$	$k_{\text{obs}} / \text{s}^{-1}$
1.05×10^{-4}	3.22×10^{-3}	31	1.98×10^{-2}
9.57×10^{-5}	5.36×10^{-3}	56	3.22×10^{-2}
9.57×10^{-5}	7.15×10^{-3}	75	4.21×10^{-2}
9.57×10^{-5}	1.43×10^{-2}	149	8.21×10^{-2}



$$k_2 = 5.61 \text{ M}^{-1} \text{ s}^{-1}$$

Rate constants for the reactions of **1d** with the anion of acetylacetonate (**2c-K**) in DMSO (stopped-flow method, 20 °C, $\lambda = 360 \text{ nm}$).

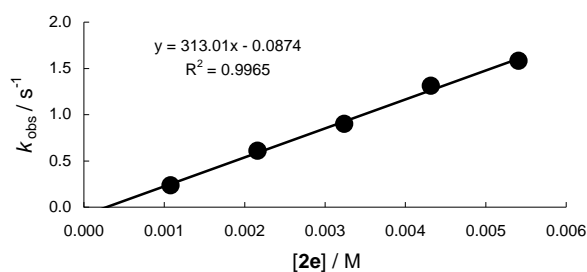
$[\mathbf{1d}]_0 / \text{M}$	$[\mathbf{2c}]_0 / \text{M}$	$[\mathbf{2c}]_0 / [\mathbf{1d}]_0$	$k_{\text{obs}} / \text{s}^{-1}$
8.68×10^{-5}	1.11×10^{-3}	13	1.21×10^{-1}
8.68×10^{-5}	2.21×10^{-3}	25	2.27×10^{-1}
8.68×10^{-5}	3.32×10^{-3}	38	3.22×10^{-1}
8.68×10^{-5}	4.42×10^{-3}	51	4.20×10^{-1}



$$k_2 = 8.98 \times 10^1 \text{ M}^{-1} \text{ s}^{-1}$$

Rate constants for the reactions of **1d** with the anion of malononitrile (**2e-K**) in DMSO (stopped-flow method, 20 °C, $\lambda = 350$ nm).

$[\mathbf{1d}]_0 / \text{M}$	$[\mathbf{2e}]_0 / \text{M}$	$[\mathbf{2e}]_0 / [\mathbf{1d}]_0$	$k_{\text{obs}} / \text{s}^{-1}$
9.57×10^{-5}	1.08×10^{-3}	11	2.37×10^{-1}
9.57×10^{-5}	2.16×10^{-3}	23	6.09×10^{-1}
9.57×10^{-5}	3.24×10^{-3}	34	9.01×10^{-1}
9.57×10^{-5}	4.32×10^{-3}	45	1.31
9.57×10^{-5}	5.41×10^{-3}	57	1.58

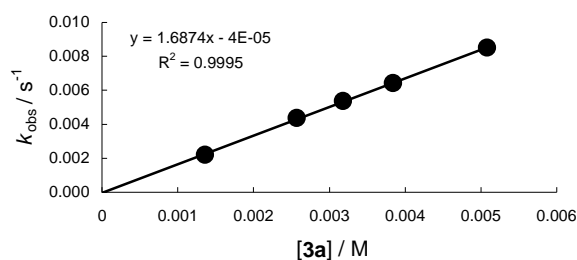


$$k_2 = 3.13 \times 10^2 \text{ M}^{-1} \text{ s}^{-1}$$

Reactions of 4-dimethylaminocarbonyl-3-methyl-1-phenylaminocarbonyl-1,2-diaza-1,3-butadiene (**1d**) with amines **3** and enamines **5**

Rate constants for the reactions of **1d** with morpholine (**3a**) in CH_3OH (conventional UV-Vis spectroscopy, 20 °C, $\lambda = 360$ nm).

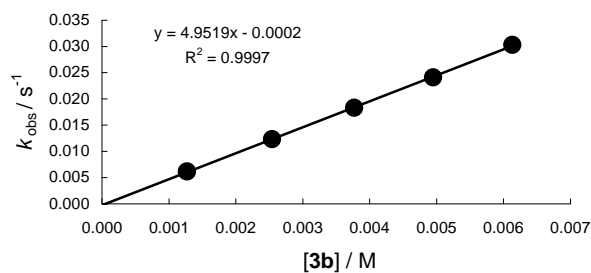
$[\mathbf{1d}]_0 / \text{M}$	$[\mathbf{3a}]_0 / \text{M}$	$[\mathbf{3a}]_0 / [\mathbf{1d}]_0$	$k_{\text{obs}} / \text{s}^{-1}$
2.62×10^{-4}	1.36×10^{-3}	5	2.20×10^{-3}
2.60×10^{-4}	2.57×10^{-3}	10	4.37×10^{-3}
2.57×10^{-4}	3.18×10^{-3}	12	5.36×10^{-3}
2.59×10^{-4}	3.84×10^{-3}	15	6.42×10^{-3}
2.57×10^{-4}	5.08×10^{-3}	20	8.51×10^{-3}



$$k_2 = 1.69 \text{ M}^{-1} \text{ s}^{-1}$$

Rate constants for the reactions of **1d** with piperidine (**3b**) in CH₃OH (conventional UV-Vis spectroscopy, 20 °C, $\lambda = 360 \text{ nm}$).

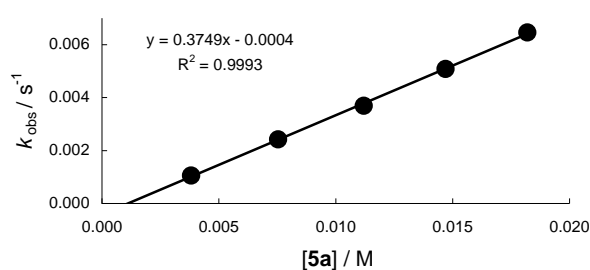
$[\mathbf{1d}]_0 / \text{M}$	$[\mathbf{3b}]_0 / \text{M}$	$[\mathbf{3b}]_0 / [\mathbf{1d}]_0$	$k_{\text{obs}} / \text{s}^{-1}$
3.26×10^{-4}	1.27×10^{-3}	4	6.16×10^{-3}
3.25×10^{-4}	2.54×10^{-3}	8	1.23×10^{-2}
3.22×10^{-4}	3.77×10^{-3}	12	1.83×10^{-2}
3.17×10^{-4}	4.95×10^{-3}	16	2.41×10^{-2}
3.14×10^{-4}	6.13×10^{-3}	20	3.03×10^{-2}



$$k_2 = 4.95 \text{ M}^{-1} \text{ s}^{-1}$$

Rate constants for the reactions of **1d** with morpholinocyclohexene (**5a**) in CH₃CN (conventional UV-Vis spectroscopy, 20 °C, $\lambda = 360$ nm).

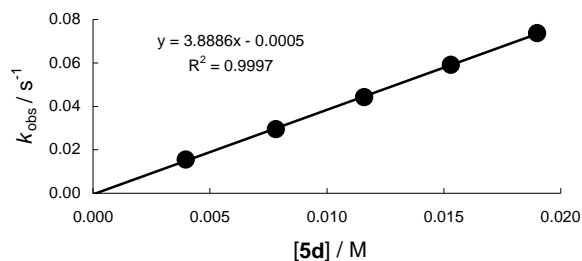
$[\mathbf{1d}]_0 / \text{M}$	$[\mathbf{5a}]_0 / \text{M}$	$[\mathbf{5a}]_0 / [\mathbf{1d}]_0$	$k_{\text{obs}} / \text{s}^{-1}$
3.13×10^{-4}	3.81×10^{-3}	12	1.05×10^{-3}
3.10×10^{-4}	7.54×10^{-3}	24	2.42×10^{-3}
3.07×10^{-4}	1.12×10^{-2}	36	3.69×10^{-3}
3.02×10^{-4}	1.47×10^{-2}	49	5.08×10^{-3}
3.00×10^{-4}	1.82×10^{-2}	61	6.46×10^{-3}



$$k_2 = 3.75 \times 10^{-1} \text{ M}^{-1} \text{ s}^{-1}$$

Rate constants for the reactions of **1d** with morpholinocyclopentene (**5d**) in CH₃CN (conventional UV-Vis spectroscopy, 20 °C, $\lambda = 360$ nm).

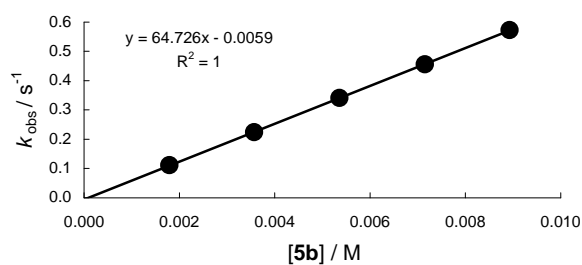
$[\mathbf{1d}]_0 / \text{M}$	$[\mathbf{5d}]_0 / \text{M}$	$[\mathbf{5d}]_0 / [\mathbf{1d}]_0$	$k_{\text{obs}} / \text{s}^{-1}$
3.15×10^{-4}	3.97×10^{-3}	13	1.54×10^{-2}
3.10×10^{-4}	7.82×10^{-3}	25	2.95×10^{-2}
3.07×10^{-4}	1.16×10^{-2}	38	4.42×10^{-2}
3.02×10^{-4}	1.53×10^{-2}	51	5.91×10^{-2}
3.01×10^{-4}	1.90×10^{-2}	63	7.36×10^{-2}



$$k_2 = 3.89 \text{ M}^{-1} \text{ s}^{-1}$$

Rate constants for the reactions of **1d** with piperidinocyclopentene (**5b**) in CH_3CN (stopped-flow method, 20°C , $\lambda = 360 \text{ nm}$).

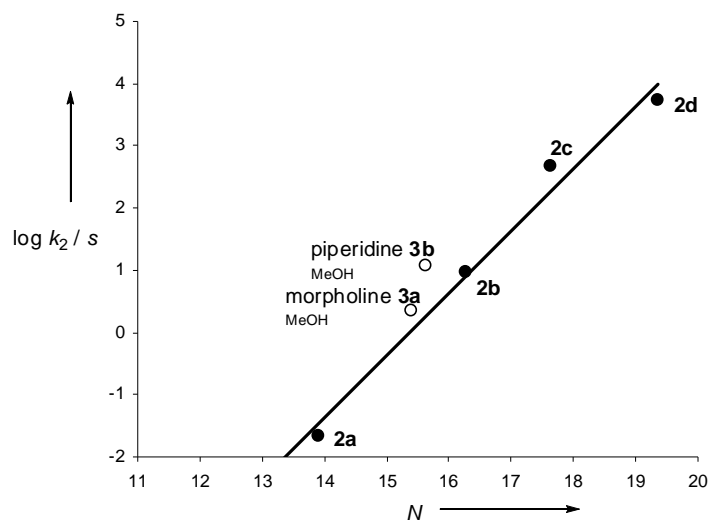
$[\mathbf{1d}]_0 / \text{M}$	$[\mathbf{5b}]_0 / \text{M}$	$[\mathbf{5b}]_0 / [\mathbf{1d}]_0$	$k_{\text{obs}} / \text{s}^{-1}$
1.03×10^{-4}	1.79×10^{-3}	17	1.11×10^{-1}
1.03×10^{-4}	3.57×10^{-3}	35	2.24×10^{-1}
1.03×10^{-4}	5.36×10^{-3}	52	3.41×10^{-1}
1.03×10^{-4}	7.15×10^{-3}	69	4.56×10^{-1}
1.03×10^{-4}	8.93×10^{-3}	87	5.73×10^{-1}



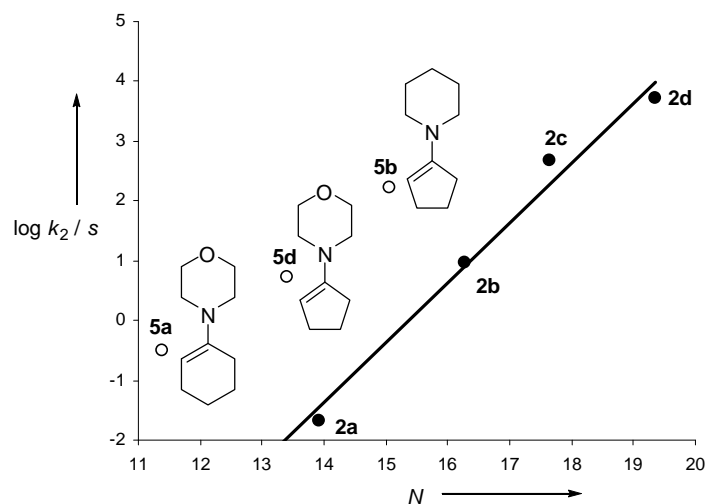
$$k_2 = 6.47 \times 10^1 \text{ M}^{-1} \text{ s}^{-1}$$

Correlations of the second-order rate constants ($\log k_2$ (20 °C)/s) of the reactions of **1d** with the nucleophiles **2-5** versus the corresponding N parameters of the nucleophiles

Plot of $\log k_2/s$ versus N for the reactions of **1d** with carbanions **2** (filled symbols) in DMSO and with amines **3** (open symbols) in different solvents.



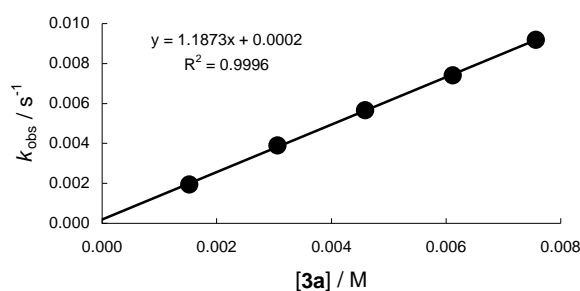
Plot of $\log k_2/s$ versus N for the reactions of **1d** with carbanions **2** (filled symbols) in DMSO and with enamines **5** (open symbols) in MeCN.



Kinetics of the reactions of ethyl 2-[2-(aminocarbonyl)-1-diazenyl]-1-cyclopentene-1-carboxylate (**1e**) with amines **3**

Rate constants for the reactions of **1e** with morpholine (**3a**) in CH₃OH (conventional UV-Vis spectroscopy, 20 °C, $\lambda = 320$ nm).

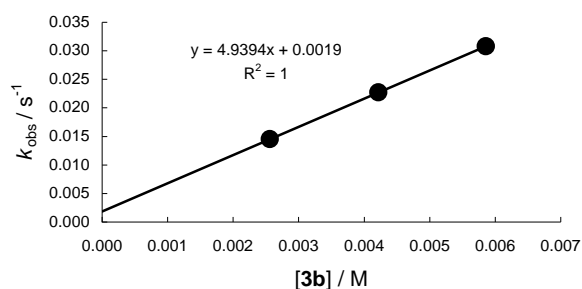
$[\mathbf{1e}]_0 / \text{M}$	$[\mathbf{3a}]_0 / \text{M}$	$[\mathbf{3a}]_0 / [\mathbf{1e}]_0$	$k_{\text{obs}} / \text{s}^{-1}$
3.75×10^{-4}	1.52×10^{-3}	4	1.94×10^{-3}
3.78×10^{-4}	3.06×10^{-3}	8	3.90×10^{-3}
3.78×10^{-4}	4.59×10^{-3}	12	5.66×10^{-3}
3.94×10^{-4}	6.12×10^{-3}	16	7.40×10^{-3}
3.90×10^{-4}	7.57×10^{-3}	20	9.19×10^{-3}



$$k_2 = 1.19 \text{ M}^{-1} \text{ s}^{-1}$$

Rate constants for the reactions of **1e** with piperidine (**3b**) in CH₃OH (conventional UV-Vis spectroscopy, 20 °C, $\lambda = 320$ nm).

$[\mathbf{1e}]_0 / \text{M}$	$[\mathbf{3b}]_0 / \text{M}$	$[\mathbf{3b}]_0 / [\mathbf{1e}]_0$	$k_{\text{obs}} / \text{s}^{-1}$
3.76×10^{-4}	2.56×10^{-3}	7	1.45×10^{-2}
3.72×10^{-4}	4.22×10^{-3}	11	2.27×10^{-2}
3.69×10^{-4}	5.86×10^{-3}	16	3.08×10^{-2}

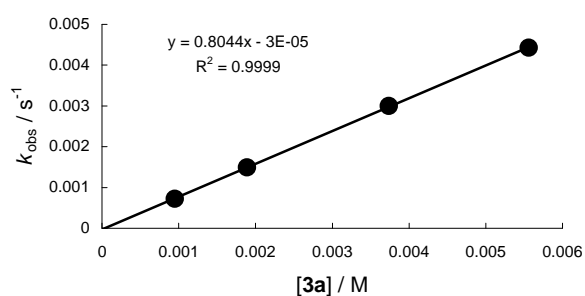


$$k_2 = 4.94 \text{ M}^{-1} \text{ s}^{-1}$$

Kinetics of the reactions of 4-dimethylaminocarbonyl-3-methyl-1-aminocarbonyl-1,2-diaza-1,3-butadiene (**1f**) with amines **3**

Rate constants for the reactions of **1f** with morpholine (**3a**) in CH₃OH (conventional UV-Vis spectroscopy, 20 °C, $\lambda = 300 \text{ nm}$).

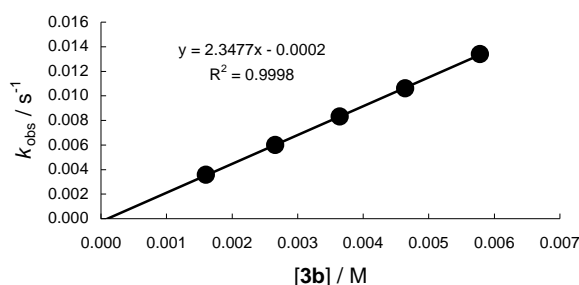
$[\mathbf{1f}]_0 / \text{M}$	$[\mathbf{3a}]_0 / \text{M}$	$[\mathbf{3a}]_0 / [\mathbf{1f}]_0$	$k_{\text{obs}} / \text{s}^{-1}$
3.09×10^{-4}	9.49×10^{-4}	3	7.26×10^{-4}
3.07×10^{-4}	1.89×10^{-3}	6	1.49×10^{-3}
3.04×10^{-4}	3.74×10^{-3}	12	3.00×10^{-3}
3.02×10^{-4}	5.56×10^{-3}	18	4.43×10^{-3}



$$k_2 = 8.04 \times 10^{-1} \text{ M}^{-1} \text{ s}^{-1}$$

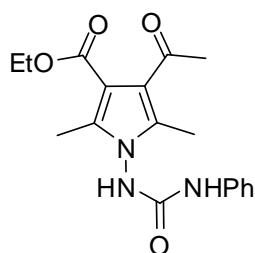
Rate constants for the reactions of **1f** with piperidine (**3b**) in CH₃OH (conventional UV-Vis spectroscopy, 20 °C, $\lambda = 300$ nm).

[1f] ₀ / M	[3b] ₀ / M	[3b] ₀ / [1f] ₀	k_{obs} / s ⁻¹
3.06×10^{-4}	1.60×10^{-3}	5	3.57×10^{-3}
3.05×10^{-4}	2.66×10^{-3}	9	5.99×10^{-3}
2.98×10^{-4}	3.64×10^{-3}	12	8.32×10^{-3}
2.96×10^{-4}	4.64×10^{-3}	16	1.06×10^{-2}
3.02×10^{-4}	5.78×10^{-3}	19	1.34×10^{-2}



$$k_2 = 2.35 \text{ M}^{-1} \text{ s}^{-1}$$

3.4.2 Synthetic Experiments

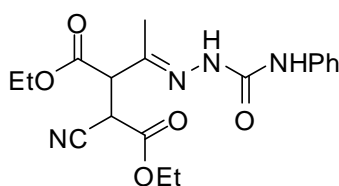


2ca

4-Ethoxycarbonyl-3-methyl-1-phenylaminocarbonyl-1,2-diaza-1,3-butadiene **1a** (130 mg, 0.498 mmol) was added to a stirred solution of acetylacetone **2c** (50 mg, 0.50 mmol) and KO^tBu (62 mg, 0.55 mmol) in dry DMSO (5 mL). After the consumption of the starting materials, the reaction was quenched with water and extracted with CH₂Cl₂. The combined organic layers were washed with water, dried over Na₂SO₄, and evaporated under reduced pressure. The crude product was purified by column chromatography on silica gel (cyclohexane/EtOAc): **2ca** (50 mg, 0.15 mmol, 30%) colorless oil.

$^1\text{H-NMR}$ (400 MHz, $\text{d}_6\text{-DMSO}$) δ = 1.26 (t, 3H, 3J = 7.0 Hz, CH_3), 2.13 (s, 3 H, CH_3), 2.27 (s, 3 H, CH_3), 2.30 (s, 3 H, CH_3), 4.21 (q, 2 H, 3J = 7.2 Hz, OCH_2), 7.00 (t, 1 H, 7.6 Hz, CH), 7.28 (t, 2 H, 8.0 Hz, $2 \times \text{CH}$), 7.46 (d, 2 H, 8.8 Hz, $2 \times \text{CH}$), 9.41 (br s, 1 H, NH), 9.48 ppm (s, 1 H, NH).

$^{13}\text{C-NMR}$ (100 MHz, $\text{d}_6\text{-DMSO}$) δ = 9.4, 9.8, 13.6, 30.4, 59.2, 107.9, 118.3, 119.6, 122.1, 128.3, 132.6, 135.3, 138.6, 153.2, 163.9, 196.3 ppm.



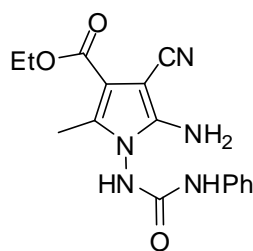
2da

4-Ethoxycarbonyl-3-methyl-1-phenylaminocarbonyl-1,2-diaza-1,3-butadiene **1a** (131 mg, 0.501 mmol) was added to a stirred solution of ethyl cyanoacetate **2d** (57 mg, 0.50 mmol) and NaOMe (30 mg, 0.56 mmol) in MeOH (5 mL). The formed precipitate was filtered and washed with diethyl ether: **2da** (40 mg, 0.11 mmol, 21%) white solid.

$^1\text{H-NMR}$ (400 MHz, $\text{d}_6\text{-DMSO}$) δ = 1.08-1.25 (m, 6 H, $2 \times \text{CH}_3$), 1.99*, 2.01 (2s, 3 H, CH_3), 4.09-4.23 (m, 4 H, $2 \times \text{OCH}_2$), 4.24-4.25 (m, 0.5 H, CH), 4.29-4.30 (m, 0.5 H, CH), 5.06-5.08 (m, 1 H, CH), 7.00-7.04 (m, 1H, CH), 7.29-7.33 (m, 2H, $2 \times \text{CH}$), 7.57-7.60 (m, 2 H, $2 \times \text{CH}$), 8.44, 8.51* (2s, 1 H, NH), 10.01, 10.05* ppm (2s, 1 H, NH).

$^{13}\text{C-NMR}$ (100 MHz, $\text{d}_6\text{-DMSO}$) δ = 13.58*, 13.61 (2q), 13.78, 13.82* (2q), 16.47*, 16.81 (2q), 37.41, 37.45* (2d), 51.23 (signals of diastereomers superimposed, d), 61.66, 61.72* (2t), 62.51, 62.54* (2t), 116.82*, 116.88 (2s), 118.60*, 118.73 (2d), 122.47 (signals of diastereomers superimposed, d), 128.66, 128.69* (2d), 138.71*, 138.73 (2s), 142.76*, 143.39 (2s), 153.03*, 153.09 (2s), 165.36*, 165.67 (2s), 168.09*, 168.20 ppm (2s).

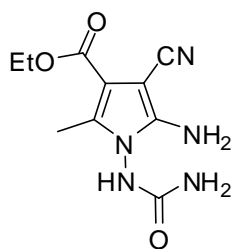
*signals belong to the major diastereomer

**2e**

4-Ethoxycarbonyl-3-methyl-1-phenylaminocarbonyl-1,2-diaza-1,3-butadiene **1a** (52 mg, 0.20 mmol) was added to a stirred solution of malononitrile **2e** (13 mg, 0.20 mmol) and KO^tBu (25 mg, 0.22 mmol) in dry DMSO (5 mL). After the consumption of the starting materials, the reaction was quenched with water and extracted with CH₂Cl₂. The combined organic layers were washed with water, dried over Na₂SO₄, and evaporated under reduced pressure. The crude product was purified by column chromatography on silica gel (cyclohexane/EtOAc): **2ea** (34 mg, 0.10 mmol, 52%) orange solid. Spectroscopic data are in agreement with previously published data.^[18]

¹H-NMR (400 MHz, d₆-DMSO) δ = 1.26 (t, 3H, ³J = 7.1 Hz, CH₃), 2.23 (s, 3 H, CH₃), 4.19 (q, 2 H, ³J = 7.1 Hz, OCH₂), 6.22 (s, 2 H, NH₂), 6.97–7.01 (m, 1 H, CH), 7.26–7.30 (m, 2 H, 2 × CH), 7.45–7.48 (m, 2 H, 2 × CH), 9.17 (s, 1 H, NH), 9.25 ppm (s, 1 H, NH).

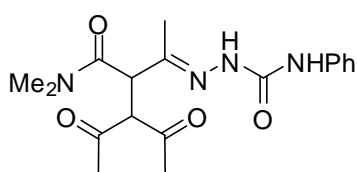
¹³C-NMR (100 MHz, d₆-DMSO) δ = 10.0 (q), 14.1 (q), 59.2 (t), 65.3 (s), 105.3 (s), 116.7 (s), 118.7 (d), 122.3 (d), 128.6 (d), 132.1 (s), 139.1 (s), 149.2 (s), 153.3 (s), 162.9 ppm (s).

**2e**

4-Ethoxycarbonyl-3-methyl-1-aminocarbonyl-1,2-diaza-1,3-butadiene **1c** (56 mg, 0.30 mmol) was added to a stirred solution of malononitrile **2e** (20 mg, 0.30 mmol) and KO^tBu (37 mg, 0.33 mmol) in dry DMSO (5 mL). After the consumption of the starting materials, the reaction was quenched with water and extracted with CH₂Cl₂. The combined organic layers were washed with water, dried over Na₂SO₄, and evaporated under reduced pressure. The crude product was purified by column chromatography on silica gel (cyclohexane/EtOAc): **2ec** (45 mg, 0.18 mmol, 60%) white solid.

¹H-NMR (400 MHz, d₆-DMSO) δ = 1.25 (t, 3H, ³J = 7.1 Hz, CH₃), 2.19 (s, 3 H, CH₃), 4.17 (q, 2 H, ³J = 7.1 Hz, OCH₂), 6.05 (s, 2 H, NH₂), 6.34 (s, 2 H, NH₂), 8.98 ppm (s, 1 H, NH).

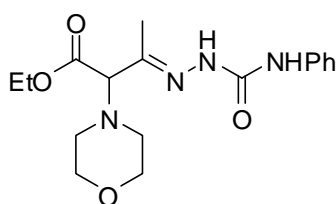
¹³C-NMR (100 MHz, d₆-DMSO) δ = 9.93 (q), 14.1 (q), 59.2 (t), 65.4 (s), 105.3 (s), 116.8 (s), 132.0 (s), 148.9 (s), 156.5 (s), 162.9 ppm (s).

**2c**

4-Dimethylaminocarbonyl-3-methyl-1-phenylaminocarbonyl-1,2-diaza-1,3-butadiene **1d** (130 mg, 0.499 mmol) was added to a stirred solution of acetylacetone **2c** (50 mg, 0.50 mmol) and KO^tBu (62 mg, 0.55 mmol) in dry DMSO (5 mL). After the consumption of the starting materials, the reaction was quenched with acetic acid (1 vol-%) and extracted with CH₂Cl₂. The combined organic layers were washed with water, dried over Na₂SO₄, and evaporated under reduced pressure. The crude product was purified by column chromatography on silica gel (cyclohexane/EtOAc): **2cd** (104 mg, 0.289 mmol, 58 %).

$^1\text{H-NMR}$ (400 MHz, d_6 -DMSO) δ = 1.76 (s, 3H, CH_3), 2.20 (s, 3 H, CH_3), 2.23 (s, 3 H, CH_3), 2.82 (s, 3 H, CH_3), 3.16 (s, 3 H, CH_3), 4.52 (d, 1 H, $^3J = 11.6$ Hz, CH), 4.66 (d, 1 H, $^3J = 10.8$ Hz, CH), 6.99–7.02 (m, 1 H, CH), 7.28–7.32 (m, 2 H, $2 \times$ CH), 7.59–7.61 (m, 2 H, $2 \times$ CH), 8.66 (s, 1 H, NH), 9.68 ppm (s, 1 H, NH).

$^{13}\text{C-NMR}$ (100 MHz, d_6 -DMSO) δ = 13.7 (q), 29.3 (q), 30.6 (q), 35.5 (q), 37.3 (q), 50.0 (d), 68.1 (d), 119.3 (d), 122.4 (d), 128.6 (d), 139.0 (s), 144.9 (s), 153.3 (s), 168.7 (s), 202.4 (s), 203.1 ppm (s).

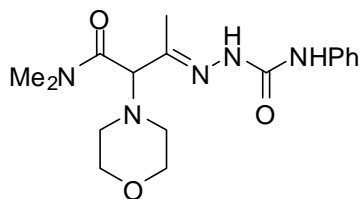


3aa

4-Ethoxycarbonyl-3-methyl-1-phenylaminocarbonyl-1,2-diaza-1,3-butadiene **1a** (261 mg, 0.999 mmol) was added to a stirred solution of morpholine **3a** (87 mg, 1.0 mmol) in methanol (10 mL). The formed precipitate was filtered and washed with diethyl ether/ petroleum ether (bp 40–60 °C): **3aa** (272 mg, 0.781 mmol, 78%).

$^1\text{H-NMR}$ (400 MHz, d_6 -DMSO) δ = 1.20 (t, 3H, $^3J = 7.1$ Hz, CH_3), 1.91 (s, 3 H, CH_3), 2.41–2.48 (m, 4 H, $2 \times$ CH_2), 3.58 (t, 4 H, $^3J = 4.6$ Hz, $2 \times$ CH_2), 3.91 (s, 1 H, CH), 4.12–4.20 (m, 2 H, CH_2), 7.00–7.03 (m, 1 H, CH), 7.27–7.31 (m, 2 H, $2 \times$ CH), 7.51–7.54 (m, 2 H, $2 \times$ CH), 8.59 (s, 1 H, NH), 9.81 ppm (s, 1 H, NH).

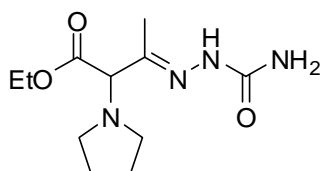
$^{13}\text{C-NMR}$ (100 MHz, d_6 -DMSO) δ = 13.2 (q), 14.0 (q), 50.2 (t), 60.4 (t), 66.2 (t), 74.3 (d), 118.9 (d), 122.4 (d), 128.6 (d), 138.7 (s), 145.7 (s), 152.9 (s), 169.1 ppm (s).

**3ad**

4-Dimethylaminocarbonyl-3-methyl-1-phenylaminocarbonyl-1,2-diaza-1,3-butadiene **1d** (164 mg, 0.630 mmol) was added to a stirred solution of morpholine **3a** (55 mg, 0.63 mmol) in methanol (10 mL). The formed precipitate was filtered and washed with diethyl ether/petroleum ether (bp 40–60 °C): **3ad** (198 mg, 0.570 mmol, 90%).

¹H-NMR (400 MHz, d₆-DMSO) δ = 1.88 (s, 3H, CH₃), 2.41-2.47 (m, 4 H, 2 × CH₂), 2.85 (s, 3 H, NCH₃), 3.09 (s, 3 H, NCH₃), 3.56–3.61 (m, 4 H, 2 × CH₂), 4.18 (s, 1 H, CH), 6.98–7.02 (m, 1 H, CH), 7.27–7.31 (m, 2 H, 2 × CH), 7.52–7.54 (m, 2 H, 2 × CH), 8.70 (s, 1 H, NH), 9.72 ppm (s, 1 H, NH).

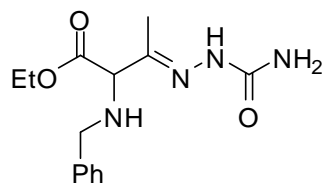
¹³C-NMR (100 MHz, d₆-DMSO) δ = 13.0 (q), 35.3 (q), 36.9 (q), 50.4 (t), 66.3 (t), 70.8 (d), 119.0 (d), 122.3 (d), 128.5 (d), 138.8 (s), 147.1 (s), 153.0 (s), 167.7 ppm (s).

**3cc**

4-Ethoxycarbonyl-3-methyl-1-aminocarbonyl-1,2-diaza-1,3-butadiene **1c** (185 mg, 0.999 mmol) was added to a stirred solution of pyrrolidine **3c** (71 mg, 1.0 mmol) in methanol (10 mL). After the typical red colour of **1c** had faded, the solvent was evaporated under reduced pressure the crude was purified by column chromatography on silica gel (cyclohexane/EtOAc). The obtained product was crystallized from EtOAc/cyclohexane: **3cc** (223 mg, 0.870 mmol, 87%).

$^1\text{H-NMR}$ (400 MHz, $\text{d}_6\text{-DMSO}$) $\delta = 1.17$ (t, 3H, $^3J = 7.1$ Hz, CH_3), 1.69–1.70 (m, 4 H, CH_2), 1.83 (s, 3 H, CH_3), 2.43–2.47 (m, 4 H, $2 \times \text{CH}_2$), 3.67 (s, 1 H, CH), 4.07–4.14 (m, 2 H, CH_2), 6.27 (brs 2 H, NH_2), 9.27 ppm (s, 1 H, NH).

$^{13}\text{C-NMR}$ (100 MHz, $\text{d}_6\text{-DMSO}$) $\delta = 12.7$ (q), 14.0 (q), 23.2 (t), 50.6 (t), 60.3 (t), 73.4 (d), 145.3 (s), 156.9 (s), 169.6 ppm (s).

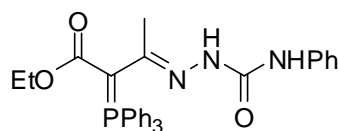


3dc

4-Ethoxycarbonyl-3-methyl-1-aminocarbonyl-1,2-diaza-1,3-butadiene **1c** (132 mg, 0.713 mmol) was added to a stirred solution of benzylamine **3d** (76 mg, 0.71 mmol) in methanol (10 mL). After the typical red colour of **1c** had faded, the solvent was evaporated under reduced pressure and the product was crystallized from diethyl ether/petroleum ether (bp 40–60 °C): **3dc** (158 mg, 0.616 mmol, 86%).

$^1\text{H-NMR}$ (400 MHz, $\text{d}_6\text{-DMSO}$) $\delta = 1.17$ (t, 3H, $^3J = 7.1$ Hz, CH_3), 1.78 (s, 3 H, CH_3), 2.99 (brs, 1 H, NH), 3.60–3.68 (m, 2 H, CH_2), 3.87 (s, 1 H, CH), 4.09–4.14 (m, 2 H, CH_2), 6.30 brs, 2 H, NH_2), 7.20–7.30 (m, 5 H, $5 \times \text{CH}$), 9.22 ppm (s, 1 H, NH).

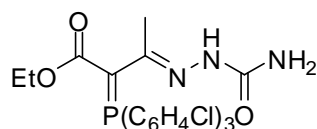
$^{13}\text{C-NMR}$ (100 MHz, $\text{d}_6\text{-DMSO}$) $\delta = 13.3$ (q), 14.1 (q), 50.4 (t), 60.5 (t), 66.3 (d), 126.6 (d), 128.00 (d), 128.04 (d), 140.0 (s), 144.7 (s), 157.0 (s), 170.9 ppm (s).

**4ba**

Triphenylphosphine **4b** (129 mg, 0.492 mmol) was added to a stirred solution of 4-ethoxycarbonyl-3-methyl-1-phenylaminocarbonyl-1,2-diaza-1,3-butadiene **1a** (128 mg, 0.490 mmol) in CH_2Cl_2 (10 mL). After the typical red colour of **1a** had faded, the solvent was removed in vacuo and the crude product was purified by column chromatography on silica gel (cyclohexane /EtOAc): **4ba** (113 mg, 0.216 mmol, 44%). Spectroscopic data are in agreement with previously published data.^[11]

$^1\text{H-NMR}$ (400 MHz, $\text{d}_6\text{-DMSO}$) δ = 0.65 (t, 3H, $^3J = 7.1$ Hz, CH_3), 2.19 (s, 3 H, CH_3), 3.63 (q, 3H, $^3J = 7.1$ Hz, CH_2), 6.66–6.68 (m, 2 H, $2 \times \text{CH}$), 6.84–6.88 (m, 1 H, CH), 7.09–7.14 (m, 2 H, $2 \times \text{CH}$), 7.52–7.77 (m, 16 H, $15 \times \text{CH}$, NH), 8.86 ppm (s, 1H, NH).

$^{13}\text{C-NMR}$ (100 MHz, $\text{d}_6\text{-DMSO}$) δ = 14.1, 18.9 (d, $J_{\text{P,C}} = 5.9$ Hz), 51.9 (d, $J_{\text{P,C}} = 120.2$ Hz), 56.7, 117.2, 121.5, 126.8 (d, $J_{\text{P,C}} = 91.8$ Hz), 128.5, 128.7 (d, $J_{\text{P,C}} = 12.0$ Hz), 131.8, 133.0 (d, $J_{\text{P,C}} = 9.6$ Hz), 138.6, 151.3 (d, $J_{\text{P,C}} = 4.9$ Hz), 152.7, 168.0 ppm (d, $J_{\text{P,C}} = 15.4$ Hz).

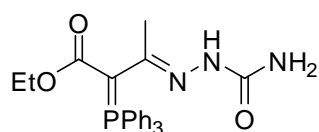
**4ac**

4-Ethoxycarbonyl-3-methyl-1-aminocarbonyl-1,2-diaza-1,3-butadiene **1c** (93 mg, 0.50 mmol) was added to a stirred solution of tris(4-chlorophenyl)phosphine **4a** (183 mg, 0.500 mmol) in CH_2Cl_2 (10 mL). After a few minutes the typical red colour of **1c** had faded. Then the solvent was removed in vacuo and the crude product was purified by column chromatography on silica gel (cyclohexane /EtOAc): **4ac** (160 mg, 0.290 mmol, 58%).

$^1\text{H-NMR}$ (400 MHz, $\text{d}_6\text{-DMSO}$) δ = 0.74 (t, 3H, 3J = 7.1 Hz, CH_3), 2.07 (2s, 3 H, CH_3), 3.68 (q, 3H, 3J = 7.1 Hz, CH_2), 7.59–7.72 (m, 14 H, $12 \times \text{CH}$, NH_2), 8.33 ppm (s, 1H, NH).

$^{13}\text{C-NMR}$ (100 MHz, $\text{d}_6\text{-DMSO}$) δ = 14.2 (q), 19.0 (qd, $J_{\text{P,C}}$ = 6.0 Hz), 50.7 (sd, $J_{\text{P,C}}$ = 122.8 Hz), 56.0 (t), 125.4 (sd, $J_{\text{P,C}}$ = 94.3 Hz), 128.9 (dd, $J_{\text{P,C}}$ = 12.9 Hz), 134.8 (dd, $J_{\text{P,C}}$ = 10.9 Hz), 137.2 (sd, $J_{\text{P,C}}$ = 3.4 Hz), 149.2 (sd, $J_{\text{P,C}}$ = 5.9 Hz), 156.8 (s), 167.9 ppm (sd, $J_{\text{P,C}}$ = 16.0 Hz).

$^{31}\text{P-NMR}$ (162 MHz, $\text{d}_6\text{-DMSO}$) δ = 18.7 ppm (s)

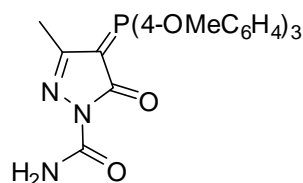


4bc

Triphenylphosphine **4b** (263 mg, 1.00 mmol) was added to a stirred solution of 4 ethoxycarbonyl-3-methyl-1-aminocarbonyl-1,2-diaza-1,3-butadiene **1c** (92.5 mg, 0.500 mmol) in CH_2Cl_2 (15 mL). After a few minutes the typical red colour of **1c** had faded. Then the solvent was removed in vacuo and the crude product was purified by column chromatography on silica gel (cyclohexane /EtOAc): **4bc** (120 mg, 0.268 mmol, 54%). Spectroscopic data are in agreement with previously published data.^[11]

$^1\text{H-NMR}$ (400 MHz, $\text{d}_6\text{-DMSO}$) δ = 0.67 (t, 3H, 3J = 6.8 Hz, CH_3), 2.10 (s, 3 H, CH_3), 7.51–7.67 (m, 17 H, $15 \times \text{CH}$, NH_2), 8.26 ppm (s, 1H, NH).

$^{13}\text{C-NMR}$ (100 MHz, $\text{d}_6\text{-DMSO}$) δ = 13.7 (d, $J_{\text{C,P}}$ = 6.1 Hz), 18.6, 50.5 (d, $J_{\text{C,P}}$ = 119.8 Hz), 56.3, 126.6 (d, $J_{\text{C,P}}$ = 91.0 Hz), 128.1 (d, $J_{\text{C,P}}$ = 11.4 Hz), 131.2, 132.5, 149.2 (d, $J_{\text{C,P}}$ = 6.0 Hz), 156.5, 167.6 ppm (s, $J_{\text{C,P}}$ = 15.1 Hz).

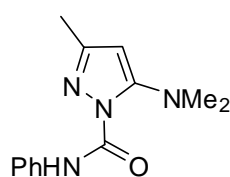
**4cc**

4-Ethoxycarbonyl-3-methyl-1-aminocarbonyl-1,2-diaza-1,3-butadiene **1c** (46 mg, 0.25 mmol) was added to a stirred solution of tris(4-methoxyphenyl)phosphine **4c** (88 mg, 0.25 mmol) in CH_2Cl_2 (5 mL). After a few minutes the typical red colour of **1c** had faded. Then the solvent was removed in vacuo and the crude product was purified by column chromatography on silica gel (MeOH/EtOAc): **4cc** (62 mg, 0.13 mmol, 50%).

$^1\text{H-NMR}$ (400 MHz, $\text{d}_6\text{-DMSO}$) δ = 1.25 (s, 3H, CH_3), 3.86 (s, 9 H, $3 \times \text{OCH}_3$), 6.92 (brs, 1 H, NH), 7.19–7.23 (m, 6 H, $6 \times \text{CH}$), 7.56–7.63 (m, 6 H, $6 \times \text{CH}$), 8.52 ppm (br s, 1 H, NH).

$^{13}\text{C-NMR}$ (100 MHz, $\text{d}_6\text{-DMSO}$) δ = 15.5 (qd, $J_{\text{C,P}} = 1.2$ Hz), 55.5 (qd, $J_{\text{C,P}} = 5.3$ Hz), 66.9 (sd, $J_{\text{C,P}} = 129.0$ Hz), 113.2 (sd, $J_{\text{C,P}} = 100.0$ Hz), 115.0 (dd, $J_{\text{C,P}} = 13.8$ Hz), 135.5 (dd, $J_{\text{C,P}} = 12.3$ Hz), 149.3 (sd, $J_{\text{C,P}} = 11.8$ Hz), 151.3 (s), 163.0 (sd, $J_{\text{C,P}} = 2.9$ Hz), 168.0 ppm (sd, $J_{\text{C,P}} = 18.1$ Hz).

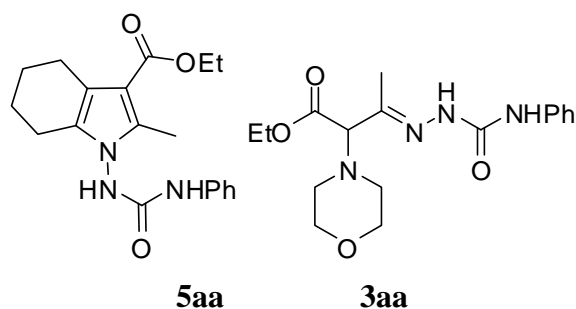
$^{31}\text{P-NMR}$ (162 MHz, $\text{d}_6\text{-DMSO}$) δ = 7.8 ppm (s)

**4ad**

4-Dimethylaminocarbonyl-3-methyl-1-phenylaminocarbonyl-1,2-diaza-1,3-butadiene **1d** (52 mg, 0.20 mmol) was added to a stirred solution of tris(4-chlorophenyl)phosphine **4a** (73 mg, 0.20 mmol) in CH_2Cl_2 (5 mL). After a few minutes the typical red colour of **1d** had faded. Then the solvent was removed in vacuo and the crude product was purified by column chromatography on silica gel (cyclohexane /EtOAc): **4ad** (30 mg, 0.12 mmol, 61%).

$^1\text{H-NMR}$ (400 MHz, d_6 -DMSO) δ = 2.52 (s, 3H, CH_3), 2.89 (2s, 6 H, $2 \times \text{CH}_3$), 5.97 (s, 1 H, CH), 7.12 (t, 1H, $^3J = 7.2$ Hz, CH), 7.36 (t, 1H, $^3J = 7.2$ Hz, CH), 7.68 ppm (d, $^3J = 8.4$ Hz, $2 \times \text{CH}$).

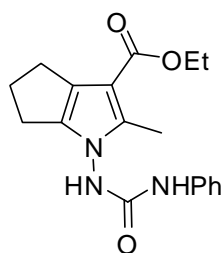
$^{13}\text{C-NMR}$ (100 MHz, d_6 -DMSO) δ = 14.0 (q), 38.7 (q), 98.6 (d), 120.1 (d), 123.5 (d), 128.6 (d), 143.6 (s), 148.7 (s), 158.4 ppm (s).



4-Ethoxycarbonyl-3-methyl-1-phenylaminocarbonyl-1,2-diaza-1,3-butadiene **1a** (287 mg, 1.10 mmol) was added to a stirred solution of morpholinocyclohexene **5a** (187 mg, 1.12 mmol) in of acetonitrile(15 mL). The formed white precipitate was filtered, washed with diethyl ether and purified by column chromatography on silica gel (cyclohexane/EtOAc). Two products could be isolated **5aa** (90 mg, 0.26 mmol, 24%) and **3aa** 100 mg, 0.29 mmol, 26%).

5aa: $^1\text{H-NMR}$ (400 MHz, d_6 -DMSO) δ = 1.25 (t, 3H, $^3J = 7.1$ Hz, CH_3), 1.66-1.68 (m, 4 H, $2 \times \text{CH}_2$), 2.23–2.44 (m, 5 H, CH_3 , $1 \times \text{CH}_2$), 2.58–2.60 (m, 2 H, CH_2), 4.12–4.18 (m, 2 H, OCH_2), 6.96–7.00 (m, 1 H, CH), 7.24–7.28 (m, 2 H, $2 \times \text{CH}$), 7.44–4.46 (m, 2 H, $2 \times \text{CH}$), 9.21 (brs, 1 H, NH), 9.26 ppm (s, 1 H, NH).

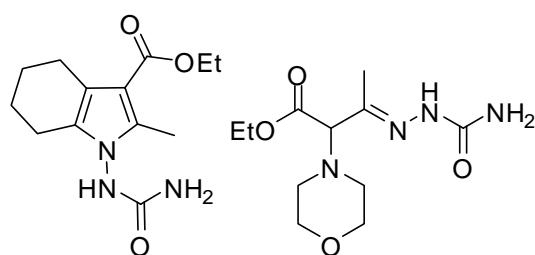
$^{13}\text{C-NMR}$ (100 MHz, d_6 -DMSO) δ = 10.4 (q), 14.4 (q), 20.2 (t), 22.1 (t), 22.9 (t), 23.1 (t), 58.4 (t), 106.9 (s), 115.0 (s), 118.7 (d), 122.2 (d), 128.6 (s), 129.4 (d), 135.5 (s), 139.2 (s), 154.0 (s), 164.9 ppm (s).

**5da**

4-Ethoxycarbonyl-3-methyl-1-phenylaminocarbonyl-1,2-diaza-1,3-butadiene **1a** (266 mg, 1.02 mmol) was added to a stirred solution of morpholinocyclopentene **5d** (156 mg, 1.02 mmol) in of acetonitrile (15 mL). After < 1 min the typical red colour of **1a** had faded. Then the solvent was evaporated under reduced pressure and the crude product was refluxed in THF for 20 h. After removing the solvent, the product was purified by column chromatography on silica gel (cyclohexane/EtOAc): **5da** (130 mg, 0.397 mmol, 39%).

$^1\text{H-NMR}$ (400 MHz, $\text{d}_6\text{-DMSO}$) δ = 1.23 (t, 3H, 3J = 7.0 Hz, CH_3), 2.23–2.31 (m, 5 H, CH_3 , CH_2), 2.53–2.60 (m, 2 H, CH_2), 2.62–2.73 (m, 2 H, CH_2), 4.12 (q, 2 H, 3J = 6.8 Hz), 6.97 (t, 1 H, CH), 7.25 (t, 2 H, $2 \times \text{CH}$), 7.45 (d, 2 H, 3J = 8.4 Hz, $2 \times \text{CH}$), 9.19 (s, 1 H, NH), 9.40 ppm (s, 1 H, NH).

$^{13}\text{C-NMR}$ (100 MHz, $\text{d}_6\text{-DMSO}$) δ = 10.2, 13.9, 23.7, 26.2, 26.7, 58.0, 105.0, 118.3, 121.8, 123.3, 128.2, 136.1.4, 138.7, 138.8, 153.6, 164.1 ppm.

**5ac****3ac**

4-Ethoxycarbonyl-3-methyl-1-aminocarbonyl-1,2-diaza-1,3-butadiene **1c** (177 mg, 0.956 mmol) was added to a solution of morpholinocyclohexene **5a** (160 mg, 0.957 mmol) in acetonitrile (10 mL). After < 1 min the typical red colour of **1c** had faded. Subsequently the solvent was evaporated under reduced pressure and the crude product was purified by column chromatography on silica gel (cyclohexane/EtOAc). Two products could be isolated **5ac** (130 mg, 0.490 mmol, 51%) and **3ac** (100 mg, 0.367 mmol, 38%).

5ac: $^1\text{H-NMR}$ (400 MHz, $\text{d}_6\text{-DMSO}$) $\delta = 1.24$ (t, 3H, $^3J = 7.1$ Hz, CH_3), 1.65–1.69 (m, 4 H, $2 \times \text{CH}_2$), 2.20–2.39 (m, 5 H, CH_3 , $1 \times \text{CH}_2$), 2.56 (m, 2 H, CH_2), 4.11–4.16 (m, 2 H, OCH_2), 6.17 (brs, 2 H, NH_2), 9.00 ppm (s, 1 H, NH).

$^{13}\text{C-NMR}$ (100 MHz, $\text{d}_6\text{-DMSO}$) $\delta = 10.3$ (q), 14.4 (q), 20.1 (t), 22.1 (t), 22.9 (t), 23.1 (t), 58.3 (t), 106.8 (s), 114.9 (s), 128.0 (s), 135.4 (s), 157.3 (s), 165.0 ppm (s).

3.5 References

- [1] Reviews: a) O. A. Attanasi, *Org. Prep. Proced. Int.* **1986**, 299–327; b) O. A. Attanasi, P. Filippone, *Synlett* **1997**, 1128–1140; c) O. A. Attanasi, L. De Crescentini, P. Filippone, F. Mantellini, S. Santeusanio, *Arkivoc* **2002**, xi, 274–292; d) O. A. Attanasi, L. De Crescentini, G. Favi, P. Filippone, F. Mantellini, F. R. Perrulli, S. Santeusanio, *Eur. J. Org. Chem.* **2009**, 3109–3127.
- [2] H. Mayr, M. Patz, *Angew. Chem.* **1994**, 106, 990–1010; *Angew. Chem. Int. Ed. Engl.* **1994**, 33, 938–957.
- [3] a) H. Mayr, T. Bug, M. F. Gotta, N. Hering, B. Irrgang, B. Janker, B. Kempf, R. Loos, A. R. Ofial, G. Remennikov, H. Schimmel, *J. Am. Chem. Soc.* **2001**, 123, 9500–9512; b) R. Lucius, R. Loos, H. Mayr, *Angew. Chem.* **2002**, 114, 97–102; *Angew. Chem. Int. Ed.* **2002**, 41, 91–95; c) H. Mayr, B. Kempf, A. R. Ofial, *Acc. Chem. Res.* **2003**, 36, 66–77; d) H. Mayr, A. R. Ofial in *Carbocation Chemistry* (G. A. Olah, G. K. S. Prakash, Eds.), Wiley, Hoboken (N.J.), **2004**, Chapt. 13, pp 331–358; e) H. Mayr, A. R. Ofial, *Pure Appl. Chem.* **2005**, 77, 1807–1821; f) H. Mayr, A. R. Ofial, *J. Phys. Org. Chem.* **2008**, 21, 584–595; g) D. Richter, N. Hampel, T. Singer, A. R. Ofial, H. Mayr, *Eur. J. Org. Chem.* **2009**, 3203–3211.
- [4] a) T. Lemek, H. Mayr, *J. Org. Chem.* **2003**, 68, 6880–6886; b) S. T. A. Berger, F. H. Seeliger, F. Hofbauer, H. Mayr, *Org. Biomol. Chem.* **2007**, 5, 3020–3026; c) F. Seeliger, S. T. A. Berger, G. Y. Remennikov, K. Polborn, H. Mayr, *J. Org. Chem.* **2007**, 72, 9170–9180; d) O. Kaumanns, H. Mayr, *J. Org. Chem.* **2008**, 73, 2738–2745; e) O. Kaumanns, R. Lucius, H. Mayr, *Chem. Eur. J.* **2008**, 14, 9675–9682.
- [5] T. B. Phan, H. Mayr, *Eur. J. Org. Chem.* **2006**, 2530–2537.

- [6] a) O. A. Attanasi, P. Bonifazi, E. Foresti, G. Pradella, *J. Org. Chem.* **1982**, *47*, 684–687; b) O. Attanasi, P. Filippone, A. Mei, S. Santeusanio, *Synthesis* **1984**, 671–672; c) O. A. Attanasi, P. Filippone, S. Santeusanio, F. Serra-Zanetti, *Synthesis* **1987**, 381–383; d) O. A. Attanasi, Z. Liao, A. McKillop, S. Santeusanio, F. Serra-Zanetti, *J. Chem. Soc. Perkin Trans. 1* **1993**, 315–320; e) A. Arcadi, O. A. Attanasi, L. De Crescentini, E. Rossi, F. Serra-Zanetti, *Tetrahedron* **1996**, *52*, 3997–4012.
- [7] M. R. Crampton, J. A. Stevens, *J. Chem. Soc. Perkin Trans. 2* **1991**, 1715–1720.
- [8] F. Terrier, S. Lakhdar, T. Boubaker, R. Goumont, *J. Org. Chem.* **2005**, *70*, 6242–6253.
- [9] a) B. Kempf, N. Hampel, A. R. Ofial, H. Mayr, *Chem. Eur. J.* **2003**, *9*, 2209–2218; b) S. Minegishi, H. Mayr, *J. Am. Chem. Soc.* **2003**, *125*, 286–295; c) B. Kempf, H. Mayr, *Chem. Eur. J.* **2005**, *11*, 917–927; d) T. B. Phan, M. Breugst, H. Mayr, *Angew. Chem.* **2006**, *118*, 3954–3959; *Angew. Chem. Int. Ed.* **2006**, *45*, 3869–3874; e) T. Kanzian, T. A. Nigst, A. Maier, S. Pichl, H. Mayr *Eur. J. Org. Chem.* **2009**, 6379–6385.
- [10] O. A. Attanasi, S. Berretta, L. De Crescentini, G. Favi, G. Giorgi, F. Mantellini, *Adv. Synth. Catal.* **2009**, *351*, 715–719.
- [11] a) O. A. Attanasi, P. Filippone, A. Mei, *Tetrahedron* **1992**, *48*, 1707–1714; b) O. A. Attanasi, P. Filippone, D. Giovagnoli, *Org. Prep. Proced. Int.* **1994**, *26*, 321–326.
- [12] a) S. Sommer, *Chem. Lett.* **1977**, 583–586; b) S. Sommer, *Angew. Chem. Int. Ed. Engl.* **1979**, *18*, 695–696; c) A. G. Schultz, W. K. Hagmann, M. Shen, *Tetrahedron Lett.* **1979**, *32*, 2965–2968; d) E. Rossi, G. Abbiati, O. A. Attanasi, S. Rizzato, S. Santeusanio, *Tetrahedron* **2007**, *63*, 11055–11065.
- [13] a) M. Hartnagel, K. Grimm, H. Mayr, *Liebigs Ann.* **1997**, 71–80; b) H. Mayr, J. Henninger, *Eur. J. Org. Chem.* **1998**, 1919–1922; c) H. Mayr, A. R. Ofial, J. Sauer, B. Schmied, *Eur. J. Org. Chem.* **2000**, 2013–2020; d) C. Fichtner, H. Mayr, *J. Chem. Soc. Perkin Trans. 2* **2002**, 1441–1444.
- [14] O. A. Attanasi, L. De Crescentini, P. Filippone, F. Fringuelli, F. Mantellini, M. Matteucci, O. Piermatti, F. Pizzo, *Helv. Chim. Acta* **2001**, *84*, 513–525.
- [15] H. G. O. Becker, *Organikum* (19 Aufl.), Edition dt. Verlag der Wissenschaften, Berlin, **1993**.
- [16] O. Attansi, P. Filippone, A. Mei, S. Santeusanio, *Synthesis* **1984**, 873–874.
- [17] H. Mayr, R. Schneider, C. Schade, J. Bartl, R. Bederke, *J. Am. Chem. Soc.* **1990**, *112*, 4446–4454.
- [18] O. A. Attanasi, S. Santeusanio, F. Serra-Zanetti, E. Foresti, A. McKillop, *J. Chem. Soc., Perkin Trans. 1* **1990**, 1669–1675.

Chapter 4

ELECTROPHILIC REACTIVITIES OF AZODICARBOXYLATES

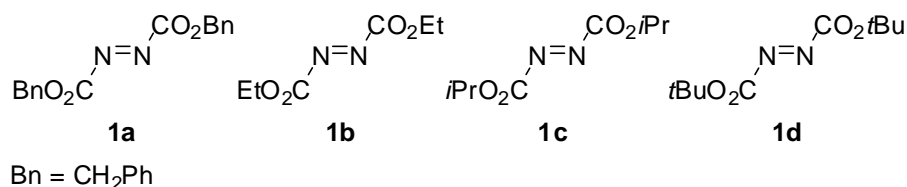
Tanja Kanzian and Herbert Mayr, *Chem. Eur. J.* **2010**, *16*, 11670-11677.

4.1 Introduction

Azodicarboxylates **1** have been used as strong electrophiles in numerous synthetic transformations,^[1] e. g., electrophilic aminations of carbonyl compounds, which have first been described in 1954 by Huisgen and Jakob.^[2] They have been reported to be highly reactive dienophiles and enophiles in Diels-Alder and ene reactions,^[3] and their reaction with phosphines represents the first step of the synthetically important Mitsunobu reaction.^[4] In recent years organocatalytic enantioselective α -aminations of aldehydes and ketones with azodicarboxylates attracted great attention,^[5] where the electrophiles **1** are attacked by intermediate enamines. Electrophiles, used for enamine activated reactions of carbonyl compounds should react fast with the enamine intermediates but not with the enols, which are present in equilibrium with the tautomeric carbonyl compounds. As the reactions of azodicarboxylates with enamines represent the key-step of organocatalytic α -aminations of carbonyl compounds,^[5] we have now quantified the electrophilic reactivities of the four azodicarboxylates **1a-d** using the linear free-energy relationship [Equation (4.1)].

$$\log k (20\text{ }^\circ\text{C}) = s(N + E) \quad (4.1)$$

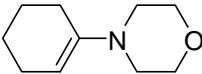
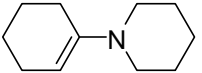
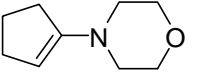
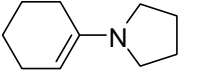
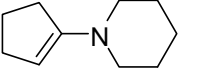
In numerous investigations we have shown that the reactions of carbocations and Michael acceptors with σ -, n-, and π -nucleophiles follow Equation (4.1), where electrophiles are described by E (electrophilicity parameter) and nucleophiles are described by N (nucleophilicity parameter) and s (nucleophile-specific slope parameter).^[6]



In this way, we were able to set up comprehensive electrophilicity and nucleophilicity scales, which allow us to predict the rates of polar organic reactions with an accuracy of better than a factor of 10^2 in a reactivity range of 40 orders of magnitude.^[7]

The nucleophile-specific parameters N and s of the enamines **2a-e** have recently been derived from the rates of their reactions with benzydrylium ions (Table 4.1).^[7a,8] These enamines have now been employed as reference nucleophiles for determining the electrophilicities E of **1a-d**.

Table 4.1. Enamines **2** used as reference nucleophiles in this study and their reactivity parameters N and s in dichloromethane.

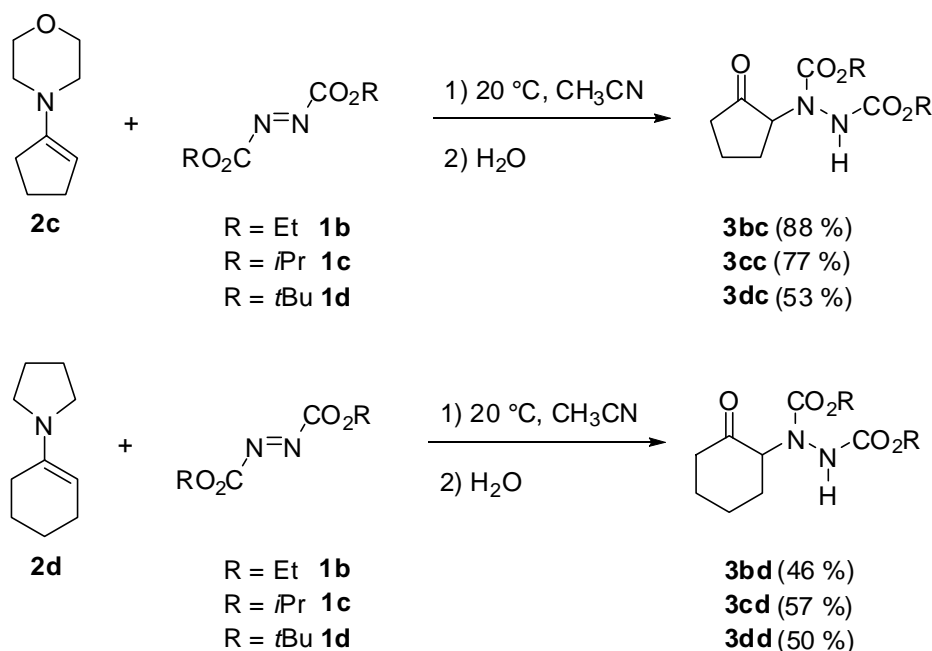
Enamine	$N(s)^{[a]}$
 2a	11.40 (0.83)
 2b	13.36 (0.81)
 2c	13.41 (0.82)
 2d	14.91 (0.86)
 2e	15.06 (0.82)

[a] Refs. [7a,8]

4.2 Results and Discussion

4.2.1 Reactions of Azodicarboxylates **1** with Enamines **2**.

Treatment of the azodicarboxylates **1b-d** with the enamines **2c** and **2d** yielded the α -hydrazino substituted ketones **3**^[2a,9] after aqueous workup (Scheme 4.1). Initial attack of the nucleophilic carbon of the enamine **2** at the azo functionality of **1** leads to zwitterionic intermediates, which are hydrolyzed with formation of the final products **3**.



Scheme 4.1. Reactions of **1b-d** with the enamines **2c** and **2d**.

The rates of the reactions of the azodicarboxylates **1** with the enamines **2** were determined photometrically in CH_3CN at $20 \text{ }^\circ\text{C}$. For the kinetic studies, the nucleophiles **2** were used in high excess over the electrophiles **1** to achieve first-order conditions. The reaction progress was monitored by following the decrease of the absorbances of the electrophiles **1** at 405 nm . From the observed mono-exponential decays the first-order rate constants k_{obs} were obtained (Figure 4.1). Details are given in the Experimental Section (Chapter 4.4).

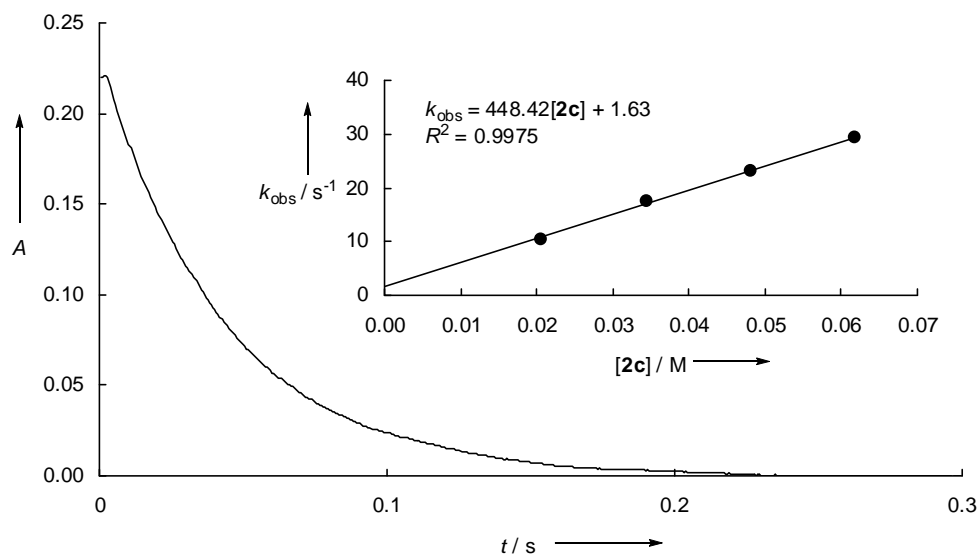


Figure 4.1. Exponential decay of the absorbance at 405 nm during the reaction of **1b** with **2c** ($[\mathbf{1b}] = 6.52 \times 10^{-3}$ M; $[\mathbf{2c}] = 4.81 \times 10^{-2}$ M; $k_{\text{obs}} = 2.32 \times 10^1$ s $^{-1}$). Insert: Determination of the second-order rate constant k_2 (4.48×10^2 M $^{-1}$ s $^{-1}$) as the slope of the correlation between the first-order rate constants k_{obs} and the concentration of the enamine **2c**.

As shown for the reaction of diethyl azodicarboxylate (**1b**) with morpholinocyclopentene (**2c**) in Figure 4.1, plots of k_{obs} versus the enamine concentrations were linear as required by Equation (4.2).

$$k_{\text{obs}} = k_2 [\mathbf{2}] \quad (4.2)$$

The slopes of these plots yielded the second-order rate constants k_2 , which are listed in Table 4.2.

Table 4.2. Second-order rate constants k_2 for the reactions of the azodicarboxylates **1a-d** with the enamines **2a-e** in acetonitrile at 20 °C.

Azodicarboxylate (<i>E</i>)	Enamine	k_2^{exp} [$\text{M}^{-1} \text{s}^{-1}$]	k_2^{calcd} [$\text{M}^{-1} \text{s}^{-1}$] [a]	$k_2^{\text{exp}}/k_2^{\text{calcd}}$
1a (-8.89)	2a	1.72×10^2	1.21×10^2	1.4
	2b	3.02×10^3	4.17×10^3	0.72
	2c	4.88×10^3	5.08×10^3	0.96
1b (-10.15)	2a	1.84×10^1	1.09×10^1	1.7
	2b	3.04×10^2	3.97×10^2	0.76
	2c	4.48×10^2	4.70×10^2	0.95
	2e	8.52×10^3	1.06×10^4	0.80
1c (-10.71)	2a	4.98	3.73	1.3
	2b	1.13×10^2	1.40×10^2	0.81
	2c	1.47×10^2	1.63×10^2	0.90
	2d	5.95×10^3	4.08×10^3	1.5
	2e	2.54×10^3	3.68×10^3	0.69
1d (-12.23)	2a	2.86×10^{-1}	2.06×10^{-1}	1.4
	2b	5.07	8.28	0.61
	2c	1.02×10^1	9.34	1.1
	2d	2.99×10^2	2.03×10^2	1.5
	2e	1.50×10^2	2.11×10^2	0.71

[a] Calculated by using Equation (4.1), N and s parameters from Table 4.1 and E from this Table.

Applicability of Equation (4.1) implies slopes of 1.0 for the plots of $(\log k_2)/s$ versus N . Figure 4.2 shows that this condition is roughly fulfilled for the reactions of **1** with the enamines **2**, where a new C-N bond is formed. Therefore, electrophilicity parameters E of **1** were determined by a least-squares fit, i.e., by minimization of $\Delta^2 = \sum (\log k_2 - s(N + E))^2$. The last column of Table 4.2 shows that calculated and experimental rate constants agree within a factor of 2, which is within the confidence limit of Equation (4.1). It is remarkable that the N and s parameters of **2a-e**, which have been derived from their reactivities toward benzhydrylium ions, also hold for their reactions with the N-electrophiles **1**. In line with this interpretation, we have previously reported that the N and s parameters of carbon nucleophiles can also be used to calculate rates of reactions with diazonium ions.^[10]

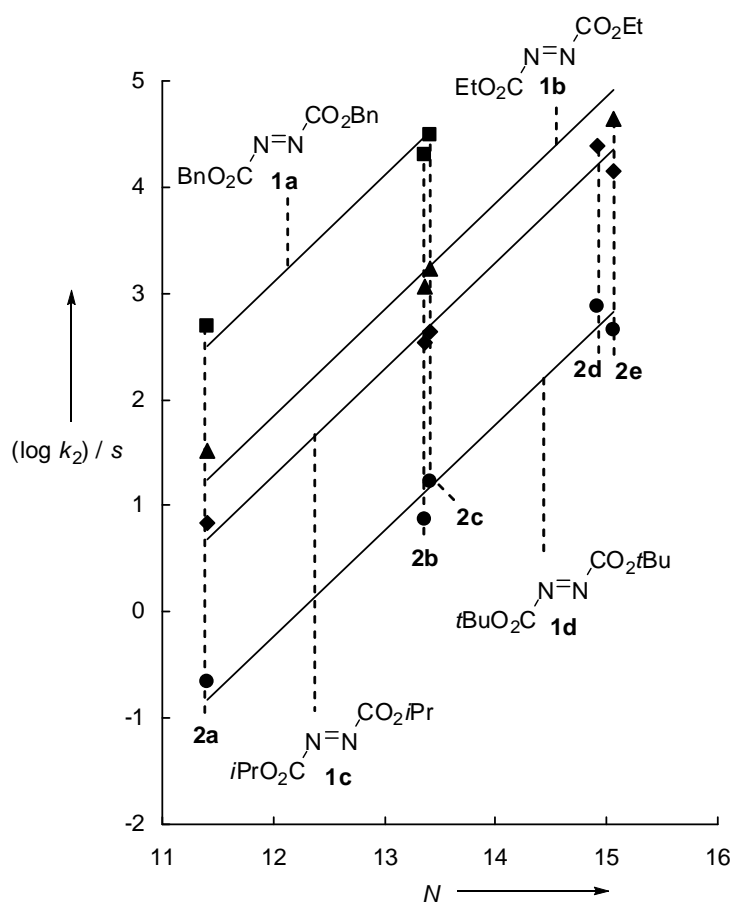


Figure 4.2. Correlation of $(\log k_2)/s$ against the corresponding nucleophile parameters N of the enamines **2a-e** for the reactions of azodicarboxylates **1a-d** with **2** (the slopes are fixed to 1.0 as required by Equation (4.1)).

The electrophilicities of the azodicarboxylates **1a-d** cover three orders of magnitude. They are only slightly less reactive than arenediazonium ions,^[10] comparable to α,β -unsaturated

iminium ions,^[11] amino-substituted benzhydrylium ions,^[7a] and ordinary Michael acceptors (Figure 4.3).^[7b,12] The slightly less electrophilic, structurally related 1,2-diaza-1,3-dienes react with nucleophiles at the alkenyl and not at the azo group.^[13]

The origin of the remarkably large effect of the different ester groups on the electrophilicities of the azodicarboxylates in the order of Bn > Et > *i*Pr > *t*Bu, as shown in Figures 4.2 and 4.3, is not known. With electrophilicity parameters between -9 and -12 azodicarboxylates are not attacked by typical enols, but react fast with enamines, comparable to other Michael acceptors, which proved to be suitable for enamine-activated reactions of carbonyl compounds.

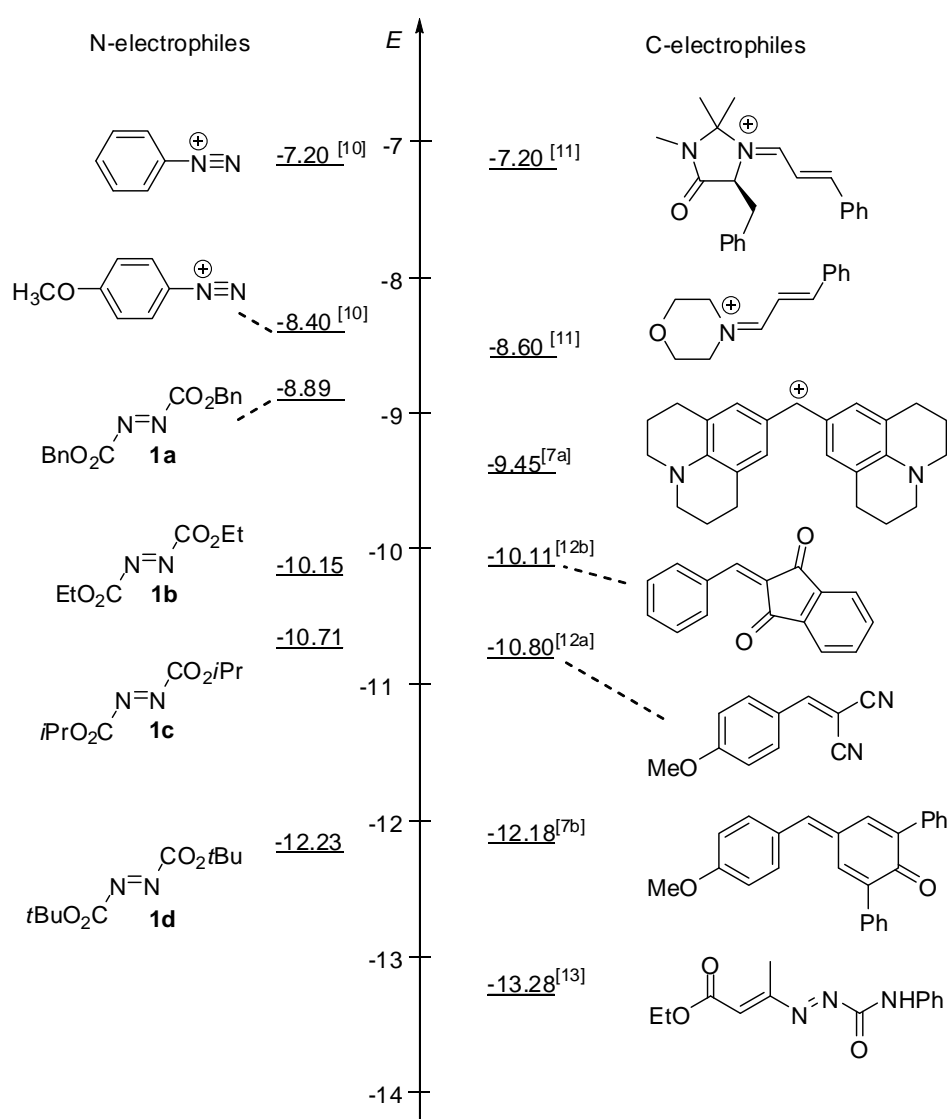


Figure 4.3. Comparison of the electrophilicity parameters of azodicarboxylates **1** with other electrophiles.

In order to compare these reactivities with rate constants determined in dichloromethane, we have also studied the influence of solvent on some of the reactions of **1** with **2**. Table 4.3 shows that the second-order rate constants for the reactions of **1** with **2** in acetonitrile (dielectric constant $\epsilon = 35.94$)^[14] and dichloromethane ($\epsilon = 8.93$)^[14] differ by less than a factor of 3. It is, therefore, not necessary to consider the effect of solvent on E when applying Equation (4.1) on reactions of **1** with nucleophiles in dichloromethane.

Table 4.3. Comparison of second-order rate constants k_2 for the reactions of the azodicarboxylates **1a-d** with the enamines **2a-e** in acetonitrile (MeCN) and dichloromethane (DCM) at 20 °C.

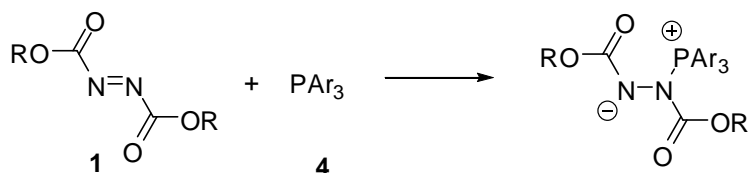
1	2	k_2^{MeCN} [M ⁻¹ s ⁻¹]	k_2^{DCM} [M ⁻¹ s ⁻¹]	$k_2^{\text{MeCN}}/k_2^{\text{DCM}}$
1a	2c	4.88×10^3	1.81×10^3	2.7
1b	2a	1.84×10^1	1.08×10^1	1.7
	2c	4.48×10^2	2.38×10^2	1.9
1c	2a	4.98	2.21	2.3
	2c	1.47×10^2	8.36×10^1	1.8
1d	2a	2.86×10^{-1}	1.24×10^{-1}	2.3
	2b	5.07	2.48	2.0
	2c	1.02×10^1	3.98	2.6
	2e	1.50×10^2	1.03×10^2	1.5

4.2.2 Reactions with Triarylphosphines **4**

In order to check whether the electrophilicity parameters E of **1a-d** (Figure 4.3) derived from the rates of their reactions with enamines **2** (carbon nucleophiles) are also suitable for the prediction of the rates of the reactions of azodicarboxylates with heteronucleophiles, we studied the kinetics of the reactions of **1a-d** with the triarylphosphines **4** and the amines **5**,

whose N and s parameters have previously been derived from the rates of their reactions with benzhydrylium ions.^[15,16]

Nucleophilic additions of the triarylphosphines **4** to dialkyl azodicarboxylates **1**, which correspond to the first step of the Mitsunobu reaction, yield the so-called Huisgen zwitterions, as depicted in Scheme 4.2.^[17]



Scheme 4.2. Reactions of **1** with phosphines **4**.

The kinetics of the reactions of **1** with triarylphosphines in CH_2Cl_2 were determined photometrically as described above for the reactions of **1** with enamines **2**. Linear plots of k_{obs} vs. $[\text{PAr}_3]$ confirmed second-order rate laws for these reactions, and the resulting second-order rate constants for the attack of PAr_3 at the $\text{N}=\text{N}$ unit are summarized in Table 4.4.

As shown in the last column of Table 4.4, the experimental rate constants for the reactions of **1** with the phosphines **4** generally agree within a factor of 10 with those calculated by Equation (4.1). This agreement is surprising: Since E parameters are generally derived from reactions with a series of C-centered nucleophiles (E of **1** from reactions with enamines, Table 4.2, Figure 4.2) and N , s parameters are generally derived from the rates of reactions with a series of C-centered electrophiles (N , s of **4** from reactions with benzhydrylium ions), Equation (4.1) can only be expected to hold for the formation of C-X bonds, i. e., for reactions where at least one of the reaction centers in electrophile or nucleophile is carbon.^[15] The unexpected observation that Equation (4.1) also holds for the formation of a N-P bond reminds one of the observation that Equation (4.1) as well as the Ritchie Equation were also found to work for the combinations of diazonium ions with several hetero-nucleophiles.^[10, 18] The comparable magnitudes of the P-N (290 kJ mol^{-1}) and C-N (305 kJ mol^{-1}) bond energies may account for this finding.^[19]

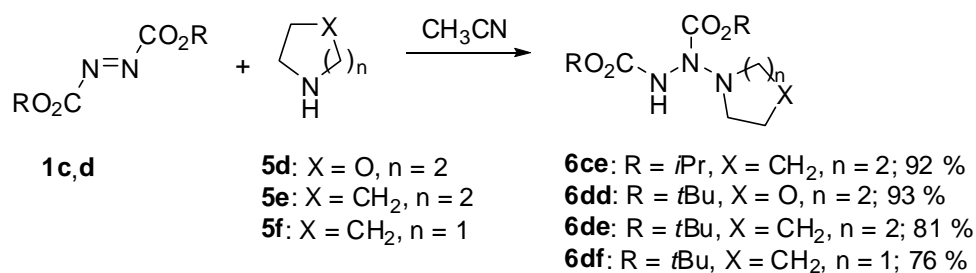
Table 4.4. Experimental and calculated second-order rate constants for the reactions of the azodicarboxylates **1** with the phosphines **4** in dichloromethane at 20 °C.

1	Phosphine 4 (<i>N/s</i>) ^[a]		k_2^{exp} [M ⁻¹ s ⁻¹]	k_2^{calcd} [M ⁻¹ s ⁻¹] ^[b]	$k_2^{\text{calcd}}/k_2^{\text{exp}}$
1a	(4-ClC ₆ H ₄) ₃ P (12.58/0.65)	4a	6.41×10^1	2.50×10^2	3.9
1a	Ph ₃ P (14.33/0.65)	4b	4.83×10^2	3.44×10^3	7.1
1a	(4-MeC ₆ H ₄) ₃ P (15.44/0.64)	4c	2.42×10^3	1.56×10^4	6.4
1a	(4-OMeC ₆ H ₄) ₃ P (16.17/0.62)	4d	1.07×10^4	3.26×10^4	3.0
1b	Ph ₃ P (14.33/0.65)	4b	1.45×10^2	5.21×10^2	3.6
1b	(4-MeC ₆ H ₄) ₃ P (15.44/0.64)	4c	6.13×10^2	2.43×10^3	3.8
1b	(4-OMeC ₆ H ₄) ₃ P (16.17/0.62)	4d	2.36×10^3	5.40×10^3	2.3
1c	(4-ClC ₆ H ₄) ₃ P (12.58/0.65)	4a	4.28	1.64×10^1	3.8
1c	Ph ₃ P (14.33/0.65)	4b	4.51×10^1	2.25×10^2	5.0
1c	(4-MeC ₆ H ₄) ₃ P (15.44/0.64)	4c	2.16×10^2	1.06×10^3	4.9
1c	(4-OMeC ₆ H ₄) ₃ P (16.17/0.62)	4d	7.25×10^2	2.43×10^3	3.3
1d	(4-ClC ₆ H ₄) ₃ P (12.58/0.65)	4a	4.83×10^{-1}	1.69	3.5
1d	Ph ₃ P (14.33/0.65)	4b	2.14	2.32×10^1	11
1d	(4-MeC ₆ H ₄) ₃ P (15.44/0.64)	4c	1.11×10^1	1.13×10^2	10

[a] *N/s*-parameters from ref. [15]. [b] Calculated by using Equation (4.1), *N* and *s* parameters from ref [15], and the *E* parameters from Table 4.2.

4.2.3 Reactions with Amines **5**

The reactions of azodicarboxylates **1** with amines **5** have been reported to yield triazanes **6** in petroleum ether solution.^[20] Scheme 4.3 shows that triazanes **6** are also formed in acetonitrile solution, i.e., the solvent in which the kinetic investigations were performed. Though N-N single bonds are generally rather weak, the triazanes **6** are stabilized by two electron withdrawing ester groups and can be isolated without problems.^[20a]



Scheme 4.3. Reactions of **1c,d** with amines **5d-5f**.

Nevertheless, the thermodynamic driving force for these additions seems to be rather low. As shown below, the relative reactivities of the azodicarboxylates **1** toward amines are the same as toward enamines **2** and phosphines **4**. For that reason, one can expect that **1a** should even react faster with amines than the azodicarboxylates **1b-d**. The fact, that no conversion was observed when **1a** was combined with morpholine **5d** and pyrrolidine **5f** must, therefore, be due to unfavourable thermodynamics (fast reverse reactions).

The reactions of **1** with the secondary amines **5a-f** were studied in CH₃CN by following the decay of the electrophiles' absorbances. When the amines were used in large excess, first-order kinetics were observed with exponential decays of the absorbances of the azodicarboxylates **1**. However, linearity of the k_{obs} vs. $[\mathbf{5}]$ plots was only observed for the reactions of **1c** with **5c** and **5e**. For all other reactions of the azodicarboxylates **1** with the secondary amines **5a-f**, the plots of the k_{obs} values vs. the amine concentrations showed concave curvatures (Figure 4.4), indicating that a second molecule of amine is involved in the rate determining step, which acts as a base catalyst (Scheme 4.4).

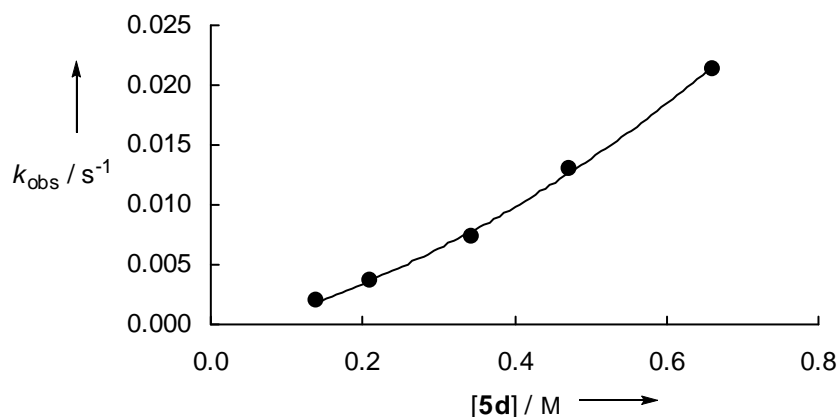
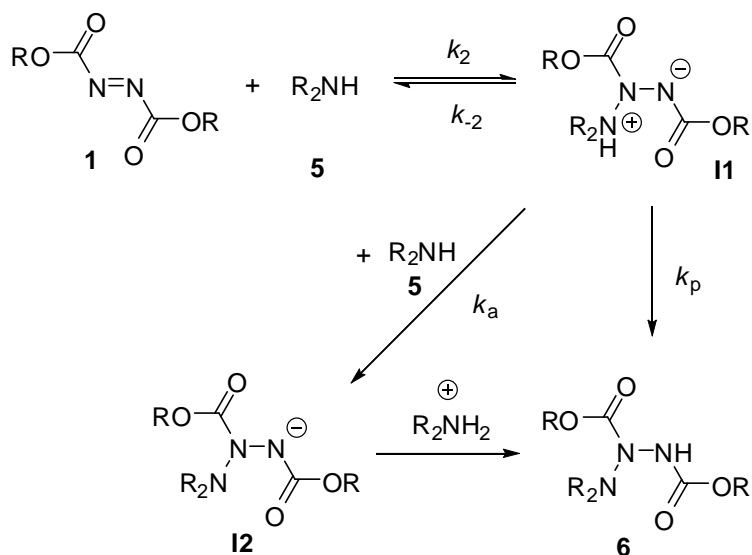


Figure 4.4. Plots of k_{obs} vs. [5d] for the reaction of 5d with the azodicarboxylate 1b (CH₃CN, 20 °C).

The assumption, that the formation of the intermediate **I1** is a reversible process, is in line with the observation that tertiary amines [e.g. DBU (1,8-diazabicyclo[5.4.0]undec-7-ene) or DABCO (1,4-diazabicyclo[2.2.2]octane)] do not react with the azodicarboxylates **1**.



Scheme 4.4. Reactions of the azodicarboxylates **1** with the amines **5**.

According to Scheme 4.4, the change of the concentration of the betaine intermediate **I1** can be expressed by Equation (4.3).

$$d[\mathbf{I1}]/dt = k_2[\mathbf{1}][\mathbf{5}] - k_{-2}[\mathbf{I1}] - k_a[\mathbf{I1}][\mathbf{5}] - k_p[\mathbf{I1}] \quad (4.3)$$

With the assumption of a steady state concentration for the intermediate **II** ($d[\mathbf{II}]/dt = 0$), the rate law can be expressed by Equations (4.4) and (4.5).

$$-d[\mathbf{1}]/dt = k_2[\mathbf{1}][\mathbf{5}](k_a[\mathbf{5}] + k_p)/(k_{-2} + k_a[\mathbf{5}] + k_p) \quad (4.4)$$

$$k_{\text{obs}} = k_2[\mathbf{5}](k_a[\mathbf{5}] + k_p)/(k_{-2} + k_a[\mathbf{5}] + k_p) \quad (4.5)$$

Let us first neglect the direct proton-transfer (k_p) from NH^+ to N^- in the zwitterionic intermediate **II**. Equation (4.5) is then reduced to Equation (4.6), which can be transformed into Equation (4.7).

$$k_{\text{obs}} = k_2[\mathbf{5}]^2 k_a/(k_{-2} + k_a[\mathbf{5}]) \quad (4.6)$$

$$[\mathbf{5}]/k_{\text{obs}} = 1/k_2 + k_{-2}/(k_2[\mathbf{5}]k_a) \quad (4.7)$$

$$k_{\text{obs}} = k_2[\mathbf{5}] \quad (4.8)$$

If $k_{-2} \ll k_a[\mathbf{5}]$, Equation 4.6 is transformed to Equation 4.8, i.e., a second-order reaction [Equation (4.2)] with rate-determining formation of the NN bond. As mentioned before, this situation was only observed for the reaction of **1c** with **5c** and **5e**. At high amine concentrations the second-order rate law [Equation (4.8)] also holds for the reactions of **1b** with **5b** and **5c**, and for **1d** with **5b**. As exemplified in Figure 4.5a for the reaction of **1d** with **5b**, $k_{\text{obs}}/[\mathbf{5b}]$ increases with increasing amine concentration $[\mathbf{5b}]$, because the proton transfer ($k_a[\mathbf{5b}]$) is getting faster. At high amine concentrations, where $k_{\text{obs}}/[\mathbf{5b}]$ is constant, the attack of the amine at the azodicarboxylate is rate limiting and $k_{\text{obs}}/[\mathbf{5b}] = k_2$ [Equation (4.8)]; the second-order rate constant equals the intercept on the y-axis. The whole range of amine concentrations can be evaluated by using Equation (4.7). The linear plot of $[\mathbf{5}]/k_{\text{obs}}$ against $1/[\mathbf{5}]$, as shown in Figure 4.5b, provides $1/k_2$ as the intercept. The second-order rate constants for the reaction of **1c** with **5d**, determined by the different evaluations, are thus in fair agreement. Equation 4.7 has analogously been used to determine the second-order rate constants k_2 for the first step of the reactions of **1b** with **5b** and **5c**.

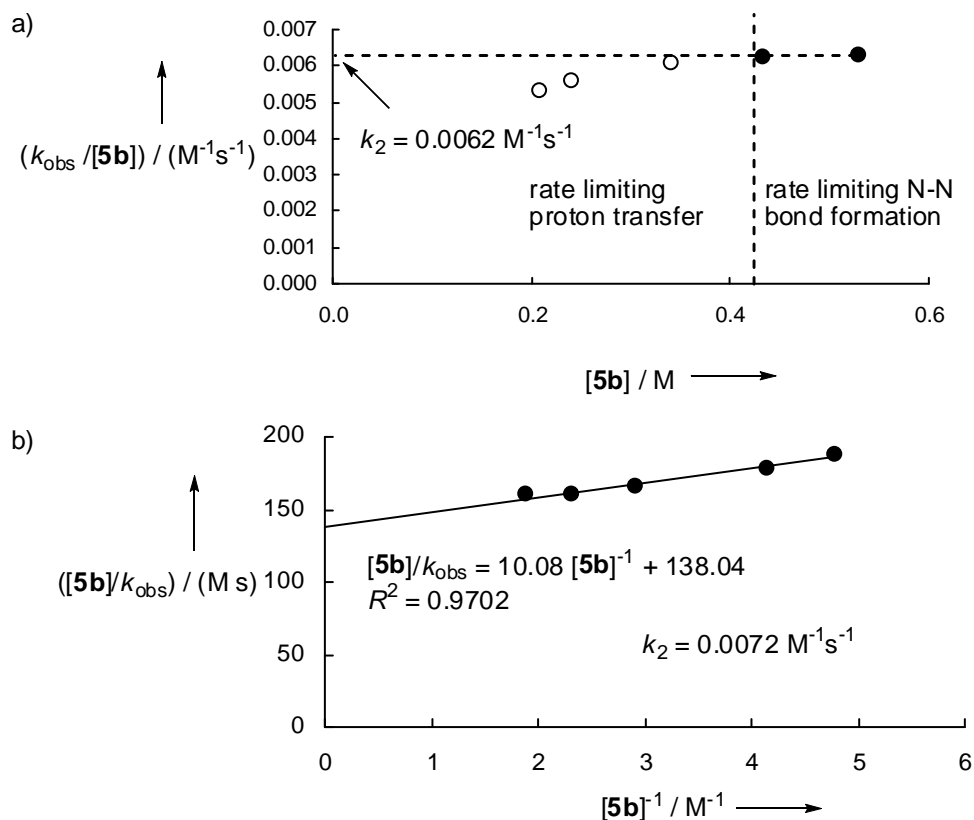


Figure 4.5. Plots of $k_{\text{obs}}/[5b]$ vs. $[5b]$ (Figure 4.5a) and $[5b]/k_{\text{obs}}$ vs. $1/[5b]$ (Figure 4.5b) for the reaction of **5b** with the azodicarboxylate **1d**.

In all other combinations of **1** and **5**, rate limiting NN bond formation was never observed, not even at high amine concentrations. The second-order rate constants for the first step of the reactions were also determined by plotting $[5b]/k_{\text{obs}}$ against $1/[5b]$. Deviations from these linear plots occur only at very low amine concentrations, probably due to the operation of k_p . If the k_{obs} values at low amine concentrations are neglected (open circles in Figure 4.6), the second-order rate constants k_2 can be obtained from the intercepts ($1/k_2$) of the linear correlations [Figure 4.6 and Equation (4.7)].

Analogous changes of the reaction order of amines have previously been reported for the reactions of secondary amines with quinone methides,^[16] thiocarbonates,^[21] thionobenzoates,^[22] and activated esters of indole-3-acetic acid.^[23] Table 4.5 shows the second-order rate constants k_2 for the reactions of **1** with **5** obtained by these evaluations.

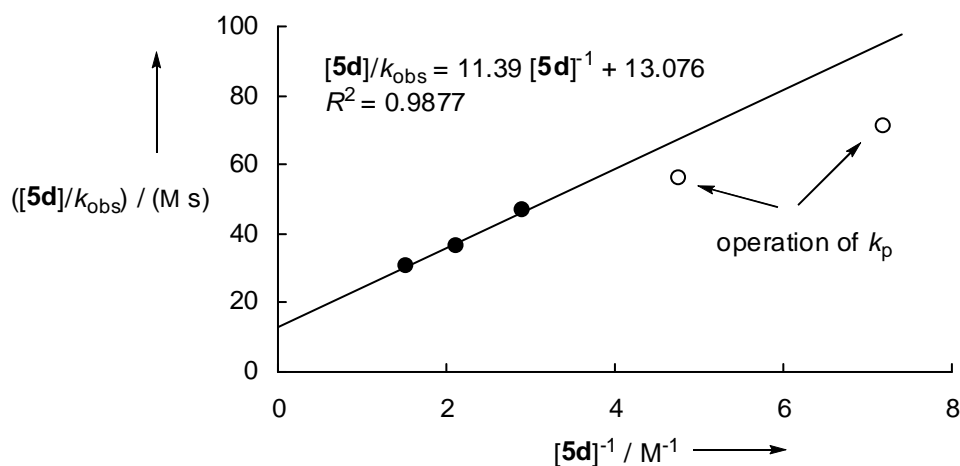


Figure 4.6. Plot of $[5d]/k_{obs}$ vs. $1/[5d]$ for the reaction of **5d** with the azodicarboxylate **1b**. (filled circles : included for the determination of k_2 ; $k_2 = 1/(13.076 M s) = 7.65 \times 10^{-2} M^{-1} s^{-1}$) ; open circles: not included for the evaluation of k_2 , because at the low concentration of **5d** the assumption that $k_p \ll k_a \times [5d]$ seems to be invalid).

The experimental rate constants are 10^3 to 10^6 times smaller than the values calculated by Equation (4.1). As described above, Equation (4.1) can only be expected to hold when at least one of the reaction centers in either electrophile or nucleophile is carbon. Table 4.5 clearly shows that Equation (4.1) cannot be applied to the N-N-bond forming reactions in the first step of Scheme 4.4. The considerably smaller N-N-bond energy (159 kJ mol^{-1}) compared with the CN-bond energy (305 kJ mol^{-1}) may account for the fact, why N -parameters of amines which have been derived from the reactivities of amines with C-electrophiles give far too low values in reactions with N-electrophiles.

Table 4.5. Experimental and calculated second-order rate constants for the reactions of azodicarboxylates **1** with amines **5** in acetonitrile at 20 °C.

1	Amine 5 (<i>N/s</i>) ^[a]	k_2^{exp} [$\text{M}^{-1} \text{s}^{-1}$]	k_2^{calcd} [$\text{M}^{-1} \text{s}^{-1}$] ^[b]	$k_2^{\text{calcd}}/k_2^{\text{exp}}$
1b	bis(2-methoxy)ethylamine 5a (13.24/0.93)	1.58×10^{-2}	7.48×10^2	4.7×10^4
1b	di- <i>n</i> -propylamine 5b (14.51/0.80)	3.34×10^{-1}	3.08×10^3	9.2×10^3
1b	diethylamine 5c (15.10/0.73)	1.00	4.11×10^3	4.1×10^3
1b	morpholine 5d (15.65/0.74)	7.65×10^{-2}	1.17×10^4	1.5×10^5
1b	piperidine 5e (17.35/0.68)	1.72	7.87×10^4	4.6×10^4
1b	pyrrolidine 5f (18.64/0.60)	2.94×10^1	1.24×10^5	4.2×10^3
1c	bis(2-methoxy)ethylamine 5a (13.24/0.93)	5.52×10^{-3}	2.25×10^2	4.1×10^4
1c	di- <i>n</i> -propylamine 5b (14.51/0.80)	9.52×10^{-2}	1.10×10^3	1.2×10^4
1c	diethylamine 5c (15.10/0.73)	3.27×10^{-1} ^[c]	1.60×10^3	4.9×10^3
1c	morpholine 5d (15.65/0.74)	1.86×10^{-2}	4.52×10^3	2.4×10^5
1c	piperidine 5e (17.35/0.68)	4.59×10^{-1} ^[c]	3.27×10^4	7.1×10^4
1c	pyrrolidine 5f (18.64/0.60)	1.55×10^1	5.73×10^4	3.7×10^3
1d	bis(2-methoxy)ethylamine 5a (13.24/0.93)	3.22×10^{-4}	8.70	2.7×10^4
1d	di- <i>n</i> -propylamine 5b (14.51/0.80)	7.24×10^{-3}	6.67×10^1	9.2×10^3
1d	diethylamine 5c (15.10/0.73)	2.60×10^{-2}	1.24×10^2	4.8×10^3
1d	morpholine 5d (15.65/0.74)	1.06×10^{-3}	3.39×10^2	3.2×10^5
1d	piperidine 5e (17.35/0.68)	3.07×10^{-2}	3.03×10^3	9.9×10^4
1d	pyrrolidine 5f (18.64/0.60)	8.09×10^{-1}	7.01×10^3	8.7×10^3

[a] *N/s*-parameters from ref. [16]. [b] Calculated by using Equation (4.1), *N* and *s* parameters from ref [16], and the *E* parameters from Table 4.2. [c] Derived from plots of k_{obs} vs. [**5**].

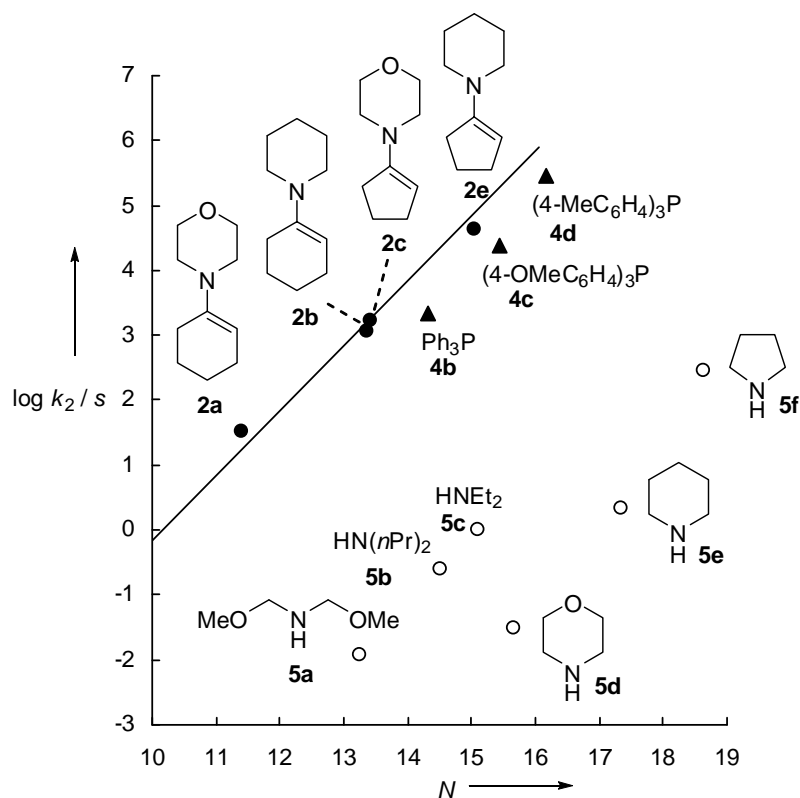


Figure 4.7. Plots of $(\log k_2)/s$ against the N -parameters of the enamines **2a-c** and **2e** (filled circles), the phosphines **4b-d** (filled triangles) and the amines **5a-f** (open circles) for the reactions of the azodicarboxylate **1b** with **2**, **4** and **5** at 20°C. The linear graph refers to the plot of $(\log k_2)/s$ against the N -parameters of the enamines **2a-c** and **2e** and the slope is fixed to unity.

Figure 4.7 illustrates that acyclic and cyclic secondary amines **5** are on different correlation lines, considerably below that for enamines **2**, from which the phosphines **4** deviate only marginally. Nevertheless, the internal consistency of the second-order rate constants k_2 for the reactions of the amines **5** with the azodicarboxylates **1b-d** is beautifully demonstrated by Figure 4.8 where the reactivities of the amines **5a-f** towards the azodicarboxylates **1c** and **1d** are plotted against the corresponding reactivities toward diethyl azodicarboxylate (**1b**).

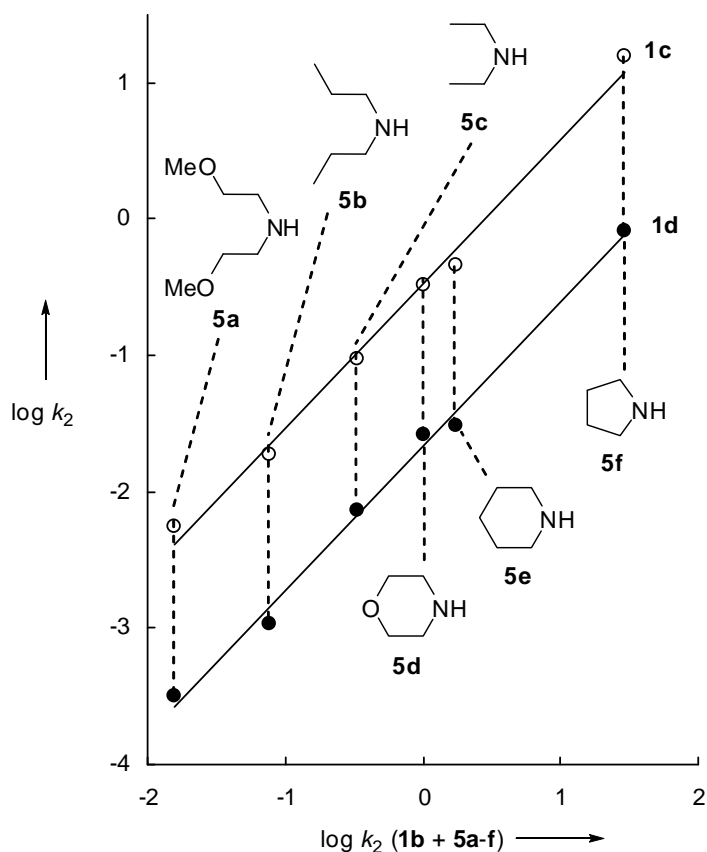


Figure 4.8. Correlation of ($\log k_2$) for the reactions of **1c** and **1d** with the amines **5a-f** against ($\log k_2$) for the reaction of **1b** with the amines **5a-f** (in CH_3CN , 20 °C).

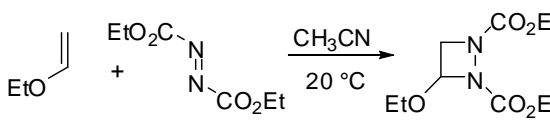
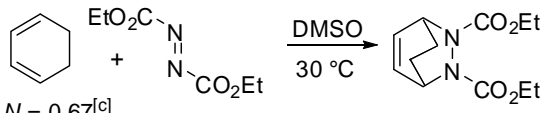
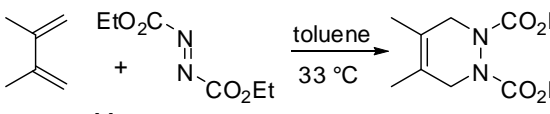
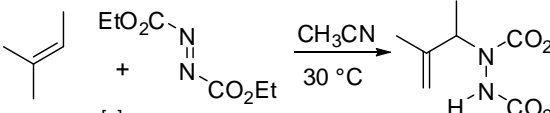
4.2.4 Pericyclic Reactions

Rate constants for the [2+2] cycloaddition of **1b** with ethyl vinyl ether,^[4d] for the Diels-Alder reactions of **1b** with cyclohexa-1,3-diene^[4b] and 2,3-dimethyl-1,3-butadiene,^[4a] and for the ene reaction of diethyl azodicarboxylate (**1b**) with 2-methyl-but-2-ene^[4c] have previously been reported (Table 4.6). Though the conditions (solvent, temperature) were not in all cases identical to those for which the reactivity parameters E , N , and s have been derived, they are similar enough that a comparison between experimental and calculated rate constants appears to be justified.

Table 4.6 shows that the reaction of **1b** with ethyl vinyl ether at 30 °C is only 36 times faster than calculated for 20 °C, i. e., the rate of the [2+2]-cycloaddition is in agreement with the predictions of Equation (4.1). As [2+2]-cycloadditions proceed stepwise and only one new σ -bonds is formed in the rate limiting step, Equation (4.1) appears to be applicable.

On the other hand, the Diels-Alder reactions as well as the ene reaction (entries 2-4 in Table 4.6) proceed 10^5 to 10^8 times faster than calculated by Equation (4.1). In these cases, the concerted formation of two new σ -bonds stabilizes the transition state and gives rise to a higher reaction rate. In cases where pericyclic processes are feasible, Equation (4.1) gives only a lower limit for the rate constant. If calculated and experimental rate constants refer to the same reaction conditions, the deviation between the two values may even be considered as a measure for the energy of concert.^[24]

Table 4.6. Comparison of experimental and calculated second-order rate constants k_2 for pericyclic reactions of **1b** with different nucleophiles.

	$k_2^{\text{exp [a]}}$ [M ⁻¹ s ⁻¹]	$k_2^{\text{calcd [b]}}$ [M ⁻¹ s ⁻¹]	$k_2^{\text{exp}}/k_2^{\text{calcd}}$
 $N = 3.92^{[c]}$ $s = 0.90$	$8.38 \times 10^{-5[d]}$	2.3×10^{-6}	36
 $N = 0.67^{[c]}$ $s = 1.10$	$7.6 \times 10^{-5[e]}$	3.4×10^{-11}	2.2×10^6
 $N = 1.17^{[c]}$ $s = 1.00$	$9.46 \times 10^{-5[f]}$	9.6×10^{-10}	9.9×10^4
 $N = 0.65^{[g]}$ $s = 1.17$	$5.7 \times 10^{-4[h]}$	6.9×10^{-12}	8.3×10^7

[a] If more than one rate constant was reported for a certain reaction, we selected that one, which was determined under conditions most similar to those we used for deriving the reactivity parameters (acetonitrile, 20 °C, 1013 mbar). [b] Calculated by using Equation (4.1). [c] Ref. [7c], [d] Ref. [3d], [e] Ref. [3b], [f] Ref. [3a], [g] Ref. [7a], [h] Ref. [3c].

4.3 Conclusion

The π -systems of azodicarboxylates and enamines combine with formation of only one new C-N bond, which allows us to derive electrophilicity parameters E for the azodicarboxylates **1a-d**. They are slightly less electrophilic than ordinary arenediazonium ions, comparable to α,β -unsaturated iminium ions and benzylidenemalononitriles. The E parameters of the azodicarboxylates determined in this work can be used to predict rate constants not only for the reactions of these electrophiles with carbon nucleophiles but unexpectedly also for the reactions with phosphines, though none of the reaction centers is carbon, a prerequisite for the application of Equation (4.1). The reported rate constants for Diels-Alder and ene reactions of diethyl azodicarboxylate are 10^5 to 10^8 times higher than calculated by Equation (4.1) indicating concerted pericyclic reactions.

4.4 Experimental Section

4.4.1 General comment

Azodicarboxylates **1a-d**, phosphines **4a-d**, and amines **5a-f** were purchased, and the amines **5** were purified by distillation prior to use. The enamines **2a-e** were synthesized by literature procedures.^[25]

The kinetics of the reactions of the azodicarboxylates with enamines, triarylphosphines, and amines were followed by UV-Vis spectroscopy at 20 °C.

For slow reactions ($\tau_{1/2} > 10$ s) the UV-Vis spectra were collected at different times by using a conventional diode array spectrophotometer (J&M TIDAS) that was connected to a Hellma 661.502-QX quartz Suprasil immersion probe (5 mm light path) by fiber optic cables with standard SMA connectors. All kinetic measurements were carried out in Schlenk glassware under exclusion of moisture. The temperature of the solutions during the kinetic studies was maintained to within ± 0.1 °C by using circulating bath cryostats and monitored with thermocouple probes that were inserted into the reaction mixture.

Stopped-flow spectrophotometer systems (Applied Photophysics SX.18MV-R or Hi-Tech SF-61DX2) were used for the investigation of fast reactions of azodicarboxylates with nucleophiles (10 ms $< \tau_{1/2} < 10$ s). The kinetic runs were initiated by mixing equal volumes of solutions of the nucleophiles and the azodicarboxylates.

From the exponential decays of the absorbances at λ_{\max} of the electrophiles **1**, the first-order rate constants k_{obs} (s^{-1}) were obtained.

The k_2 values were obtained as slopes of the plots of k_{obs} vs. the nucleophile concentrations unless noted otherwise.

4.4.2 Kinetic Experiments

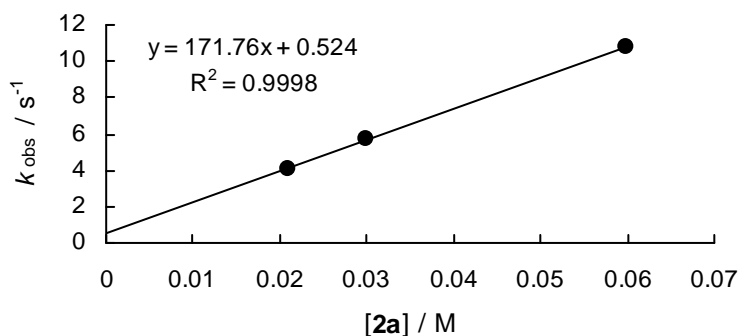
Kinetics of the reactions of dibenzyl azodicarboxylate (**1a**) with nucleophiles

Rate constants for the reactions of dibenzyl azodicarboxylate (**1a**) with enamines **2**

Reactions in CH_3CN

Rate constants for the reaction of **1a** with morpholinocyclohexene **2a** (stopped-flow method, $20\text{ }^\circ\text{C}$, $\lambda = 405\text{ nm}$) in CH_3CN .

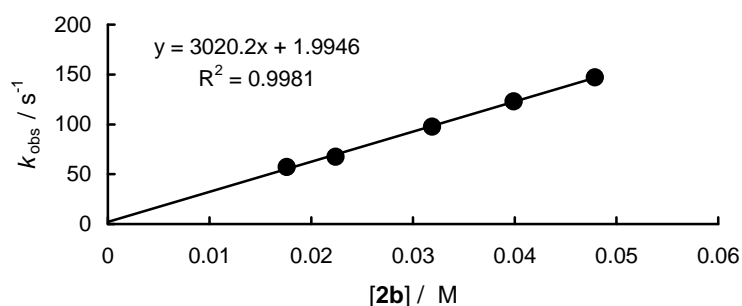
$[\mathbf{1a}]_0 / \text{M}$	$[\mathbf{2a}]_0 / \text{M}$	$[\mathbf{2a}]_0 / [\mathbf{1a}]_0$	$k_{\text{obs}} / \text{s}^{-1}$
1.96×10^{-3}	2.10×10^{-2}	11	4.09×10^0
1.96×10^{-3}	3.00×10^{-2}	15	5.73×10^0
1.96×10^{-3}	5.99×10^{-2}	30	1.08×10^1



$$k_2 = 1.72 \times 10^2 \text{ M}^{-1} \text{ s}^{-1}$$

Rate constants for the reaction of **1a** with piperidinocyclohexene **2b** (stopped-flow method, 20 °C, $\lambda = 405$ nm) in CH₃CN.

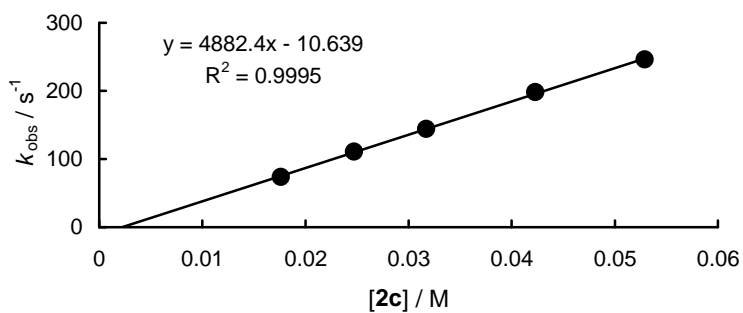
[1a] ₀ / M	[2b] ₀ / M	[2b] ₀ / [1a] ₀	k_{obs} / s ⁻¹
2.00×10^{-3}	1.76×10^{-2}	9	5.73×10^1
2.00×10^{-3}	2.24×10^{-2}	11	6.74×10^1
2.00×10^{-3}	3.19×10^{-2}	16	9.76×10^1
2.00×10^{-3}	3.99×10^{-2}	20	1.23×10^2
2.00×10^{-3}	4.79×10^{-2}	24	1.47×10^2



$$k_2 = 3.02 \times 10^3 \text{ M}^{-1} \text{ s}^{-1}$$

Rate constants for the reaction of **1a** with morpholinocyclopentene **2c** (stopped-flow method, 20 °C, $\lambda = 405$ nm) in CH₃CN.

[1a] ₀ / M	[2c] ₀ / M	[2c] ₀ / [1a] ₀	k_{obs} / s ⁻¹
1.92×10^{-3}	1.76×10^{-2}	9	7.39×10^1
1.92×10^{-3}	2.47×10^{-2}	13	1.11×10^2
1.92×10^{-3}	3.17×10^{-2}	17	1.44×10^2
1.92×10^{-3}	4.23×10^{-2}	22	1.98×10^2
1.92×10^{-3}	5.29×10^{-2}	28	2.46×10^2

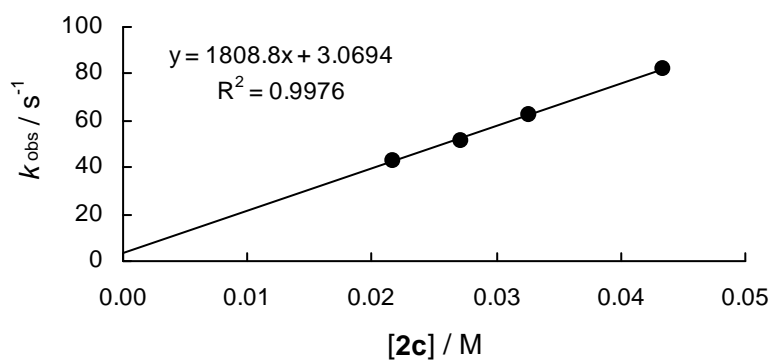


$$k_2 = 4.88 \times 10^3 \text{ M}^{-1} \text{ s}^{-1}$$

Reactions in CH_2Cl_2

Rate constants for the reaction of **1a** with morpholinocyclopentene **2c** (stopped-flow method, 20 °C, $\lambda = 405 \text{ nm}$) in CH_2Cl_2 .

$[\mathbf{1a}]_0 / \text{M}$	$[\mathbf{2c}]_0 / \text{M}$	$[\mathbf{2c}]_0 / [\mathbf{1a}]_0$	$k_{\text{obs}} / \text{s}^{-1}$
2.02×10^{-3}	2.17×10^{-2}	11	4.31×10^1
2.02×10^{-3}	2.72×10^{-2}	13	5.10×10^1
2.02×10^{-3}	3.26×10^{-2}	16	6.23×10^1
2.02×10^{-3}	4.34×10^{-2}	22	8.18×10^1

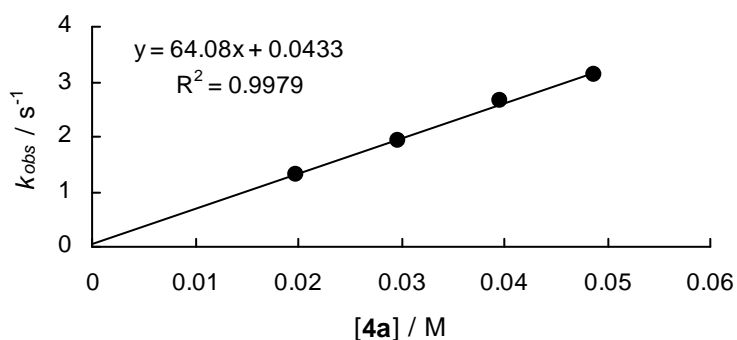


$$k_2 = 1.81 \times 10^3 \text{ M}^{-1} \text{ s}^{-1}$$

Rate constants for the reactions of dibenzyl azodicarboxylate (**1a**) with phosphines **4** in CH_2Cl_2

Rate constants for the reaction of **1a** with tris(4-chlorophenyl)phosphine **4a** (stopped-flow method, 20 °C, $\lambda = 405 \text{ nm}$) in CH_2Cl_2 .

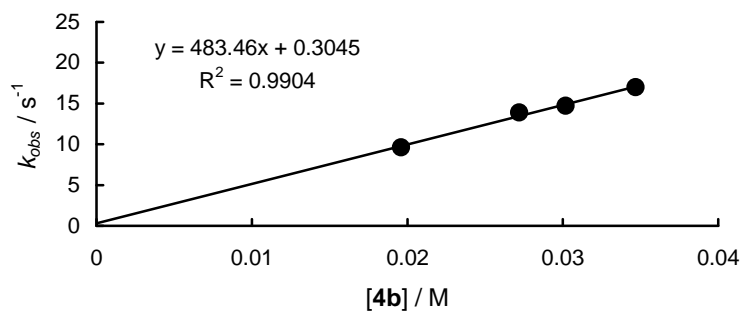
$[\mathbf{1a}]_0 / \text{M}$	$[\mathbf{4a}]_0 / \text{M}$	$[\mathbf{4a}]_0 / [\mathbf{1a}]_0$	$k_{\text{obs}} / \text{s}^{-1}$
2.06×10^{-3}	1.98×10^{-2}	10	1.30
2.06×10^{-3}	2.97×10^{-2}	14	1.94
2.06×10^{-3}	3.97×10^{-2}	19	2.64
2.06×10^{-3}	4.87×10^{-2}	24	3.13



$$k_2 = 6.41 \times 10^1 \text{ M}^{-1} \text{ s}^{-1}$$

Rate constants for the reaction of **1a** with triphenylphosphine **4b** (stopped-flow method, 20 °C, $\lambda = 405 \text{ nm}$) in CH_2Cl_2 .

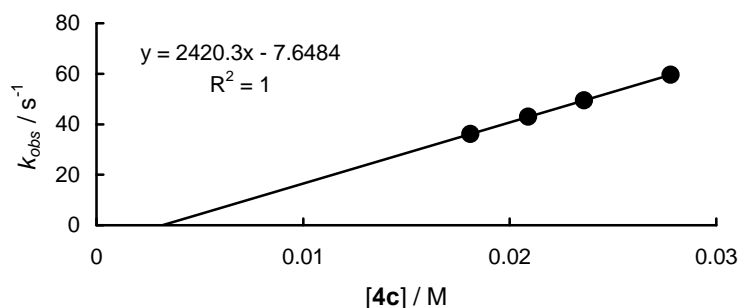
$[\mathbf{1a}]_0 / \text{M}$	$[\mathbf{4b}]_0 / \text{M}$	$[\mathbf{4b}]_0 / [\mathbf{1a}]_0$	$k_{\text{obs}} / \text{s}^{-1}$
2.01×10^{-3}	1.96×10^{-2}	10	9.62
2.01×10^{-3}	2.72×10^{-2}	14	1.39×10^1
2.01×10^{-3}	3.02×10^{-2}	15	1.47×10^1
2.01×10^{-3}	3.47×10^{-2}	17	1.70×10^1



$$k_2 = 4.83 \times 10^2 \text{ M}^{-1} \text{ s}^{-1}$$

Rate constants for the reaction of **1a** with tris(4-methylphenyl)phosphine **4c** (stopped-flow method, 20 °C, $\lambda = 405 \text{ nm}$) in CH_2Cl_2 .

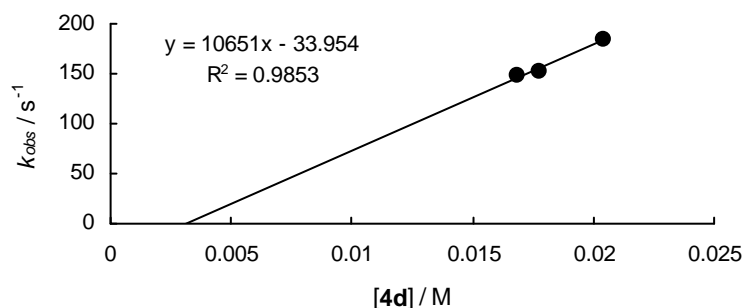
$[\mathbf{1a}]_0 / \text{M}$	$[\mathbf{4c}]_0 / \text{M}$	$[\mathbf{4c}]_0 / [\mathbf{1a}]_0$	$k_{\text{obs}} / \text{s}^{-1}$
2.06×10^{-3}	1.81×10^{-2}	9	3.61×10^1
2.06×10^{-3}	2.09×10^{-2}	10	4.30×10^1
2.06×10^{-3}	2.36×10^{-2}	11	4.95×10^1
2.06×10^{-3}	2.78×10^{-2}	13	5.96×10^1



$$k_2 = 2.42 \times 10^3 \text{ M}^{-1} \text{ s}^{-1}$$

Rate constants for the reaction of **1a** with tris(4-methoxyphenyl)phosphine **4d** (stopped-flow method, 20 °C, $\lambda = 405 \text{ nm}$) in CH_2Cl_2 .

$[\mathbf{1a}]_0 / \text{M}$	$[\mathbf{4d}]_0 / \text{M}$	$[\mathbf{4d}]_0 / [\mathbf{1a}]_0$	$k_{\text{obs}} / \text{s}^{-1}$
2.01×10^{-3}	1.69×10^{-2}	8	1.48×10^2
2.01×10^{-3}	1.78×10^{-2}	9	1.53×10^2
2.01×10^{-3}	2.04×10^{-2}	10	1.84×10^2



$$k_2 = 1.07 \times 10^4 \text{ M}^{-1} \text{ s}^{-1}$$

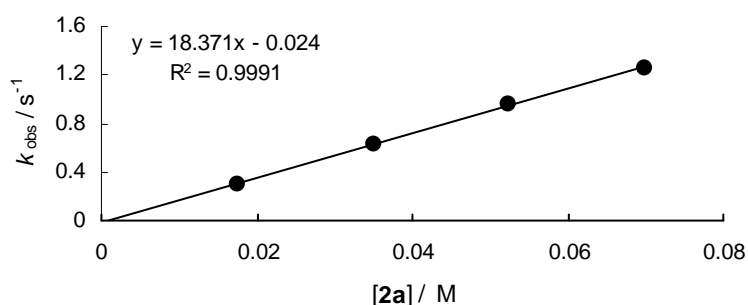
Kinetics of the reactions of diethyl azodicarboxylate (**1b**) with nucleophiles

Rate constants for the reactions of diethyl azodicarboxylate (**1b**) with enamines **2**

Reactions in CH₃CN

Rate constants for the reaction of **1b** with morpholinocyclohexene **2a** (stopped-flow method, 20 °C, $\lambda = 405 \text{ nm}$) in CH₃CN.

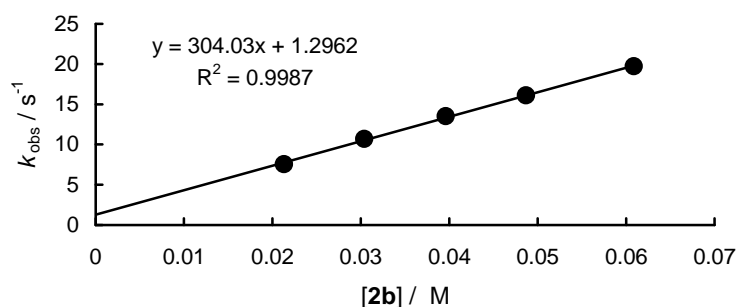
[1b] ₀ / M	[2a] ₀ / M	[2a] ₀ / [1b] ₀	$k_{\text{obs}} / \text{s}^{-1}$
2.05×10^{-3}	1.75×10^{-2}	9	2.90×10^{-1}
2.05×10^{-3}	3.50×10^{-2}	17	6.22×10^{-1}
2.05×10^{-3}	5.25×10^{-2}	26	9.57×10^{-1}
2.05×10^{-3}	7.00×10^{-2}	34	1.25



$$k_2 = 1.84 \times 10^1 \text{ M}^{-1} \text{ s}^{-1}$$

Rate constants for the reaction of **1b** with piperidinocyclohexene **2b** (stopped-flow method, 20 °C, $\lambda = 405$ nm) in CH₃CN.

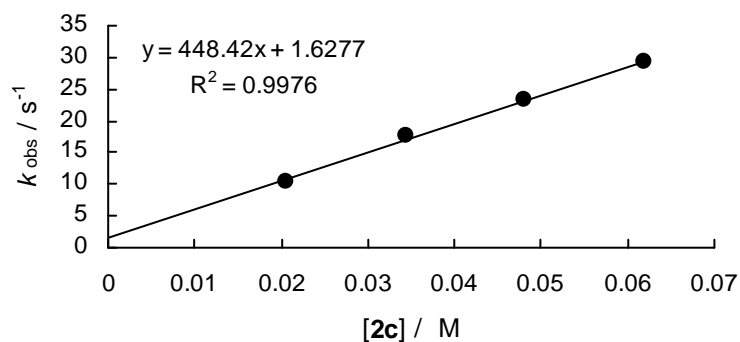
$[\mathbf{1b}]_0 / \text{M}$	$[\mathbf{2b}]_0 / \text{M}$	$[\mathbf{2b}]_0 / [\mathbf{1b}]_0$	$k_{\text{obs}} / \text{s}^{-1}$
1.99×10^{-3}	2.13×10^{-2}	11	7.56
1.99×10^{-3}	3.04×10^{-2}	15	1.07×10^1
1.99×10^{-3}	3.96×10^{-2}	20	1.35×10^1
1.99×10^{-3}	4.87×10^{-2}	25	1.61×10^1
1.99×10^{-3}	6.09×10^{-2}	31	1.97×10^1



$$k_2 = 3.04 \times 10^2 \text{ M}^{-1} \text{ s}^{-1}$$

Rate constants for the reaction of **1b** with morpholinocyclopentene **2c** (stopped-flow method, 20 °C, $\lambda = 405$ nm) in CH₃CN.

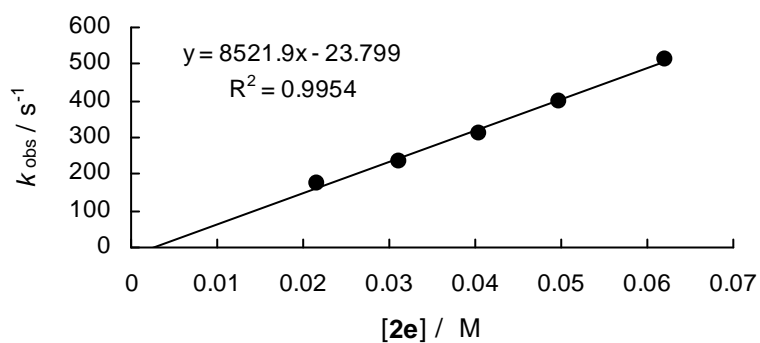
$[\mathbf{1b}]_0 / \text{M}$	$[\mathbf{2c}]_0 / \text{M}$	$[\mathbf{2c}]_0 / [\mathbf{1b}]_0$	$k_{\text{obs}} / \text{s}^{-1}$
6.52×10^{-3}	2.06×10^{-2}	3	1.05×10^1
6.52×10^{-3}	3.44×10^{-2}	5	1.76×10^1
6.52×10^{-3}	4.81×10^{-2}	7	2.32×10^1
6.52×10^{-3}	6.19×10^{-2}	9	2.92×10^1



$$k_2 = 4.48 \times 10^2 \text{ M}^{-1} \text{ s}^{-1}$$

Rate constants for the reaction of **1b** with piperidinocyclopentene **2e** (stopped-flow method, 20 °C, $\lambda = 405 \text{ nm}$) in CH_3CN .

$[\mathbf{1b}]_0 / \text{M}$	$[\mathbf{2e}]_0 / \text{M}$	$[\mathbf{2e}]_0 / [\mathbf{1b}]_0$	$k_{\text{obs}} / \text{s}^{-1}$
2.34×10^{-3}	2.17×10^{-2}	9	1.72×10^2
2.34×10^{-3}	3.11×10^{-2}	13	2.35×10^2
2.34×10^{-3}	4.04×10^{-2}	17	3.09×10^2
2.34×10^{-3}	4.97×10^{-2}	21	4.00×10^2
2.34×10^{-3}	6.21×10^{-2}	27	5.12×10^2

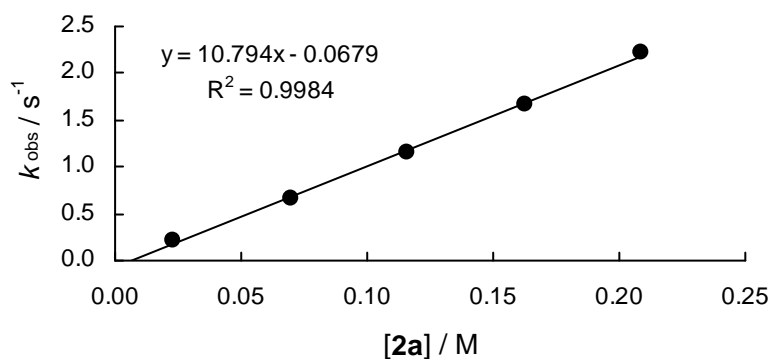


$$k_2 = 8.52 \times 10^3 \text{ M}^{-1} \text{ s}^{-1}$$

Reactions in CH₂Cl₂

Rate constants for the reaction of **1b** with morpholinocyclohexene **2a** (stopped-flow method, 20 °C, $\lambda = 405$ nm) in CH₂Cl₂.

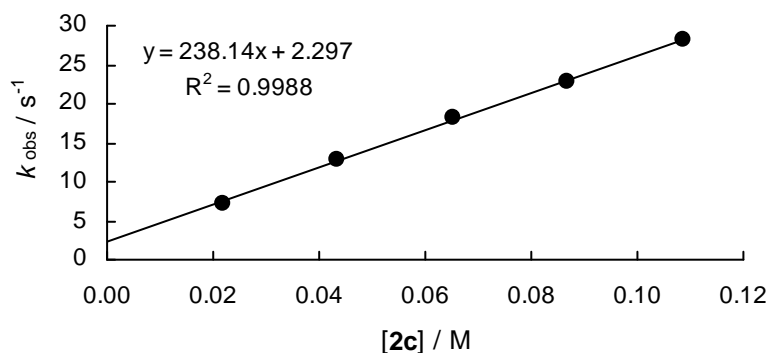
[1b] ₀ / M	[2a] ₀ / M	[2a] ₀ / [1b] ₀	k_{obs} / s ⁻¹
2.07×10^{-3}	2.32×10^{-2}	11	2.17×10^{-1}
2.07×10^{-3}	6.96×10^{-2}	34	6.66×10^{-1}
2.07×10^{-3}	1.16×10^{-1}	56	1.15
2.07×10^{-3}	1.62×10^{-1}	78	1.67
2.07×10^{-3}	2.09×10^{-1}	101	2.22



$$k_2 = 1.08 \times 10^1 \text{ M}^{-1} \text{ s}^{-1}$$

Rate constants for the reaction of **1b** with morpholinocyclopentene **2c** (stopped-flow method, 20 °C, $\lambda = 405$ nm) in CH₂Cl₂.

[1b] ₀ / M	[2c] ₀ / M	[2c] ₀ / [1b] ₀	k_{obs} / s ⁻¹
2.06×10^{-3}	2.17×10^{-2}	11	7.17
2.06×10^{-3}	4.34×10^{-2}	21	1.29×10^1
2.06×10^{-3}	6.52×10^{-2}	32	1.82×10^1
2.06×10^{-3}	8.69×10^{-2}	42	2.28×10^1
2.06×10^{-3}	1.09×10^{-1}	53	2.81×10^1

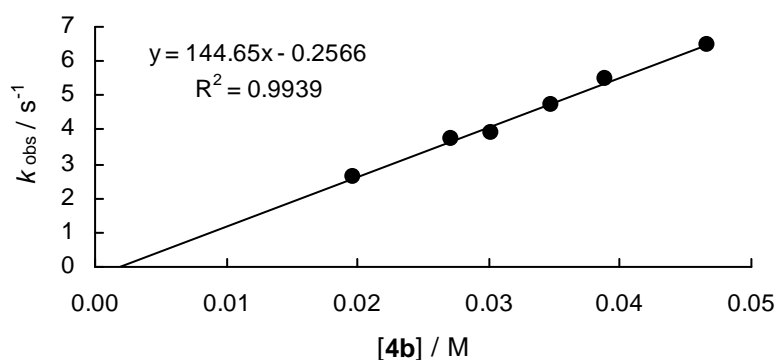


$$k_2 = 2.38 \times 10^2 \text{ M}^{-1} \text{ s}^{-1}$$

Rate constants for the reactions of diethyl azodicarboxylate (**1b**) with phosphines **4** in CH_2Cl_2

Rate constants for the reaction of **1b** with triphenylphosphine **4b** (stopped-flow method, 20 °C, $\lambda = 405 \text{ nm}$) in CH_2Cl_2 .

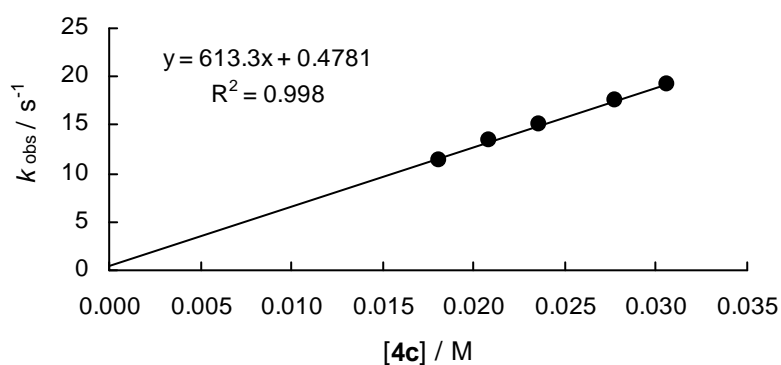
$[\mathbf{1b}]_0 / \text{M}$	$[\mathbf{4b}]_0 / \text{M}$	$[\mathbf{4b}]_0 / [\mathbf{1b}]_0$	$k_{\text{obs}} / \text{s}^{-1}$
1.72×10^{-3}	1.96×10^{-2}	11	2.62
1.72×10^{-3}	2.72×10^{-2}	16	3.76
1.72×10^{-3}	3.02×10^{-2}	18	3.92
1.72×10^{-3}	3.47×10^{-2}	20	4.73
1.72×10^{-3}	3.88×10^{-2}	23	5.46
1.72×10^{-3}	4.66×10^{-2}	27	6.48



$$k_2 = 1.45 \times 10^2 \text{ M}^{-1} \text{ s}^{-1}$$

Rate constants for the reaction of **1b** with tris(4-methylphenyl)phosphine **4c** (stopped-flow method, 20 °C, $\lambda = 405$ nm) in CH_2Cl_2 .

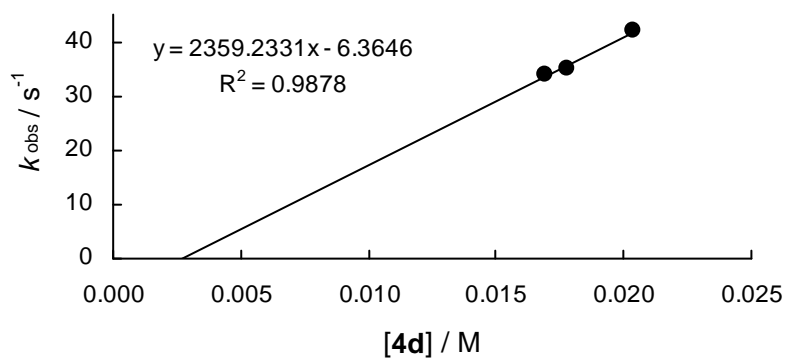
$[\mathbf{1b}]_0 / \text{M}$	$[\mathbf{4c}]_0 / \text{M}$	$[\mathbf{4c}]_0 / [\mathbf{1b}]_0$	$k_{\text{obs}} / \text{s}^{-1}$
2.08×10^{-3}	1.81×10^{-2}	9	1.14×10^1
2.08×10^{-3}	2.09×10^{-2}	10	1.35×10^1
2.08×10^{-3}	2.36×10^{-2}	11	1.50×10^1
2.08×10^{-3}	2.78×10^{-2}	13	1.75×10^1
2.08×10^{-3}	3.06×10^{-2}	15	1.92×10^1



$$k_2 = 6.13 \times 10^2 \text{ M}^{-1} \text{ s}^{-1}$$

Rate constants for the reaction of **1b** with tris(4-methoxyphenyl)phosphine **4d** (stopped-flow method, 20 °C, $\lambda = 405$ nm) in CH_2Cl_2 .

$[\mathbf{1b}]_0 / \text{M}$	$[\mathbf{4d}]_0 / \text{M}$	$[\mathbf{4d}]_0 / [\mathbf{1b}]_0$	$k_{\text{obs}} / \text{s}^{-1}$
1.72×10^{-3}	1.69×10^{-2}	10	3.39×10^1
1.72×10^{-3}	1.78×10^{-2}	10	3.51×10^1
1.72×10^{-3}	2.04×10^{-2}	12	4.19×10^1

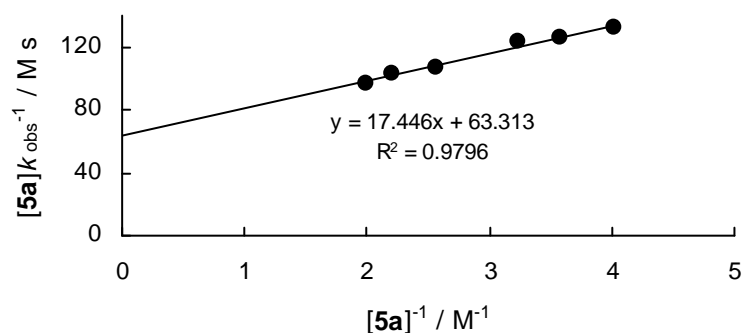
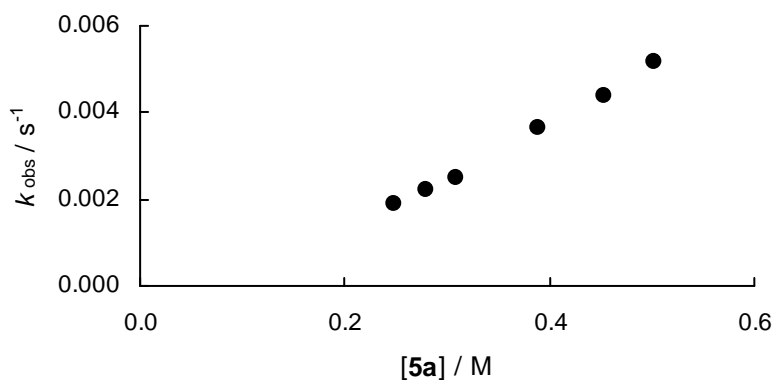


$$k_2 = 2.36 \times 10^3 \text{ M}^{-1} \text{ s}^{-1}$$

Rate constants for the reactions of diethyl azodicarboxylate (**1b**) with amines **5** in CH₃CN

Rate constants for the reaction of **1b** with bis(2-methoxyethyl)amine **5a** (conventional UV-Vis spectroscopy, 20 °C, $\lambda = 405 \text{ nm}$) in CH₃CN.

$[\mathbf{1b}]_0 / \text{M}$	$[\mathbf{5a}]_0 / \text{M}$	$[\mathbf{5a}]_0^{-1} / \text{M}^{-1}$	$[\mathbf{5a}]_0 / [\mathbf{1b}]_0$	$k_{\text{obs}} / \text{s}^{-1}$	$[\mathbf{5a}]_0 \times k_{\text{obs}}^{-1} / \text{Ms}$
2.71×10^{-2}	2.49×10^{-1}	4.02	9	1.89×10^{-3}	1.32×10^2
2.70×10^{-2}	2.79×10^{-1}	3.58	10	2.22×10^{-3}	1.26×10^2
2.69×10^{-2}	3.09×10^{-1}	3.24	11	2.51×10^{-3}	1.23×10^2
2.66×10^{-2}	3.89×10^{-1}	2.57	15	3.66×10^{-3}	1.06×10^2
2.63×10^{-2}	4.53×10^{-1}	2.21	17	4.39×10^{-3}	1.03×10^2
2.57×10^{-2}	5.02×10^{-1}	1.99	20	5.18×10^{-3}	9.69×10^1

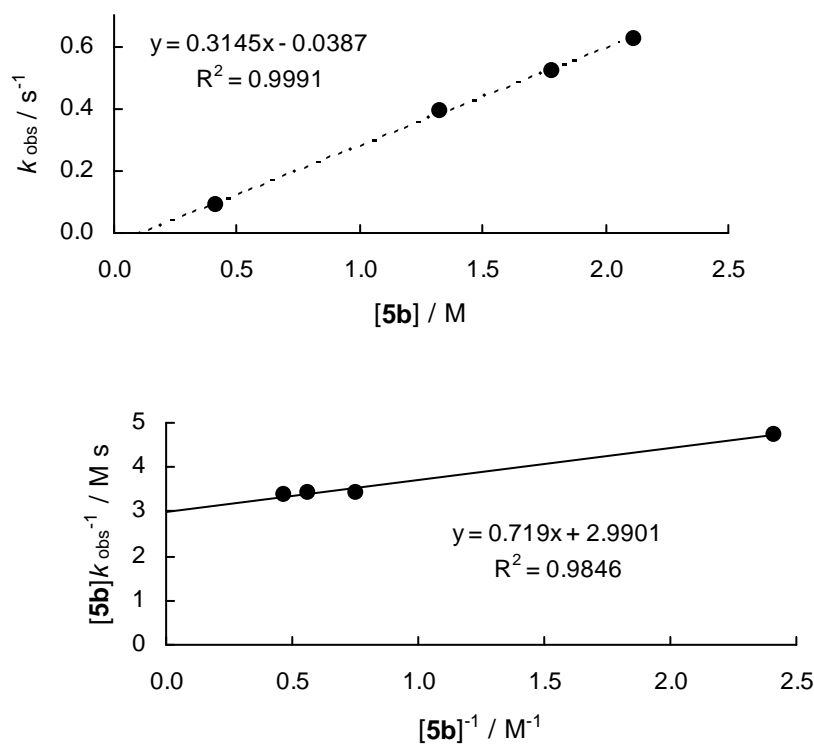


$$k_2 = 1.58 \times 10^{-2} \text{ M}^{-1} \text{ s}^{-1}$$

k_2 determined by plot of $[5a]/k_{\text{obs}}$ vs. $1/[5a]$

Rate constants for the reaction of **1b** with di-*n*-propylamine **5b** (stopped-flow method, 20 °C, $\lambda = 405 \text{ nm}$) in CH_3CN .

$[1b]_0 / \text{M}$	$[5b]_0 / \text{M}$	$[5b]_0^{-1} / \text{M}^{-1}$	$[5b]_0 / [1b]_0$	$k_{\text{obs}} / \text{s}^{-1}$	$[5b]_0 \times k_{\text{obs}}^{-1} / \text{MS}$
1.96×10^{-2}	4.14×10^{-1}	2.42	21	8.73×10^{-2}	4.74
1.94×10^{-2}	1.33	7.52×10^{-1}	69	3.90×10^{-1}	3.41
1.94×10^{-2}	1.78	5.62×10^{-1}	92	5.18×10^{-1}	3.44
1.89×10^{-2}	2.12	4.72×10^{-1}	112	6.25×10^{-1}	3.39

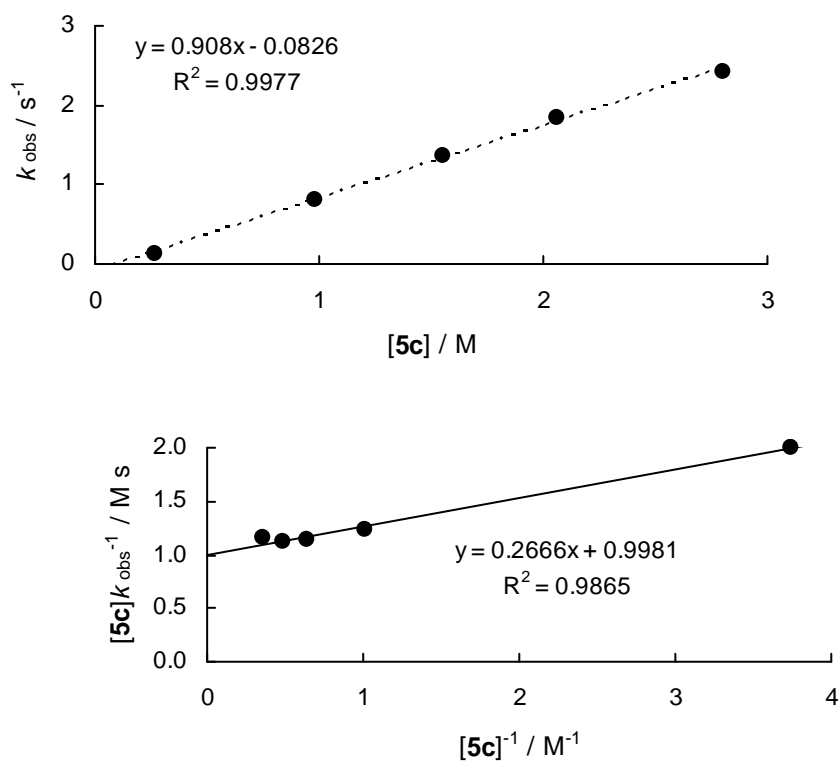


$$k_2 = 3.34 \times 10^{-1} \text{ M}^{-1} \text{ s}^{-1}$$

k_2 determined by plot of $[\mathbf{5b}]/k_{\text{obs}}$ vs. $1/[\mathbf{5b}]$

Rate constants for the reaction of **1b** with diethylamine **5c** (stopped-flow method, 20 °C, $\lambda = 405 \text{ nm}$) in CH_3CN .

$[\mathbf{1b}]_0 / \text{M}$	$[\mathbf{5c}]_0 / \text{M}$	$[\mathbf{5c}]_0^{-1} / \text{M}^{-1}$	$[\mathbf{5c}]_0 / [\mathbf{1b}]_0$	$k_{\text{obs}} / \text{s}^{-1}$	$[\mathbf{5c}]_0 \times k_{\text{obs}}^{-1} / \text{Ms}$
2.81×10^{-2}	2.67×10^{-1}	3.75	10	1.33×10^{-1}	2.01
2.81×10^{-2}	9.83×10^{-1}	1.02	35	7.99×10^{-1}	1.23
2.81×10^{-2}	1.55	6.45×10^{-1}	55	1.37	1.13
2.81×10^{-2}	2.06	4.85×10^{-1}	73	1.83	1.13
2.81×10^{-2}	2.80	3.57×10^{-1}	100	2.41	1.16

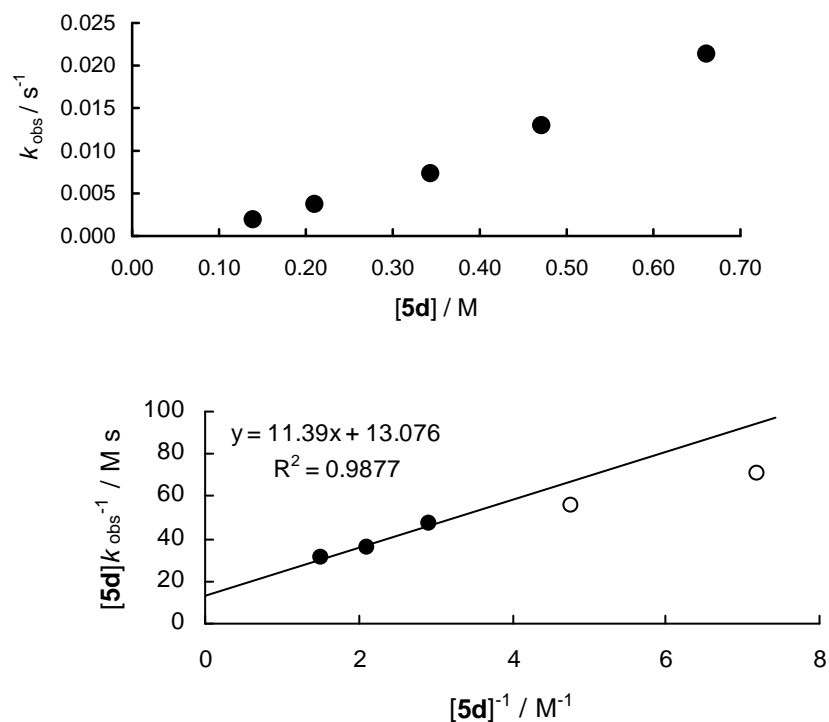


$$k_2 = 1.00 \text{ M}^{-1} \text{ s}^{-1}$$

k_2 determined by plot of $[\mathbf{5c}]/k_{\text{obs}}$ vs. $1/[\mathbf{5c}]$

Rate constants for the reaction of **1b** with morpholine **5d** (conventional UV-Vis spectroscopy, 20 °C, $\lambda = 405 \text{ nm}$) in CH_3CN .

$[\mathbf{1b}]_0 / \text{M}$	$[\mathbf{5d}]_0 / \text{M}$	$[\mathbf{5d}]_0^{-1} / \text{M}^{-1}$	$[\mathbf{5d}]_0 / [\mathbf{1b}]_0$	$k_{\text{obs}} / \text{s}^{-1}$	$[\mathbf{5d}]_0 \times k_{\text{obs}}^{-1} / \text{Ms}$
3.24×10^{-2}	1.39×10^{-1}	7.19	4	1.96×10^{-3}	7.09×10^1
3.27×10^{-2}	2.10×10^{-1}	4.76	6	3.75×10^{-3}	5.60×10^1
3.21×10^{-2}	3.43×10^{-1}	2.92	11	7.34×10^{-3}	4.67×10^1
3.14×10^{-2}	4.71×10^{-1}	2.12	15	1.30×10^{-2}	3.62×10^1
3.09×10^{-2}	6.61×10^{-1}	1.51	21	2.14×10^{-2}	3.09×10^1

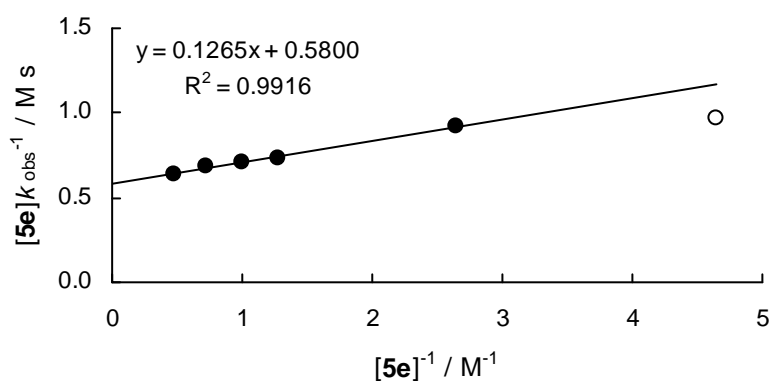
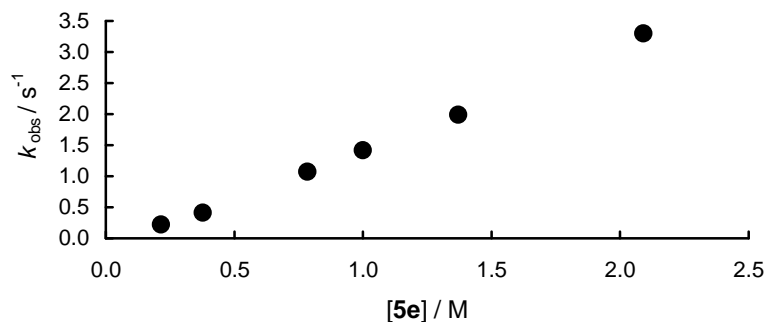


$$k_2 = 7.65 \times 10^{-2} \text{ M}^{-1} \text{ s}^{-1}$$

k_2 determined by plot of $[\mathbf{5d}]/k_{\text{obs}}$ vs. $1/[\mathbf{5d}]$

Rate constants for the reaction of **1b** with piperidine **5e** (stopped-flow method, 20 °C, $\lambda = 405 \text{ nm}$) in CH_3CN .

$[\mathbf{1b}]_0 / \text{M}$	$[\mathbf{5e}]_0 / \text{M}$	$[\mathbf{5e}]_0^{-1} / \text{M}^{-1}$	$[\mathbf{5e}]_0 / [\mathbf{1b}]_0$	$k_{\text{obs}} / \text{s}^{-1}$	$[\mathbf{5e}]_0 \times k_{\text{obs}}^{-1} / \text{Ms}$
3.12×10^{-2}	2.15×10^{-1}	4.65	7	2.22×10^{-1}	9.68×10^{-1}
3.12×10^{-2}	3.77×10^{-1}	2.65	12	4.11×10^{-1}	9.17×10^{-1}
3.12×10^{-2}	7.84×10^{-1}	1.28	25	1.07	7.33×10^{-1}
3.12×10^{-2}	1.00	1.00	32	1.42	7.04×10^{-1}
3.12×10^{-2}	1.37	7.30×10^{-1}	44	1.99	6.88×10^{-1}
3.12×10^{-2}	2.09	4.78×10^{-1}	67	3.30	6.33×10^{-1}

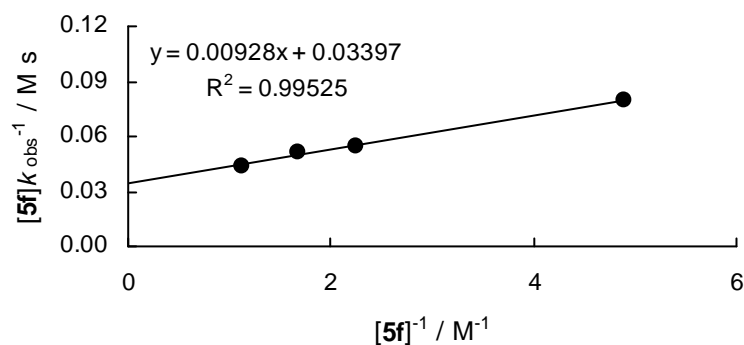
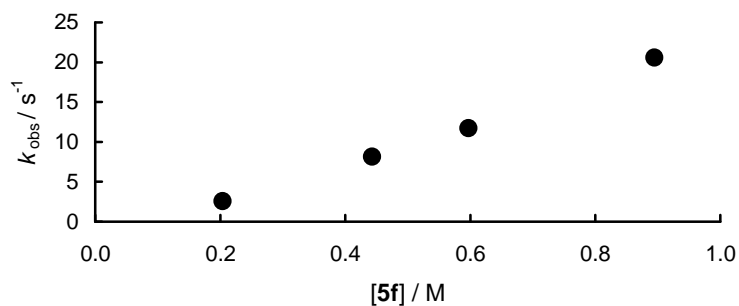


$$k_2 = 1.72 \text{ M}^{-1} \text{ s}^{-1}$$

k_2 determined by plot of $[\mathbf{5e}]/k_{\text{obs}}$ vs. $1/[\mathbf{5e}]$

Rate constants for the reaction of **1b** with pyrrolidine **5f** (stopped-flow method, 20 °C, $\lambda = 405 \text{ nm}$) in CH_3CN .

$[\mathbf{1b}]_0 / \text{M}$	$[\mathbf{5f}]_0 / \text{M}$	$[\mathbf{5f}]_0^{-1} / \text{M}^{-1}$	$[\mathbf{5f}]_0 / [\mathbf{1b}]_0$	$k_{\text{obs}} / \text{s}^{-1}$	$[\mathbf{5f}]_0 \times k_{\text{obs}}^{-1} / \text{Ms}$
3.12×10^{-2}	2.04×10^{-1}	4.90	7	2.57	7.94×10^{-2}
3.12×10^{-2}	4.43×10^{-1}	2.26	14	8.15	5.44×10^{-2}
3.12×10^{-2}	5.97×10^{-1}	1.68	19	1.17×10^1	5.10×10^{-2}
3.12×10^{-2}	8.95×10^{-1}	1.12	29	2.06×10^1	4.34×10^{-2}



$$k_2 = 2.94 \times 10^1 \text{ M}^{-1} \text{ s}^{-1}$$

k_2 determined by plot of $[5\text{f}]/k_{\text{obs}}$ vs. $1/[5\text{f}]$

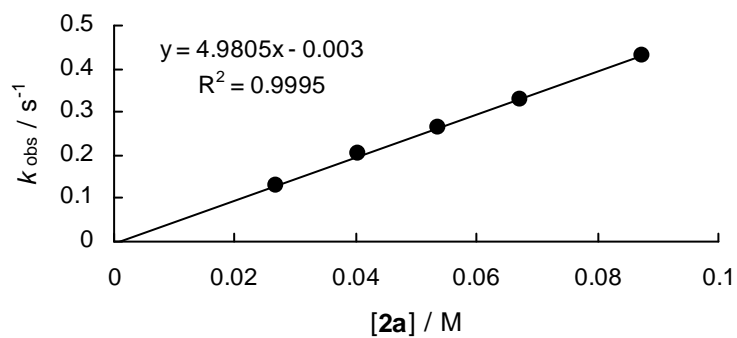
Kinetics of the reactions of di-isopropyl azodicarboxylate (**1c**) with nucleophiles

Rate constants for the reactions of di-isopropyl azodicarboxylate (**1c**) with enamines **2**

Reactions in CH_3CN

Rate constants for the reaction of **1c** with morpholinocyclohexene **2a** (stopped-flow method, 20°C , $\lambda = 405 \text{ nm}$) in CH_3CN .

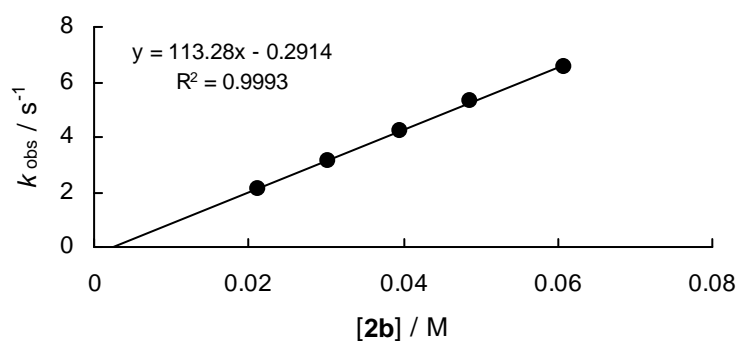
$[1\text{c}]_0 / \text{M}$	$[2\text{a}]_0 / \text{M}$	$[2\text{a}]_0 / [1\text{c}]_0$	$k_{\text{obs}} / \text{s}^{-1}$
2.54×10^{-3}	2.69×10^{-2}	11	1.29×10^{-1}
2.54×10^{-3}	4.03×10^{-2}	16	2.02×10^{-1}
2.54×10^{-3}	5.37×10^{-2}	21	2.62×10^{-1}
2.54×10^{-3}	6.71×10^{-2}	26	3.31×10^{-1}
2.54×10^{-3}	8.73×10^{-2}	34	4.32×10^{-1}



$$k_2 = 4.98 \text{ M}^{-1} \text{ s}^{-1}$$

Rate constants for the reaction of **1c** with piperidinocyclohexene **2b** (stopped-flow method, 20 °C, $\lambda = 405 \text{ nm}$) in CH_3CN .

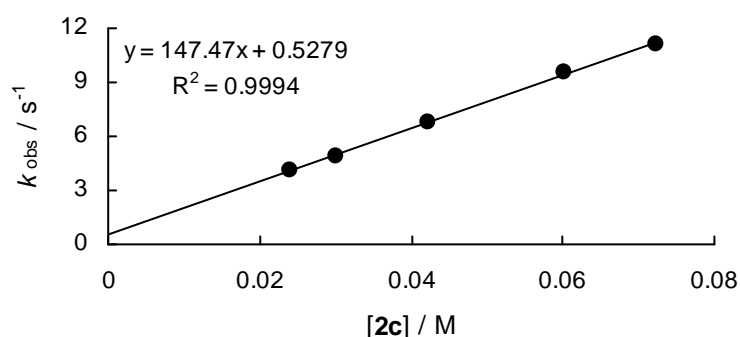
$[\mathbf{1c}]_0 / \text{M}$	$[\mathbf{2b}]_0 / \text{M}$	$[\mathbf{2b}]_0 / [\mathbf{1c}]_0$	$k_{\text{obs}} / \text{s}^{-1}$
2.35×10^{-3}	2.13×10^{-2}	11	2.12
2.35×10^{-3}	3.04×10^{-2}	15	3.12
2.35×10^{-3}	3.96×10^{-2}	20	4.20
2.35×10^{-3}	4.87×10^{-2}	25	5.30
2.35×10^{-3}	6.09×10^{-2}	31	6.56



$$k_2 = 1.13 \times 10^2 \text{ M}^{-1} \text{ s}^{-1}$$

Rate constants for the reaction of **1c** with morpholinocyclopentene **2c** (stopped-flow method, 20 °C, $\lambda = 405$ nm) in CH₃CN.

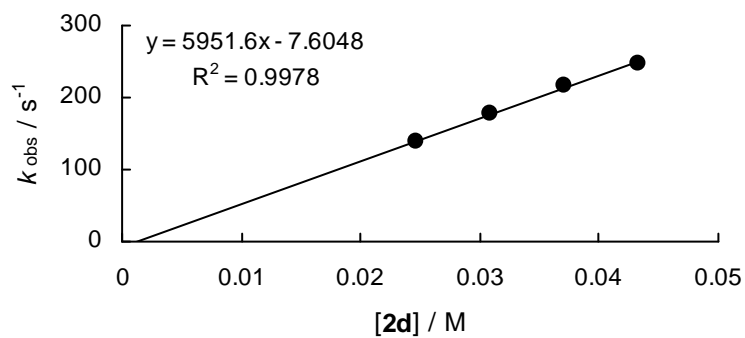
$[\mathbf{1c}]_0 / \text{M}$	$[\mathbf{2c}]_0 / \text{M}$	$[\mathbf{2c}]_0 / [\mathbf{1c}]_0$	$k_{\text{obs}} / \text{s}^{-1}$
2.37×10^{-3}	2.41×10^{-2}	10	4.06
2.37×10^{-3}	3.01×10^{-2}	13	4.94
2.37×10^{-3}	4.22×10^{-2}	18	6.78
2.37×10^{-3}	6.03×10^{-2}	25	9.53
2.37×10^{-3}	7.23×10^{-2}	30	1.11×10^1



$$k_2 = 1.47 \times 10^2 \text{ M}^{-1} \text{ s}^{-1}$$

Rate constants for the reaction of **1c** with pyrrolidinocyclohexene **2d** (stopped-flow method, 20 °C, $\lambda = 405$ nm) in CH₃CN.

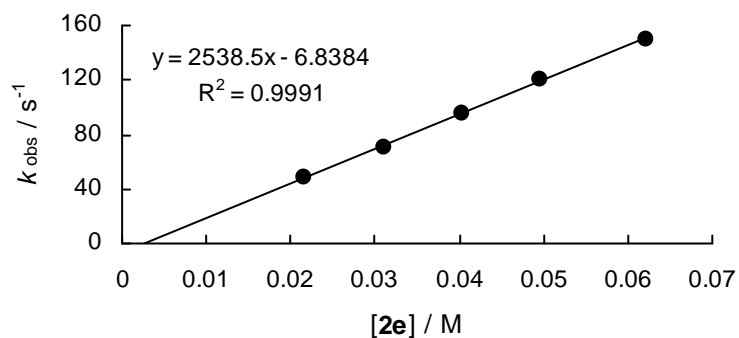
$[\mathbf{1c}]_0 / \text{M}$	$[\mathbf{2d}]_0 / \text{M}$	$[\mathbf{2d}]_0 / [\mathbf{1c}]_0$	$k_{\text{obs}} / \text{s}^{-1}$
2.54×10^{-3}	2.47×10^{-2}	10	1.38×10^2
2.54×10^{-3}	3.09×10^{-2}	12	1.77×10^2
2.54×10^{-3}	3.71×10^{-2}	15	2.16×10^2
2.54×10^{-3}	4.33×10^{-2}	17	2.48×10^2



$$k_2 = 5.95 \times 10^3 \text{ M}^{-1} \text{ s}^{-1}$$

Rate constants for the reaction of **1c** with piperidinocyclopentene **2e** (stopped-flow method, 20 °C, $\lambda = 405 \text{ nm}$) in CH_3CN .

$[\mathbf{1c}]_0 / \text{M}$	$[\mathbf{2e}]_0 / \text{M}$	$[\mathbf{2e}]_0 / [\mathbf{1c}]_0$	$k_{\text{obs}} / \text{s}^{-1}$
2.37×10^{-3}	2.17×10^{-2}	9	4.88×10^1
2.37×10^{-3}	3.11×10^{-2}	13	7.08×10^1
2.37×10^{-3}	4.04×10^{-2}	17	9.56×10^1
2.37×10^{-3}	4.97×10^{-2}	21	1.21×10^2
2.37×10^{-3}	6.21×10^{-2}	26	1.50×10^2

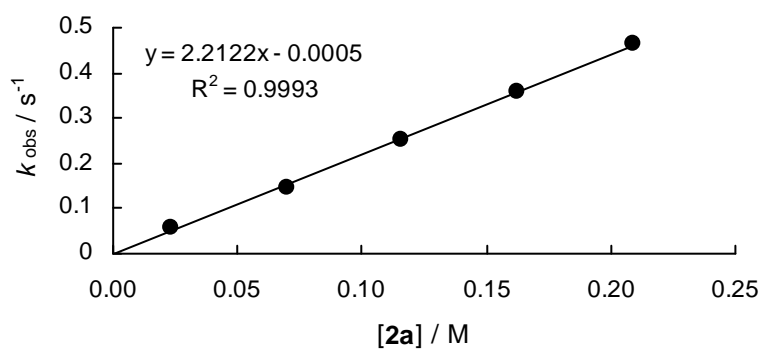


$$k_2 = 2.54 \times 10^3 \text{ M}^{-1} \text{ s}^{-1}$$

Reactions in CH₂Cl₂

Rate constants for the reaction of **1c** with morpholinocyclohexene **2a** (stopped-flow method, 20 °C, $\lambda = 405$ nm) in CH₂Cl₂.

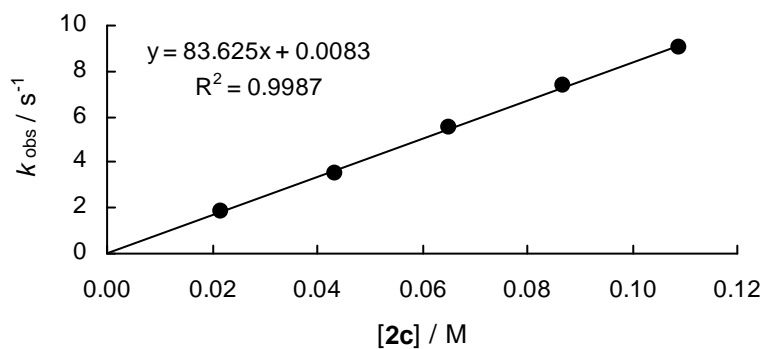
[1c] ₀ / M	[2a] ₀ / M	[2a] ₀ / [1c] ₀	k_{obs} / s ⁻¹
1.84×10^{-3}	2.32×10^{-2}	13	5.61×10^{-2}
1.84×10^{-3}	6.96×10^{-2}	38	1.48×10^{-1}
1.84×10^{-3}	1.16×10^{-1}	63	2.54×10^{-1}
1.84×10^{-3}	1.62×10^{-1}	88	3.59×10^{-1}
1.84×10^{-3}	2.09×10^{-1}	113	4.64×10^{-1}



$$k_2 = 2.21 \text{ M}^{-1} \text{ s}^{-1}$$

Rate constants for the reaction of **1c** with morpholinocyclopentene **2c** (stopped-flow method, 20 °C, $\lambda = 405$ nm) in CH₂Cl₂.

[1c] ₀ / M	[2c] ₀ / M	[2c] ₀ / [1c] ₀	k_{obs} / s ⁻¹
2.19×10^{-3}	2.17×10^{-2}	10	1.85
2.19×10^{-3}	4.34×10^{-2}	20	3.52
2.19×10^{-3}	6.52×10^{-2}	30	5.52
2.19×10^{-3}	8.69×10^{-2}	40	7.40
2.19×10^{-3}	1.09×10^{-1}	50	9.03

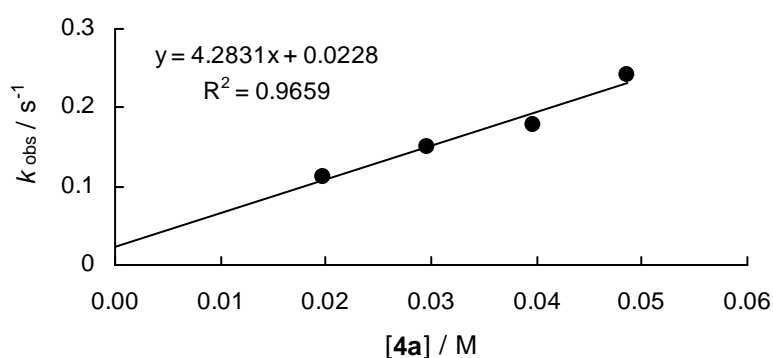


$$k_2 = 8.36 \times 10^1 \text{ M}^{-1} \text{ s}^{-1}$$

Rate constants for the reactions of di-isopropyl azodicarboxylate (**1c**) with phosphines **4** in CH_2Cl_2

Rate constants for the reaction of **1c** with tris(4-chlorophenyl)phosphine **4a** (stopped-flow method, 20 °C, $\lambda = 405 \text{ nm}$) in CH_2Cl_2 .

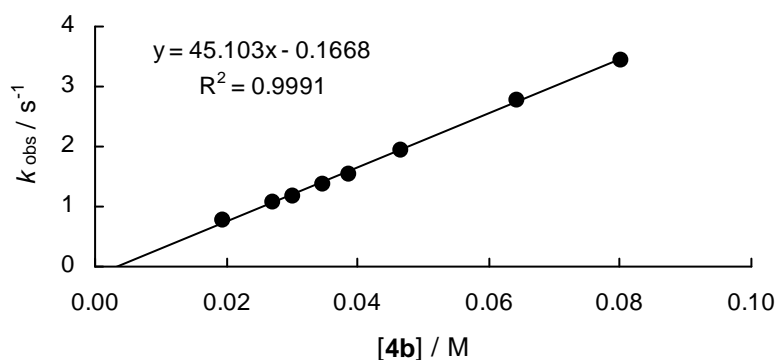
$[1\text{c}]_0 / \text{M}$	$[4\text{a}]_0 / \text{M}$	$[4\text{a}]_0 / [1\text{c}]_0$	$k_{\text{obs}} / \text{s}^{-1}$
2.17×10^{-3}	1.98×10^{-2}	9	1.12×10^{-1}
2.17×10^{-3}	2.97×10^{-2}	14	1.50×10^{-1}
2.17×10^{-3}	3.97×10^{-2}	18	1.79×10^{-1}
2.17×10^{-3}	4.87×10^{-2}	22	2.41×10^{-1}



$$k_2 = 4.28 \text{ M}^{-1} \text{ s}^{-1}$$

Rate constants for the reaction of **1c** with triphenylphosphine **4b** (stopped-flow method, 20 °C, $\lambda = 405$ nm) in CH_2Cl_2 .

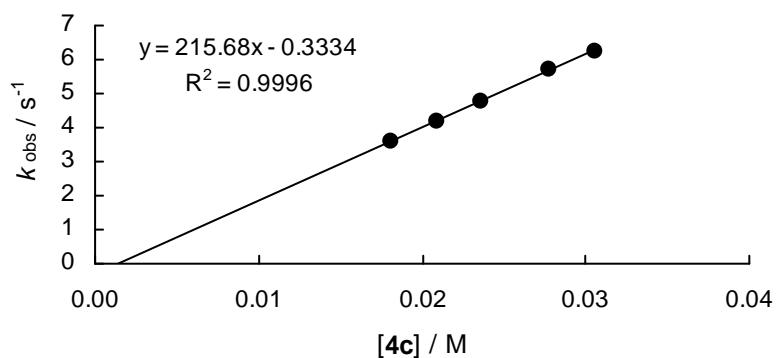
$[\mathbf{1c}]_0 / \text{M}$	$[\mathbf{4b}]_0 / \text{M}$	$[\mathbf{4b}]_0 / [\mathbf{1c}]_0$	$k_{\text{obs}} / \text{s}^{-1}$
1.87×10^{-3}	1.96×10^{-2}	10	7.58×10^{-1}
1.87×10^{-3}	2.72×10^{-2}	15	1.06
1.87×10^{-3}	3.02×10^{-2}	16	1.18
1.87×10^{-3}	3.47×10^{-2}	19	1.38
1.87×10^{-3}	3.88×10^{-2}	21	1.55
1.87×10^{-3}	4.66×10^{-2}	25	1.93
1.87×10^{-3}	6.42×10^{-2}	34	2.77
1.87×10^{-3}	8.02×10^{-2}	43	3.44



$$k_2 = 4.51 \times 10^1 \text{ M}^{-1} \text{ s}^{-1}$$

Rate constants for the reaction of **1c** with tris(4-methylphenyl)phosphine **4c** (stopped-flow method, 20 °C, $\lambda = 405$ nm) in CH_2Cl_2 .

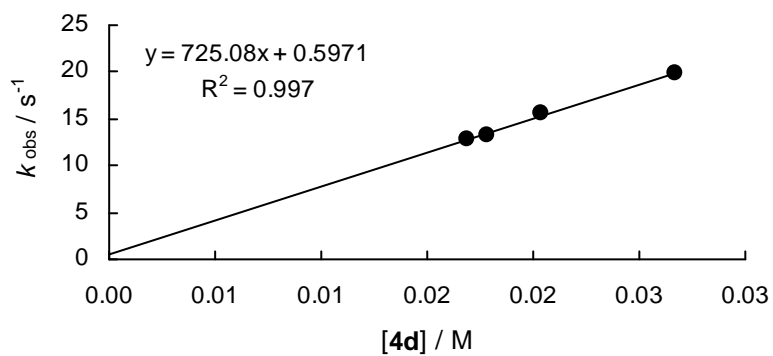
$[\mathbf{1c}]_0 / \text{M}$	$[\mathbf{4c}]_0 / \text{M}$	$[\mathbf{4c}]_0 / [\mathbf{1c}]_0$	$k_{\text{obs}} / \text{s}^{-1}$
2.17×10^{-3}	1.81×10^{-2}	8	3.56
2.17×10^{-3}	2.09×10^{-2}	10	4.17
2.17×10^{-3}	2.36×10^{-2}	11	4.77
2.17×10^{-3}	2.78×10^{-2}	13	5.69
2.17×10^{-3}	3.06×10^{-2}	14	6.24



$$k_2 = 2.16 \times 10^2 \text{ M}^{-1} \text{ s}^{-1}$$

Rate constants for the reaction of **1c** with tris(4-methoxyphenyl)phosphine **4d** (stopped-flow method, 20 °C, $\lambda = 405 \text{ nm}$) in CH_2Cl_2 .

$[\mathbf{1c}]_0 / \text{M}$	$[\mathbf{4d}]_0 / \text{M}$	$[\mathbf{4d}]_0 / [\mathbf{1c}]_0$	$k_{\text{obs}} / \text{s}^{-1}$
1.87×10^{-3}	1.69×10^{-2}	9	1.29×10^1
1.87×10^{-3}	1.78×10^{-2}	10	1.33×10^1
1.87×10^{-3}	2.04×10^{-2}	11	1.56×10^1
1.87×10^{-3}	2.67×10^{-2}	14	1.99×10^1

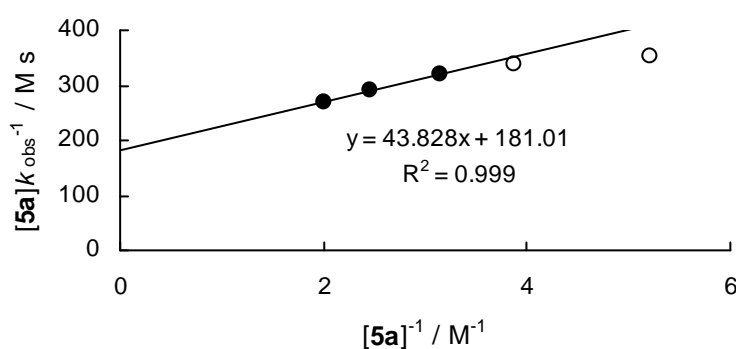
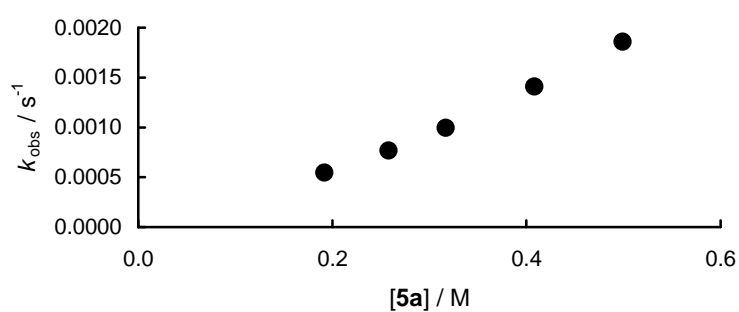


$$k_2 = 7.25 \times 10^2 \text{ M}^{-1} \text{ s}^{-1}$$

Rate constants for the reactions of di-isopropyl azodicarboxylate (**1c**) with amines **5** in CH_3CN

Rate constants for the reaction of **1c** with bis(2-methoxyethyl)amine **5a** (conventional UV-Vis spectroscopy, 20 °C, $\lambda = 405 \text{ nm}$) in CH_3CN .

$[\mathbf{1c}]_0 / \text{M}$	$[\mathbf{5a}]_0 / \text{M}$	$[\mathbf{5a}]_0^{-1} / \text{M}^{-1}$	$[\mathbf{5a}]_0 / [\mathbf{1c}]_0$	$k_{\text{obs}} / \text{s}^{-1}$	$[\mathbf{5a}]_0 \times k_{\text{obs}}^{-1} / \text{MS}$
2.63×10^{-2}	1.92×10^{-1}	5.21	7	5.47×10^{-4}	3.51×10^2
2.59×10^{-2}	2.58×10^{-1}	3.88	10	7.67×10^{-4}	3.36×10^2
2.62×10^{-2}	3.17×10^{-1}	3.15	12	9.94×10^{-4}	3.19×10^2
2.62×10^{-2}	4.08×10^{-1}	2.45	16	1.41×10^{-3}	2.89×10^2
2.62×10^{-2}	4.99×10^{-1}	2.00	19	1.86×10^{-3}	2.68×10^2

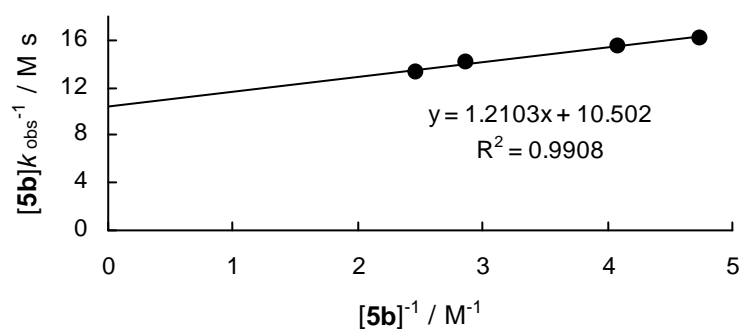
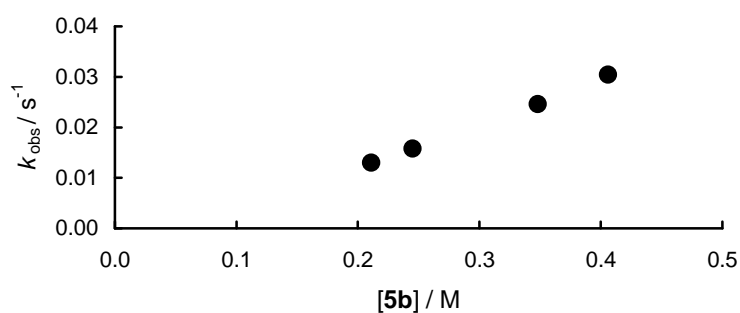


$$k_2 = 5.52 \times 10^{-3} \text{ M}^{-1} \text{ s}^{-1}$$

k_2 determined by plot of $[\mathbf{5a}]/k_{\text{obs}}$ vs. $1/[\mathbf{5a}]$

Rate constants for the reaction of **1c** with di-*n*-propylamine **5b** (conventional UV-Vis spectroscopy, 20 °C, $\lambda = 405$ nm) in CH₃CN.

[1c] ₀ / M	[5b] ₀ / M	[5b] ₀ ⁻¹ / M ⁻¹	[5b] ₀ / [1c] ₀	k_{obs} / s ⁻¹	[5b] ₀ × k_{obs} ⁻¹ / Ms
2.55×10^{-2}	2.11×10^{-1}	4.74	8	1.30×10^{-2}	1.62×10^1
2.54×10^{-2}	2.45×10^{-1}	4.08	10	1.59×10^{-2}	1.54×10^1
2.53×10^{-2}	3.48×10^{-1}	2.87	14	2.46×10^{-2}	1.41×10^1
2.46×10^{-2}	4.06×10^{-1}	2.46	17	3.04×10^{-2}	1.34×10^1

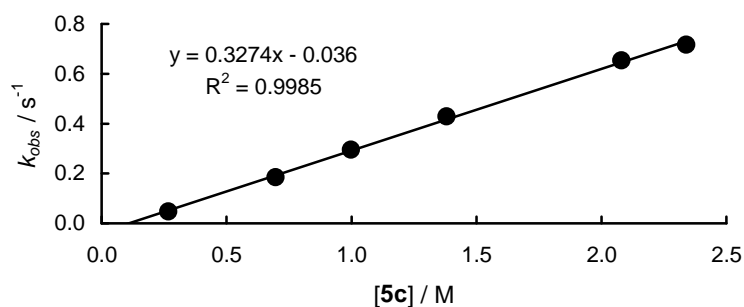


$$k_2 = 9.52 \times 10^{-2} \text{ M}^{-1} \text{ s}^{-1}$$

k_2 determined by plot of $[\mathbf{5b}]_0/k_{\text{obs}}$ vs. $1/[\mathbf{5b}]_0$

Rate constants for the reaction of **1c** with diethylamin **5c** (stopped-flow method, 20 °C, $\lambda = 405$ nm) in CH₃CN.

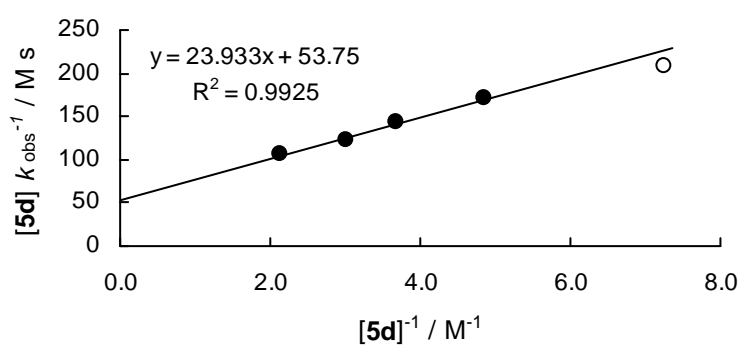
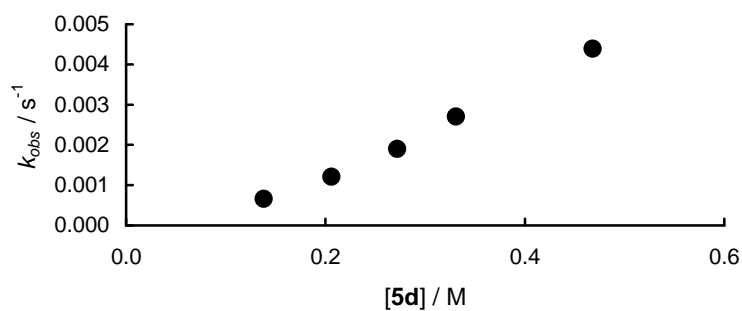
[1c] ₀ / M	[5c] ₀ / M	[5c] ₀ / [1b] ₀	$k_{\text{obs}} / \text{s}^{-1}$
2.87×10^{-2}	2.67×10^{-1}	9	4.71×10^{-2}
2.87×10^{-2}	6.96×10^{-1}	24	1.85×10^{-1}
2.87×10^{-2}	9.98×10^{-1}	35	2.95×10^{-1}
2.87×10^{-2}	1.38	48	4.29×10^{-1}
2.87×10^{-2}	2.08	73	6.53×10^{-1}
2.87×10^{-2}	2.34	82	7.16×10^{-1}



$$k_2 = 3.27 \times 10^{-1} \text{ M}^{-1} \text{ s}^{-1}$$

Rate constants for the reaction of **1c** with morpholine **5d** (conventional UV-Vis spectroscopy, 20 °C, $\lambda = 405$ nm) in CH₃CN.

[1c] ₀ / M	[5d] ₀ / M	[5d] ₀ ⁻¹ / M ⁻¹	[5d] ₀ / [1c] ₀	$k_{\text{obs}} / \text{s}^{-1}$	[5d] ₀ × k_{obs} ⁻¹ / MS
2.71×10^{-2}	1.38×10^{-1}	7.25	5	6.59×10^{-4}	2.09×10^2
2.98×10^{-2}	2.06×10^{-1}	4.85	7	1.21×10^{-3}	1.70×10^2
2.95×10^{-2}	2.72×10^{-1}	3.68	9	1.90×10^{-3}	1.43×10^2
2.87×10^{-2}	3.31×10^{-1}	3.02	12	2.70×10^{-3}	1.23×10^2
2.90×10^{-2}	4.68×10^{-1}	2.14	16	4.39×10^{-3}	1.07×10^2

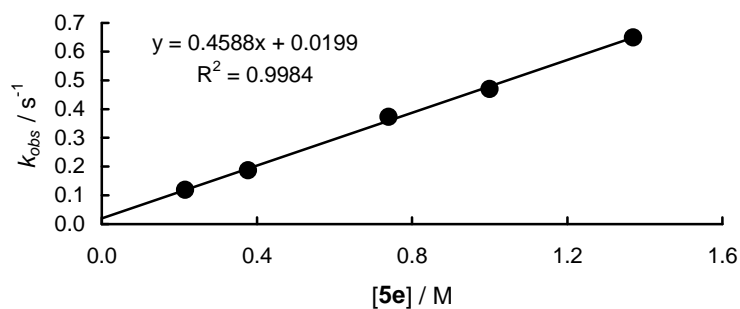


$$k_2 = 1.86 \times 10^{-2} \text{ M}^{-1} \text{ s}^{-1}$$

k_2 determined by plot of $[\mathbf{5d}]/k_{\text{obs}}$ vs. $1/[\mathbf{5d}]$

Rate constants for the reaction of **1c** with piperidine **5e** (stopped-flow method, 20 °C, $\lambda = 405 \text{ nm}$) in CH_3CN .

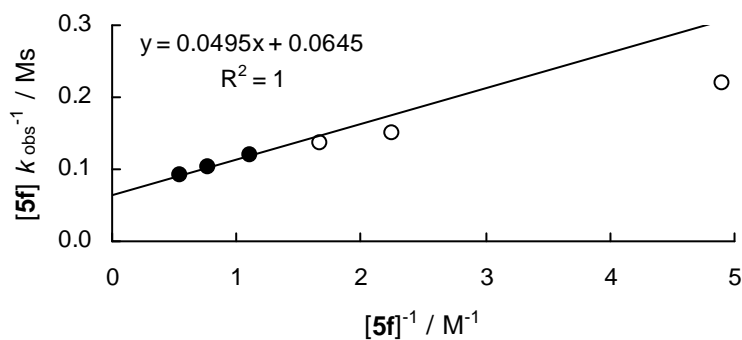
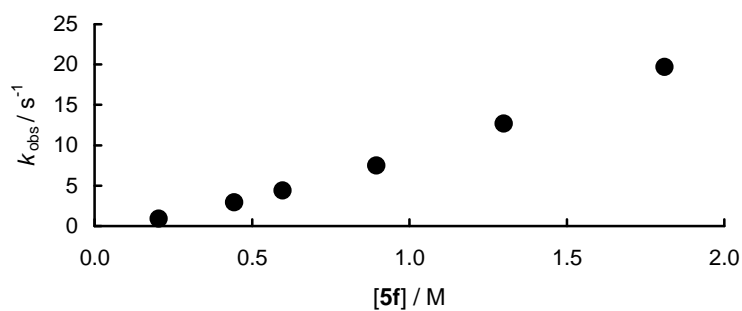
$[\mathbf{1c}]_0 / \text{M}$	$[\mathbf{5e}]_0 / \text{M}$	$[\mathbf{5e}]_0 / [\mathbf{1c}]_0$	$k_{\text{obs}} / \text{s}^{-1}$
3.12×10^{-2}	2.15×10^{-1}	7	1.19×10^{-1}
3.12×10^{-2}	3.77×10^{-1}	12	1.87×10^{-1}
3.12×10^{-2}	7.84×10^{-1}	24	3.73×10^{-1}
3.12×10^{-2}	1.00	32	4.70×10^{-1}
3.12×10^{-2}	1.37	44	6.49×10^{-1}



$$k_2 = 4.59 \times 10^{-1} \text{ M}^{-1} \text{ s}^{-1}$$

Rate constants for the reaction of **1c** with pyrrolidine **5f** (stopped-flow method, 20 °C, $\lambda = 405$ nm) in CH₃CN.

$[\mathbf{1c}]_0 / \text{M}$	$[\mathbf{5f}]_0 / \text{M}$	$[\mathbf{5f}]_0^{-1} / \text{M}^{-1}$	$[\mathbf{5f}]_0 / [\mathbf{1c}]_0$	$k_{\text{obs}} / \text{s}^{-1}$	$[\mathbf{5f}]_0 \times k_{\text{obs}}^{-1} / \text{Ms}$
3.12×10^{-2}	2.04×10^{-1}	4.90	7	9.30×10^{-1}	2.19×10^{-1}
3.12×10^{-2}	4.43×10^{-1}	2.26	14	2.95	1.50×10^{-1}
3.12×10^{-2}	5.97×10^{-1}	1.68	19	4.39	1.36×10^{-1}
3.12×10^{-2}	8.95×10^{-1}	1.12	29	7.47	1.20×10^{-1}
3.12×10^{-2}	1.30	7.69×10^{-1}	42	1.27×10^1	1.02×10^{-1}
3.12×10^{-2}	1.81	5.52×10^{-1}	58	1.97×10^1	9.19×10^{-2}



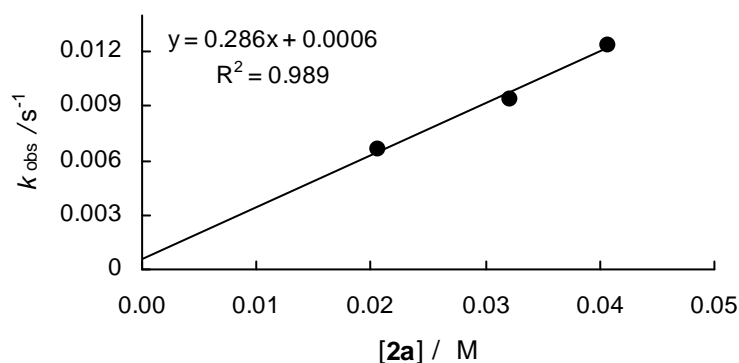
$$k_2 = 1.55 \times 10^1 \text{M}^{-1} \text{s}^{-1}$$

k_2 determined by plot of $[\mathbf{5f}]/k_{\text{obs}}$ vs. $1/[\mathbf{5f}]$

Kinetics of the reactions of di-*t*-butyl azodicarboxylate (1d) with nucleophilesRate constants for the reactions of di-*t*-butyl azodicarboxylate (1d) with enamines 2Reactions in CH₃CN

Rate constants for the reaction of **1d** with morpholinocyclohexene **2a** (conventional UV-Vis spectroscopy, 20 °C, $\lambda = 405$ nm) in CH₃CN.

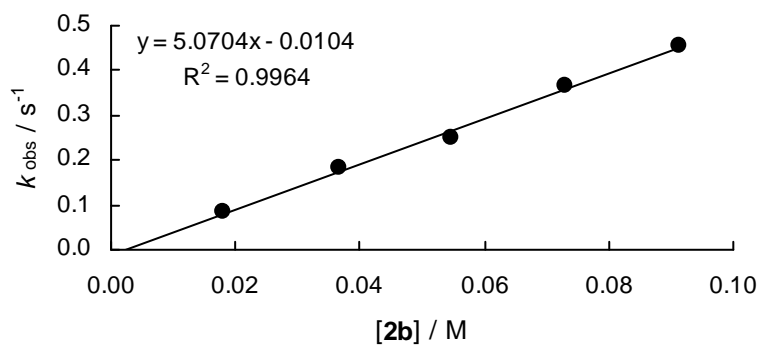
[1d] ₀ / M	[2a] ₀ / M	[2a] ₀ / [1d] ₀	$k_{\text{obs}} / \text{s}^{-1}$
1.93×10^{-3}	2.06×10^{-2}	11	6.60×10^{-3}
1.90×10^{-3}	3.21×10^{-2}	17	9.39×10^{-3}
1.96×10^{-3}	4.07×10^{-2}	21	1.24×10^{-2}



$$k_2 = 2.86 \times 10^{-1} \text{ M}^{-1} \text{ s}^{-1}$$

Rate constants for the reaction of **1d** with piperidinocyclohexene **2b** (stopped-flow method, 20 °C, $\lambda = 405$ nm) in CH₃CN.

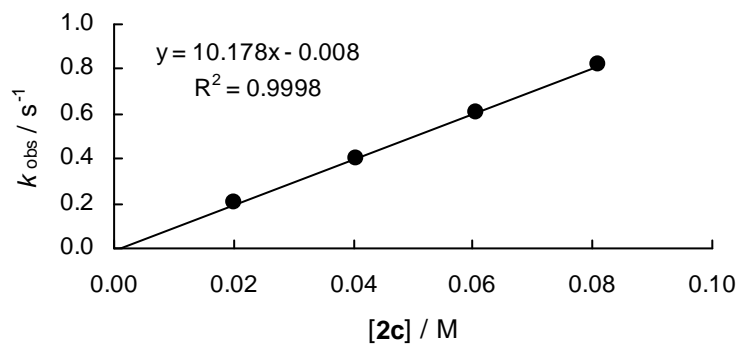
[1d] ₀ / M	[2b] ₀ / M	[2b] ₀ / [1d] ₀	$k_{\text{obs}} / \text{s}^{-1}$
2.08×10^{-3}	1.80×10^{-2}	9	8.28×10^{-2}
2.08×10^{-3}	3.66×10^{-2}	18	1.81×10^{-1}
2.08×10^{-3}	5.48×10^{-2}	26	2.52×10^{-1}
2.08×10^{-3}	7.31×10^{-2}	35	3.66×10^{-1}
2.08×10^{-3}	9.14×10^{-2}	44	4.55×10^{-1}



$$k_2 = 5.07 \text{ M}^{-1} \text{ s}^{-1}$$

Rate constants for the reaction of **1d** with morpholinocyclopentene **2c** (stopped-flow method, 20 °C, $\lambda = 405 \text{ nm}$) in CH_3CN .

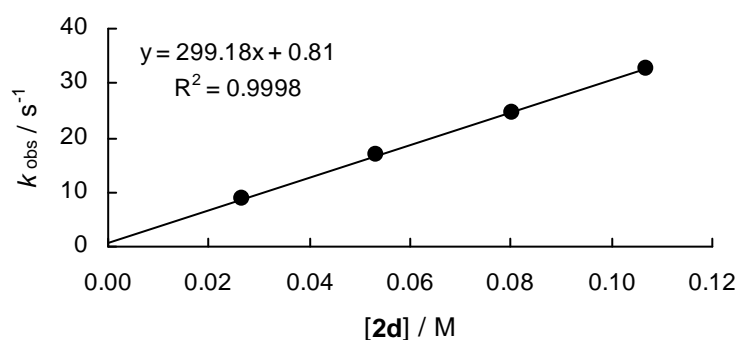
$[\mathbf{1d}]_0 / \text{M}$	$[\mathbf{2c}]_0 / \text{M}$	$[\mathbf{2c}]_0 / [\mathbf{1d}]_0$	$k_{\text{obs}} / \text{s}^{-1}$
2.11×10^{-3}	2.02×10^{-2}	10	2.01×10^{-1}
2.11×10^{-3}	4.04×10^{-2}	19	3.99×10^{-1}
2.11×10^{-3}	6.07×10^{-2}	29	6.08×10^{-1}
2.11×10^{-3}	8.09×10^{-2}	38	8.18×10^{-1}



$$k_2 = 1.02 \times 10^1 \text{ M}^{-1} \text{ s}^{-1}$$

Rate constants for the reaction of **1d** with pyrrolidinocyclohexene **2d** (stopped-flow method, 20 °C, $\lambda = 405$ nm) in CH₃CN.

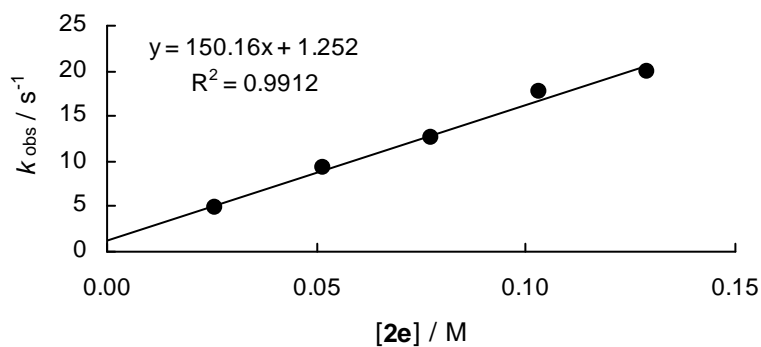
$[\mathbf{1d}]_0 / \text{M}$	$[\mathbf{2d}]_0 / \text{M}$	$[\mathbf{2d}]_0 / [\mathbf{1d}]_0$	$k_{\text{obs}} / \text{s}^{-1}$
1.95×10^{-3}	2.67×10^{-2}	14	8.68
1.95×10^{-3}	5.34×10^{-2}	27	1.70×10^1
1.95×10^{-3}	8.01×10^{-2}	41	2.47×10^1
1.95×10^{-3}	1.07×10^{-1}	55	3.28×10^1



$$k_2 = 2.99 \times 10^2 \text{ M}^{-1} \text{ s}^{-1}$$

Rate constants for the reaction of **1d** with piperidinocyclopentene **2e** (stopped-flow method, 20 °C, $\lambda = 405$ nm) in CH₃CN.

$[\mathbf{1d}]_0 / \text{M}$	$[\mathbf{2e}]_0 / \text{M}$	$[\mathbf{2e}]_0 / [\mathbf{1d}]_0$	$k_{\text{obs}} / \text{s}^{-1}$
1.95×10^{-3}	2.58×10^{-2}	13	4.79
1.95×10^{-3}	5.16×10^{-2}	27	9.28
1.95×10^{-3}	7.74×10^{-2}	40	1.27×10^1
1.95×10^{-3}	1.03×10^{-1}	53	1.76×10^1
1.95×10^{-3}	1.29×10^{-1}	66	2.00×10^1

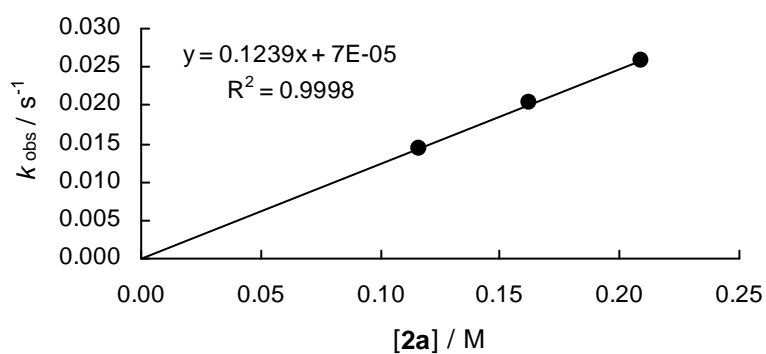


$$k_2 = 1.50 \times 10^2 \text{ M}^{-1} \text{ s}^{-1}$$

Reactions in CH_2Cl_2

Rate constants for the reaction of **1d** with morpholinocyclohexene **2a** (stopped-flow method, 20 °C, $\lambda = 405 \text{ nm}$) in CH_2Cl_2 .

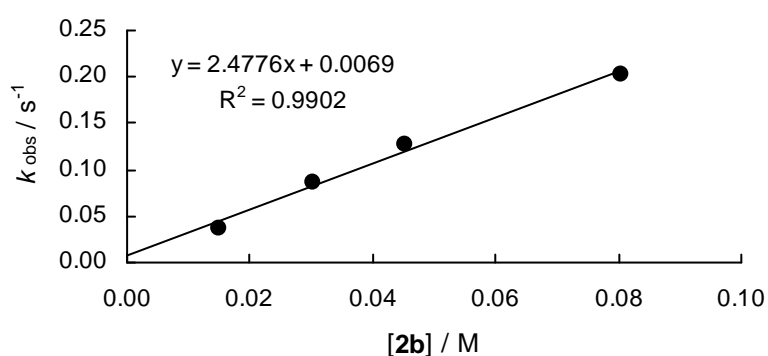
$[\mathbf{1d}]_0 / \text{M}$	$[\mathbf{2a}]_0 / \text{M}$	$[\mathbf{2a}]_0 / [\mathbf{1d}]_0$	$k_{\text{obs}} / \text{s}^{-1}$
2.05×10^{-3}	1.16×10^{-1}	56	1.44×10^{-2}
2.05×10^{-3}	1.62×10^{-1}	79	2.03×10^{-2}
2.05×10^{-3}	2.09×10^{-1}	102	2.59×10^{-2}



$$k_2 = 1.24 \times 10^1 \text{ M}^{-1} \text{ s}^{-1}$$

Rate constants for the reaction of **1d** with piperidinocyclohexene **2b** (stopped-flow method, 20 °C, $\lambda = 405$ nm) in CH_2Cl_2 .

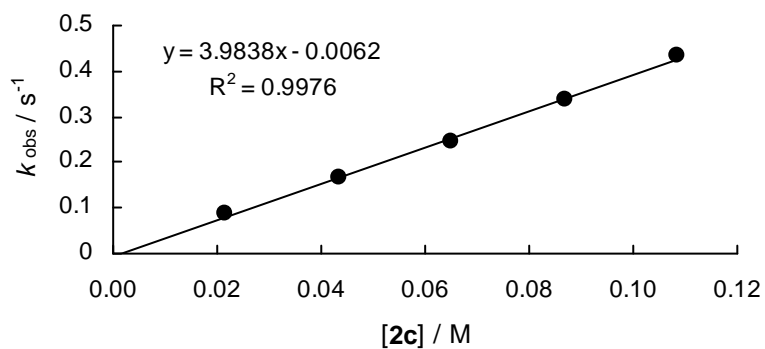
$[\mathbf{1d}]_0 / \text{M}$	$[\mathbf{2b}]_0 / \text{M}$	$[\mathbf{2b}]_0 / [\mathbf{1d}]_0$	$k_{\text{obs}} / \text{s}^{-1}$
2.05×10^{-3}	1.51×10^{-2}	7	3.73×10^{-2}
2.05×10^{-3}	3.02×10^{-2}	15	8.53×10^{-2}
2.05×10^{-3}	4.53×10^{-2}	22	1.27×10^{-1}
2.05×10^{-3}	8.06×10^{-2}	39	2.02×10^{-1}



$$k_2 = 2.48 \text{ M}^{-1} \text{ s}^{-1}$$

Rate constants for the reaction of **1d** with morpholinocyclopentene **2c** (stopped-flow method, 20 °C, $\lambda = 405$ nm) in CH_2Cl_2 .

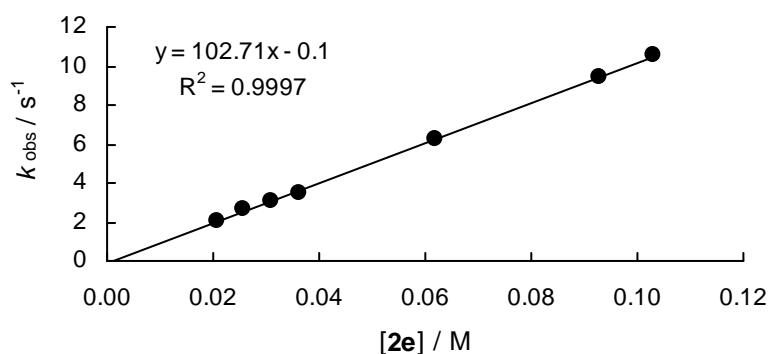
$[\mathbf{1d}]_0 / \text{M}$	$[\mathbf{2c}]_0 / \text{M}$	$[\mathbf{2c}]_0 / [\mathbf{1d}]_0$	$k_{\text{obs}} / \text{s}^{-1}$
2.18×10^{-3}	2.17×10^{-2}	10	8.63×10^{-2}
2.18×10^{-3}	4.35×10^{-2}	20	1.66×10^{-1}
2.18×10^{-3}	6.52×10^{-2}	30	2.45×10^{-1}
2.18×10^{-3}	8.69×10^{-2}	40	3.36×10^{-1}
2.18×10^{-3}	1.09×10^{-1}	50	4.34×10^{-1}



$$k_2 = 3.98 \text{ M}^{-1} \text{ s}^{-1}$$

Rate constants for the reaction of **1d** with piperidinocyclopentene **2e** (stopped-flow method, 20 °C, $\lambda = 405 \text{ nm}$) in CH_2Cl_2 .

$[\mathbf{1d}]_0 / \text{M}$	$[\mathbf{2e}]_0 / \text{M}$	$[\mathbf{2e}]_0 / [\mathbf{1d}]_0$	$k_{\text{obs}} / \text{s}^{-1}$
2.18×10^{-3}	2.06×10^{-2}	9	2.07
2.18×10^{-3}	2.58×10^{-2}	12	2.64
2.18×10^{-3}	3.10×10^{-2}	14	3.03
2.18×10^{-3}	3.61×10^{-2}	17	3.52
2.18×10^{-3}	6.19×10^{-2}	28	6.22
2.18×10^{-3}	9.29×10^{-2}	43	9.46
2.18×10^{-3}	1.03×10^{-1}	47	1.05×10^1

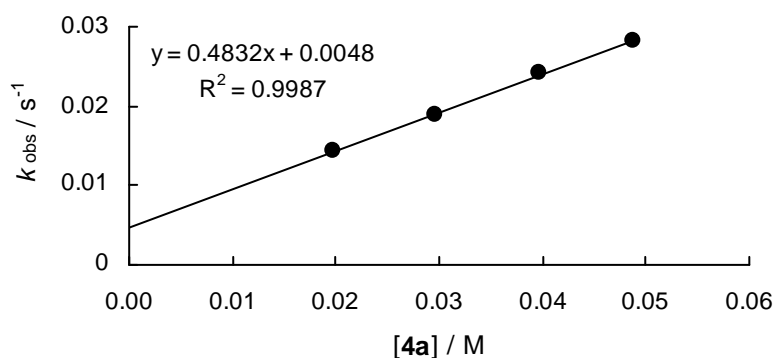


$$k_2 = 1.03 \times 10^2 \text{ M}^{-1} \text{ s}^{-1}$$

Rate constants for the reactions of di-*t*-butyl azodicarboxylate (**1d**) with phosphines **4** in CH₂Cl₂

Rate constants for the reaction of **1d** with tris(4-chlorophenyl)phosphine **4a** (stopped-flow method, 20 °C, $\lambda = 405$ nm) in CH₂Cl₂.

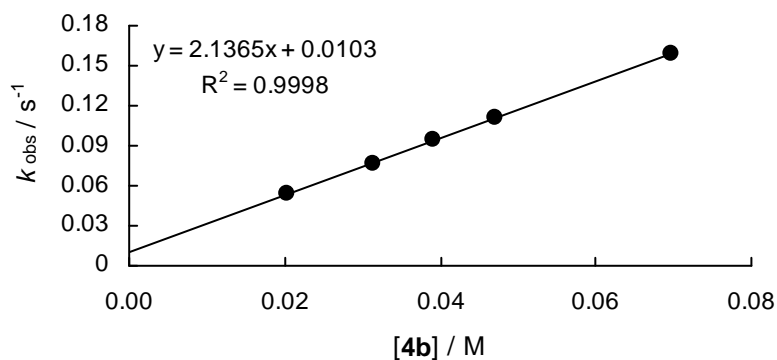
[1d] ₀ / M	[4a] ₀ / M	[4a] ₀ / [1d] ₀	$k_{\text{obs}} / \text{s}^{-1}$
1.92×10^{-3}	1.98×10^{-2}	10	1.44×10^{-2}
1.92×10^{-3}	2.97×10^{-2}	15	1.90×10^{-2}
1.92×10^{-3}	3.97×10^{-2}	21	2.43×10^{-2}
1.92×10^{-3}	4.87×10^{-2}	25	2.82×10^{-2}



$$k_2 = 4.83 \times 10^{-1} \text{ M}^{-1} \text{ s}^{-1}$$

Rate constants for the reaction of **1d** with triphenylphosphine **4b** (stopped-flow method, 20 °C, $\lambda = 405$ nm) in CH₂Cl₂.

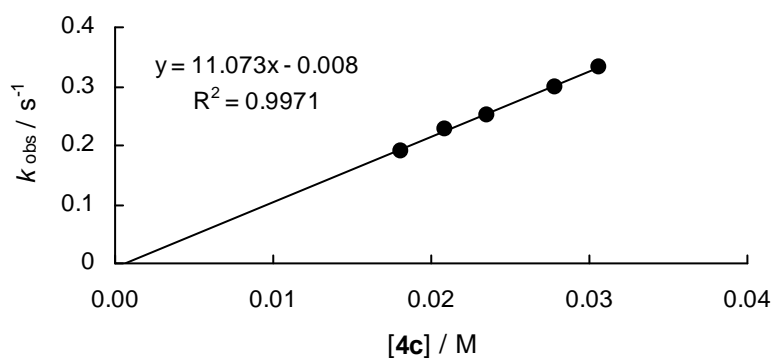
[1d] ₀ / M	[4b] ₀ / M	[4b] ₀ / [1d] ₀	$k_{\text{obs}} / \text{s}^{-1}$
2.13×10^{-3}	2.04×10^{-2}	10	5.37×10^{-2}
2.13×10^{-3}	3.14×10^{-2}	15	7.70×10^{-2}
2.13×10^{-3}	3.92×10^{-2}	18	9.50×10^{-2}
2.13×10^{-3}	4.71×10^{-2}	22	1.11×10^{-1}
2.13×10^{-3}	6.97×10^{-2}	33	1.59×10^{-1}
2.13×10^{-3}	9.37×10^{-2}	44	2.15×10^{-1}



$$k_2 = 2.14 \text{ M}^{-1} \text{ s}^{-1}$$

Rate constants for the reaction of **1d** with tris(4-methylphenyl)phosphine **4c** (stopped-flow method, 20 °C, $\lambda = 405 \text{ nm}$) in CH_2Cl_2 .

$[\mathbf{1d}]_0 / \text{M}$	$[\mathbf{4c}]_0 / \text{M}$	$[\mathbf{4c}]_0 / [\mathbf{1d}]_0$	$k_{\text{obs}} / \text{s}^{-1}$
1.92×10^{-3}	1.81×10^{-2}	9	1.91×10^{-1}
1.92×10^{-3}	2.09×10^{-2}	11	2.28×10^{-1}
1.92×10^{-3}	2.36×10^{-2}	12	2.50×10^{-1}
1.92×10^{-3}	2.78×10^{-2}	14	2.99×10^{-1}
1.92×10^{-3}	3.06×10^{-2}	16	3.32×10^{-1}

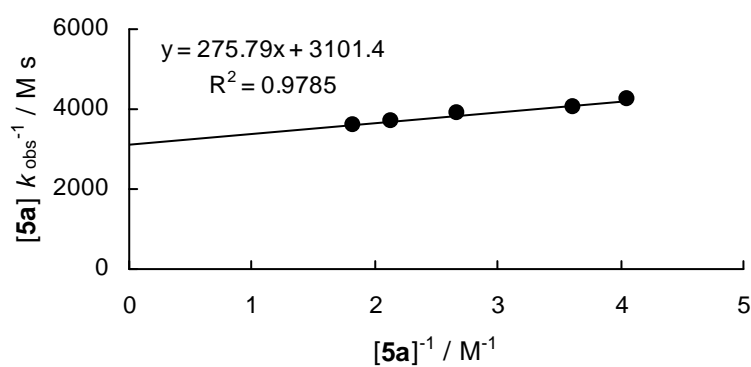
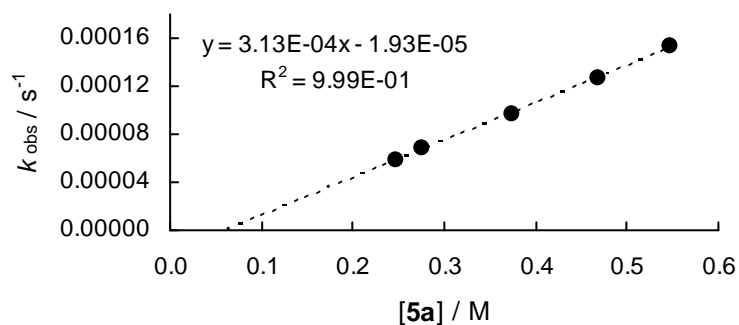


$$k_2 = 1.11 \times 10^1 \text{ M}^{-1} \text{ s}^{-1}$$

Rate constants for the reactions of di-*t*-butyl azodicarboxylate (**1d**) with amines **5** in CH₃CN

Rate constants for the reaction of **1d** with bis(2-methoxyethyl)amine **5a** (conventional UV-Vis spectroscopy, 20 °C, $\lambda = 405$ nm) in CH₃CN.

$[\mathbf{1d}]_0 / \text{M}$	$[\mathbf{5a}]_0 / \text{M}$	$[\mathbf{5a}]_0^{-1} / \text{M}^{-1}$	$[\mathbf{5a}]_0 / [\mathbf{1d}]_0$	$k_{\text{obs}} / \text{s}^{-1}$	$[\mathbf{5a}]_0 \times k_{\text{obs}}^{-1} / \text{Ms}$
2.60×10^{-2}	2.47×10^{-1}	4.05	10	5.84×10^{-5}	4.23×10^3
2.58×10^{-2}	2.76×10^{-1}	3.62	11	6.80×10^{-5}	4.06×10^3
2.49×10^{-2}	3.74×10^{-1}	2.67	15	9.60×10^{-5}	3.90×10^3
2.43×10^{-2}	4.69×10^{-1}	2.13	19	1.27×10^{-4}	3.96×10^3
2.43×10^{-2}	5.47×10^{-1}	1.83	23	1.53×10^{-4}	3.58×10^3

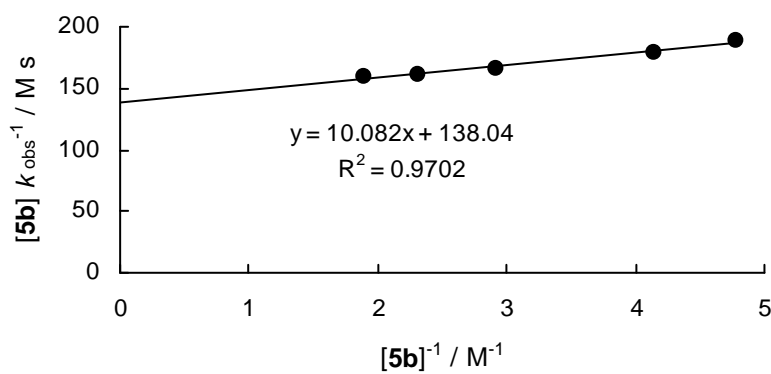
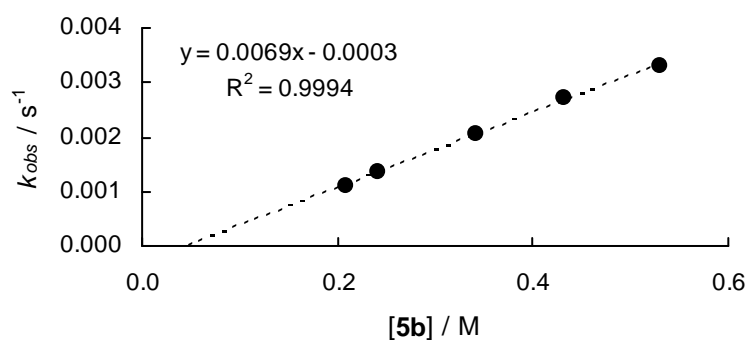


$$k_2 = 3.22 \times 10^{-4} \text{ M}^{-1} \text{ s}^{-1}$$

k_2 determined by plot of $[\mathbf{5a}]/k_{\text{obs}}$ vs. $1/[\mathbf{5a}]$

Rate constants for the reaction of **1d** with di-*n*-propylamine **5b** (conventional UV-Vis spectroscopy, 20 °C, $\lambda = 405$ nm) in CH₃CN.

$[\mathbf{1d}]_0 / \text{M}$	$[\mathbf{5b}]_0 / \text{M}$	$[\mathbf{5b}]_0^{-1} / \text{M}^{-1}$	$[\mathbf{5b}]_0 / [\mathbf{1d}]_0$	$k_{\text{obs}} / \text{s}^{-1}$	$[\mathbf{5b}]_0 \times k_{\text{obs}}^{-1} / \text{Ms}$
2.48×10^{-2}	2.09×10^{-1}	4.78	8	1.11×10^{-3}	1.88×10^2
2.46×10^{-2}	2.41×10^{-1}	4.15	10	1.35×10^{-3}	1.79×10^2
2.44×10^{-2}	3.42×10^{-1}	2.92	14	2.07×10^{-3}	1.65×10^2
2.38×10^{-2}	4.33×10^{-1}	2.31	18	2.70×10^{-3}	1.60×10^2
2.37×10^{-2}	5.30×10^{-1}	1.89	22	3.32×10^{-3}	1.60×10^2

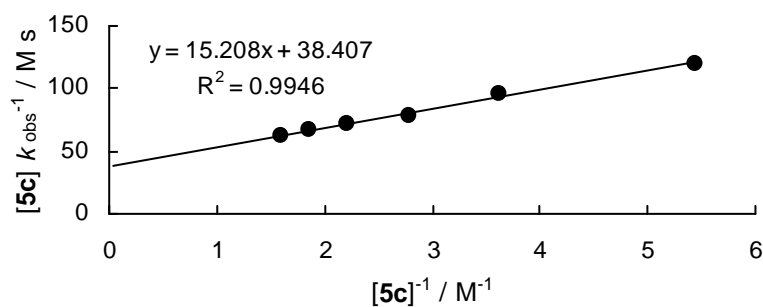
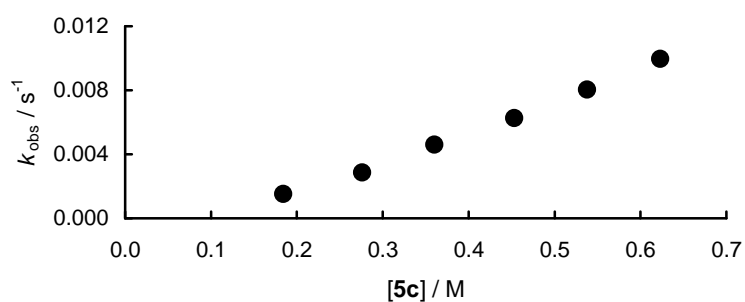


$$k_2 = 7.24 \times 10^{-3} \text{ M}^{-1} \text{ s}^{-1}$$

k_2 determined by plot of $[\mathbf{5b}]/k_{\text{obs}}$ vs. $1/[\mathbf{5b}]$

Rate constants for the reaction of **1d** with diethylamine **5c** (conventional UV-Vis spectroscopy, 20 °C, $\lambda = 405$ nm) in CH_3CN .

$[\mathbf{1d}]_0 / \text{M}$	$[\mathbf{5c}]_0 / \text{M}$	$[\mathbf{5c}]_0^{-1} / \text{M}^{-1}$	$[\mathbf{5c}]_0 / [\mathbf{1d}]_0$	$k_{\text{obs}} / \text{s}^{-1}$	$[\mathbf{5c}]_0 \times k_{\text{obs}}^{-1} / \text{Ms}$
2.32×10^{-2}	1.84×10^{-1}	5.43	8	1.53×10^{-3}	1.20×10^2
2.34×10^{-2}	2.76×10^{-1}	3.62	12	2.87×10^{-3}	9.62×10^1
2.28×10^{-2}	3.60×10^{-1}	2.78	16	4.59×10^{-3}	7.84×10^1
2.30×10^{-2}	4.53×10^{-1}	2.21	20	6.26×10^{-3}	7.24×10^1
2.27×10^{-2}	5.38×10^{-1}	1.86	24	8.04×10^{-3}	6.69×10^1
2.25×10^{-2}	6.23×10^{-1}	1.61	28	9.96×10^{-3}	6.26×10^1

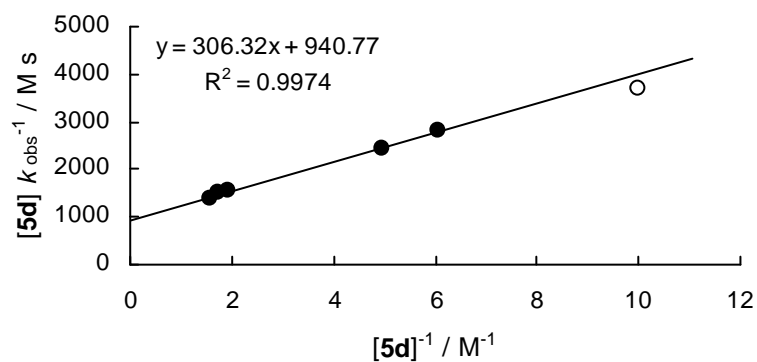
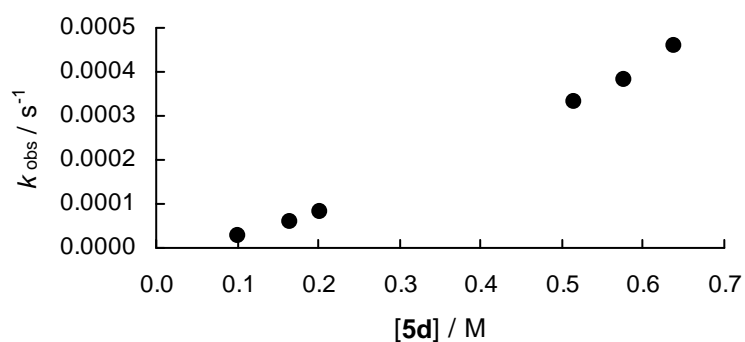


$$k_2 = 2.60 \times 10^{-2} \text{ M}^{-1} \text{ s}^{-1}$$

k_2 determined by plot of $[\mathbf{5c}]/k_{\text{obs}}$ vs. $1/[\mathbf{5c}]$

Rate constants for the reaction of **1d** with morpholine **5d** (conventional UV-Vis spectroscopy, 20 °C, $\lambda = 405$ nm) in CH₃CN.

$[\mathbf{1d}]_0 / \text{M}$	$[\mathbf{5d}]_0 / \text{M}$	$[\mathbf{5d}]_0^{-1} / \text{M}^{-1}$	$[\mathbf{5d}]_0 / [\mathbf{1d}]_0$	$k_{\text{obs}} / \text{s}^{-1}$	$[\mathbf{5d}]_0 \times k_{\text{obs}}^{-1} / \text{Ms}$
2.56×10^{-2}	1.00×10^{-1}	1.00×10^1	4	2.71×10^{-5}	3.69×10^3
2.25×10^{-2}	1.65×10^{-1}	6.06	7	5.84×10^{-5}	2.83×10^3
2.56×10^{-2}	2.01×10^{-1}	4.98	8	8.29×10^{-5}	2.42×10^3
2.47×10^{-2}	5.15×10^{-1}	1.94	21	3.32×10^{-4}	1.55×10^3
2.19×10^{-2}	5.76×10^{-1}	1.74	26	3.84×10^{-4}	1.50×10^3
2.44×10^{-2}	6.39×10^{-1}	1.56	26	4.60×10^{-4}	1.39×10^3

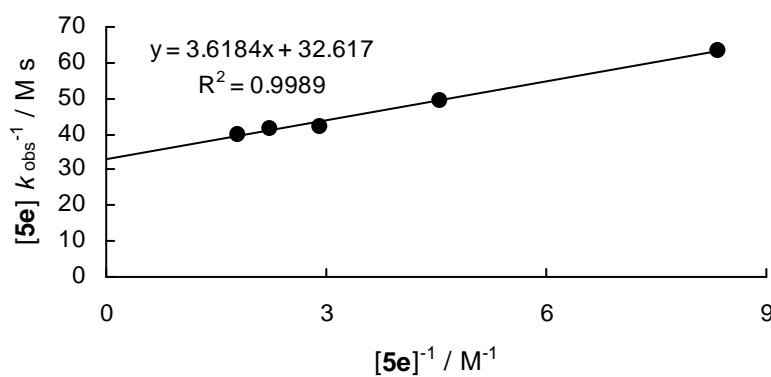
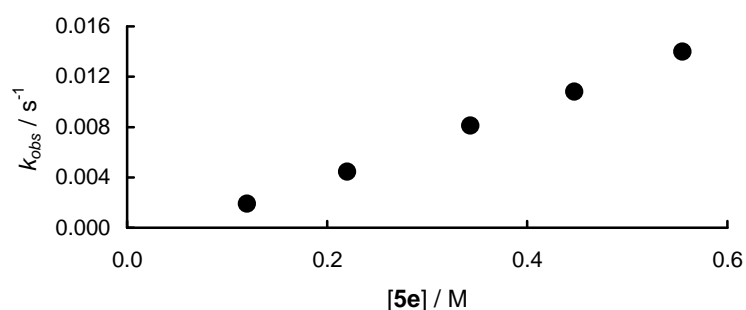


$$k_2 = 1.06 \times 10^{-3} \text{ M}^{-1} \text{ s}^{-1}$$

k_2 determined by plot of $[\mathbf{5d}]/k_{\text{obs}}$ vs. $1/[\mathbf{5d}]$

Rate constants for the reaction of **1d** with piperidine **5e** (conventional UV-Vis spectroscopy, 20 °C, $\lambda = 405$ nm) in CH₃CN.

$[\mathbf{1d}]_0 / \text{M}$	$[\mathbf{5e}]_0 / \text{M}$	$[\mathbf{5e}]_0^{-1} / \text{M}^{-1}$	$[\mathbf{5e}]_0 / [\mathbf{1d}]_0$	$k_{\text{obs}} / \text{s}^{-1}$	$[\mathbf{5e}]_0 \times k_{\text{obs}}^{-1} / \text{Ms}$
2.12×10^{-2}	1.20×10^{-1}	8.33	6	1.90×10^{-3}	6.32×10^1
2.32×10^{-2}	2.20×10^{-1}	4.55	9	4.44×10^{-3}	4.95×10^1
2.41×10^{-2}	3.43×10^{-1}	2.92	14	8.12×10^{-3}	4.22×10^1
2.36×10^{-2}	4.47×10^{-1}	2.24	19	1.08×10^{-2}	4.14×10^1
2.34×10^{-2}	5.55×10^{-1}	1.80	24	1.40×10^{-2}	3.97×10^1

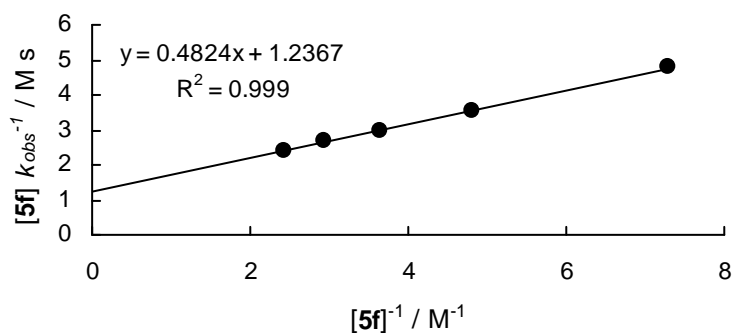
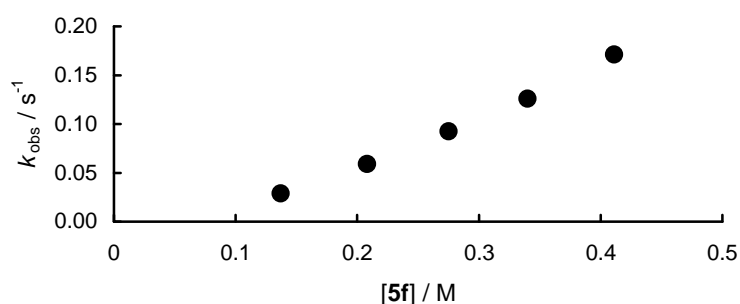


$$k_2 = 3.07 \times 10^{-2} \text{ M}^{-1} \text{ s}^{-1}$$

k_2 determined by plot of $[\mathbf{5e}]/k_{\text{obs}}$ vs. $1/[\mathbf{5e}]$

Rate constants for the reaction of **1d** with pyrrolidine **5f** (conventional UV-Vis spectroscopy, 20 °C, $\lambda = 405$ nm) in CH₃CN.

$[\mathbf{1d}]_0 / \text{M}$	$[\mathbf{5f}]_0 / \text{M}$	$[\mathbf{5f}]_0^{-1} / \text{M}^{-1}$	$[\mathbf{5f}]_0 / [\mathbf{1d}]_0$	$k_{\text{obs}} / \text{s}^{-1}$	$[\mathbf{5f}]_0 \times k_{\text{obs}}^{-1} / \text{Ms}$
2.47×10^{-2}	1.37×10^{-1}	7.30	6	2.87×10^{-2}	4.77
2.50×10^{-2}	2.08×10^{-1}	4.81	8	5.90×10^{-2}	3.52
2.48×10^{-2}	2.75×10^{-1}	3.64	11	9.26×10^{-2}	2.97
2.52×10^{-2}	3.40×10^{-1}	2.94	13	1.26×10^{-1}	2.70
2.47×10^{-2}	4.11×10^{-1}	2.43	17	1.71×10^{-1}	2.40



$$k_2 = 8.09 \times 10^{-1} \text{ M}^{-1} \text{ s}^{-1}$$

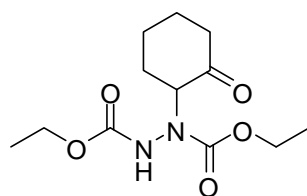
k_2 determined by plot of $[\mathbf{5f}]/k_{\text{obs}}$ vs. $1/[\mathbf{5f}]$

4.4.3 Synthetic Experiments

Syntheses of α -substituted carbonyl compounds **3**

General procedure for the syntheses of compounds **3**:

The azodicarboxylate **1** (1 equivalent) dissolved in acetonitrile was added dropwise to a stirred solution of the enamine **2** in dry acetonitrile. The reaction mixture was stirred until the yellow color of the azodicarboxylate had disappeared. The reaction mixture was quenched with water and the organic layer was dried over MgSO_4 . The solvent was removed in vacuo. The crude products were purified by column chromatography (pentane/ethyl acetate).

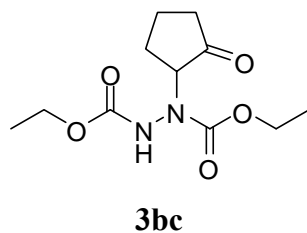


3bd

N,N'-Bis(ethoxycarbonyl)-2-hydrazino-cyclohexanone **3bd**^[2a,9a,9d,9e,9g,9h,9i] was synthesized from 202 mg (1.16 mmol) diethyl azodicarboxylate (**1b**) and 176 mg (1.16 mmol) pyrrolidinocyclohexene (**2d**) (white solid, yield 46 %, 144 mg, 0.529 mmol).

^1H NMR (CDCl_3 , 300 MHz): δ = 1.23 (t, 3J = 6.1 Hz, 6 H), 1.54–1.57 (m, 1 H), 1.68–1.80 (m, 2 H), 1.95–2.01 (m, 2 H), 2.28–2.49 (m, 3 H), 4.12–4.18 (m, 4 H), 4.87–4.97 (m, 1H), 6.69 (br s, 1H).

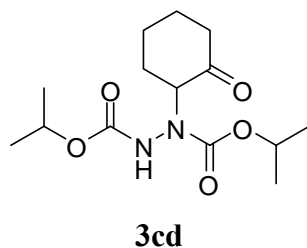
^{13}C NMR (CDCl_3 , 75 MHz): δ = 14.3 (q), 14.4 (q), 24.2 (t), 26.7 (t), 30.6 (t), 41.2 (t), 61.8 (t), 62.7 (t), 65.6 (d), 156.3 (s, 2C), 207.7 (s).



N,N'-Bis(ethoxycarbonyl)-2-hydrazino-cyclopentanone **3bc**^[2a,9a] was synthesized from 255 mg (1.46 mmol) diethyl azodicarboxylate (**1b**) and 224 mg (1.46 mmol) morpholinocyclopentene (**2c**) (white solid, yield 88 %, 327 mg, 1.27 mmol).

¹H NMR (CDCl₃, 300 MHz): δ = 1.25 (t, ³*J* = 7.1 Hz, 6 H), 1.68–2.19 (m, 4 H), 2.28–2.39 (m, 2 H), 4.15–4.21 (m, 4 H), 4.42–4.69 (m, 1H), 6.56 (br s, 1H).

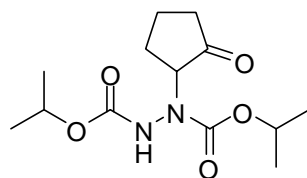
¹³C NMR (CDCl₃, 75 MHz): δ = 14.4 (q, 2C), 18.0 (t), 26.0 (t), 35.3 (t), 62.2 (t), 63.0 (t), 66.3 (d), 155.9 (s), 156.2 (s), 219.9 (s).



N,N'-Bis(isopropoxycarbonyl)-2-hydrazino-cyclohexanone **3cd**^[9e] was synthesized from 163 mg (0.806 mmol) di-isopropyl azodicarboxylate (**1c**) and 122 mg (0.807 mmol) pyrrolidinocyclohexene (**2d**) (white solid, yield 57 %, 137 mg, 0.456 mmol).

¹H NMR (CDCl₃, 600 MHz): δ = 1.22–1.25 (m, 12 H), 1.51–1.60 (m, 1 H), 1.72–1.85 (m, 2 H), 1.96–2.07 (m, 2 H), 2.30–2.47 (m, 3 H), 4.81–4.97 (m, 3 H), 6.58 (br s, 1H).

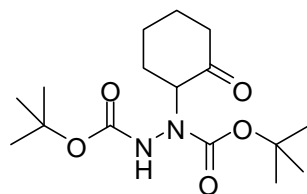
¹³C NMR (CDCl₃, 125 MHz): δ = 21.81 (q), 21.84 (q), 21.9 (q), 22.0 (q), 24.3 (t), 26.7 (t), 30.7 (t), 41.3 (t), 65.3 (d), 69.3 (d), 70.4 (d), 155.9 (s), 156.0 (s), 207.8 (s).

**3cc**

N,N'-Bis(isopropoxycarbonyl)-2-hydrazino-cyclopentanone **3cc** was synthesized from 179 mg (0.885 mmol) di-isopropyl azodicarboxylate (**1c**) and 136 mg (0.888 mmol) morpholinocyclopentene (**2c**) (white solid, yield 77 %, 195 mg, 0.681 mmol).

^1H NMR (CDCl_3 , 600 MHz): δ = 1.24–1.26 (m, 12 H), 1.76–1.84 (m, 1 H), 1.92–2.18 (m, 3 H), 2.26–2.43 (m, 2 H), 4.52–4.69 (m, 1H), 4.93–4.98 (m, 2 H), 6.45 (br s, 1H).

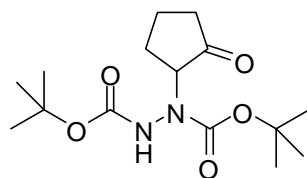
^{13}C NMR (CDCl_3 , 125 MHz): δ = 18.0 (t), 21.9 (q, 2C), 22.0 (q, 2C), 25.9 (t), 35.4 (t), 66.0 (d), 69.8 (d), 70.6 (d), 155.4 (s), 156.0 (s), 214.3 (s).

**3dd**

N,N'-Bis(*t*-butoxycarbonyl)-2-hydrazino-cyclohexanone **3dd**^[9b-f] was synthesized from 121 mg (0.525 mmol) di-*t*-butyl azodicarboxylate (**1d**) and 79 mg (0.52 mmol) pyrrolidinocyclohexene (**2d**) (white solid, yield 50 %, 85 mg, 0.26 mmol).

^1H NMR (CDCl_3 , 300 MHz): δ = 1.45–1.80 (m, 21 H), 1.95–2.09 (m, 2 H), 2.19–2.49 (m, 21 H), 4.82–4.87 (m, 1H), 6.48 (s br, 1H).

^{13}C NMR (CDCl_3 , 75 MHz): δ = 24.4 (t), 26.7 (t), 28.1 (q, 3C), 28.2 (q, 3C), 30.7 (t), 41.4 (t), 64.9 (d), 81.6 (s), 80.6 (s), 155.27 (s), 155.33 (s), 208.0 (s).

**3dc**

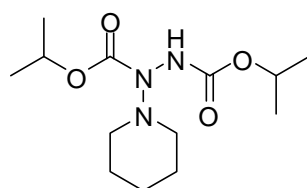
N,N'-Bis(*t*-butoxycarbonyl)-2-hydrazino-cyclopentanone **3dc** was synthesized from 458 mg (1.99 mmol) di-*t*-butyl azodicarboxylate (**1d**) and 304 mg (1.98 mmol) morpholino-cyclopentene (**2c**) (white solid, yield 53 %, 326 mg, 1.04 mmol).

^1H NMR (CDCl_3 , 300 MHz): δ = 1.45 (s, 18 H), 1.66–2.35 (m, 6 H), 4.47–4.67 (m, 1H), 6.35 (br s, 1H).

^{13}C NMR (CDCl_3 , 75 MHz): δ = 18.0 (t), 25.8 (t), 28.1 (q, 6C), 35.4 (t), 65.5 (d), 81.1 (s), 81.7 (s), 154.7 (s), 155.3 (s), 214.5 (s).

Syntheses of triazanes **6**

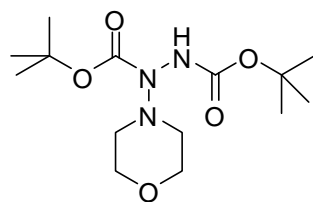
General procedure for the syntheses of compounds **6**: The amines **5** (2 equiv.) were added to solutions of the azodicarboxylates **1** in acetonitrile at 20 °C, and the mixture was stirred until the yellow color of the azodicarboxylates had disappeared. The solvent was evaporated in vacuo.

**6ce**

N,N'-Bis(*i*-propoxycarbonyl)-1-hydrazino-piperidine **6ce**^[20a] was synthesized from 82 mg (0.41 mmol) di-isopropyl azodicarboxylate (**1c**) and 70 mg (0.82 mmol) piperidine (**5e**) (white solid, yield 92 %, 109 mg, 0.379 mmol).

^1H NMR (CD_3CN , 400 MHz): δ = 1.19–1.23 (m, 12 H), 1.27–1.39 (m, 2 H), 1.57–1.63 (m, 4 H), 2.56–2.82 (m, 4 H), 4.77–4.91 (m, 2H), 7.43 (br s, 1H).

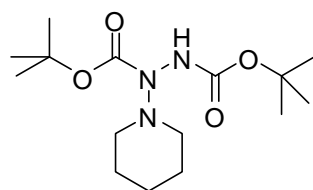
^{13}C NMR (CD_3CN , 100 MHz): 22.2 (q, 4C), 24.0 (t), 26.5 (t, 2 C), 52.8 (t, 2 C), 70.6 (d, 2C), 157.3 (s, 2C).

**6dd**

N,N'-Bis(*t*-butoxycarbonyl)-1-hydrazino-morpholine **6dd** was synthesized from 102 mg (0.443 mmol) di-*t*-butyl azodicarboxylate (**1d**) and 77 mg (0.88 mmol) morpholine (**5d**) (white solid, yield 93 %, 130 mg, 0.410 mmol).

^1H NMR (CD_3CN , 400 MHz): δ = 1.42 (s, 9 H), 1.44 (s, 9 H), 2.57–2.93 (m, 4 H), 3.65 (t, 3J = 4.74 Hz, 4 H), 7.32 (br s, 1H).

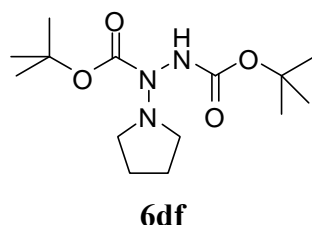
^{13}C NMR (CD_3CN , 100 MHz): 28.30 (q, 3C), 28.33 (q, 3C), 52.1 (t, 2C), 67.3 (t, 2C), 81.6 (s, 2 C), 156.7 (s, 2 C).

**6de**

N,N'-Bis(*t*-butoxycarbonyl)-1-hydrazino-piperidine **6de** was synthesized from 104 mg (0.452 mmol) di-*t*-butyl azodicarboxylate (**1d**) and 77 mg (0.90 mmol) piperidine (**5e**) (white solid, yield 81 %, 115 mg, 0.365 mmol).

^1H NMR (CD_3CN , 400 MHz): δ = 1.25–1.43 (m, 20 H), 1.56–1.61 (m, 4 H), 2.50–2.87 (m, 4 H), 7.27 (br s, 1H).

^{13}C NMR (CD_3CN , 100 MHz): 24.0 (t), 26.5 (t, 2 C), 28.30 (q, 3 C), 28.33 (q, 3 C), 52.8 (t, 2 C), 81.2 (s, 2 C), 156.6 (s, 2C).



N,N'-Bis(*t*-butoxycarbonyl)-1-hydrazino-pyrrolidine **6df** was synthesized from 100 mg (0.434 mmol) di-*t*-butyl azodicarboxylate (**1d**) and 62 mg (0.87 mmol) pyrrolidine (**5f**) (white solid, yield 76 %, 98 mg, 0.33 mmol).

^1H NMR (CD_3CN , 400 MHz): δ = 1.42 (s, 9 H), 1.44 (s, 9 H), 1.69–1.74 (m, 4 H), 2.72–2.80 (m, 4 H), 7.30 (br s, 1H).

^{13}C NMR (CD_3CN , 100 MHz): 22.5 (t, 2C), 28.3 (q, 6C), 49.5 (t, 2C), 81.3 (s, 2C), 156.7 (s, 2 C).

4.5 References

- [1] V. Nair, A. T. Biju, S. C. Mathew, B. P. Babu, *Chem. Asian J.* **2008**, *3*, 810–820.
- [2] a) R. Huisgen, F. Jakob, *Justus Liebigs Ann. Chem.* **1954**, *590*, 37–54; b) E. Erdik, *Tetrahedron* **2004**, *60*, 8747–8782; c) J. M. Janey, *Angew. Chem.* **2005**, *117*, 4364–4372, *Angew. Chem. Int. Ed.* **2005**, *44*, 4292–4300.
- [3] a) G. Desimoni, G. Faita, P. P. Righetti, L. Toma, *Tetrahedron* **1990**, *46*, 7951–7970; b) G. Jenner, R. B. Salem, *J. Chem. Soc. Perkin Trans. 2* **1990**, 1961–1964; c) G. Desimoni, G. Faita, P. P. Righetti, A. Sfulcini, D. Tsyganov, *Tetrahedron* **1994**, *50*, 1821–1832; d) M. R. Gholami, A. Habibi Yangjeh, *J. Phys. Org. Chem.* **2000**, *13*, 468–472; e) A. Chanda, V. V. Fokin, *Chem. Rev.* **2009**, *109*, 725–748.

- [4] a) O. Mitsunobu, M. Eguchi, *Bull. Chem. Soc. Jpn.* **1971**, *44*, 3427–3430; b) V. Nair, R. S. Menon, A. R. Sreekanth, N. Abhilash, A. T. Biju, *Acc. Chem. Res.* **2006**, *39*, 520–530; c) T. Y. S. But, P. H. Toy, *Chem. Asian J.* **2007**, *2*, 1340–1355; d) K. C. K. Swamy, N. N. B. Kumar, E. Balaraman, K. V. P. P. Kumar, *Chem. Rev.* **2009**, *109*, 2551–2651.
- [5] a) B. List, *J. Am. Chem. Soc.* **2002**, *124*, 5656–5657; b) A. Bøgevig, K. Juhl, N. Kumaragurubaran, W. Zhuang, K. A. Jørgensen, *Angew. Chem.* **2002**, *114*, 1868–1871, *Angew. Chem. Int. Ed.* **2002**, *41*, 1790–1793; for reviews: c) A. Berkessel, H. Gröger, *Asymmetric Organocatalysis*, Wiley-VCH, Weinheim, **2005**; d) *Enantioselective Organocatalysis* (Ed.: P. I. Dalko), Wiley-VCH, Weinheim, **2007**; e) S. Mukherjee, J. W. Yang, S. Hoffman, B. List, *Chem. Rev.* **2007**, *107*, 5471–5569.
- [6] H. Mayr, M. Patz, *Angew. Chem.* **1994**, *106*, 990–1010; *Angew. Chem. Int. Ed. Engl.* **1994**, *33*, 938–957.
- [7] a) H. Mayr, T. Bug, M. F. Gotta, N. Hering, B. Irrgang, B. Janker, B. Kempf, R. Loos, A. R. Ofial, G. Remennikov, H. Schimmel, *J. Am. Chem. Soc.* **2001**, *123*, 9500–9512; b) R. Lucius, R. Loos, H. Mayr, *Angew. Chem.* **2002**, *114*, 97–102; *Angew. Chem. Int. Ed.* **2002**, *41*, 91–95; c) H. Mayr, B. Kempf, A. R. Ofial, *Acc. Chem. Res.* **2003**, *36*, 66–77; d) H. Mayr, A. R. Ofial in *Carbocation Chemistry* (Eds.: G. A. Olah, G. K. S. Prakash,), Wiley, Hoboken (NJ), **2004**, Chapt. 13, pp 331–358; e) H. Mayr, A. R. Ofial, *Pure Appl. Chem.* **2005**, *77*, 1807–1821; f) H. Mayr, A. R. Ofial, *J. Phys. Org. Chem.* **2008**, *21*, 584–595; g) D. Richter, N. Hampel, T. Singer, A. R. Ofial, H. Mayr, *Eur. J. Org. Chem.* **2009**, 3203–3211.
- [8] B. Kempf, N. Hampel, A. R. Ofial, H. Mayr, *Chem. Eur. J.* **2003**, *9*, 2209–2218.
- [9] a) R. M. Moriarty, I. Prakash, *Synth. Commun.* **1985**, *15*, 649–655; b) S. Fioravanti, L. Pellacani, P. A. Tardella, *Gazz. Chim. Ital.* **1997**, *127*, 41–44; c) D. Enders, R. Joseph, C. Poiesz, *Tetrahedron* **1998**, *54*, 10069–10078; d) S. Fioravanti, L. Olivieri, L. Pellacani, P. A. Tardella, *J. Chem. Research (S)* **1998**, 338–339; e) N. Kumaragurubaran, K. Juhl, W. Zhuang, A. Bøgevig, K. A. Jørgensen, *J. Am. Chem. Soc.* **2002**, *124*, 6254–6255; f) G. Dessole, L. Bernardi, B. F. Bonini, E. Capitò, M. Fochi, R. P. Herrera, A. Ricci, G. Cahiez, *J. Org. Chem.* **2004**, *69*, 8525–8528; g) P. Kotrusz, S. Alemayehu, Š. Toma, H.-G. Schmalz, A. Adler, *Eur. J. Org. Chem.* **2005**, 4904–4911; h) C. Thomassigny, D. Prim, C. Greck, *Tetrahedron Lett.* **2006**, *47*, 1117–1119; i) Y. Hayashi, S. Aratake, Y. Imai, K. Hibino, Q.-Y. Chen, J. Yamaguchi, T. Uchamaru, *Chem. Asian J.* **2008**, *3*, 225–232.

- [10] H. Mayr, M. Hartnagel, K. Grimm, *Liebigs Ann.* **1997**, 55–69.
- [11] S. Lakhdar, T. Tokuyasu, H. Mayr, *Angew. Chem.* **2008**, *120*, 8851–8854, *Angew. Chem. Int. Ed.* **2008**, *47*, 8723–8726.
- [12] a) T. Lemek, H. Mayr, *J. Org. Chem.* **2003**, *68*, 6880–6886; b) S. T. A. Berger, F. H. Seeliger, F. Hofbauer, H. Mayr, *Org. Biomol. Chem.* **2007**, *5*, 3020–3026; c) O. Kaumanns, H. Mayr, *J. Org. Chem.* **2008**, *73*, 2738–2745.
- [13] T. Kanzian, S. Nicolini, L. De Crescentini, O. A. Attanasi, A. R. Ofial, H. Mayr, *Chem. Eur. J.* **2010**, accepted (DOI: 10.1002/chem.201000828).
- [14] C. Reichardt, *Solvents and Solvent Effects in Organic Chemistry*; Wiley: Weinheim, **2003**.
- [15] B. Kempf, H. Mayr, *Chem. Eur. J.* **2005**, *11*, 917–927.
- [16] T. Kanzian, T. A. Nigst, A. Maier, S. Pichl, H. Mayr, *Eur. J. Org. Chem.* **2009**, 6379–6385.
- [17] a) D. C. Morrison, *J. Org. Chem.* **1958**, *23*, 1072–1074; b) E. Brunn, R. Huisgen, *Angew. Chem.* **1969**, *81*, 534–536; *Angew. Int. Ed. Engl.* **1969**, *8*, 513–515; c) R. D. Guthrie, I. D. Jenkins, *Aust. J. Chem.* **1982**, *35*, 767–774. d) S. Moebis-Sanchez, G. Bouhadir, N. Saffon, L. Maron, D. Bourissou, *Chem. Commun.* **2008**, 3435–3437.
- [18] a) C. D. Ritchie, *Acc. Chem. Res.* **1972**, *5*, 348–354; b) C. D. Ritchie, *Can. J. Chem.* **1986**, *64*, 2239–2250.
- [19] N. Wiberg, A. F. Holleman, E. Wiberg, *Lehrbuch der Anorganischen Chemie*, 102nd Ed., Walter de Gruyter, Berlin, New York, **2007**, p 143.
- [20] a) K.-H. Linke, H. J. Göhausen, *Chem. Ber.* **1971**, *104*, 301–306; b) N. Egger, L. Hoesch, A. S. Dreiding, *Helv. Chim. Acta* **1983**, *66*, 1416–1426.
- [21] a) I.-H. Um, S. Yoon, H.-R. Park, H.-J. Han, *Org. Biomol. Chem.* **2008**, *6*, 1618–1624; b) E. A. Castro, *Pure Appl. Chem.* **2009**, *81*, 685–696.
- [22] I.-H. Um, J.-A. Seok, H.-T. Kim, S.-K. Bae, *J. Org. Chem.* **2003**, *68*, 7742–7746.
- [23] M. J. Pfeiffer, S. B. Hanna, *J. Org. Chem.* **1993**, *58*, 735–740.
- [24] a) W. v. E. Doering, W. R. Roth, R. Breuckmann, L. Figge, H.-W. Lennartz, W.-D. Fessner, H. Prinzbach, *Chem. Ber.* **1988**, *121*, 1–9; b) M. Hartnagel, K. Grimm, H. Mayr, *Liebigs Ann.* **1997**, 71–80; c) H. Mayr, A. R. Ofial, J. Sauer, B. Schmied, *Eur. J. Org. Chem.* **2000**, 2013–2020.
- [25] H. G. O. Becker, *Organikum* (19 Aufl.), Edition dt. Verlag der Wissenschaften, Berlin, **1993**.

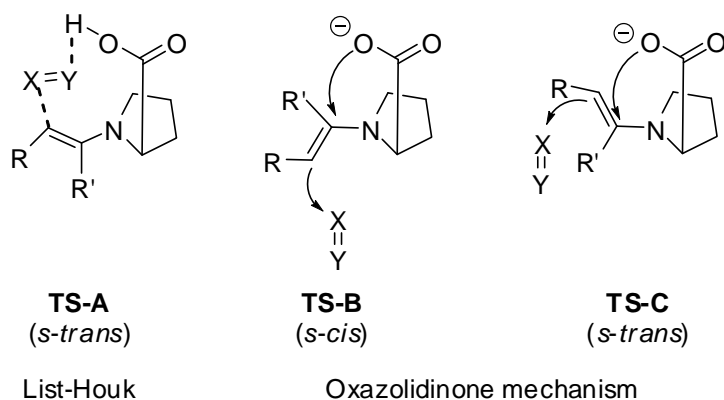
Chapter 5

KINETIC EVIDENCE FOR OXAZOLIDINONE FORMATION IN THE STEREOGENIC STEP OF PROLINE-CATALYZED REACTIONS

Tanja Kanzian, Sami Lakhdar, and Herbert Mayr, *Angew. Chem.* **2010**, accepted:
The results obtained by S. Lakhdar are not listed in the Experimental Section.

5.1 Introduction

The stereoselectivity of proline-catalyzed reactions of aldehydes or ketones with electrophiles^[1] is usually rationalized by activation of the electrophile by the proton of the carboxy group as depicted in the List-Houk transition state (**TS-A**) of Scheme 5.1.^[2]

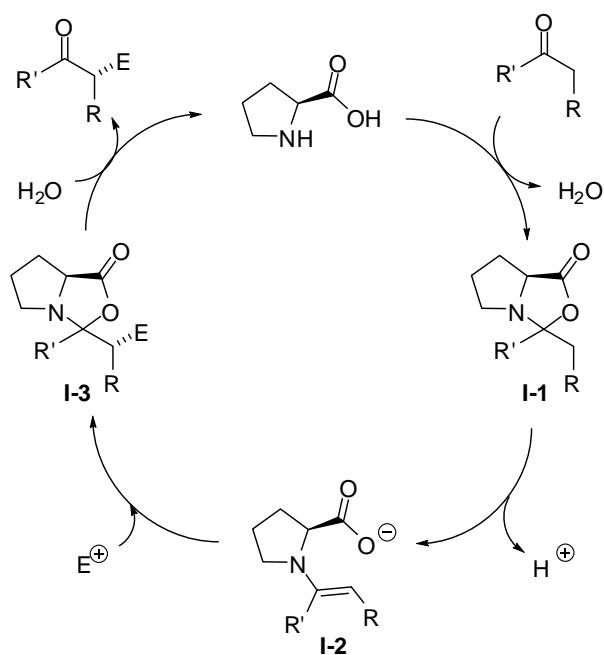


Scheme 5.1. Transition state models of the proline-catalyzed reactions of carbonyl compounds with electrophiles.

Oxazolidinone formation had generally been considered as an unproductive dead end of the reaction cascade^[2g] until Seebach and Eschenmoser suggested that oxazolidinones, rather than being ‘parasitic species’, may also play a decisive role in determining the stereochemical course of proline-catalyzed reactions.^[3] In this mechanism, illustrated in Scheme 5.2, proline and the carbonyl compound combine with formation of the oxazolidinone **I-1**, which

undergoes ring-opening to furnish the *s-cis* and/or *s-trans* conformer of the enaminocarboxylate **I-2**. In order to account for the observed stereoselectivities, it was assumed that **TS-B** (Scheme 5.1), which yields the more stable oxazolidinone, is favored over the stereoelectronically preferred **TS-C**.^[3] Support for the involvement of an enamine carboxylate **I-2** has recently been provided by Blackmond and Armstrong, who reported that the enantioselectivities of proline catalyzed reactions of aliphatic aldehydes with azodicarboxylates are reversed in the presence of tertiary amines.^[4] This reversal was explained by a change from **TS-A** (Scheme 5.1) in the reactions without tertiary amines to **TS-C** in the presence of amines, where the attack of the electrophile occurs at the *s-trans* isomer of the enamine carboxylate. The role of the carboxylate group could not be clarified, however, and it was suggested that CO_2^- either acts as a steric blocking group, or in accordance with Seebach/Eschenmoser, participates in the addition step.^[4]

Traditionally, anchimeric assistance (neighboring group participation) has been derived from stereochemical as well as kinetic investigations in a variety of reactions, e.g., solvolytic displacement reactions, electrophilic additions and eliminations.^[5] Due to the conformational flexibility of the intermediate enamines stereochemical investigations did not provide unequivocal evidence for or against the formation of oxazolidinones in the stereogenic step.^[1e] Therefore, we have now approached this problem with kinetic methods.



Scheme 5.2. Crucial role of oxazolidinones in proline catalyzed reactions according to Seebach and Eschenmoser.^[3]

In order to separate steric and electronic effects, we have studied the kinetics of the reactions of the proline-, pyrrolidine-, and proline methyl ester derived enamines **1⁻**, **2**, and **3** toward the benzhydrylium ions **4a–4f** and the quinone methides **4g–4j** (Table 5.1). As shown previously, their electrophilicities can be fine-tuned by variation of the para- and meta-substituents, while keeping the steric surroundings of the reaction centers constant.^[6] The empirical electrophilicity parameters listed in Table 5.1 show a continuous decrease of reactivity from top to bottom by 8 orders of magnitude.

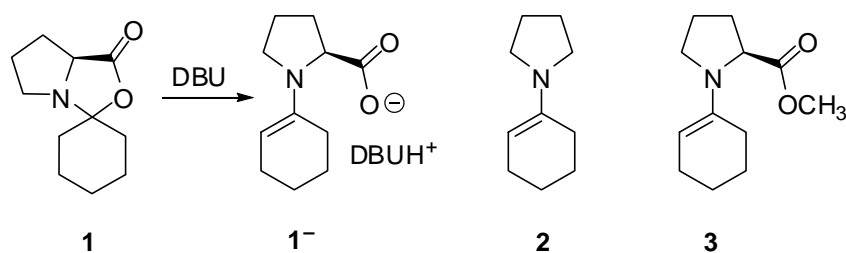


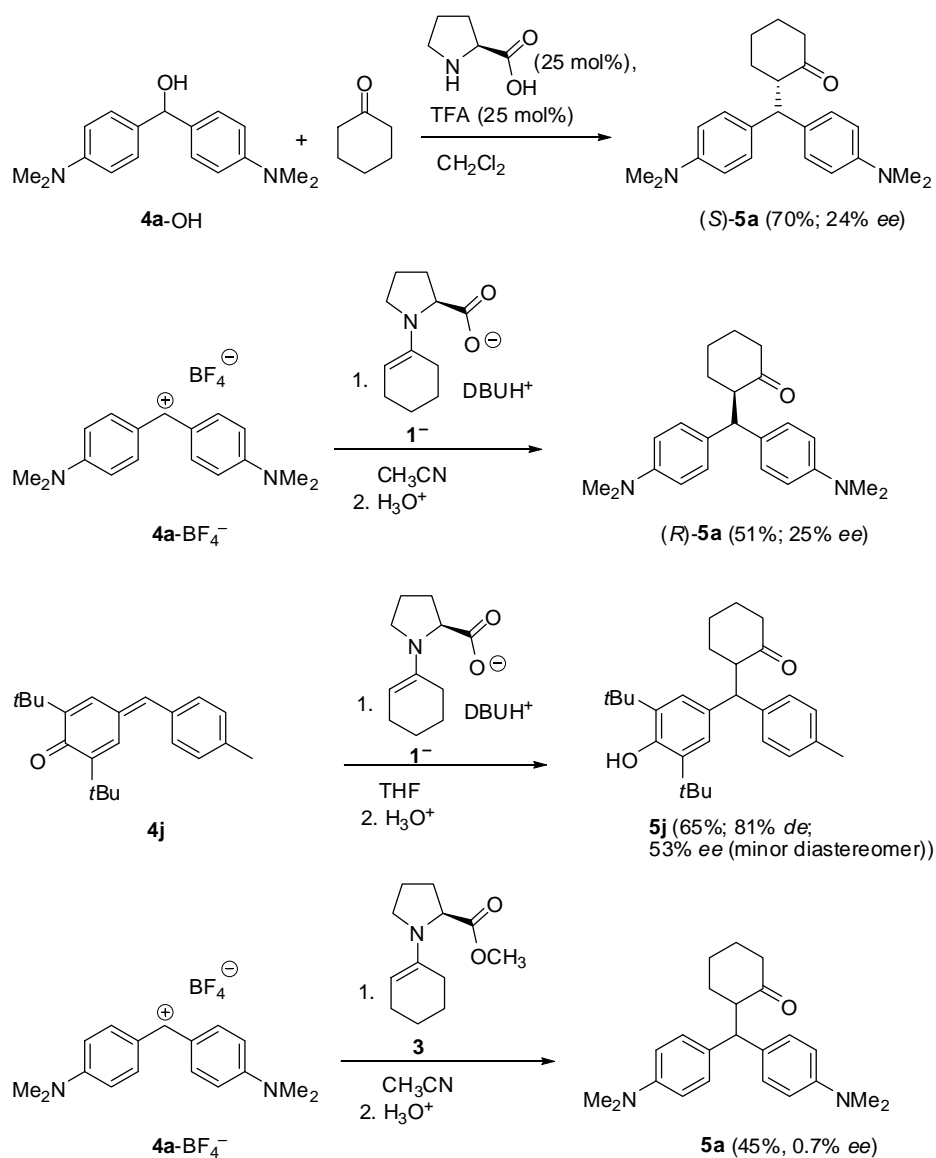
Table 5.1. Benzhydrylium ions **4a–f** and quinone methides **4g–j** employed as reference electrophiles.

Electrophile		E [a]
4a		X = NMe ₂ -7.02
4b		X = N(CH ₂) ₄ -7.69
4c		n = 2 -8.22
4d		n = 1 -8.76
4e		n = 2 -9.45
4f		n = 1 -10.04
4g		Y = Ph; Z = OMe -12.18
4h		Y = Ph; Z = NMe ₂ -13.39
4i		Y = <i>t</i> Bu; Z = NO ₂ -14.36
4j		Y = <i>t</i> Bu; Z = Me -15.83

[a] Empirical electrophilicity parameter E for **4a–f** from ref. [6] and for **4g–j** from ref. [7].

5.2 Results and Discussion

The proline-catalyzed reaction of cyclohexanone with 4,4'-bis(dimethylamino)benzhydrol (**4a-OH**) was recently reported by Cheng et al. to yield (*S*)-**5a** with 16% *ee*.^[8] Under the same conditions we have obtained (*S*)-**5a** with an *ee* of 24% (Scheme 5.3). The corresponding reaction of the benzhydrylium salt **4a-BF₄⁻** with the enaminocarboxylate **1⁻**, which was obtained by treatment of the oxazolidinone **1** with 1,8-diazabicyclo[5.4.0]undec-7-ene (DBU) gave (*R*)-**5a** with 25% *ee*. The reaction of the quinone methide **4j** with **1⁻** yielded the α -substituted cyclohexanone **5j** with 81% *de*. While the enantiomeric excess of the major diastereomer could not be determined, an *ee* of 53% was found for the minor diastereoisomer. The reaction of **4a-BF₄⁻** with the proline ester **3** yielded **5a** almost in racemic form (0.7% *ee*).



Scheme 5.3. Stereoselectivities of the reactions of cyclohexanone derived enamines with the reference electrophiles **4a** and **4j**.

The rates of the reactions of **1**⁻, **2**, and **3** with the electrophiles **4** were determined photometrically in CH₃CN at 20 °C by following the decrease of the absorbances of the colored electrophiles **4**. Reactions with $k_2 < 10^6 \text{ M}^{-1} \text{ s}^{-1}$ were studied with stopped-flow techniques, while the Laser-flash-photolytic generation of benzhydrylium ions was employed for determining rate constants $k_2 > 10^6 \text{ M}^{-1} \text{ s}^{-1}$ as described previously.^[9] By using the enamines **1**⁻, **2** and **3** in high excess over the electrophiles **4**, first-order conditions were achieved, and the first-order rate constants k_{obs} were obtained from the observed mono-exponential decays (Figure 5.1). From the linear plots of k_{obs} vs [**1**⁻], [**2**], or [**3**] the second-order rate constants k_2 were obtained which are listed in Table 5.2.

While the enamines **2** and **3** were used as pure samples, solutions of **1**⁻ were freshly prepared by treatment of **1** with one equivalent of DBU.^[3] The quantitative conversion of **1** to **1**⁻ under these conditions was demonstrated by kinetic investigations with solutions obtained from **1** with 0.95 or 1.3 equivalents of DBU.^[10] Details are given in the Experimental Section (Chapter 5.4).

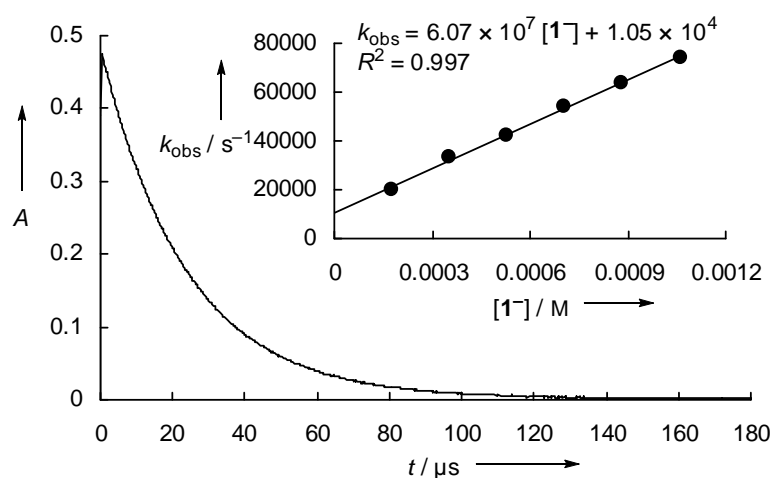


Figure 5.1. Exponential decay of the absorbance at 611 nm during the reaction of **1**⁻ ($5.27 \times 10^{-4} \text{ M}$) with laser-flash-photolytically generated **4b** at 20 °C in acetonitrile ($k_{\text{obs}} = 4.25 \times 10^4 \text{ s}^{-1}$). Insert: Determination of the second-order rate constant $k_2 = 6.07 \times 10^7 \text{ M}^{-1} \text{ s}^{-1}$ as the slope of the correlation between the first-order rate constant k_{obs} and the concentration of the enamine **1**⁻.

Table 5.2. Second-order rate constants for the reactions of **1**⁻, **2** and **3** with reference electrophiles **4** in acetonitrile at 20 °C.

Nucleophile	Electrophile	$k_2 / \text{M}^{-1} \text{s}^{-1}$
1 ⁻	4b	6.07×10^7
	4c	3.03×10^7
	4d	1.31×10^7
	4g	4.41×10^4
	4h	1.35×10^4
	4i	8.58×10^2
2	4c	6.43×10^5
	4d	2.12×10^5
	4e	7.62×10^4
	4f	3.25×10^4
3	4c	3.74×10^4
	4d	1.40×10^4
	4e	5.98×10^3
	4f	2.02×10^3

[a] From ref. [18].

The second-order rate constants for the reactions of **2** with **4c–4f** in acetonitrile (Table 5.2) deviate from those, previously measured in dichloromethane solution^[11] by less than a factor of 3, in line with our previous observations that the rates of the reactions of carbocations with neutral π -systems are only slightly affected by the nature of the solvent.^[12] Plots of the logarithms of the second-order rate constants against the empirical electrophilicity parameters E of the reference electrophiles **4** are linear, showing that Equation (5.1)^[13] is applicable (Figure 5.2) which allows us to calculate the nucleophile-specific parameters N and s for the enamines **1**⁻ ($N = 18.86$; $s = 0.70$), **2** ($N = 16.42$; $s = 0.70$), and **3** ($N = 14.96$; $s = 0.68$) in acetonitrile.

$$\log k_2(20 \text{ }^\circ\text{C}) = s(N + E) \quad (5.1)$$

s = nucleophile specific slope parameter

N = nucleophilicity parameter

E = electrophilicity parameter

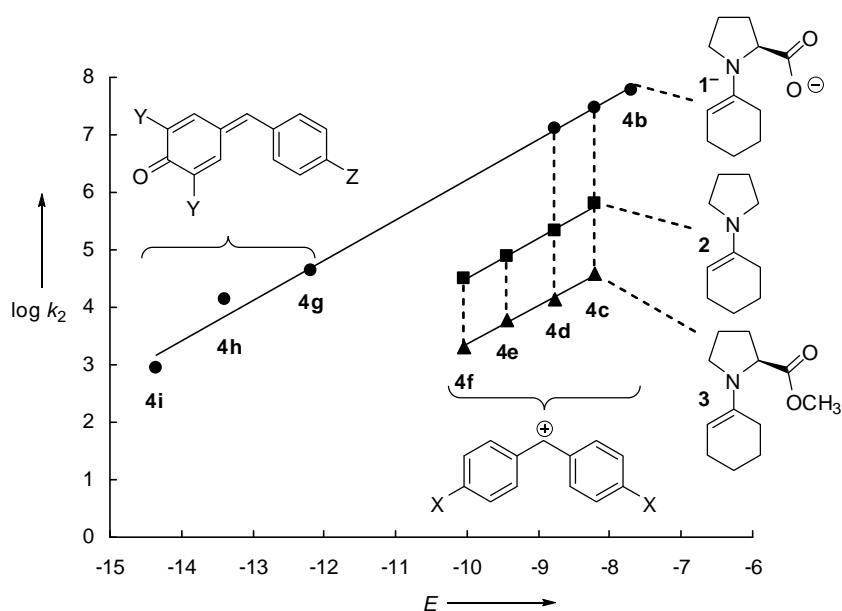


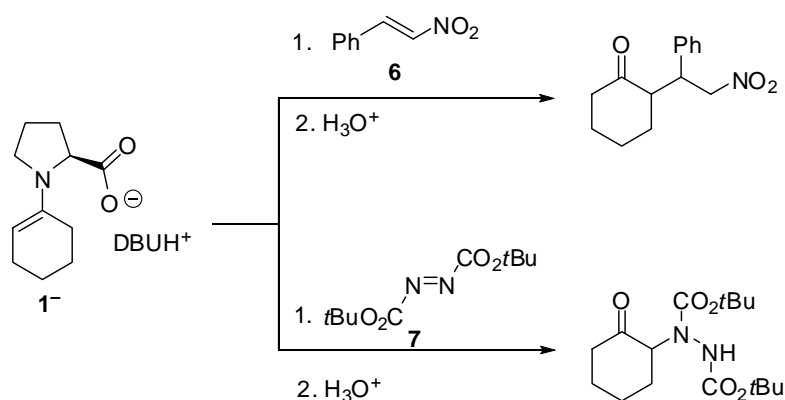
Figure 5.2. Plots of $\log k_2$ for the reactions of the enamines **1⁻**, **2**, and **3** with the reference electrophiles **4b–i** at 20 °C in acetonitrile versus their electrophilicity parameters E .

The enamine ester **3** is about 15 times less reactive than the unsubstituted enamine **2**, which reflects the electron-withdrawing effect of the ester group. In contrast, the enamino carboxylate **1⁻** is 50 to 60 times more reactive than **2** and even 800 to 900 times more reactive than **3** (Table 5.2, Figure 5.2). In line with earlier observations, the reactions of ordinary enamines with the quinone methides **4g–4i** in dichloromethane solution are thermodynamically unfavorable, and **2** was found not to react with **4g–4i**.^[14]

Can one rule out that the second-order rate constants listed for **1⁻** in Table 5.2 reflect the rates of addition of the carboxylate group to the electrophiles **4** and that the isolated products **5** are the result of thermodynamic product control? This possibility can rigorously be excluded for the reactions of **1⁻** with the quinone methides **4g–4i**, as no decrease of absorbance was observed when these electrophiles were combined with carboxylate ions, e.g., tetrabutylammonium acetate in acetonitrile (thermodynamically unfavorable). The disappearance of the benzhydrylium ions **4b–4d** in the reactions with **1⁻** also cannot be due to initial reactions of the carbocations with the carboxylate group, because previous studies on the kinetics of the reactions of the amino-substituted benzhydrylium ions **4a–4f** with tetrabutylammonium acetate^[15] have shown that the reactions with carboxylate anions are approximately 10 times slower than the reactions with **1⁻** (Table 5.2).

Two reasons may account for the fact that **1**⁻ is by far the most reactive enamine of this series (Figure 5.2). One is anchimeric assistance of the electrophilic attack by the carboxylate group as shown in **TS-B/C** of Scheme 5.1. The second one is electrostatic attraction between the cationic electrophiles and the anionic nucleophile **1**⁻, which may contribute in the reactions with the benzhydrylium ions **4b–4d**. From the comparison of the rate constants for the reactions of **4a** with aniline ($k_2 = 7.16 \times 10^3 \text{ M}^{-1} \text{ s}^{-1}$)^[16] and the 3-aminobenzenesulfonate anion ($k_2 = 7.68 \times 10^4 \text{ M}^{-1} \text{ s}^{-1}$) in acetonitrile, one can derive that Coulombic attractions may be responsible for an acceleration of the cation-anion combinations in acetonitrile by a factor of approximately 10.^[17] As a consequence, Coulomb attraction can only partially account for the high reactivity of **1**⁻ with **4b**, **4c**, and **4d**, and anchimeric assistance by the carboxylate group must play a significant role.

This interpretation is corroborated by comparing the reactivities of the enamines **1**⁻ and **2** toward the neutral electrophiles β-nitrostyrene (**6**) and di-*t*-butyl azodicarboxylate (**7**), where Coulombic attractions cannot contribute (Scheme 5.4). The observation that the enamino-carboxylate **1**⁻ reacts 107 times faster with β-nitrostyrene (**6**), but only 6 times faster with the azodicarboxylate **7** than the enamine **2** (Table 5.3) indicates that the magnitude of the anchimeric assistance is strongly dependent on the nature of the electrophiles.



Scheme 5.4. Reactions of β-nitrostyrene (**6**)^[3] and di-*t*-butyl azodicarboxylate (**7**) with the enamine **1**⁻.

Table 5.3. Second order rate constants for the reactions of **1**⁻ and **2** with β-nitrostyrene (**6**) and di-*t*-butyl azodicarboxylate (**7**) in acetonitrile at 20 °C.

Electrophile	Nucleophile	$k_2 / \text{M}^{-1} \text{s}^{-1}$
6	1 ⁻	2.43×10^3
	2	2.27×10^1
7	1 ⁻	1.80×10^3
	2	$2.99 \times 10^{2[\text{a}]}$

From ref. [19].

5.3 Conclusion

The kinetic data presented herein thus provide clear evidence for anchimeric assistance by the carboxylate group in electrophilic additions to the enamino carboxylate **1**⁻. In combination with the results of Blackmond and Armstrong^[4] these data support the proposal that oxazolidinone formation may occur in the stereogenic step of proline-catalyzed reactions,^[3] particularly in the presence of strong bases. Our results do not affect the rationalization of the stereoselectivities of a manifold of proline-catalyzed reactions by **TS-A** when the effective nucleophile is an enamino carboxylic acid^[1e,20] and not an enamino carboxylate anion.

5.4 Experimental Section

5.4.1 General comment

The kinetics of the reactions of the enamines **1**⁻, **2** and **3** with the electrophiles **4-6** were followed by UV-Vis spectroscopy at 20 °C.

For the reactions with $k_2 < 10^6 \text{ M}^{-1} \text{ s}^{-1}$ a stopped-flow spectrophotometer system (Applied Photophysics SX.18MV-R or Hi-Tech SF-61DX2) was used. The kinetic runs were initiated by mixing equal volumes of acetonitrile solutions of the electrophiles and the enamines **1**⁻, **2**, and **3**.

For determining the rates of the reactions of the benzhydrylium ions **4** with **1**⁻ with reaction times below 10 ms, benzhydrylium ions were generated by laser-flash photolysis of solutions of benzhydryl tri-*n*-butylphosphonium tetrafluoroborates (P-salt) in acetonitrile at 20 °C. A solution of known concentration of the precursor in acetonitrile was mixed with a known concentration of the enamine carboxylate **1**⁻ and the resulting colorless solution was then irradiated with a 6.5-ns laser pulse (Innolas SpitLight 600 Nd:YAG laser, fourth harmonic at $\lambda = 266 \text{ nm}$: power/pulse of 40-60 mJ) to generate the benzhydrylium ions Ar_2CH^+ .

From the exponential decays of the absorbances at λ_{max} of the electrophiles **4**, **6**, and **7**, the first-order rate constants k_{obs} (s^{-1}) were obtained. All kinetic measurements were carried out in Schlenk glassware under exclusion of moisture. The temperature of the solutions during the kinetic studies was maintained to within $\pm 0.1 \text{ }^\circ\text{C}$ by using circulating bath cryostats and monitored with thermo-couple probes that were inserted into the reaction mixture.

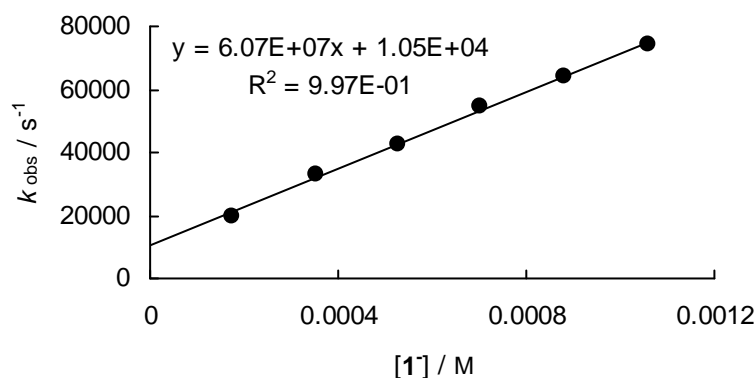
Solutions of **1**⁻ were freshly prepared by treatment of **1** with one equivalent of DBU.

5.4.2 Kinetic Experiments

Kinetics of the reactions of the enamine carboxylate **1**⁻ with the electrophiles **4b-d**, **4g-i**, **6** and **7**

Rate constants for the reaction of **1**⁻ with **4b** (precursor: **4b**⁻P(*n*-butyl)₃BF₄⁻, **4b**-P(*n*Bu)₃-salt) in CH₃CN laser flash photolysis, 20 °C, λ = 620 nm).

[1 ⁻] ₀ / M	[4b -P(<i>n</i> Bu) ₃ -salt] ₀ / M	<i>k</i> _{obs} / s ⁻¹
1.76 × 10 ⁻⁴	1.14 × 10 ⁻⁵	1.98 × 10 ⁴
3.52 × 10 ⁻⁴	1.14 × 10 ⁻⁵	3.31 × 10 ⁴
5.27 × 10 ⁻⁴	1.14 × 10 ⁻⁵	4.25 × 10 ⁴
7.03 × 10 ⁻⁴	1.14 × 10 ⁻⁵	5.44 × 10 ⁴
8.79 × 10 ⁻⁴	1.14 × 10 ⁻⁵	6.39 × 10 ⁴
1.06 × 10 ⁻³	1.14 × 10 ⁻⁵	7.40 × 10 ⁴

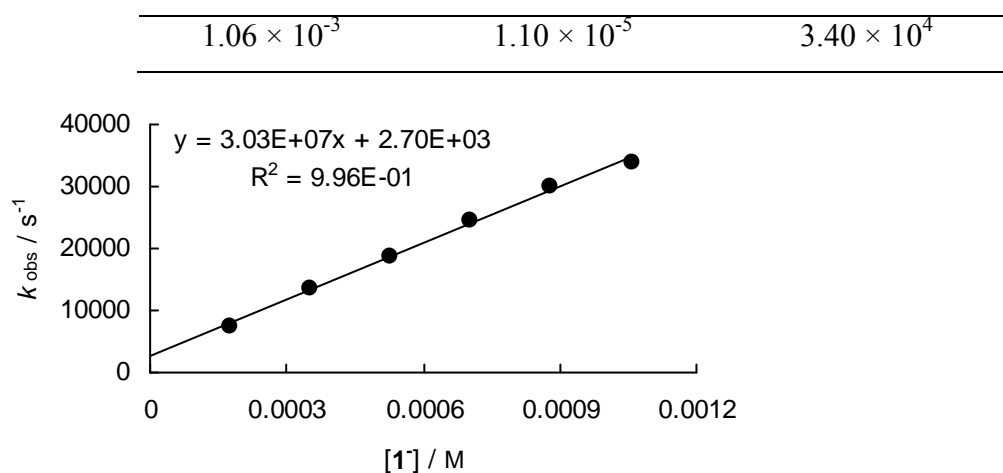


$$k_2 = 6.07 \times 10^7 \text{ M}^{-1} \text{ s}^{-1}$$

Rate constants for the reaction of **1**⁻ with **4c** (precursor: **4c**⁻P(*n*-butyl)₃BF₄⁻, **4c**-P(*n*Bu)₃-salt) in CH₃CN laser flash photolysis, 20 °C, λ = 611 nm).

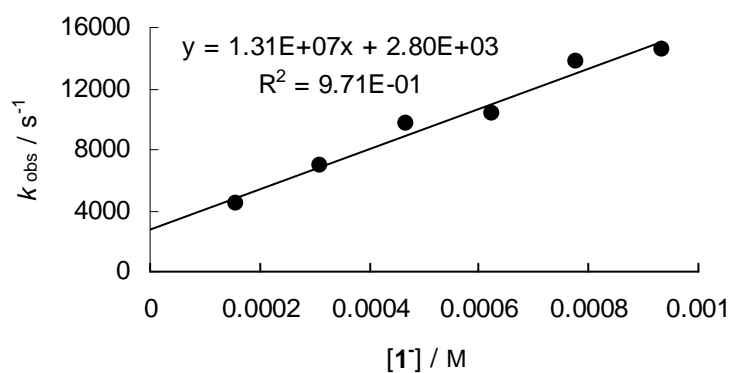
[1 ⁻] ₀ / M	[4c -P(<i>n</i> Bu) ₃ -salt] ₀ / M	<i>k</i> _{obs} / s ⁻¹
1.76 × 10 ⁻⁴	1.10 × 10 ⁻⁵	7.48 × 10 ³
3.52 × 10 ⁻⁴	1.10 × 10 ⁻⁵	1.37 × 10 ⁴
5.27 × 10 ⁻⁴	1.10 × 10 ⁻⁵	1.87 × 10 ⁴
7.03 × 10 ⁻⁴	1.10 × 10 ⁻⁵	2.44 × 10 ⁴
8.79 × 10 ⁻⁴	1.10 × 10 ⁻⁵	3.01 × 10 ⁴

Chapter 5: Kinetic Evidence for Oxazolidinone Formation in the Stereogenic Step of Proline-Catalyzed Reactions



Rate constants for the reaction of $\mathbf{1}^-$ with $\mathbf{4d}$ (precursor: $\mathbf{4d}^- \text{P}(n\text{-butyl})_3\text{BF}_4^-$, $\mathbf{4d}\text{-P}(n\text{Bu})_3\text{-salt}$) in CH_3CN laser flash photolysis, 20 °C, $\lambda = 627 \text{ nm}$).

$[\mathbf{1}^-]_0 / \text{M}$	$[\mathbf{4d}\text{-P}(n\text{Bu})_3\text{-salt}]_0 / \text{M}$	$k_{\text{obs}} / \text{s}^{-1}$
1.56×10^{-4}	1.02×10^{-5}	4.43×10^3
3.11×10^{-4}	1.02×10^{-5}	6.92×10^3
4.67×10^{-4}	1.02×10^{-5}	9.75×10^3
6.23×10^{-4}	1.02×10^{-5}	1.03×10^4
7.79×10^{-4}	1.02×10^{-5}	1.38×10^4
9.34×10^{-4}	1.02×10^{-5}	1.45×10^4

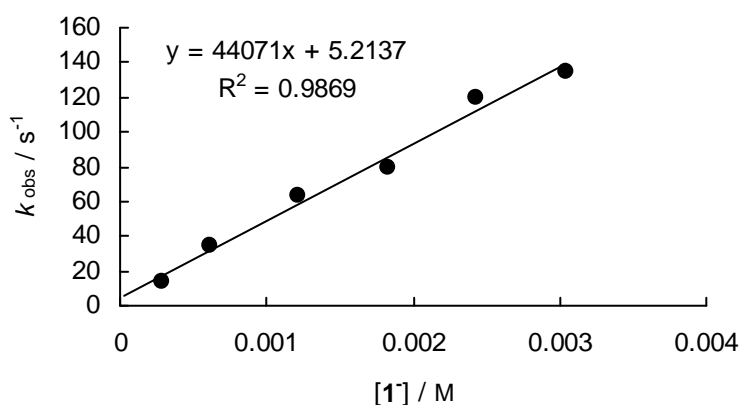


Chapter 5: Kinetic Evidence for Oxazolidinone Formation in the Stereogenic Step of Proline-Catalyzed Reactions

Rate constants for the reaction of **1**⁻ with **4g** in CH₃CN (stopped-flow method, 20 °C, λ = 422 nm).

[1 ⁻] ₀ / M	[4g] ₀ / M	[1 ⁻] ₀ / [4g] ₀	<i>k</i> _{obs} / s ⁻¹
2.87 × 10 ⁻⁴	1.54 × 10 ⁻⁵	19	1.43 × 10 ^{1[a]}
6.08 × 10 ⁻⁴	4.12 × 10 ⁻⁵	15	3.40 × 10 ¹
1.22 × 10 ⁻³	4.12 × 10 ⁻⁵	30	6.30 × 10 ¹
1.83 × 10 ⁻³	4.12 × 10 ⁻⁵	44	7.96 × 10 ¹
2.43 × 10 ⁻³	4.12 × 10 ⁻⁵	59	1.20 × 10 ²
3.04 × 10 ⁻³	4.12 × 10 ⁻⁵	74	1.35 × 10 ²

[a] Deprotonated with 1.34 equivalents DBU.

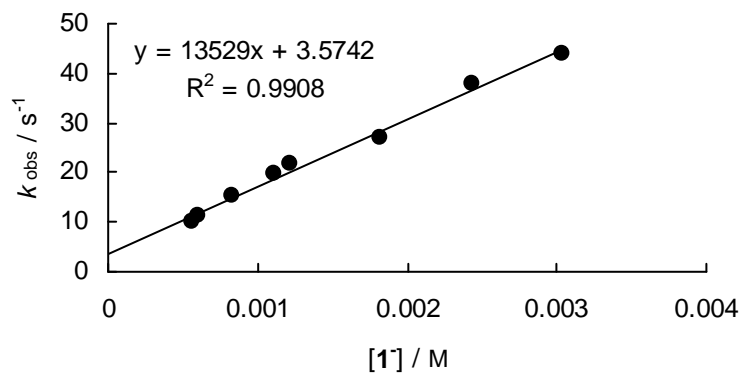


$$k_2 = 4.41 \times 10^4 \text{ M}^{-1} \text{ s}^{-1}$$

Rate constants for the reaction of **1**⁻ with **4h** in CH₃CN (stopped-flow method, 20 °C, λ = 533 nm).

[1 ⁻] ₀ / M	[4h] ₀ / M	[1 ⁻] ₀ / [4h] ₀	<i>k</i> _{obs} / s ⁻¹
5.57 × 10 ^{-4[a]}	2.28 × 10 ⁻⁵	24	9.90
6.08 × 10 ⁻⁴	4.17 × 10 ⁻⁵	15	1.12 × 10 ¹
8.36 × 10 ^{-4[a]}	2.28 × 10 ⁻⁵	37	1.52 × 10 ¹
1.11 × 10 ^{-3[a]}	2.28 × 10 ⁻⁵	49	1.96 × 10 ¹
1.22 × 10 ⁻³	4.17 × 10 ⁻⁵	29	2.16 × 10 ¹
1.83 × 10 ⁻³	4.17 × 10 ⁻⁵	44	2.69 × 10 ¹
2.43 × 10 ⁻³	4.17 × 10 ⁻⁵	58	3.78 × 10 ¹
3.04 × 10 ⁻³	4.17 × 10 ⁻⁵	73	4.38 × 10 ¹

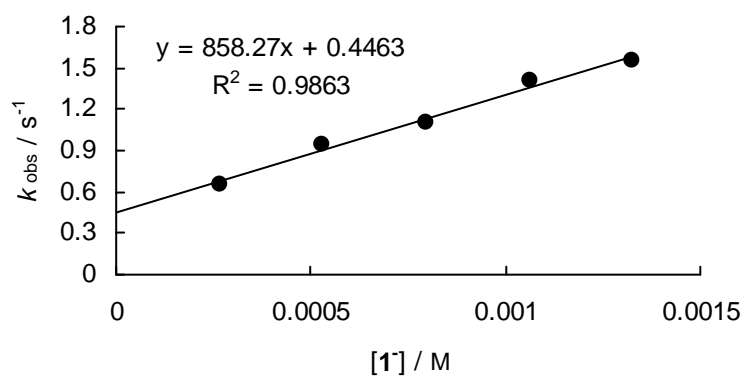
[a] Deprotonated with 0.95 equiv. DBU.



$$k_2 = 1.35 \times 10^4 \text{ M}^{-1} \text{ s}^{-1}$$

Rate constants for the reaction of $\mathbf{1}^-$ with $\mathbf{4i}$ in CH_3CN (stopped-flow method, 20°C , $\lambda = 374 \text{ nm}$).

$[\mathbf{1}^-]_0 / \text{M}$	$[\mathbf{4i}]_0 / \text{M}$	$[\mathbf{1}^-]_0 / [\mathbf{4i}]_0$	$k_{\text{obs}} / \text{s}^{-1}$
2.65×10^{-4}	1.71×10^{-5}	16	6.46×10^{-1}
5.31×10^{-4}	1.71×10^{-5}	31	9.41×10^{-1}
7.96×10^{-4}	1.71×10^{-5}	47	1.10
1.06×10^{-3}	1.71×10^{-5}	62	1.41
1.33×10^{-3}	1.71×10^{-5}	78	1.55

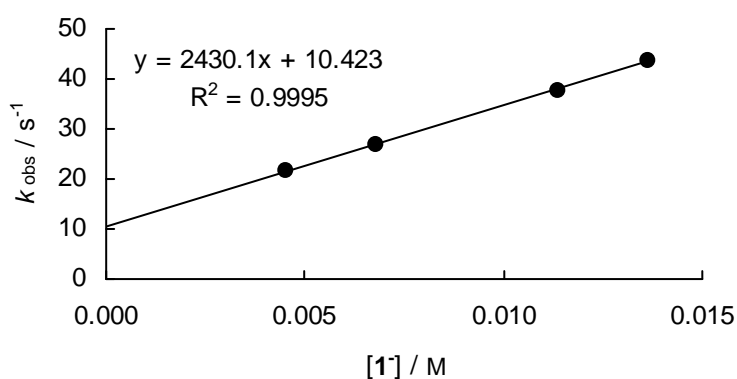


$$k_2 = 8.58 \times 10^2 \text{ M}^{-1} \text{ s}^{-1}$$

Chapter 5: Kinetic Evidence for Oxazolidinone Formation in the Stereogenic Step of Proline-Catalyzed Reactions

Rate constants for the reaction of **1**⁻ with **6** in CH₃CN (stopped-flow method, 20 °C, λ = 340 nm).

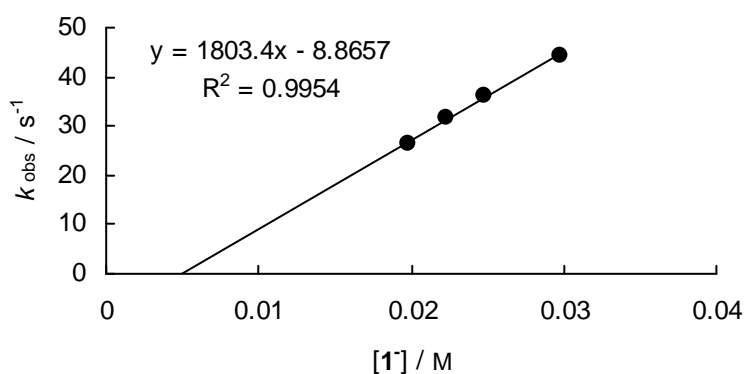
[1 ⁻] ₀ / M	[6] ₀ / M	[1 ⁻] ₀ / [6] ₀	<i>k</i> _{obs} / s ⁻¹
4.54 × 10 ⁻³	1.85 × 10 ⁻⁴	25	2.16 × 10 ¹
6.82 × 10 ⁻³	1.85 × 10 ⁻⁴	37	2.69 × 10 ¹
1.14 × 10 ⁻²	1.85 × 10 ⁻⁴	61	3.78 × 10 ¹
1.36 × 10 ⁻²	1.85 × 10 ⁻⁴	74	4.38 × 10 ¹



$$k_2 = 2.43 \times 10^3 \text{ M}^{-1} \text{ s}^{-1}$$

Rate constants for the reaction of **1**⁻ with **7** in CH₃CN (stopped-flow method, 20 °C, λ = 410 nm).

[1 ⁻] ₀ / M	[7] ₀ / M	[1 ⁻] ₀ / [7] ₀	<i>k</i> _{obs} / s ⁻¹
1.98 × 10 ⁻²	3.19 × 10 ⁻³	6	2.63 × 10 ¹
2.23 × 10 ⁻²	3.19 × 10 ⁻³	7	3.18 × 10 ¹
2.48 × 10 ⁻²	3.19 × 10 ⁻³	8	3.62 × 10 ¹
2.97 × 10 ⁻²	3.19 × 10 ⁻³	9	4.44 × 10 ¹

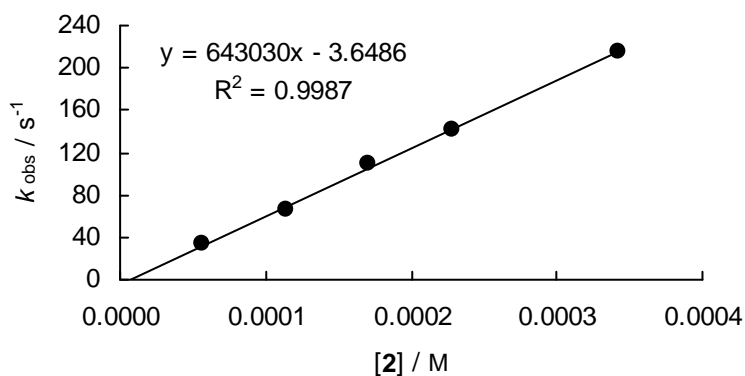


$$k_2 = 1.80 \times 10^3 \text{ M}^{-1} \text{ s}^{-1}$$

Kinetics of the reactions of the 1-(pyrrolidino)cyclohexene **2 with the electrophiles **4c-f** and **6****

Rate constants for the reaction of **2** with **4c** in CH₃CN (stopped-flow method, 20 °C, λ = 620 nm).

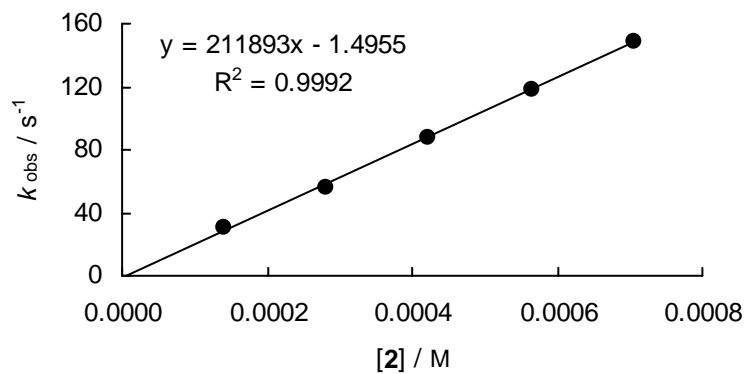
[2] ₀ / M	[4c] ₀ / M	[2] ₀ / [4c] ₀	<i>k</i> _{obs} / s ⁻¹
5.70 × 10 ⁻⁵	8.87 × 10 ⁻⁶	6	3.37 × 10 ¹
1.14 × 10 ⁻⁴	8.87 × 10 ⁻⁶	13	6.65 × 10 ¹
1.71 × 10 ⁻⁴	8.87 × 10 ⁻⁶	19	1.10 × 10 ²
2.28 × 10 ⁻⁴	8.87 × 10 ⁻⁶	26	1.42 × 10 ²
3.42 × 10 ⁻⁴	8.87 × 10 ⁻⁶	39	2.16 × 10 ²



$$k_2 = 6.43 \times 10^5 \text{ M}^{-1} \text{ s}^{-1}$$

Rate constants for the reaction of **2** with **4d** in CH₃CN (stopped-flow method, 20 °C, λ = 630 nm).

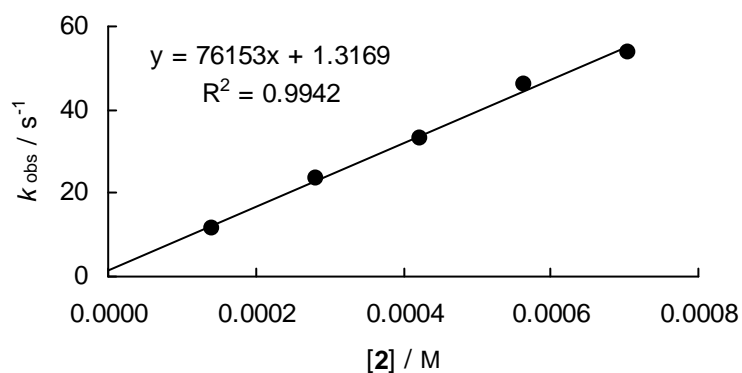
[2] ₀ / M	[4d] ₀ / M	[2] ₀ / [4d] ₀	<i>k</i> _{obs} / s ⁻¹
1.41 × 10 ⁻⁴	7.91 × 10 ⁻⁶	18	3.01 × 10 ¹
2.82 × 10 ⁻⁴	7.91 × 10 ⁻⁶	36	5.64 × 10 ¹
4.23 × 10 ⁻⁴	7.91 × 10 ⁻⁶	53	8.76 × 10 ¹
5.65 × 10 ⁻⁴	7.91 × 10 ⁻⁶	71	1.18 × 10 ²
7.06 × 10 ⁻⁴	7.91 × 10 ⁻⁶	89	1.49 × 10 ²



$$k_2 = 2.12 \times 10^5 \text{ M}^{-1} \text{ s}^{-1}$$

Rate constants for the reaction of **2** with **4e** in CH₃CN (stopped-flow method, 20 °C, $\lambda = 630 \text{ nm}$).

[2] ₀ / M	[4e] ₀ / M	[2] ₀ / [4e] ₀	$k_{\text{obs}} / \text{s}^{-1}$
1.41×10^{-4}	7.88×10^{-6}	18	1.13×10^1
2.82×10^{-4}	7.88×10^{-6}	36	2.36×10^1
4.23×10^{-4}	7.88×10^{-6}	54	3.29×10^1
5.65×10^{-4}	7.88×10^{-6}	72	4.62×10^1
7.06×10^{-4}	7.88×10^{-6}	90	5.38×10^1

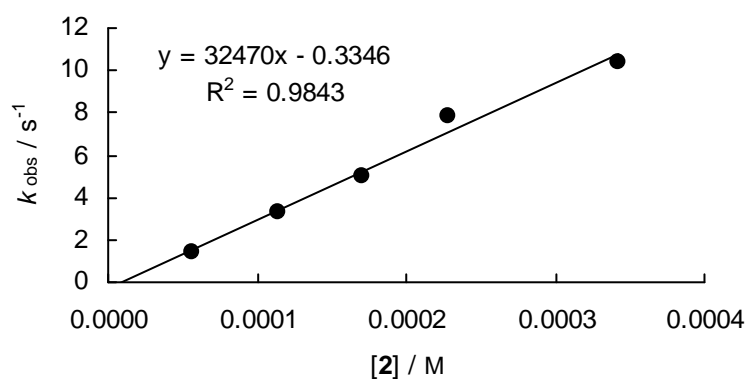


$$k_2 = 7.62 \times 10^4 \text{ M}^{-1} \text{ s}^{-1}$$

Chapter 5: Kinetic Evidence for Oxazolidinone Formation in the Stereogenic Step of Proline-Catalyzed Reactions

Rate constants for the reaction of **2** with **4f** in CH₃CN (stopped-flow method, 20 °C, λ = 620 nm).

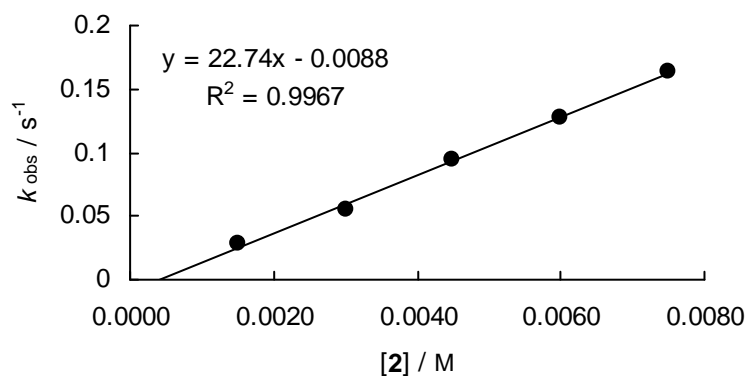
[2] ₀ / M	[4f] ₀ / M	[2] ₀ / [4f] ₀	<i>k</i> _{obs} / s ⁻¹
5.70 × 10 ⁻⁵	7.69 × 10 ⁻⁶	7	1.40
1.14 × 10 ⁻⁴	7.69 × 10 ⁻⁶	15	3.27
1.71 × 10 ⁻⁴	7.69 × 10 ⁻⁶	22	5.02
2.28 × 10 ⁻⁴	7.69 × 10 ⁻⁶	30	7.85
3.42 × 10 ⁻⁴	7.69 × 10 ⁻⁶	44	1.04 × 10 ¹



$$k_2 = 3.25 \times 10^4 \text{ M}^{-1} \text{ s}^{-1}$$

Rate constants for the reaction of **2** with **6** in CH₃CN (stopped-flow method, 20 °C, λ = 340 nm).

[2] ₀ / M	[6] ₀ / M	[2] ₀ / [6] ₀	<i>k</i> _{obs} / s ⁻¹
1.50 × 10 ⁻³	9.55 × 10 ⁻⁵	16	2.87 × 10 ⁻²
3.00 × 10 ⁻³	9.55 × 10 ⁻⁵	31	5.45 × 10 ⁻²
4.50 × 10 ⁻³	9.55 × 10 ⁻⁵	47	9.45 × 10 ⁻²
6.00 × 10 ⁻³	9.55 × 10 ⁻⁵	63	1.27 × 10 ⁻¹
7.50 × 10 ⁻³	9.55 × 10 ⁻⁵	79	1.63 × 10 ⁻¹

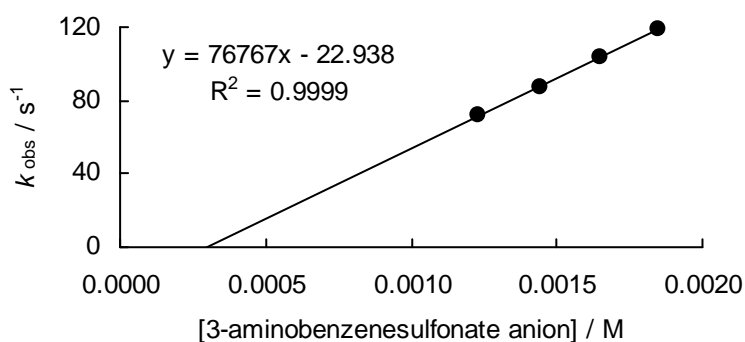


$$k_2 = 2.27 \times 10^1 \text{ M}^{-1} \text{ s}^{-1}$$

Kinetics of the reactions of 3-aminobenzenesulfonate anion with **4a**

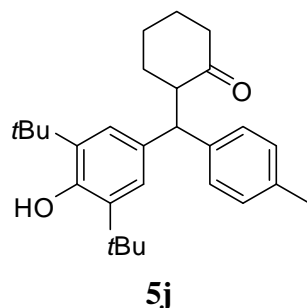
Rate constants for the reaction of 3-aminobenzenesulfonate anion (Nu) with **4a** in CH₃CN (stopped-flow method, 20 °C, $\lambda = 613$ nm, the solution of 3-aminobenzenesulfonate anion was freshly prepared before the experiment by adding one equivalent of NEt₃ to a solution of 3-aminobenzenesulfonic acid).

[Nu] ₀ / M	[4a] ₀ / M	[Nu] ₀ / [4a] ₀	$k_{\text{obs}} / \text{s}^{-1}$
1.23×10^{-3}	1.08×10^{-5}	114	7.16×10^1
1.44×10^{-3}	1.08×10^{-5}	133	8.73×10^1
1.65×10^{-3}	1.08×10^{-5}	153	1.04×10^2
1.85×10^{-3}	1.08×10^{-5}	171	1.19×10^2



$$k_2 = 7.68 \times 10^4 \text{ M}^{-1} \text{ s}^{-1}$$

5.4.3 Synthetic Experiments



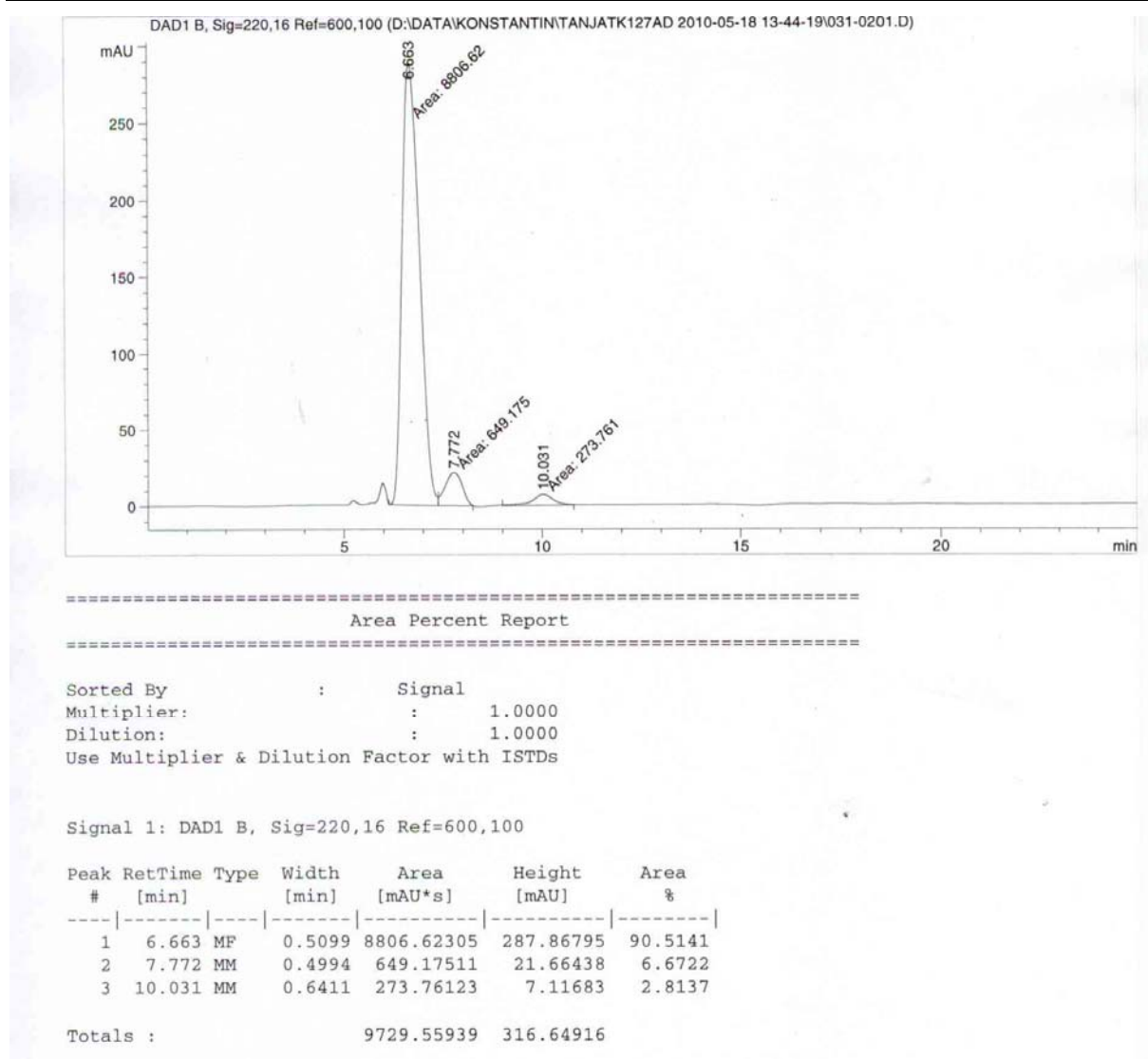
The oxazolidinone **1** (43 mg, 0.22 mmol) was dissolved in dry THF (10 ml) under Ar in a two-necked flask (dried by heat gun at 1.2 mbar). The solution was cooled to 0 °C, DBU (33 μ l, 0.22 mmol) was added, and the mixture was stirred for 30 min. Then a solution of **4j** in THF was added (68 mg, 0.22 mmol). The mixture was stirred for 1 h, and the reaction was quenched with a diluted solution of acetic acid (5 ml) and extracted with ethyl acetate (3 \times). The organic layer was dried over MgSO₄, filtered, and concentrated under vacuum. The residue was purified by column chromatography on silica gel (15% AcOEt/pentane) to give **5j** as white solid (59 mg, 0.15 mmol, 68%, 81% *de*, 53% *ee* of the minor diastereomer). The enantiomeric excess was determined by HPLC analysis on a Chiralpak AD-H column, λ = 254 nm, eluent *i*-PrOH/*n*-hexane (2:98), flow rate = 0.7 mL/min; major diastereoisomer: t_R = 6.66 min; minor diastereoisomer: t_R = 7.77 (major enantiomer), 10.03 min (minor enantiomer).

Major isomer:

¹H NMR (300 MHz, CDCl₃): δ = 1.41 (s, 18 H), 1.62-1.70 (m, 1 H), 1.75-2.02 (m, 5 H), 2.27-2.35 (m, 4 H), 2.39-2.47 (m, 1 H), 3.23-3.31 (m, 1 H), 4.28 (d, 1 H, J = 10.4 Hz), 4.97, (s, 1 H), 7.01-7.22 (m, 6 H). Additionally the following chemical shifts were found for the minor isomer: δ = 4.18 (d, J = 11.1), 5.01 (s).

Major isomer:

¹³C NMR (75.5 MHz, CDCl₃): δ = 21.0 (q), 23.9 (t), 29.2 (t), 30.36 (q), 33.1 (t), 34.3 (q), 42.0 (t), 50.2 (d), 55.7 (d), 124.3 (d), 128.2 (d), 129.1 (d), 134.2 (s), 135.3 (s), 135.5 (s), 140.7 (s), 151.9, 212.8 (s). Additionally the following chemical shifts were found for the minor isomer: δ = 30.34, 124.5, 127.5, 129.0, 133.4, 135.7, 141.4, 152.1, 213.1.



5.5 References

- [1] a) Z. G. Hajos, D. R. Parrish, *J. Org. Chem.* **1974**, *39*, 1615–1621; b) C. Puchot, O. Samuel, E. Duñach, S. Zhao, C. Agami, H. B. Kagan, *J. Am. Chem. Soc.* **1986**, *108*, 2353–2357; c) D. Rajagopal, M. S. Moni, S. Subramanian, S. Swaminathan, *Tetrahedron: Asymmetry* **1999**, *10*, 1631–1634; d) K. N. Rankin, J. W. Gauld, R. J. Boyd, *J. Phys. Chem. A* **2002**, *106*, 5155–5159; e) M. B. Schmid, K. Zeitler, R. M. Gschwind, *Angew. Chem.* **2010**, *122*, 5117–5123; *Angew. Chem. Int. Ed.* **2010**, *49*, 4997–5003.

- [2] a) B. List, R. A. Lerner, C. F. Barbas, III, *J. Am. Chem. Soc.* **2000**, *122*, 2395–2396; b) S. Bahmanyar, K. N. Houk, *J. Am. Chem. Soc.* **2001**, *123*, 12911–12912; c) L. Hoang, S. Bahmanyar, K. N. Houk, B. List, *J. Am. Chem. Soc.* **2003**, *125*, 16–17; d) S. Bahmanyar, K. N. Houk, H. J. Martin, B. List, *J. Am. Chem. Soc.* **2003**, *125*, 2475–2479; e) F. R. Clemente, K. N. Houk, *Angew. Chem.* **2004**, *116*, 5890–5892; *Angew. Chem. Int. Ed.* **2004**, *43*, 5766–5768; f) P. H.-Y. Cheong, K. N. Houk, *J. Am. Chem. Soc.* **2004**, *126*, 13912–13913; g) B. List, L. Hoang, H. J. Martin, *Proc. Nat. Acad. Sci. U.S.A.* **2004**, *101*, 5839–5842; h) B. List, *Acc. Chem Res.* **2004**, *37*, 548–557; i) C. Allemann, R. Gordillo, F. R. Clemente, P. H.-Y. Cheong, K. N. Houk, *Acc. Chem. Res.* **2004**, *37*, 558–569; j) P. H.-Y. Cheong, K. N. Houk, *Synthesis* **2005**, *9*, 1533–1537; k) F. R. Clemente, K. N. Houk, *J. Am. Chem. Soc.* **2005**, *127*, 11294–11302; l) B. List, *Chem. Commun.* **2006**, 819–824; m) S. Mukherjee, J. W. Yang, S. Hoffmann, B. List, *Chem. Rev.* **2007**, *107*, 5471–5569; n) D. W. C. McMillan, *Nature* **2008**, *455*, 304–308.
- [3] D. Seebach, A. K. Beck, D. M. Badine, M. Limbach, A. Eschenmoser, A. M. Treasurywala, R. Hobi, W. Prikoszovich, B. Lindner, *Helv. Chim. Acta* **2007**, *90*, 425–471.
- [4] D. G. Blackmond, A. Moran, M. Hughes, A. Armstrong, *J. Am. Chem. Soc.* **2010**, *132*, 7598–7599.
- [5] B. Capon, S. P. McManus, *Neighboring Group Participation*, Vol. 1, Plenum Press, New York, **1976**.
- [6] H. Mayr, T. Bug, M. F. Gotta, N. Hering, B. Irrgang, B. Janker, B. Kempf, R. Loos, A. R. Ofial, G. Remennikov, H. Schimmel, *J. Am. Chem. Soc.* **2001**, *123*, 9500–9512.
- [7] a) R. Lucius, R. Loos, H. Mayr, *Angew. Chem.* **2002**, *114*, 97–102; *Angew. Chem. Int. Ed.* **2002**, *41*, 91–95; b) D. Richter, N. Hampel, T. Singer, A. R. Ofial, H. Mayr *Eur. J. Org. Chem.* **2009**, 3203–3211.
- [8] L. Zhang, L. Cui, X. Li, J. Li, S. Luo, J.-P. Cheng, *Chem. Eur. J.* **2010**, *16*, 2045–2049.
- [9] J. Ammer, H. Mayr, *Macromolecules* **2010**, *43*, 1719–1723.
- [10] With $N = 15.29$ and $s = 0.70$ (M. Baidya, H. Mayr, *Chem. Commun.* **2008**, 1792–1794) the reactions of DBU with **4a-4j** are much slower than the reactions under consideration.
- [11] B. Kempf, N. Hampel, A. R. Ofial, H. Mayr, *Chem. Eur. J.* **2003**, *9*, 2209–2218.

- [12] a) H. Mayr, R. Schneider, C. Schade, J. Bartl, R. Bederke, *J. Am. Chem. Soc.* **1990**, *112*, 4446–4454; b) H. Mayr, *Angew. Chem.* **1990**, *102*, 1415–1428; *Angew. Chem. Int. Ed. Engl.* **1990**, *29*, 1371–1384.
- [13] a) H. Mayr, M. Patz, *Angew. Chem.* **1994**, *106*, 990–1010; *Angew. Chem. Int. Ed. Engl.* **1994**, *33*, 938–957; b) H. Mayr, B. Kempf, A. R. Ofial, *Acc. Chem. Res.* **2003**, *36*, 66–77.
- [14] B. Kempf, *Dissertation*, Ludwig-Maximilians-Universität München, **2003**.
- [15] H. F. Schaller, A. A. Tishkov, X. Feng, H. Mayr, *J. Am. Chem. Soc.* **2008**, *130*, 3012–3022.
- [16] F. Brotzel, Y. C. Chu, H. Mayr, *J. Org. Chem.* **2007**, *72*, 3679–3688.
- [17] The σ_m value of 0.05 for SO_3^- excludes a noticeable substituent effect on the nucleophilicity of the amino group: D. H. McDaniel, H. C. Brown, *J. Org. Chem.* **1958**, *23*, 420–427.
- [18] T. Kanzian, H. Mayr, *Chem. Eur. J.*, accepted (DOI: 10.1002/chem.201001598).
- [19] See also [3] and B. List, P. Pojarliev, H. J. Martin, *Org. Lett.* **2001**, *3*, 2423–2425.

LEBENS LAUF

Persönliche Daten

Tanja Kanzian

geboren am 10.01.1980

ledig, Staatsangehörigkeit: deutsch

Geburtsort Füssen

Schulen

1986-1990 Grundschule Rieden

1990-1999 Gymnasium Füssen

Jun 1999 Abitur

Studium und Promotion

Okt 1999-Mai 2000 Betriebswirtschaftsstudium an der Universität Augsburg

Okt 2000-Mai 2005 Chemiestudium an der Ludwig-Maximilians-Universität
München, Wahlfach Patentrecht

Jun 2005-Dez 2005 Diplomarbeit im Arbeitskreis Prof. H. Mayr, LMU, Titel:
„Kinetik der Reaktionen elektronenarmer Arene mit Amininen
und Enaminen“

Jan 2006-Dez 2010 Wissenschaftliche Mitarbeiterin im Arbeitskreis Prof. H. Mayr

Feb 2009-Apr 2009 Forschungsaufenthalt im Arbeitskreis Prof. Dr. O. Attanasi,
Università degli Studi di Urbino Carlo Bo, Italien

München, 02.08.2010

